CRANFIELD INSTITUTE OF TECHNOLOGY

Aerodynamics Division

College of Aeronautics

Ph.D. Thesis

M. E. ESHELBY

A Non-Linear Analysis of the Longitudinal Static Stability of Light, Multi-Engined Aircraft

Part I

January 1979

SUMMARY

The longitudinal handling qualities of light aircraft have traditionally been assessed in terms of the slope of the static stability trim curves. This method of assessment is simple in terms of analysis as well as being a relatively easy task for the pilot to perform. The theory is however based on a simple linearised model of the aircraft and omits, amongst other things, the effects of power. A comparison between the estimated and measured trim curves of a typical light aircraft shows that the linearised theory severely overestimates its static stability. A design based on the linear assumptions would be unlikely to comply with airworthiness requirements.

In Part II the main omissions from the linearised model are considered individually and their effect on the trim curves found. In Part I the individual contributions from Part II are used to complete the full, non-linear, trim equations and these are solved in terms of elevator angle and incidence to trim, $\bar{\eta}$ and $\bar{\alpha}$. The solution shows that the non-linear analysis provides a good simulation of the flight measured trim curve data thus verifying the methods of estimation developed in Part II.

The trim curves are considered in terms of incidence and lift coefficient and show that assumption of a linear lift-incidence relationship may cause some misleading interpretations of the trim curves drawn in terms of lift coefficient.

AUTHORS NOTE

This thesis is the result of a long term investigation into the handling qualities of a light aircraft which was sponsored, in the initial stages, by the Ministry of Defence (Procurement Executive). As the work progressed each completed phase was published in the Cranfield Aero Report series and these reports, in their original form, are included as Part II of the thesis. I would like to thank M.O.D.(P.E.) for permission to use the flight data and other material from the light aircraft handling research in the preparation of the thesis.

I would also express my gratitude to Mrs.P.A.Forrest-Holden for typing the thesis and to the staff of the Flight Department for their assistance with the experimental work and flight trials.

CONTENTS

Notation

A	Aspect Ratio, Temperature lapse rate
a	Lift curve slope, $dC_L/d\alpha$
a_1, a_2, a_3	Lift curve slopes of tail, elevator and tab respectively
$B_1 C_1 D_1 E_1$	Stability Quartic Coefficients (eqns 2.5 to 2.8)
b_1, b_2, b_3	Elevator Hinge moment parameters due to tail, elevator and tab respectively.
C_D	Drag coefficient, $D/\frac{1}{2}\rho V^2 S$
C_L	Lift coefficient, $L/\frac{1}{2}\rho V^2 S$
C_m	Pitching moment coefficient, $M/\frac{1}{2}\rho V^2 S\bar{c}$
C_P	Power coefficient, $P/\frac{1}{2}\rho n^3 D^5$
C_Z	Normal Force coefficient, $Z_p/\frac{1}{2}\rho V^2 D^2$
c	cylinder compression ratio
$\bar{c}$	mean aerodynamic chord, (m.a.c.)
D	Propeller diameter, Drag
e	Span efficiency factor
g_o	Gravitational constant, standard sea level value.
H	Geopotential Height
H_p	Pressure altitude
h	C.G.Position, aft of L.E. of m.a.c.
h_o	Aerodynamic centre, aft of L.E. of m.a.c.
h_f h_n	Aerodynamic centres of fuselage, nacelle, aft of L.E. of m.a.c.

I	Moment of Inertia
i_B	Moment of Inertia in pitch
k	General constant
L	Lift force
L_T	Tail lift force
l_T	Tail arm
M	Pitching moment, Mach number
M_a	Aerodynamic pitching moment
M_c	Propeller pitching moment coefficient, $M_p/\frac{1}{2}\rho V^2 D^3$
m	Aircraft mass, tailplane-tab gearing
$m_u, m_w, m_{\dot{w}}$ m_q, m_η	Non-dimensional pitching moment derivatives
N	Number of propellers
P	Engine shaft Power
p	pressure, atmospheric
q	pitch rate, dynamic head, $\frac{1}{2}\rho V^2$
R	Gas constant
r	Engine manifold pressure ratio, p_i/p
S	Wing area

T	Temperature, Thrust
T_c, T_c'	Thrust coefficient, $T/\frac{1}{2}\rho V^2 D^2$; $T/\frac{1}{2}\rho V^2 S$ respectively.
t	Time, thickness
u	Forward velocity disturbance
V	True airspeed
V_e	Equivalent airspeed
V_o	Undisturbed (true) airspeed
$\bar{V}$	Tail volume coefficient
V_T	$\bar{V}/(1 + F)$, tail volume defined in ref.9.
W	Aircraft weight
w	Vertical speed disturbance
X_a, X_g	Forces in X axis, aerodynamic, gravitational
x_u, x_w, x_q, x_n	Non-dimensional force component derivatives
Z_a Z_g	Forces in Z axis, aerodynamic, gravitational
Z_c	Propeller normal force coefficient, $Z_p/\frac{1}{2}\rho V^2 D^2$
Z_p	Propeller normal force
z	Vertical position of C.G. above m.a.c.
z_u z_w z_q z_n	Non-dimensional force component derivatives

α	Incidence angle
β	Elevator tab angle, sideslip angle
γ	Flight Path angle
ε	Downwash angle
η	Elevator angle, propeller efficiency
θ	Inclination of O_X axis to horizontal in steady state
θ	Pitch attitude disturbance, relative temperature
λ	Root of stability quartic
ρ	Density
ρ_1 ρ_2 ρ_3	Constants
σ	Relative density
δ	Relative pressure
τ	Aerodynamic time
μ_1	Aircraft longitudinal density parameter
Δ	Error or change

<u>Superscripts</u>

$\cdot$	rate of change with time
$\hat{}$	Relative to undisturbed forward speed, V_o
m'	Alternative form of pitching moment coefficient (e.g. $m'_w = m_w/i_B$)
-	Trim value

<u>Subscripts</u>

o	Reference value, sea level I.S.A.
T	Tail
f	Fuselage
n	Nacelle
b	Body
w	Wing
P	Power, propeller

A Non-Linear Analysis of the Longitudinal Static Stability of Light, Multi-Engined Aircraft

1. Introduction - An aircraft's handling qualities and its relationship to pilot ability

The longitudinal stability characteristics of low speed, light aircraft are normally assessed from the trim curves of elevator angle to trim, $\bar{n}$, with lift coefficient, C_L, and elevator hinge moment to trim, $\bar{C}_H$, with C_L. This method is used because of its simplicity in terms of flight measurement technique and the analysis of the flight data. Both these features make the method particularly attractive for the assessment of light aircraft stability since the cost of flight trials and the associated instrumentation necessary to undertake a full investigation of the dynamic stability of the aircraft would be prohibitively expensive in relation to the other development costs. The only special instrumentation required to measure the trim curves is a control position indicator and a control load sensor to detect the load applied by the pilot to the elevator control. The flight lift coefficient can be calculated from the aircraft weight and the airspeed.

The derivation of the method of measurement is outlined in section 2. Fundamentally the flight technique is simple; with the elevator trim tab set in a fixed position the aircraft is flown through a series of steady speed trims at intervals through the speed range. At each steady speed the elevator angle to trim and elevator out of trim force are recorded and used to construct the trim curves, fig.1.1. By considering the slope of the trim curves it can be determined whether or not the aircraft can be regarded as stable, see section 2.

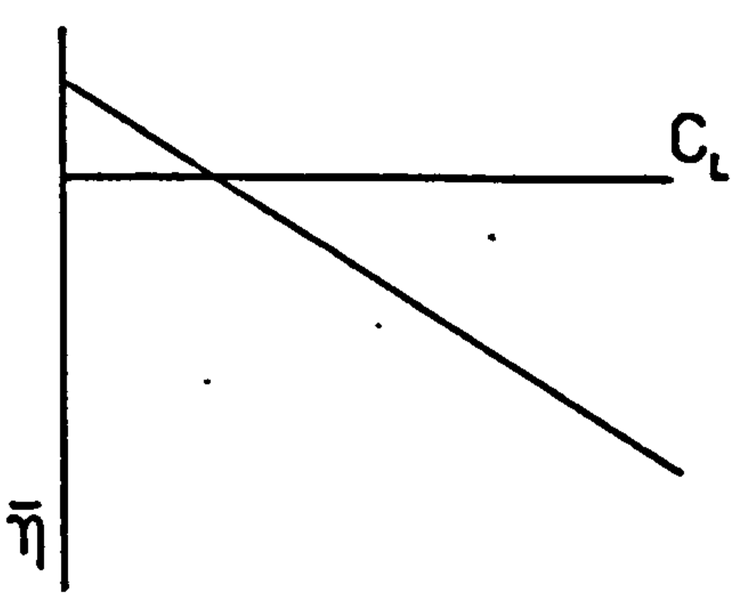

Controls Fixed

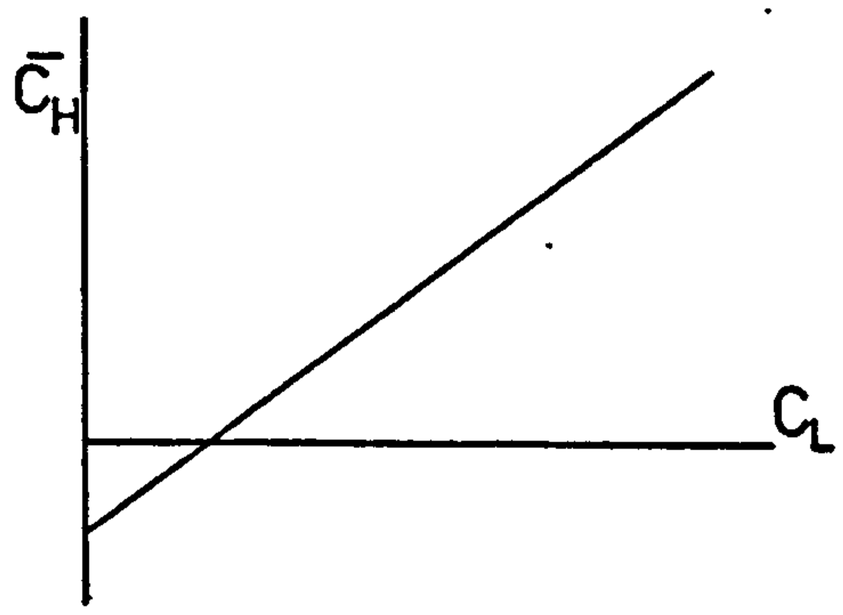

Controls Free

This method simply determines that the aircraft, if stable under the definition of static stability, will produce a restoring pitching moment following a small disturbance in incidence. This has been referred to as Pitch Stiffness by Etkin, ref.1, and this term is a good illustration of the meaning of static stability. Static stability does not include any pilot input, it is regarded as purely an aerodynamic characteristic of the aircraft. When the pitch stiffness is high then the aircraft will produce a strong restoring moment following a small disturbance and the recovery to equilibrium will be rapid. The pilot may have no need to make any conscious effort to assist the recovery. As the pitch stiffness decreases so the restoring moment decreases and the recovery to equilibrium will be less rapid. To maintain flight within reasonable speed and height variation limits it will now be necessary for the pilot to make compensatory control inputs to assist the aircraft to return to its equilibrium within a reasonable time. If the pitch stiffness becomes zero, (neutral static stability), then the pilot is wholly responsible for producing the restoring moment and an unstable aircraft, (negative pitch stiffness), demands that the pilot is also required to produce control inputs to oppose the aerodynamic pitching moments produced by the aircraft.

From this it can be seen that as pitch stiffness reduces the pilot is required to dedicate more effort into maintaining equilibrium. The limit is reached when the pilot is no longer able to guarantee that control can be maintained. It is not possible to put a simple quantitative measure on this limit since it depends on the individual pilot experience and the requirement to maintain control in other degrees of freedom. His task is time shared between longitudinal, lateral and directional control and his other flight deck duties. If the pilot has to devote some of his available effort to maintaining lateral and directional control then he has less effort available for longitudinal control. This means that his overall ability to maintain longitudinal control will be a function of the longitudinal stability, the other aircraft handling qualities, the additional flight deck activities and his individual pilot experience and personal ability.

It is not possible to quantify the individual pilot ability in simple terms, neither is there any simple and convenient means of assessing the influence of the lateral and directional handling qualities

on the longitudinal handling qualities. This influence is transferred through the pilot and is likely to be further complicated by the human element in the transfer function. The longitudinal handling should therefore be treated on its own as a critical handling quality of the aircraft, and a reasonable limit set on the magnitude of some parameter which will ensure that an average pilot will be able to maintain control under reasonable flight conditions.

The airworthiness requirements relating to handling, ref.4, do not generally consider other than smooth air conditions and steady flight between airspeed limits, generally 1.2 times the stalling speed and the maximum design speed in the configuration considered. Within these considerations the usual limit accepted for the longitudinal handling qualities is determined by the pitch stiffness being "not less than zero". This is based on the measured static stability of the aircraft, determined by the slope of trim curves, showing that the aircraft will not be divergent.

According to the classical theory of static stability using a simple, linearised model of the aircraft the trim curves should be linear which implies a constant pitch stiffness at all values of incidence for a particular C.G. location. This result may influence the interpretation of measured trim data and lead to a constant value of pitch stiffness being accepted whereas a more detailed examination would reveal that the measured data describes a curve indicating a variable pitch stiffness with incidence. The curvature may arise from design features of the aircraft which produce handling characteristics which vary with incidence. It is important to know the source of such variations and the likely contribution to the static stability so that the effect can be allowed for in the aircraft design.

In the investigation of the handling qualities of a light twin engined aircraft it was noticed that the static stability trim curves were non-linear and the general level of static stability was very much lower than the simple theory predicted. The non-linearity indicated that the aircraft would tend to become less stable as C_L increased, the effect increasing as power increased. It appeared that at aft C.G. loadings with high power the static stability could approach zero as speed was reduced. The class of aircraft under test is typically used for training purposes and may be flown by relatively inexperienced pilots. The danger of an aircraft which is

inherently unstable under low speed - high power conditions is that these are among the worst conditions for an inexperienced pilot to cope with since the aircraft is approaching a power on stall.. If the speed is allowed to become too low and power is applied for recovery the handling will become very light and the aircraft may demand an unusual pilot skill for recovery. In the case of the inexperienced pilot this may lead to excursions of speed and height beyond reasonable limits and an excessive recovery time during which the aircraft is at risk. The study of the trim curves to determine the reasons for the destabilisation and non-linearity was considered to be a worthwhile exercise if it could predict such handling qualities.

Normally the instrumentation used for the measurement of the static stability of a light aircraft is very basic. The quality of the flight test data is low and may be insufficiently good to show any non-linearity effectively; only a general level of static stability can be demonstrated. To determine the trim curves more accurately requires a very much more sophisticated instrumentation system. The aircraft used for the flight trials was extensively instrumented for handling qualities investigation (ref.2) and included trace recording of the flight data. This enabled the data to be inspected for quality and steady state conditions verified at the point of data acquisition. Using this system showed the trim curves to have some non-linear tendencies but as there were still some data points which showed experimental errors it was not possible to make an absolute definition of the trim curves. It was necessary to analyse the aircraft theoretically to determine its static stability and to compare it with the measured flight data to verify the analysis. In this thesis the development of a more complete aircraft model is described and used to show that it is possible to predict the trim curves with a good degree of precision.

Initially the approach was to consider the known deficiencies of the simple theory model of the aircraft and to develop individual corrections to the pitching moment equation to account for each in turn. In this way it was possible to develop the theory for the corrections and to assess their effect, in isolation, on the longitudinal static stability trim curves. The development of the individual corrections forms Part II of the thesis.

The complete model of the aircraft could then be built up using the expressions developed for individual corrections in the pitching moment equation and lift equation and solved for the trim condition in terms of incidence and elevator angle. The process is described fully in section 5. From the solution the trim curves can be constructed and compared with the measured flight data.

2. A Determination of the Stability Criteria

A full analysis of the motion of an aircraft following a disturbance is not always necessary to show whether or not the aircraft is stable. It is possible to examine the full analysis to determine the criteria for stability and then to find a simple means of showing that the criteria can be satisfied.

2.1 The Conditions for Stability

The equations of motion of a conventional aircraft in its plane of symmetry can be written in their non-dimensional form, (Ref 3. eqns 7.70-7.74), as

$$\frac{d\hat{u}}{d\tau} - \left\{\hat{u}x_u + \hat{w}x_w + \frac{d\theta}{d\tau}\,x_q\right\} + \tfrac{1}{2}C_L\theta = \Delta\eta x_\eta \qquad (2.1)$$

$$\frac{d\hat{w}}{d\tau} - \left\{\hat{u}z_u + \hat{w}z_w + \frac{d\theta}{d\tau}\,(1 + \frac{z_q}{\mu_1})\right\} + \tfrac{1}{2}C_L\theta\tan\Theta = \Delta\eta z_\eta \qquad (2.2)$$

$$\frac{d^2\theta}{d\tau^2} - \left\{\mu_1\hat{u}m'_u + \mu_1\hat{w}\,m'_w + \mu_1\frac{d\hat{w}}{d\tau}\,m'_{\dot{w}} + \frac{d\theta}{d\tau}\,m'_q\right\} + 0 = \mu_1\Delta\eta m'_\eta \qquad (2.3)$$

In the controls fixed sense the elevator disturbance $\Delta\eta$ is zero and the equations can be solved by the substitution

$$\hat{u} = \rho_1 e^{\lambda\tau}, \quad \hat{w} = \rho_2 e^{\lambda\tau} \quad \text{and} \quad \theta = \rho_3 e^{\lambda\tau},$$

where ρ_1, ρ_2 and ρ_3 and λ are constants.

For a low speed conventional aircraft the derivatives m'_u and z_q/μ_1 are negligible, the controls fixed equations give rise to the determinantal equation

$$\begin{vmatrix} \lambda - x_u & -x_w & \tfrac{1}{2}C_L \\ -z_u & \lambda - z_w & -\lambda + \tfrac{1}{2}C_L\tan\theta \\ 0 & -\mu_1 m'_{\dot{w}}\lambda - \mu_1 m'_w & \lambda^2 - m'_q\lambda \end{vmatrix} = 0 \qquad (2.4)$$

Expansion produces a quartic equation in λ which can be written

$$\lambda^4 + B_1\lambda^3 + C_1\lambda^2 + D_1\lambda + E_1 = 0,$$

in which the coefficients B_1, C_1, D_1 and E_1 are given by

$$B_1 = -(x_u + z_w) - m'_q - \mu_1 m'_{\dot{w}} \tag{2.5}$$

$$C_1 = (x_u z_w - x_w z_u) - \mu_1 m'_w + (x_u + z_w) m'_q + \mu_1 m'_{\dot{w}} (x_u + \frac{C_L}{2} \tan\Theta) \tag{2.6}$$

$$D_1 = \mu_1 m'_w (x_u + \frac{C_L}{2} \tan\Theta) - m'_q (x_u z_w - x_w z_u) + \mu_1 m'_{\dot{w}} \frac{C_L}{2} (z_u - x_u \tan\Theta) \tag{2.7}$$

$$E_1 = \frac{C_L}{2} \mu_1 m'_w (z_u - x_u \tan\Theta) \tag{2.8}$$

Equations (2.5) to (2.8) represent the quartic coefficients in their simplest form.

For a conventional aircraft the coefficients D and E are usually small compared with C and the quartic can be approximately factorised into the form

$$(\lambda^2 + B_1\lambda + C_1)(\lambda^2 + \frac{C_1 D_1 - B_1 E_1}{C_1{}^2} \cdot \lambda + \frac{E_1}{C_1}) = 0 \tag{2.9}$$

where the first quadratic contains a pair of large complex roots describing a short period heavily damped oscillation and the second quadratic contains a pair of small complex roots describing a long period lightly damped oscillation, the phugoid.

The simplest set of requirements for stability can be shown to be

$$B_1 > 0 \tag{2.10}$$

$$D_1 > 0 \tag{2.11}$$

$$E_1 > 0 \tag{2.12}$$

and $$R = B_1 C_1 D_1 - B_1{}^2 E_1 - D_1{}^2 > 0 \tag{2.13}$$

where R is known as Rouths Discriminant,(Ref.3 eqns 9.38 - 9.41).

Normally B_1 and D_1 will be positive leaving $E_1 > 0$ and $R > 0$ as the critical requirements, although R will generally be positive.

Eqn (2.8) can be written in the form

$$E_1 = -\frac{C_L{}^2}{2} \mu_1 m'_w (1 - \frac{x_u}{z_u} \tan\Theta) \tag{2.14}$$

since $z_u \doteq -C_L$

Also $x_u \doteq -C_D$, and the angle between the undisturbed body axis and the horizontal, Θ, will not generally be large thus tan Θ will be less than unity. Since x_u/z_u is approximately the drag/lift ratio of the aircraft this too will be small and the bracket in eqn.2.14 will be positive. This implies that the sign of E_1 depends only on the sign of m_w' and therefore if m_w' becomes positive the quadratic representing the phugoid, eqn (2.9), will have a real, positive root representing a divergence. The derivative m_w' is therefore critical since it is capable of producing an instability if it is allowed to become positive.

2.2 The Derivative m_w, Static Stability

Since m_w determines the sign of E_1, and hence the roots of the stability quartic, it is necessary to find a test for m_w to determine its magnitude and sign. From the equations of motion the pitching moment equation (2.3) can be considered under steady flight conditions, which are

$$\frac{d^2\theta}{d\tau^2} = \dot{q} = 0 \qquad (2.15)$$

$$\frac{d\hat{w}}{d\tau} = 0 \qquad (2.16)$$

and

$$\frac{d\theta}{d\tau} = q = 0 \qquad (2.17)$$

When these conditions are applied eqn.(2.3) gives the trim condition in which the overall pitching moment is zero, thus

$$-\mu_1 \alpha m_w' = \mu_1 \bar{\eta} m_\eta'$$

since $m_u' = 0$ and $\hat{w} = \alpha$. The elevator angle $\bar{\eta}$ is the elevator angle necessary to maintain zero pitching moment at that particular incidence.

The rate of change of elevator angle to trim with incidence will determine the value of m_w',

$$-m_w' = m_\eta' \frac{d\bar{\eta}}{d\alpha} \qquad (2.18)$$

If a curve of elevator angle to trim, $\bar{\eta}$, against incidence, α, is drawn then the slope of the curve will be proportional to the value of m_w. Using the conclusions of section 2.1, the trim curve slope $d\bar{\eta}/d\alpha$ is therefore an indicator of aircraft longitudinal stability since the sign of m_w is the criterion of stability.

It is usual to consider the slope of the curve of $\bar{\eta}$ against C_L since the flight lift coefficient is normally more easily measured than incidence,

$$\frac{d\bar{\eta}}{d\alpha} = \frac{d\bar{\eta}}{dC_L} \cdot \frac{dC_L}{d\alpha} \qquad (2.19)$$

If the $C_L - \alpha$ characteristic of the aircraft is linear this does not affect the value of m_w estimated from the trim curve slope. However in the full model of the aircraft the propeller and its slip-stream will both contribute to the lift of the aircraft and the trim incidence will therefore be a function of power. This will cause the $C_L - \alpha$ characteristic to be generally non-linear and the value of m_w estimated from the trim curve slope will be a function of incidence.

If the non-linearity is small then the now non-linear trim equations can be assumed to be quasi-linear, (i.e. of the same form as eqns 2.1 to 2.3), and solved in terms of trim incidence to give the value of the derivative m_w at specified values of incidence.

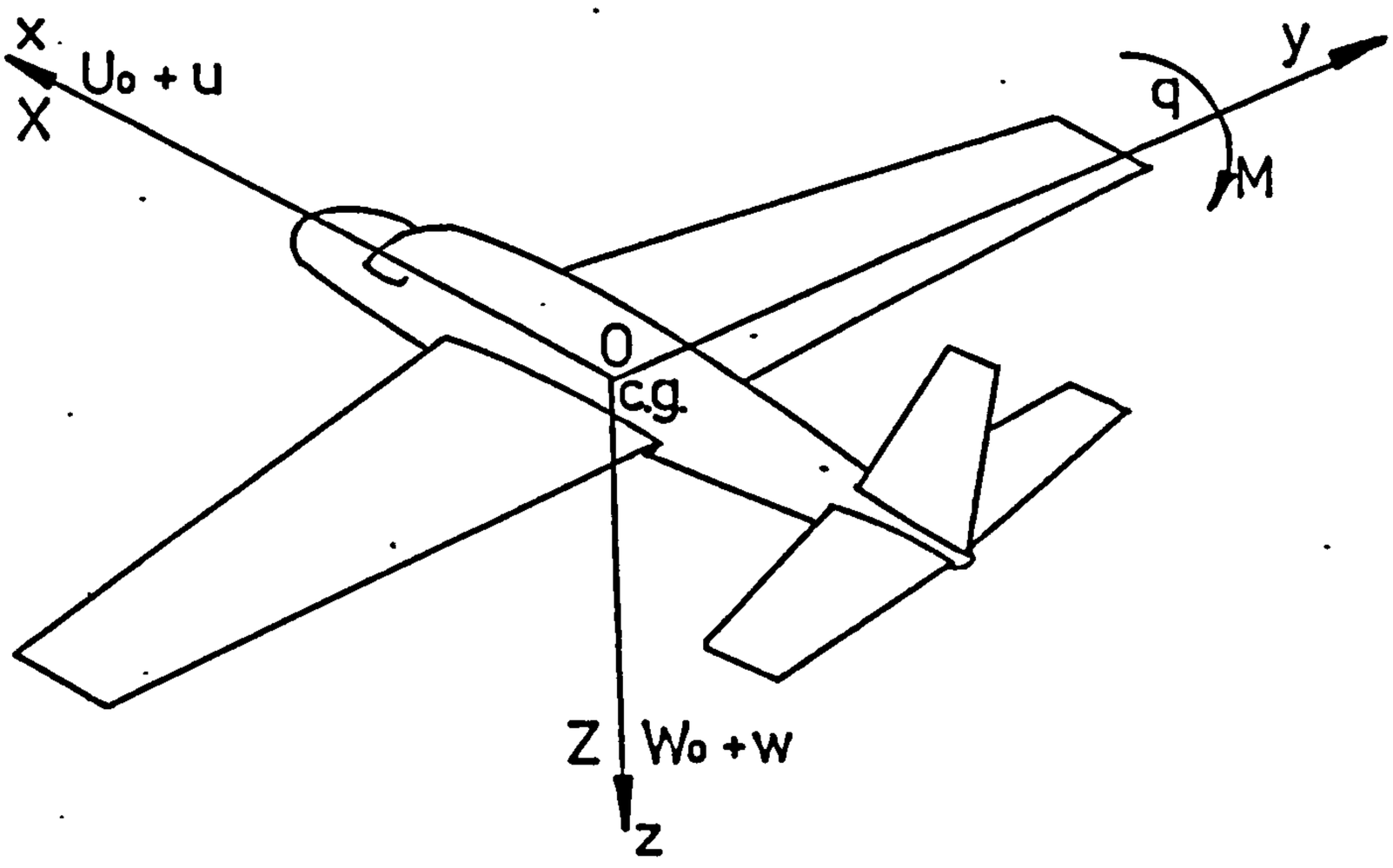

FIG.2.1. Notation for Body Axes in Symmetric Flight

3. Measurement of Longitudinal Trim Curves

The trim curves which are used to determine the static stability of an aircraft are measured by flying the aircraft under steady speed trim conditions and measuring the elevator control position, $\bar{\eta}$, and hinge moment, $\bar{C}_H$, to trim. These quantities are then plotted against flight lift coefficient, C_L, to produce curves of $\bar{\eta}$ against C_L and $\bar{C}_H$ against C_L, the slopes of which determine the levels of static stability.

The instruments available to the pilot to establish the steady flight conditions are his airspeed indicator and altimeter together with a visual reference to the natural horizon and physical sensation of sideslip and normal acceleration. The airspeed indicator reading (A.S.I.R.) must be corrected for instrument error, system pressure error and scale altitude error to give the equivalent airspeed, V_e. At a steady speed (A.S.I.R.) the instrument error will be constant and the maximum error should be small, less than 2 kts, also the rate of change of error with indicator speed should also be small so that a negative rate of change cannot cancel out an acceleration. These conditions can generally be met by selecting an instrument with a suitable calibration characteristic for the test aircraft. The system pressure error is an incidence dependant quantity and therefore under steady flight (α constant) this should be constant. It is desirable to have a small pressure error correction and to avoid those of high negative slope, $d(\Delta V_R)/dV_R$, which may reduce the apparent acceleration of the aircraft. The scale altitude correction is generally very small at speeds less than 200 kts below 10,000ft and the rates of change involved with light aircraft operations may be safely disregarded.

The airspeed can therefore be considered in the form

ASIR + Inst.Error Corr. + System P.E.C. + Scale Alt.Corr. = Ve

and for a suitable system the errors will be constant thus

$$\frac{d}{dt}(\text{ASIR}) = \frac{d}{dt}(\text{Ve}) \qquad (3.1)$$

for small rates of change.

It can therefore be considered that if the pilot flies at a steady indicated airspeed the equivalent airspeed will also be steady.

The same analysis can be applied to the altimeter readings to relate the indicated altitude, I alt, to pressure altitude H_p

$$\text{I.Alt} + \text{Inst.Corr.} + \text{System P.E.C.} = H_p$$

By similar reasoning for a steady flight state,

$$\frac{d}{dt}(\text{I.alt}) = \frac{d}{dt}(H_p) \qquad (3.2)$$

The true rate of change of height will be a function of the temperature of the atmosphere and the I.S.A. standard temperature at the same altitude. A correction to true rate of change of height dH/dt is given by the approximation,

$$\frac{dH}{dt} = \frac{dH_p}{dt} \times \left(\frac{\text{temperature at test altitude}}{\text{I.S.A.temp at test altitude}}\right)$$

thus the true vertical velocity dH/dt is proportional to the indicated rate of change of altitude.

The other pilot indications are subjective, relying on the pilots interpretation of observed external reference or physical stimulus to indicate a steady state. Observation of the natural horizon is often accepted as a good indication of a constant pitch attitude although a combination of heaving and pitching motions can produce a constant indication of attitude in a non-steady flight condition. This implies that the observed pitch attitude is not reliable as an indication of steady state in the short term although long term heaving or pitching will become obvious as speed and height changes. Sideslip and normal acceleration sensed by the pilot through the 'seat of the pants' should not be considered as reliable data due to the inherent inability to calibrate the sensor involved.

Steady state flight should be defined to the pilot by indications from calibrated flight instruments which implies the determination of the flight conditions in terms of indicated airspeed and altitude and an engine power condition.

3.1 Flight conditions to guarantee 'steady state"

To give a true steady flight state the net forces acting at the C.G. and moment about the C.G. must be zero. This condition is met by the simultaneous, and continuous, solution of the statements

$$\Sigma F_x = m\dot{V} = 0$$
$$\Sigma F_z = mV\dot{\gamma} = 0 \qquad (3.3)$$

and $\Sigma M_y = I_y \dot{q} = 0$ (3.3)

The flight conditions which satisfy the statements,

$$\dot{V} = 0$$
$$V\dot{\gamma} = 0 \quad (3.4)$$
$$\dot{q} = 0,$$

will therefore produce a true steady state.

3.1.1. Longitudinal acceleration $\dot{V}$ (parallel to flight path)

Since the pilot has only indications of altitude and airspeed $\dot{V}$ must be written in terms of these quantities. It will be assumed that the indicated airspeed is equal to the equivalent airspeed plus a constant error, see section 3.

$$Ve = IAS + \Delta V_R$$

such that

$$\frac{dVe}{dt} = \frac{d(IAS)}{dt}$$

$$\dot{V} = \frac{dV}{dt} = \frac{d}{dt}\left(\frac{Ve}{\sigma^{1/2}}\right)$$

$$= \frac{1}{\sigma^{1/2}}\frac{dVe}{dt} - \frac{1}{2}\frac{Ve}{\sigma^{3/2}}\frac{d\sigma}{dt}$$

$$= \frac{1}{\sigma^{1/2}}\left\{\frac{dVe}{dt} - \frac{1}{2}\frac{Ve}{\sigma}\frac{d\sigma}{dH}\frac{dH}{dt}\right\}$$

$$\text{thus, } \frac{dV}{dt} = \frac{1}{\sigma^{1/2}}\left\{\frac{dVe}{dt} - \frac{1}{2}\frac{Ve^2}{\sigma^{3/2}}\frac{d\sigma}{dH}\gamma\right\} \quad (3.5)$$

The condition for steady flight is thus met if $\frac{dVe}{dt} = 0$ and $\gamma = 0$, which is indicated to the pilot by steady indicated speed and altitude.

3.1.2. Normal Acceleration $V\dot{\gamma}$ (normal to flight path)

$$V\dot{\gamma} = V\frac{\partial\gamma}{\partial t} = V\frac{\partial}{\partial t}\left(\frac{1}{V}\frac{\partial H}{\partial t}\right)$$

thus $$V\dot{\gamma} = \frac{\partial^2 H}{\partial t^2} - \gamma\frac{\partial V}{\partial t} \qquad (3.6)$$

The condition is satisfied by $\frac{\partial V}{\partial t} = 0$ and $\frac{\partial^2 H}{\partial t^2} = 0$

This implies that the steady condition requires $\frac{\partial Ve}{\partial t} = 0$ and $\gamma = 0$ from 3.1.1. and that the vertical acceleration $\frac{\partial^2 H}{\partial t^2} = 0$, or 1g flight conditions.

3.1.3. Acceleration in pitch about the C.G., $\dot{q}$

The pitch acceleration $\dot{q}$ is given by $\frac{d^2\theta}{dt^2}$ where

$$\theta = \alpha + \gamma,$$

thus

$$\dot{q} = \frac{d^2\alpha}{dt^2} + \frac{d^2\gamma}{dt^2}$$

From the lift incidence characteristic of the aircraft the incidence α can be defined as

$$\alpha = L / \tfrac{1}{2}\rho_o Ve^2 Sa$$

and the lift given by

$$L = W\cos\gamma + Zp$$

where Zp is the propeller normal force

hence
$$\alpha = \frac{W\cos\gamma}{\tfrac{1}{2}\rho_o Ve^2 Sa} + \frac{Zp}{\tfrac{1}{2}\rho_o Ve^2 Sa}$$

Differentiating with respect to time to give $\ddot{\alpha}$,

$$\ddot{\alpha} = \frac{1}{a}\left\{C_L\cos\gamma\,\frac{1}{W}\frac{\partial^2 W}{\partial t^2} - C_Z\frac{D^2N}{S}\,\frac{1}{Z_p}\,\frac{\partial^2 Zp}{\partial t^2} - C_L\cos\gamma\,\frac{\partial^2\gamma}{\partial t^2}\right.$$

$$\left. + (C_L\cos\gamma - C_Z\frac{D^2N}{S})\,\frac{6}{Ve^2}\,\frac{\partial}{\partial t}\left(\frac{\partial Ve}{\partial t}\right)\right\}$$

where $C_L = W/\tfrac{1}{2}\rho_o Ve^2 S$ and $C_Z = Z_p/\tfrac{1}{2}\rho_o Ve^2 D^2$

Now $\frac{\partial W}{\partial t} = Q_f$, the fuel flow rate, thus

$$\ddot{\alpha} = \frac{1}{a}\left\{\left[C_L \cos\gamma \frac{1}{W} \frac{\partial Q_f}{\partial t} - C_Z \frac{D^2N}{S} \frac{1}{Z_p} \frac{\partial^2 Z_p}{\partial t^2}\right] - C_L \cos\gamma \cdot \ddot{\gamma}\right.$$

$$\left. + \left(C_L \cos\gamma - C_Z \frac{D^2N}{S}\right) \frac{6}{Ve^2} \frac{\partial}{\partial t}\left(\frac{\partial Ve}{\partial t}\right)\right\} \qquad (3.7)$$

The second derivative of γ with respect to time is given by

$$\ddot{\gamma} = \frac{1}{V} \frac{\partial^3 H}{\partial t^3} - \frac{2}{V^2} \frac{\partial^2 H}{\partial t^2} \frac{\partial V}{\partial t} + \frac{2}{V} \frac{\partial H}{\partial t} \frac{\partial^2 V}{\partial t^2} \qquad (3.8)$$

Thus from (3.7) and (3.8) the condition for $\dot{q} = 0$ is given by either

$\ddot{\alpha} = 0$ and $\ddot{\gamma} = 0$,

or $\ddot{\alpha} = -\ddot{\gamma}$

The latter condition will however require a rate of climb or acceleration to be present, since $\ddot{\gamma} \neq 0$, and is therefore not compatible with conditions 3.1.1 and 3.1.2.

The condition $\ddot{\gamma} = 0$ requires that the first and second derivatives of true airspeed and altitude with respect to time are zero, if this is true then it is reasonable to assume that the third derivative of height with respect to time will also be zero. This implies a constant T.A.S. and zero rate of climb.

The condition $\ddot{\alpha} = 0$ implies a constant E.A.S. such that $\frac{\partial Ve}{\partial t} = 0$, and hence $\frac{\partial}{\partial t}\left(\frac{\partial Ve}{\partial t}\right) = 0$, this requires both constant T.A.S. and $\gamma = 0$ from 3.1.1.

Since the fuel flow Q_f is a function of power and the propeller normal force Z_p is also a power dependent term the terms in the square bracket of eqn.3.7 will only be zero if the power is constant, thus an additional requirement is for a constant engine power setting during the trim if $\ddot{\alpha}$ is to be zero.

3.1.4 Engine Power Characteristic

The power developed by a piston engine can be shown to be a function of the pressure and temperature of the ambient atmosphere, ref.2, and expressed in the form

$$P = P_o \left[\frac{pi - pe/c}{T + 127}\right]_{test} \left[\frac{T + 127}{p_i - pe/_c}\right]_{I.S.A.,SL} \qquad (3.9)$$

where P = power output and P_o the sea level ISA reference power,
pi = inlet manifold pressure
pe = exhaust back pressure
c = cylinder compression ratio, and
T = static air temperature, ^oK.

The exhaust back pressure can be considered to be equal to atmospheric pressure and the manifold pressure to be proportional to atmospheric pressure for a fixed throttle setting, thus (3.9) can be written in the form

$$P = p^{\frac{(r - 1/c)}{T + 127}} Po$$

(the constant 127^o is the assumed temperature rise between the free air and the inlet valve of the engine, r is the pressure ratio p_i/p).

If it is assumed that the airspeed produces no supercharging effect on the inlet pressure then the variation of power with time can be expressed as

$$\frac{dP}{dt} = Po \left[\frac{(r - 1/c)}{(T + 127)} \frac{\partial p}{\partial t} - \frac{p(r - 1/c)}{(T + 127)} \frac{\partial T}{\partial t} \right] \left[\frac{T + 127}{pi - pe/c} \right] S.L.$$

therefore,

$$\frac{dP}{dt} = P \left[\frac{1}{p} \frac{\partial p}{\partial H} - \frac{A}{(T + 127)} \right] \frac{\partial H}{\partial t} \qquad (3.10)$$

where A is the temperature lapse rate of the atmosphere, dT/dH. The general condition for constant power is therefore level flight since the bracket will only be zero for very particular atmospheric characteristics.

3.2 Summary of Conditions for Steady Flight

A true condition of steady flight can only be given by simultaneously satisfying the following conditions.

i) Constant E.A.S., from constant indicated airspeed, eqns.3.1 and 3.5,
ii) Zero flight path angle γ, or indicated altitude constant from eqns. 3.2 and 3.5, and
iii) Constant engine power, indicated by constant manifold pressure and engine speed together with constant indicated altitude, from eqns. 3.7 and 3.10 and condition ii) above.

4. Practical Flight Conditions for Measurement of Trim Curves.

In practice the measurement of the trim curves will be made under the best approximation possible to the required state described in section 3.2. The assessment of the conditions is made by the pilot, and possibly the flight observer, at the time of the test and will assume the constraints put on the pilot by the conditions of the test, for example a constant engine power setting. The final compliance will depend on the instrumentation available for the test; if only a minimum instrumentation is available, (airspeed indicator, altimeter and external visual cues), then the pilot can only assume that the conditions of section 3.2 are acceptable when his indicators are steady and no angular rotation in pitch is apparent. If an extensive instrumentation fit is available then the airspeed, altitude, incidence, pitch attitude and normal acceleration can be recorded and data collected over a period of several seconds. The record can then be used to ascertain the steady state and the data collected from that point.

The tests considered in this analysis were for the purpose of measuring the propeller slipstream at the tail and assessing its effect on the static stability of the aircraft which constrained the flight conditions to a large degree. Previous flying had shown that some slipstream effects of power on the trim curves could be expected and the flight conditions were arranged to produce trim curves under the influence of a known power condition. Since the power was the important parameter in the tests it was decided to keep the power constant and to accept a steady flight path gradient at constant indicated airspeed. Since for the class of aircraft considered the flight path gradient, γ, would not be large, any errors in the conditions for steady flight would be acceptably small. From section 3.1, the value of the errors can be estimated.

4.1 Error in $\dot{V}$ due to flight path gradient γ

From eqn (3.5) the acceleration of the aircraft is given by

$$\frac{dV}{dt} = \frac{1}{\sigma^{1/2}} \frac{\partial Ve}{\partial t} - \frac{Ve^2}{2\sigma^2} \frac{\partial \sigma}{\partial H} \gamma \qquad (4.1)$$

Thus if a steady equivalent airspeed is maintained the error in the acceleration is given by

$$\frac{\Delta dV}{dt} = -\frac{Ve^2}{2\sigma^2} \quad \frac{\partial \sigma}{\partial H} \quad \gamma \tag{4.2}$$

From the model of the standard atmosphere the relative pressure δ is given by

$$\delta = \left[1 + \frac{AH}{T_o}\right]^{-g_o/AR} \tag{4.3}$$

and for an adiabatic process

$$\delta = \sigma^{\gamma} \tag{4.4}$$

thus from (4.3) and (4.4)

$$\sigma = \left[1 + \frac{AH}{T_o}\right]^{-g_o/AR\gamma} \tag{4.5}$$

$$\text{Thus } \frac{\partial \sigma}{\partial H} = -\frac{g_o}{R\gamma T_o}\left[1 + \frac{AH}{To}\right]^{-(g_o/AR\gamma)-1} \tag{4.6}$$

Numerically this is given by

$$\frac{\partial \sigma}{\partial H} = -0.0000258\ [\ 1 - 0.00000687\ H\ ]^{2.76}$$

and evaluating for sea level and 10,000 ft gives

$$\frac{\partial \sigma}{\partial H} = -0.0000258 \text{ at Sea level}$$

$$\frac{\partial \sigma}{\partial H} = -0.0000212 \text{ at 10,000 ft}$$

From (4.2) the error in acceleration can be assessed for typical speeds and altitudes and assuming a rate of climb of 1,000 ft/min which would be the worst case possible.

Speeds E.A.S. Kts		100	200
Acceleration error	S.L.	0.0363	0.0725
$\Delta\dot{V}$, ft/sec^2	10,000 ft.	0.0471	0.0895
Thrust Error lbf	S.L.	4.0	8.1
(Aircraft weight 3600 lbf)	10,000 ft.	5.3	10.0
Equivalent Horse Power	S.L.	1.23	4.98
Error	10,000 ft	1.62	6.13

TABLE 1

This indicates that the maximum errors which are likely to be encountered by allowing a rate of climb will be equivalent to a thrust error of less than 10 lbf. or approximately 3% of the drag.

4.2 Error in $V\dot{\gamma}$ due to flight path gradient γ

From eqn (3.6) the vertical acceleration of the aircraft is given by

$$V\dot{\gamma} = \frac{\partial^2 H}{dt^2} - \gamma \frac{\partial V}{\partial t} \tag{4.7}$$

If γ is steady then $\frac{\partial^2 H}{\partial t^2}$ is zero and the error in normal acceleration becomes

$$\Delta V\dot{\gamma} = -\gamma \quad \Delta\frac{\partial V}{\partial t} \tag{4.8}$$

and from (4.2) this can be written

$$\Delta V\dot{\gamma} = \frac{Ve^2}{2\sigma^2} \quad \frac{\partial \sigma}{\partial H} \quad \gamma^2 \tag{4.9}$$

which from (4.7) gives a normal acceleration and lift force error based on a 1,000 ft/min rate of climb.

Speed E.A.S.kts		100	200
Normal Acceleration error, ft/sec^2	S.L.	0.00358	0.00357
	10,000 ft.	0.00583	0.00555
Lift Force Error lbf (Aircraft weight 3600 lbf)	S.L.	0.40	0.40
	10,000 ft.	0.65	0.62

Table 2

This error is negligibly small for all cases

4.3 Error in $\dot{q}$ due to flight path gradient γ

In section 3.1 it is seen that the primary cause of any change in $\dot{q}$ is the change of power with height. Eqn 3.10 shows the rate of change of power with time to be given by

$$\frac{dP}{dt} = P\left[\frac{1}{p} \frac{\partial p}{\partial H} - \frac{A}{(T + 127)}\right] \frac{\partial H}{\partial t} \tag{4.10}$$

From the model of the standard atmosphere the pressure is related to the geopotential height by the relationship

$$p = p_o \left[1 + \frac{AH}{To} \right]^{- g_o/AR}$$

thus

$$\frac{\partial p}{\partial H} = \frac{-g_o p_o}{RT_o} \left[1 + \frac{AH}{T_o} \right]^{(-g_o/AR) - 1} \qquad (4.11)$$

Thus the rate of change of power with height can be expressed as

$$\frac{dP}{dt} = P \left\{ \frac{-g_o p_o}{pRT_o} \left[1 + \frac{AH}{T_o} \right]^{(-g_o/AR)-1} - \frac{A}{(T + 127)} \right\} \frac{dH}{dt} \qquad (4.12)$$

and evaluating this for sea level and 10,000ft I.S.A. conditions and a rate of climb of 1000 ft/min gives

	Sea level	10,000ft	
$\frac{dP}{dt}$ =	-0.00068	-0.001255	H.P./H.P./Sec

or a power change of 1% in 15 secs at sea level or 8 secs at 10,000ft at that rate of climb.

A power change of this magnitude will not cause a sufficient rate of change in fuel flow or normal force to alter $\ddot{\alpha}$ and hence $\dot{q}$ to any significant degree.

4.4 Acceptability of Test Conditions

From these errors it can be concluded that for normal light aircraft a test conducted under constant power and steady speed conditions, and allowing a rate of climb or descent to occur, will not be significantly in error with respect to the ideal conditions of section 3. The constraints placed on the test procedure are therefore acceptable for the purpose considered; that is to provide a basis for the measurement of static stability trim curves for the verification of the theoretically derived curves.

During the flight tests more data than the minimum necessary were recorded so that steady state conditions could be established. The channels of data recorded on the trace record were:- Elevator angle, Elevator stick force, Elevator tab trim setting, normal acceleration and airspeed.

The elevator angle and stick force together with the airspeed gave the basic data from which the trim curves were drawn. The elevator tab trim setting established that the tab was at the same setting for each set of data and remained constant through the test run. This parameter was also fed to a visual display for the purpose of setting up the test conditions. The normal acceleration trace was used to establish steady flight conditions under 1g loading and free from turbulence. As no pitch attitude or incidence information was available at the time the fact that steady speed and 1g normal acceleration were held for several seconds was accepted as a good enough test for steady flight. The weight of the aircraft could be determined reasonably accurately from the total fuel burned during the test flight, the fuel state being accepted as proportional to the time of flight. Since the aircraft only consumed about 100 lbs of fuel per hour the error involved in this estimate was very small.

During the flight at constant power and varying speed a climb or descent is inevitable. An effort was made to maintain the test altitude limits to a band of not more than 3000 ft, i.e. ±1500 ft about the datum. Most of the data was collected well within these limits.

The tests were conducted at several engine power conditions from flight idle to maximum continuous power, (climb power). In Part II section 2 it is seen that at the very low powers the propeller slip-stream could not be adequately simulated since the propeller changed from a thrust producer to a windmill and there is no way of estimating the power absorption of the engine under these conditions. The analysis was therefore limited to the three power settings normally used for flight. These are summarised in table 4.1.

Power Condition	Boost/RPM	Shaft H.P.	Thrust H.P.
Approach power	15"/2400	65	56
Cruise power	20"/2400	100	84
Climb power (M.C.P.)	24"/2400	120	99

TABLE 4.1

The engine powers were calculated from observed manifold boost pressure (ins Hg), engine rotational speed (R.P.M.) and atmospheric data using the engine manufacturers standard engine curves, ref.8. The shaft horsepower thus obtained was converted to thrust horsepower using such manufacturers data as could be obtained for propeller efficiency updating this from Part II section 3 as necessary.

The weight and C.G.location of the aircraft prepared for flight, zero fuel and no crew, was established by weighing the aircraft. The flight weight and C.G. at the time of test were calculated from the crew weight and seat location and the mid flight fuel weight. Since the fuel was in wing tanks disposed approximately at the C.G. the shift of C.G. with fuel state was minimal. In one hour the C.G. shift would be less than 0.1 ins (or 0.15%$\bar{c}$). This rate of change can be regarded as negligible on a flight lasting less than one hour. The maximum effect, shown above, is felt at forward C.G.; at aft C.G. the rate of change of C.G. with fuel is almost zero.

5. Simple Linear Theory Prediction of Static Stability

In the simple theory of static stability the aircraft is reduced to two lifting surfaces, one representing the wing, fuselage and nacelles and the other representing the tail, fig.5.1.

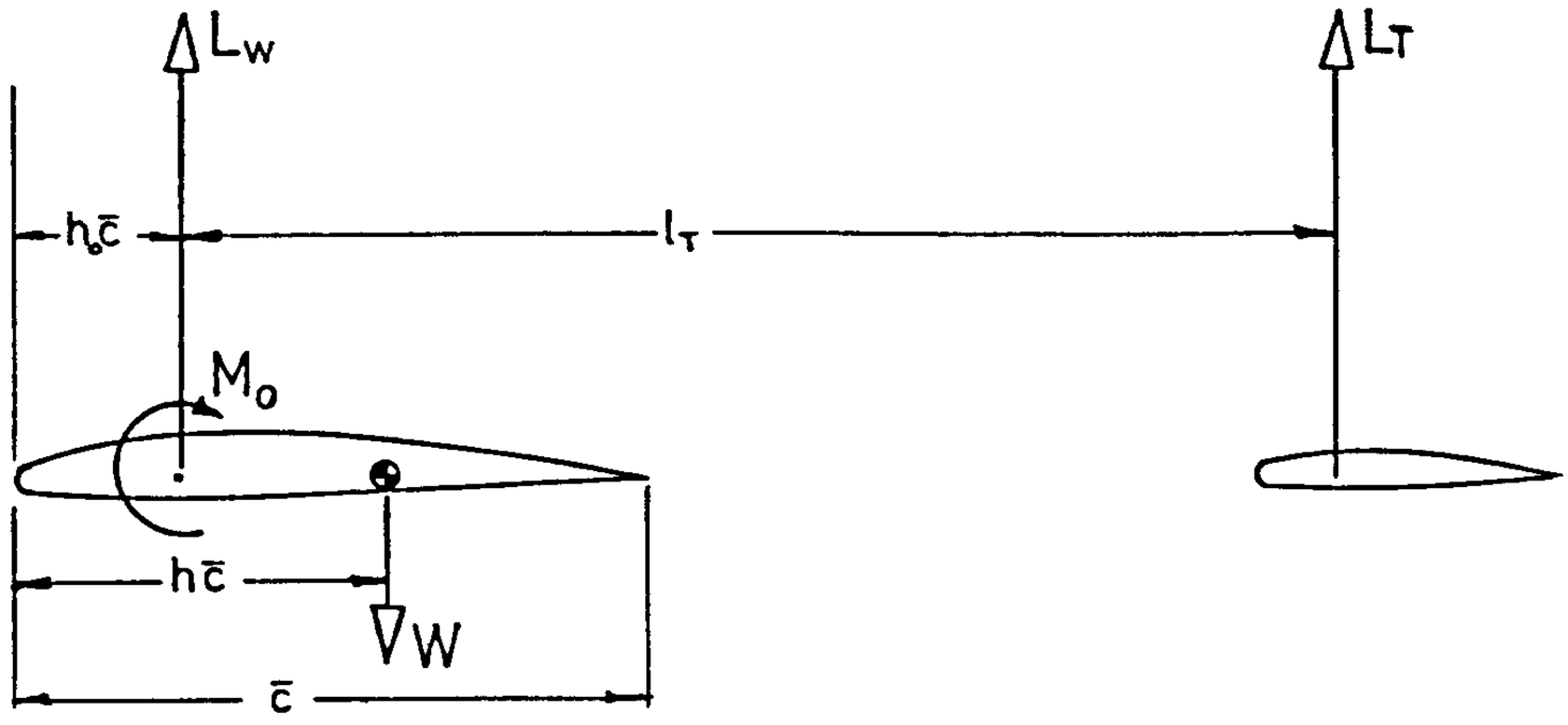

Fig.5.1 Simple Model of Aircraft

By considering the pitching moments about the C.G. of the aircraft model the well known pitching moment equation can be found, (Ref.3.ch.3 and Ref.9.Chs.4 and 5),

$$C_{mCG} = C_{mo} + C_L(h-h_o) - V_T\left\{\frac{a_1}{a}(1 - \frac{d\varepsilon}{d\alpha})C_L + a_1\eta_T + a_2\eta + a_3\beta\right\} \quad (5.1)$$

In the controls fixed condition η and β are constants and the differentiation of 5.1 with respect to incidence, α, gives the pitching moment derivative, m_w

$$\frac{dC_m}{d\alpha} = \frac{2l_r}{\bar{c}} m_w = a(h-h_o) - V_T a_1(1 - \frac{d\varepsilon}{d\alpha}) \quad (5.2)$$

By considering the pitching moment equation with the aircraft in trim, $C_{mCG} = 0$, then the elevator angle to trim, $\bar{\eta}$, can be expressed as

$$V_T a_2\bar{\eta} = C_{mo} + C_L(h-h_o) - V_T\left\{\frac{a_1}{a}(1 - \frac{d\varepsilon}{d\alpha})\, C_L + a_1\eta_T + a_3\beta\right\} \quad (5.3)$$

and the rate of change of elevator angle to trim with incidence, assuming that the trim tab angle, β, is fixed, is given by

$$V_T a_2\frac{d\bar{\eta}}{d\alpha} = a(h-h_o) - V_T a_1(1 - \frac{d\varepsilon}{d\alpha}) \quad (5.4)$$

By comparing eqns 5.2 and 5.4 it can be seen that the value of the pitching moment derivative, m_w, is given by

$$m_w = \frac{\bar{c}}{2l_T} V_T a_2 \frac{d\bar{\eta}}{d\alpha} \qquad (5.5)$$

and from eqns 5.5 and 2.18

$$m_\eta = -\frac{1}{2} \frac{S_T}{S} a_2$$

Using the result of eqn.2.19 eqn 5.5 can be written in terms of lift coefficient by dividing by the lift curve slope, $\frac{dCL}{d\alpha}$. Since in the linear model this is taken to be constant the value of m_w should not be affected,

$$m_w = \frac{\bar{c}}{2l_T} \frac{V_T a_2}{a} \frac{d\bar{\eta}}{dC_L}$$

This now shows the value of m_w to be proportional to the slope of the trim curve $\bar{\eta}$ against C_L, a negative slope indicating static stability. This form of trim curve is often more convenient for general use since the measurement of lift coefficient can be made from airspeed and weight thus avoiding the need to install and calibrate an incidence probe on the aircraft. Incidence is an unusual measurement to make on a light aircraft and particularly difficult in the case of a single engined aircraft on which a fuselage mounted probe is generally ruled out. Wing mounted probes are often subject to aeroelastic effects from the bending of the wing which can make the accurate determination of the indicated incidence very difficult.

5.1 Comparison with Measured Trim Curve Data

The linear theory pitching moment equation, eqn.5.1, can be used to estimate the elevator angle to trim. By using the estimated aerodynamic characteristics from table 6.2 the equation can be solved for $\bar{\eta}$ at the assumed trim condition $C_m = 0$. Evaluating eqn.5.1 using the values of the characteristics given in table 6.2 and the flight measured trim tab angle, -3.65^o, the elevator angle to trim is given by

Forward C.G. $\quad \bar{\eta} = -3.35\, C_L + 3.02$

Aft C.G. $\quad \bar{\eta} = -2.14\, C_L + 3.02$

Comparing these values with the measured trim curves shows that the estimated trim curve has a very much steeper slope than the measured data indicating that the actual static stability of the aircraft is far less than the estimated value. Fig.5.2 shows the comparison for the approach and climb power conditions.

Two other characteristics of the measured data are also evident, firstly the general slope of the measured trim curve is less at climb power than at approach power and, secondly that there is evidence to suggest that the trim curves in terms of C_L are not linear. Due to experimental scatter of the data the curvature is not initially obvious.

From the comparison of the estimated and measured trim curve data it is clear that there is a general reduction in the level of static stability which may be a function of the trimmed lift coefficient.

The simplified theory of static stability is inadequate in its description of the real aircraft since it neglects the effects of compressibility, aeroelasticity, slipstream, power and incidence all or any of which can lead to a non-linear trim curve characteristic and a change in the general level of static stability.

Returning to the conditions of stability, eqns.2.1 - 2.3, it is seen that for the aircraft to be in true trim three conditions must be simultaneously satisfied. They are that at any trim condition, all time dependent terms being zero,

$$\Sigma X = \Sigma Z = \Sigma M = 0 \qquad (5.6)$$

These can be written in coefficient form as

$$\bar{C}_D = \frac{W\sin\gamma}{\frac{1}{2}\rho V^2 S} = C_{D_{wfn}} + \frac{S_T}{S} C_{DT} + \frac{ND^2}{S}(Z_c \sin\alpha_p - T_c \cos\alpha_p)$$

$$\bar{C}_L = \frac{W\cos\gamma}{\frac{1}{2}\rho V^2 S} = C_{L_{wfn}} + \frac{S_T}{S} C_{L_T} + \frac{ND^2}{S}(Z_c \cos\alpha_p + T_c \sin\alpha_p) \qquad (5.7.)$$

$$\bar{C}_m = 0 = C_{m_o} + C_{m_{wfn}} + \frac{S_T}{S} C_{m_T} + \frac{ND^3}{Sc} M_c + (T_c z_p + Z_c h_p)\frac{ND^2}{S}$$

where $\bar{C}_L$, $\bar{C}_D$ and $\bar{C}_m$ are the trim conditions.

Now the wing, fuselage and nacelle contributions are functions of incidence, and possibly power; the tail contributions are functions of incidence and elevator angle; the propeller contributions are functions of incidence and forward speed. The simultaneous solution of 5.6 will therefore require a solution of trim equations 5.7 in terms of $\bar{\alpha}$ and $\bar{\eta}$, the trim incidence and elevator angle.

In the linearised theory of static stability the derivative m'_u is taken to be zero since compressibility and speed dependent terms are assumed negligible. The full expression for E_1, (see ref.3), is

$$E_1 = \frac{C_L}{2} \mu_1 [m'_w(z_u - x_u \tan\theta) - m'_u(z_w - x_w \tan\theta)] \quad (5.8)$$

This can be approximated to

$$E_1 = \frac{C_L^2}{2} \mu_1 [-m'_w + \tfrac{1}{2} m'_u \frac{a}{C_L}] = -\frac{C_L^2}{2} \mu_1 m'_{weff} \quad (5.9)$$

since $x_u << z_u$, $x_w << z_w$ and θ is small

m'_{weff} is an effective value of m'_w, see below.

The coefficient E_1 will therefore be influenced by the derivative m'_u which implies that the static stability criterion, E_1 positive, is a function of incidence and speed. Thus the static stability becomes a two parameter problem and requires definition in terms of incidence and speed.

The major part of the contribution to the speed dependent part of E_1 , m'_u, arises from the effects of power and slipstream, the remainder comes from compressibility which is small, see section 6.1. In the development of the slipstream and propeller direct force contributions to the pitching moment equation the flight conditions at

the time of test have been used. In this way incidence has been used as the prime variable and the speed dependent parameters expressed in terms of flight incidence and aircraft weight. The combined term in eqn.5.9 involving m'_w and m'_u can thus be considered to be a quasi-linear function of $\bar{\alpha}$ for a given aircraft weight and power. This approach enables the static stability to be considered as a function of incidence only. Strictly this requires that the forward and aft C.G. cases should be flown at the same all up weight so that the speed-incidence relationship is the same in each case and the power contribution should therefore be similar. The value of E_1 estimated under these conditions can be assumed proportional to $m'_{w.eff}$, an effective value of m'_w including the terms in m'_u.

To achieve the solution of the equations it is necessary to estimate the lift and drag of the various components of the aircraft under the conditions of flight in trim. Firstly these are used in the lift equation to find the trim incidence, $\bar{\alpha}$, and then the trim incidence used to calculate the pitching moment coefficient, which should be zero. The drag equation can be used, if the flight path angle γ is known with sufficient accuracy, as a check on the estimated values of drag. This can be treated as a low priority since the effect of drag on the pitching moment equation is usually small.

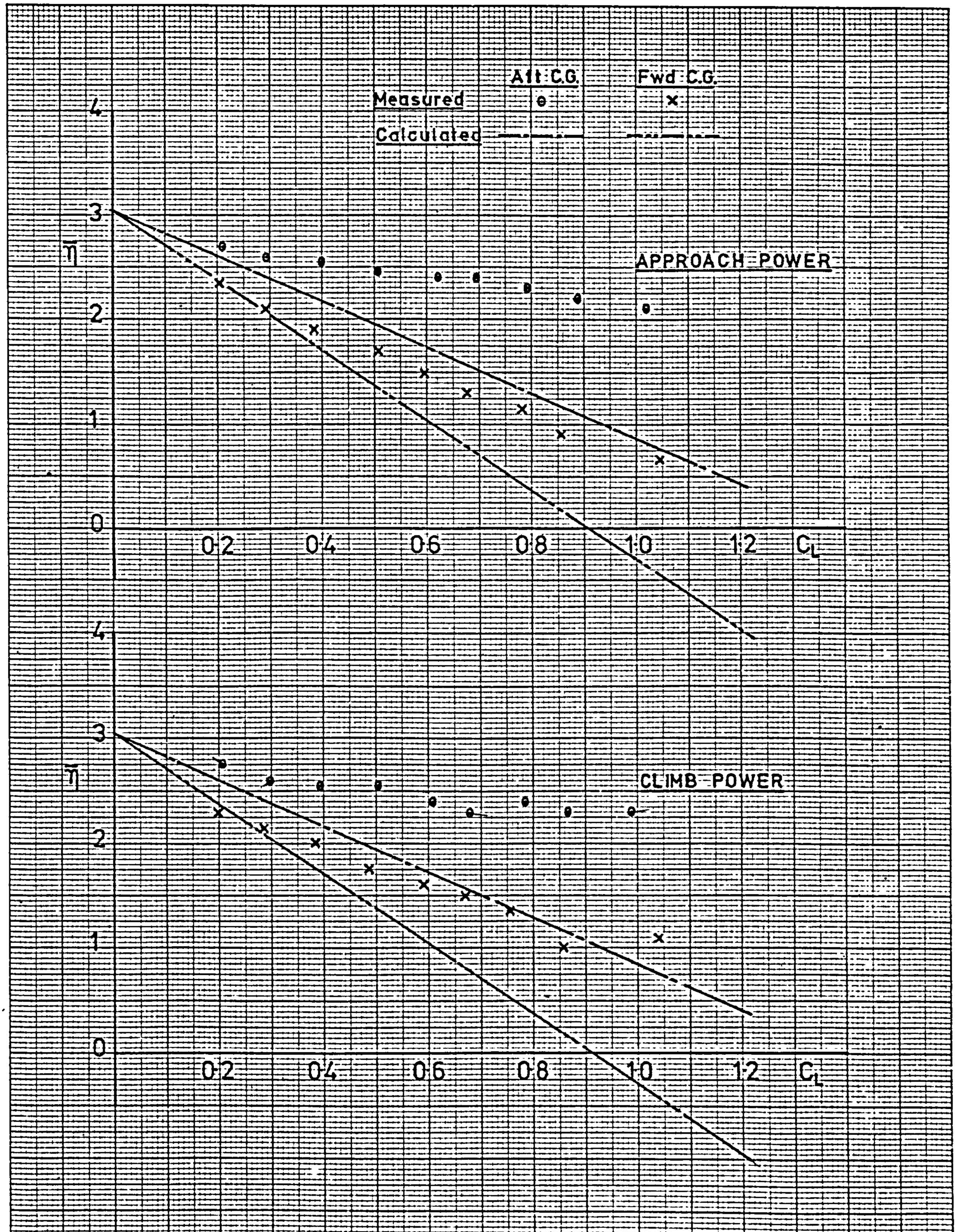

FIG.5.2 Comparison between Measured and Calculated Trim Curves (Simple Theory)

6. Development of the Non-Linear Trim Equations

The solution of the trim equation depends on being able to predict with reasonable accuracy the effects of incidence, power, compressibility and aeroelasticity on the lift and pitching moment equations. When these effects are known they can be used to give the complete trim equations which can then be solved.

The initial approach to this problem was to consider each effect in isolation to establish an expression for its effect on the longitudinal static stability as defined in the simple theory. The more complex of these are included in their original form in section II and the results will be used in the full trim equations. The individual effects can now be discussed.

6.1 Compressibility effects

Aircraft certified in the light aircraft category (section K of B.C.A.R., ref.4) are normally limited to operations below a Mach number of 0.3. At low Mach numbers the only significant compressibility effect is the modification of the lift curve slope of the lifting surfaces, the wing and tail. An approximate correction for an unswept wing is found in ref.5 and gives

$$\frac{a}{a_o} = \frac{A + 2}{A(1-M^2)^{\frac{1}{2}} + 2}$$

where a_o is the lift curve slope at M = 0

In the case of the aircraft used for the flight trials the Aspect ratios of wing and tail were 7.28 and 4.8 respectively and the effects of compressibility are summarised in table 6.1.

The effects only become significant at the lowest values of C_L and are generally small. Using the values given in table 6.1 the basic lift curve slopes can be corrected to allow for the compressibility effect.

6.2 Aeroelastic Distortion of the Structure

Before aeroelastic effects can be included flight loads must be known and as the tail lift force is not known at this stage the

	FORWARD C.G.							AFT C.G.					
C_L	0.2	0.4	0.6	0.8	1.0	1.2		0.2	0.4	0.6	0.8	1.0	1.2
M	.277	.196	.160	.139	.124	.113		.283	.200	.163	.14	.126	.115
$(a/a_o)_w$	1.032	1.015	1.010	1.008	1.006	1.005		1.033	1.016	1.011	1.008	1.006	1.005
$(a/a_o)_T$	1.028	1.014	1.009	1.007	1.005	1.005		1.029	1.014	1.009	1.007	1.005	1.005

TABLE 6.1 Compressibility Effect on Lift Curve Slope

allowance cannot be made. However as will be seen in section 8, the magnitude of the fuselage bending of the aircraft tested is negligible under the loads calculated and can therefore be discounted at this stage. Other local structural deformations may however be significant but cannot be generalized.

6.3 Incidence Effects

In Part II section 1 the simple model of the aircraft is extended to account for the offset of the C.G. from the mean aerodynamic chord and the height of the tail above the extended chord line. This also enabled the drag contribution from each part of the aircraft to be considered as well as the lift. The pitching moment equation modified for incidence effects on the moment arms of the main forces is given in Part II section 1 eqn.13. In that section it is shown that the effect of incidence on the static stability is that it causes a progressive loss of stability as incidence increases in the case of the aircraft considered. This will be generally true for all low wing aircraft.

From eqn.13 the incidence variable moment arms can be determined for each part of the aircraft and used in the general pitching moment equation.

6.4 Power effects on the trim equations

The power effects on the static stability of the aircraft arise from two sources. Firstly there will be the slipstream interference with the airframe, secondly the direct force effects of the propeller will produce moments about the C.G. and will need to be added to general pitching moment equation.

The slipstream interference is found by projecting the slipstream aft from the propeller under the general influence of the aircraft. This process is described in Part II section 2 Appendix A.1. in which a programme is developed to simulate the propeller slipstream characteristics of a twin engined aircraft. The programme shows that the slipstream interference at the tail of the aircraft is variable. The extent of immersion of the tail is a function of incidence and, to a lesser extent, the C.G. position of the aircraft. The wing and nacelles will be influenced by the slipstream which will modify the

lift produced by them. The general influence of the slipstream is discussed in Part II section 2 and is seen to produce a general destabilising effect which tends to increase at high values of C_L.

From Part II section 2 the characteristics of the slipstream are found and used in the pitching moment equation to account for the slipstream interference effect. From eqns 42 and 52 the lift increments to the wing and nacelle can be found in terms of the engine power, aircraft speed and incidence. The tail immersion in the high energy slipstream, together with the modified downwash, can also be found under the same flight conditions. These effects can now be included in the general trim equations.

The direct propeller forces are calculated in Part II section 3. A propeller acting in a flow at incidence to its axis of rotation will produce not only thrust along its axis but also a normal force in the plane of the disc. This force will produce a moment about the C.G. of the aircraft to give a nose up pitching effect as power increases at a positive incidence. There is also a small pure pitching moment produced by the propeller arising from the wing induced upwash over the propeller disc. The forces and moments are developed in terms of engine power and aircraft incidence as functions of propeller advance ratio. In Part II section 4 the propeller characteristics are converted into non-dimensional quantities based on aircraft parameters and included in the pitching moment equation. It was seen that this produced a general destabilising effect at all values of C_L and increased with power.

From eqns (4) and (10) the direct propeller forces and moments can be included in the general trim equations.

6.5 The Basic Aerodynamic Characteristics of the Aircraft

The aerodynamic characteristics of the aircraft can be estimated from the usual data sources and from any wind tunnel data available. In the case of the test aircraft there has been considerable interest in its handling qualities and an extensive study of its aerodynamic characteristics was published by NASA, ref.6. In general this is a reliable source of the basic data but there are some parameters which require further investigation. Other data is available in a wind tunnel study of the aircraft, ref.7, from which some of the data in ref.6 is drawn.

Ref.6 provides a good guide to the values of lift curve slope and drag characteristics for the aircraft as well as some of the dimensional data. A Summary of the aerodynamic data used in this analysis is given in table 6.2.

6.6 Evaluation of the Trim Equations

For the purpose of estimation of the overall lift and pitching moment of the aircraft it can be assumed that the aircraft can be separated into several independent components, the wing, fuselage, nacelles, propeller and tail. Each component can then be treated separately as a simple body, the estimation of its characteristics made from table 6.2 and sections 6.1 - 6.5.

6.6.1 The Wing

The lift of the wing is modified by the increased velocity of the slipstream over a portion of the wing and by the modified flow direction in the slipstream. Also the lift curve slope is a function of Mach Number. The wing lift can be expressed as

$$C_{L_W} = a_o\left(\frac{a}{a_o}\right)_w \bar{\alpha} \left\{ 1 + 2\,\frac{\Delta V}{V} + \frac{\Delta \alpha}{\alpha} \right\}$$

and the drag as

$$C_{D_W} = 0.00826 + 0.0418\, C_{L_W}^{\,2} \qquad (6.1)$$

The wing pitching moment is given by

$$C_{mw} = C_{mo} + C_{L_W} \left\{ (h-h_o)\cos\alpha_b + z \sin\alpha_b \right\} \qquad (6.2)$$
$$+ C_{D_W} \left\{ (h-h_o)\sin\alpha_b - z \cos\alpha_b \right\}$$

where α_b is the fuselage datum line incidence angle and

$$\alpha_b = \bar{\alpha} - 4^0 \qquad (6.3)$$

6.6.2 The Fuselage

The fuselage is treated as an equivalent body of revolution set 3^0 nose down to the datum line. The lift and drag are given by

$$C_{L_f} = a_f (\alpha_b - 3)$$

and

$$C_{D_f} = 0.00755 + C_{L_f} \frac{(\alpha_b - 3)}{57.3} \qquad (6.4)$$

The pitching moment of the fuselage is given by the moment of the lift and drag forces about the C.G. assuming them to act at the quarter chord point of the body.

$$C_{m_f} = C_{L_f} \left\{ (h-h_f)\cos\alpha_b + (z-z_f)\sin\alpha_b \right\} + C_{D_f} \left\{ (h-h_f)\sin\alpha_b - (z-z_f)\cos\alpha_b \right\} \qquad (6.5)$$

where h_f and z_f are the coordinates of the aerodynamic centre of the fuselage with respect to the leading edge of the m.a.c.

6.6.3 The Nacelles

The nacelles are also treated as bodies of revolution set parallel to the fuselage datum line and influenced by the propeller slipstream. The lift and drag are given by

$$C_{L_n} = N\, a_n\, \alpha_b \left\{ 1 + 2\frac{\Delta V}{V} + \frac{\Delta\alpha}{\alpha} \right\}$$

and

$$C_{D_n} = 0.00724 + C_{L_n} \frac{\alpha_b}{57.3} \qquad (6.6)$$

The pitching moment is given by

$$C_{m_n} = C_{L_n} \left\{ (h-h_n)\cos\alpha_b + (z-z_n)\sin\alpha_b \right\} + C_{D_n} \left\{ (h-h_n)\sin\alpha_b - (z-z_n)\cos\alpha_b \right\} \qquad (6.7)$$

where h_n and z_n are the coordinates of the aerodynamic centre of the nacelle with respect to the leading edge of the m.a.c.

6.6.4 The Propellers

The propeller action was analysed in Part II section 3 and showed that both a thrust and normal force relative to the axis of rotation occurred. The propeller axis is parallel to the aircraft datum and so the lift and drag forces are given by

$$C_{L_P} = \left\{T_c \sin\alpha_b + Z_c \cos\alpha_b\right\} \frac{ND^2}{S} \qquad (6.8)$$

and

$$C_{D_P} = \left\{-T_c \cos\alpha_b + Z_c \sin\alpha_b\right\} \frac{ND^2}{S} \qquad (6.9)$$

The pitching moment is given by

$$C_{m_p} = \left\{T_c z_p + Z_c h_p\right\} \frac{ND^2}{S} + M_c \frac{ND^3}{S\bar{c}} \qquad (6.10)$$

where M_c is the direct pitching moment coefficient.

6.6.5 The Tail

The tail lift is complicated by the partial immersion in the propeller slipstream. The extent of the immersion and the velocity and downwash are estimated in part II section 2 and can be used to produce an expression for the lift in terms of power, immersed area and a downwash factor to allow for the increase in downwash in the slipstream at the tail.

For the estimation of the tail lift of an all moving tail the tail incidence α_T and tailplane angle to trim $\bar{n}$ must be separated. A datum tail setting is defined to be parallel to the fuselage datum line and tailplane movements are made relative to this, fig.6.1. With the tailplane set to datum the tailplane incidence α_T due to the aircraft incidence is given by

$$\alpha_T = (\bar{\alpha} - \varepsilon) - \alpha_0$$

where α_o is the wing zero lift incidence relative to fuselage datum and $\bar{\alpha}$ is the aircraft trim incidence relative to α_o.

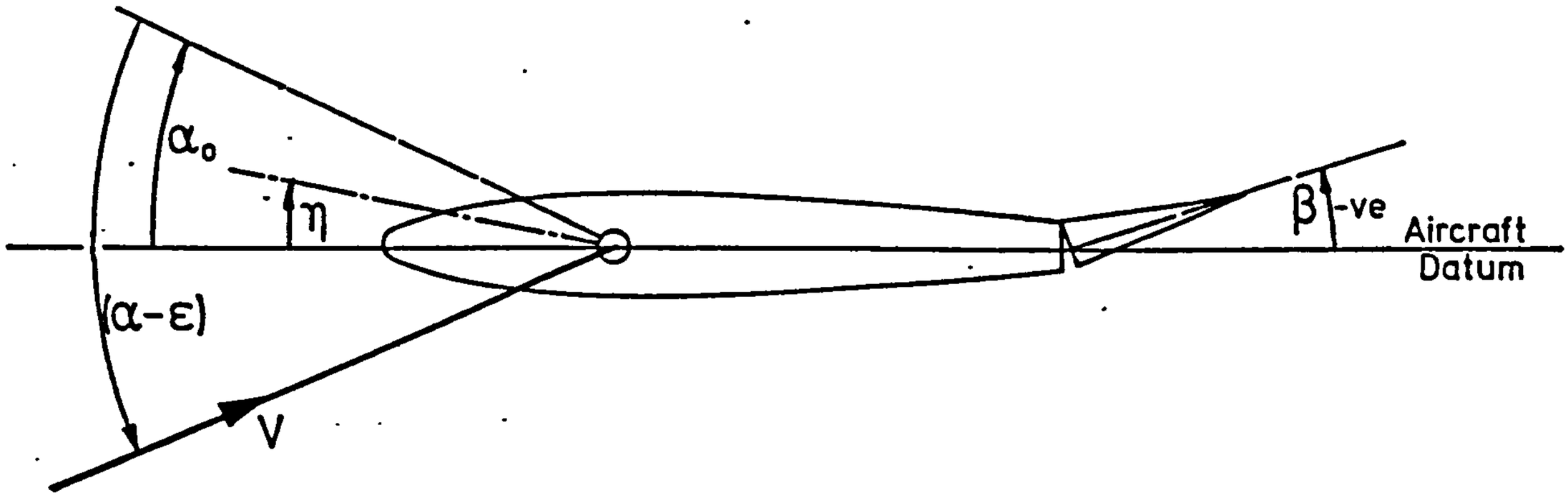

FIG.6:1. Tailplane Incidence Notation

The tailplane incidence thus produces a lift contribution which is a function of the trim incidence $\bar{\alpha}$ together with a constant term. In the absence of other effects this would be

$$C_{L_T}(\bar{\alpha}) = a_1 (\bar{\alpha} - \varepsilon) + a_1 \alpha_o$$

The tailplane movement to trim $\bar{\eta}$ will involve the geared tab contribution and can be expressed as

$$C_{L_T}(\bar{\eta}) = a_2\bar{\eta} = (a_1 + a_3 m)\bar{\eta}$$

If the trim tab is set neutral with the tailplane set on datum it will produce no lift contribution, ($\beta = 0$), all the tab movement being part of the elevator effectiveness. It is usually necessary to set the trim tab to some arbitrary datum so that the forces on the pilots stick remain within manageable limits and a tab offset is necessary. This will be a constant value for a given trim wheel setting and thus the lift contribution will be

$$C_{L_T}(\beta) = a_3\beta$$

The above contributions will be modified by the slipstream effects as indicated in Part II section 2. When these are taken into account the overall lift can be expressed as

$$C_{L_T} = \left(\frac{a}{a_{0_T}}\right)\Big[a_1\bar{\alpha}\left\{(1 - \frac{d\epsilon_0}{d\alpha})(1 + \frac{S_s}{S_T}\frac{q_T}{q}) - \frac{d\epsilon_0}{d\alpha}\frac{S_s}{S_T}(1 + \frac{q_T}{q})(\frac{\epsilon_p}{\epsilon_0} - 1)\right\}$$

$$+ (1 + \frac{S_s}{S_T}\frac{q_T}{q})(a_2\bar{\eta} + a_3\beta + a_1\alpha_0)\Big] \qquad (6.11)$$

where $\frac{S_s}{S_T}$ is the immersed area ratio

$\frac{\epsilon_p}{\epsilon_0}$ is the downwash power factor

and $\frac{q_T}{q}$ is the slipstream energy factor at the tail

The drag is given by

$$C_{D_T} = 0.00843 + 0.0669\ C_{L_T}^2 \qquad (6.12)$$

Using the lift and drag contributions to find the pitching moment gives

$$C_{m_T} = C_{L_T}\left\{\left[\frac{\ell_T}{\bar{c}} - (h-h_o)\right]\cos\alpha_b - (z - z_T)\sin\alpha_b\right\}$$

$$+ C_{D_T}\left\{\left[\frac{\ell_T}{\bar{c}} - (h-h_o)\right]\sin\alpha_b + (z-z_T)\cos\alpha_b\right\} \qquad (6.13)$$

where z_T is the tail height above the m.a.c. line extended.

Collecting the expressions for lift and pitching moment contributions from 6.6.1 to 6.6.5 now enables the trim equations, eqn.5.7, to be evaluated.

Parameter	Description	Value		Source
WING				
a	Lift curve slope	4.35/rad	0.0759/deg	NASA TN-D6800 Table 4.2-1
h_o	Aerodynamic centre	0.192$\bar{c}$ aft of L.E. m.a.c.		ESDU Wings 76003 and 70011
C_{D_W}	Drag coefficient	0.00826 + 0.0418 $C_{L_W}^2$		NASA TN-D6800 Tables 4.12.1-2 and 4.12.4-1
C_{m_o}	Pitching moment coeff.zero lift	-0.02323		NASA TN-D6800 Table 4.5-1
-	General geometric data	-		NASA TN-D6800 + Piper aircraft manual.
TAIL		Wing area	Tail area	
a_1	Lift curve slope	0.01298/deg	.0711/deg	NASA TN-D6800 Table 4.2-1
a_3	Tab lift curve slope	-	.0279/deg	ESDU & NASA TN-D6800 Table 4.13.1-1
a_2	(a_1+a_3m)elevator effectiveness	0.02039	.1120/deg	Calculated from a_1 and a_3
m	Tab gearing	1.5		Measured on subject aircraft and Piper data.
ℓ_T	Tail arm, aft of L.E. m.a.c.	3.023$\bar{c}$		NASA TN-D6800 Fig.3.2-1 & 3.2-2
y_T	Tail height above m.a.c.	0.298$\bar{c}$		NASA TN-D6800 Fig.5.2 & Piper data
C_{D_T}	Drag coefficient	0.0154 + 0.0122 $C_{L_T}^2$		NASA TN-D6800 Tables 4.12.1-2 and 4.12.4-1

N.B. All values based on wing area of 178 ft^2

TABLE 6.2 Aerodynamic Data

Parameter	Description	Value	Source
FUSELAGE			
a_f	Lift curve slope	0.00211	NASA TN-D6800 4.3-1
C_{D_f}	Drag coefficient	$0.00755 + C_{L_f} \frac{\alpha f}{57.3}$	NASA TN-D6800 4.12.2-1 & 4.12.5-1
h_f	Centre of lift fwd of L.E. m.a.c.	$0.347\bar{c}$	¼ chord of equivalent body of revolution.
z_f	Height of centre line above m.a.c	$0.137\bar{c}$	(NASA TN-D6800 & Piper data)
α_f	Fuselage incidence	$\alpha_w - 7^0$	NASA TN-D6800 Fig.4.3-5
NACELLE			
a_n	Lift curve slope (2 nacelles)	0.00155	NASA TN-D6800 Table 4.3-1
C_{D_n}	Drag coefficient (2 nacelles)	$.00724 + C_{L_n} \frac{\alpha_n}{57.3}$	NASA TN-D6800 4.12.2-1 & 4.12.5-1
h_n	Centre of lift fwd of L.E.m.a.c.	$0.4454\bar{c}$	¼ chord of equivalent body of revolution
z_n	Height of centre line above m.a.c	$0.137\bar{c}$	(NASA TN-D6800 & Piper data)
α_n	Nacelle incidence	$\alpha_w - 4^0$	NASA TN-D6800 Fig.4.3-5

TABLE 6.2 Continued

Parameter	Description	Value	Source
PROPELLERS			
T_c, Z_c, M_c	Thrust Normal force and moment coefficient	-	C of A Reports Aero 33-34 Part II sections 3 & 4
h_p	Height of thrust line above m.a.c	$0.9608\bar{c}$	NASA TN-D6800 & Piper data
z_p	Propeller station fwd of L.E.m.a.c	$0.137\bar{c}$	NASA TN-D6800 & Piper data
GENERAL			
$\frac{d\epsilon_o}{d\alpha}$	Downwash rate at the tail	0.64 (power off)	NASA TN-D4983 Fig.73
ϵ_p/ϵ_o	Downwash power factor	(function of power)	NASA TN-D4983 Fig.73 & Part II Section 3.

TABLE 6.2 Continued

7. Solution of the Trim Equations

Since the lift characteristics of the various parts of the aircraft which depend on incidence have been evaluated the lift equation, 5.7, may now be completed and solved to determine the trim value of incidence for specified values of trim lift coefficient $\bar{C}_L$.

The value of incidence determined by the lift equation can then be used to evaluate the pitching moment equation. If this process is repeated for values of C_L through the normal flight range of the aircraft then the rate of change of pitching moment with $\bar{\alpha}$ can be found for the evaluation of the static stability of the aircraft.

Strictly the drag equation should also be shown to be in equilibrium but since the flight trials were not intended for this depth of analysis no flight path angle information was recorded. It is therefore not possible to determine $\bar{C}_D$ since this involves sin γ. The cos γ term in the lift equation is much less important and up to flight path angles of 8^0 the error in accepting cos γ = 1 is only 1% in $\bar{C}_L$, this can be regarded as small enough to be insignificant. Only at the very low powers at high speeds and high powers at low speeds is a flight path angle of 8^0 liable to be exceeded since it corresponds to a rate of descent of about 2600 ft/min at C_L = 0.2 and a climb of 1100 ft/min at C_L = 1.2 at average aircraft weights. Since the aircraft was flown at constant speed the longitudinal acceleration of the aircraft should be zero, see section 4.1, which implies that the aircraft was in trim in this respect. The only virtue in including the drag equation would be a check on the engine power to verify that the estimated power and propeller efficiency were reasonably accurate.

The first stage in the solution is to evaluate the lift coefficients due to the wing, nacelle, fuselage, propellers and tail in terms of $\bar{\alpha}$. For this a value of elevator angle to trim, $\bar{\eta}$, is needed and the measured flight value is used for this purpose. From eqns.6.1 to 6.13 it can be seen that the lift contribution will be given by a "constant" term and an incidence dependent term at each value of $\bar{C}_L$. Since the variation in the "constant" term with increase in $\bar{C}_L$ is generally small the lift characteristics can be assumed to be quasi-linear at each increment in $\bar{C}_L$. In the case of the propeller contribution this is no longer true and fig.7.1 shows the propeller lift contribution as a function of incidence. Each curve can be fitted with a second degree

polynomial which gives the lift contribution of the propeller as a function of incidence.

Adding the contributions produces a quadratic in $\bar{\alpha}$ which can be solved to give the trim incidence under the particular values of power and weight. The process and its results are shown in tables 7.1 to 7.3.

The value of $\bar{\alpha}$ obtained from the lift equation is now used in the pitching moment equation and should produce a trim value of zero. If this is not achieved then the elevator angle to trim must be varied to produce a new value of $\bar{\alpha}$ and the process repeated until a compatible trim value is found. If the measured values of the elevator angle are known then it is possible to establish the trim state very quickly; if the elevator angle is unknown then an initial estimate is required and may need several iterations for convergence. A convergence to $\pm 0.01^0$ for $\bar{\eta}$ is attempted in the calculation. The limit of confidence in the flight measurements was $\pm 0.05^0$. The measured and calculated elevator angles are given in table 7.4

The results of the evaluation of the pitching moment equation are shown in table 7.5 and the comparative magnitudes of the moments due to the individual parts of the aircraft, tail off, are shown in figs. 7.9 and 7.10. They are separated into a tail off moment and a moment due to the tail for convenience. The tail off and tail moments are then summed and should produce a zero result. The error ΔC_m shows that the zero state is very nearly achieved and an approximate correction to the elevator angle to trim, $\Delta\bar{\eta}$, based on the out of trim moment is shown to be generally well within the limit of accuracy of the measured data. The estimated and measured trim curve data, controls fixed, are shown in figs.7.2 to 7.4 for the three power settings used for the simulation of the propeller slipstream and force estimation. From these figures it can be seen that the estimated data lies very close to the measured data indicating that the simulation of the aircraft must correspond well with the actual aircraft under the same flight conditions.

Some small error is seen between the measured and calculated elevator angles at aft C.G.. Above $C_L = 0.6$ it appears that at all power conditions the elevator angle to trim is increased by about 0.2^0. Fig.7.5 shows the tail load of the aircraft, given in table 7.5, and it is apparent that the tail produces a net upload under these conditions.

It is possible that a structural distortion due to the load reversal may occur and this could cause such an effect. This suggestion is considered further in section 8.

Whereas the measured and calculated elevator angles to trim agree closely at forward C.G. the aft C.G. cases all indicate a small systematic error. The reason for this has not been firmly established but one remaining possibility is that there may have been a loading error in the declared equipment on board the aircraft. The loading sheet was checked by the flight test observer, (the author), and independently by the design authority before clearance for flight was given. This does not however eliminate the possibility of the removal or replacement of some item of equipment without proper notification and consequent untraceable errors in the declared loading. The systematic error is equivalent to about a 1% error in C.G. position, equivalent to a total moment error of 0.7% or 2200 lbf-ins.

An alternative possibility is that the trim tab position may have been in error due to backlash in the tab setting mechanism. The tab angle was sensed by a potentiometer on the indicator operating wire, not at the tab itself, and there was no measurement of the tab position relative to the elevator control. This arrangement was chosen to enable the tab to be set to a known datum in flight. Since the tab was geared to the elevator the separation of the trim function of the tab from its geared function to establish the datum trim was necessary. On the ground there was no evidence of any problem regarding the validity of the calibration of the transducer for tab setting angle but in flight the aerodynamic loading may have caused some mistrim to occur. The magnitude of the error is about 0.1 deg in elevator angle and this would be caused by an error of 0.4 deg in the tab setting angle. Considering the tab trim setting angle of -3.65^0 it can be seen that for elevator angles less than 2.4^0 the gearing of 1.5 will produce a tab deflection relative to the elevator which is negative. Figs.7.2 to 7.4 show that at forward C.G. a negative tab deflection will always be produced whilst at aft C.G. the tab deflection will change from negative to positive as speed increases thus producing a load reversal on the tab linkage. It is significant that such a load change occurs at about $C_L = 0.6$ since this is also the condition under which the total tail-plane loading reverses at the bearing. The concurrence of these effects

leaves any attempt at analysis very doubtful and it can only be regarded as unfortunate that such a loading and tab setting should have occurred. The tab setting was chosen to provide a pilot stick force which was acceptable at both forward and aft C.G. loadings throughout the speed range of the aircraft.

The solution of the trim equations gave the trim incidence and elevator angle at selected values of $\bar{C}_L$. This enables the trim curves to be drawn both in terms of $\bar{\eta}$ against $\bar{C}_L$ and $\bar{\eta}$ against $\bar{\alpha}$. Figs.7.2 to 7.4 show the alternative forms indicating the considerable difference between them.

If the curves are plotted in terms of $\bar{C}_L$, as they would be for convenience if the aircraft had no incidence measurement system, then they would show a non-linear form. There is a slight inflexion and a tendency to reduced slope at high C_L, particularly at high powers.

In contrast the same data plotted in terms of $\bar{\alpha}$ is linear. This is a most significant finding since it indicates that the value of $m'_{w.eff}$ which is determined by $dCm/d\bar{\alpha}$, is constant through the whole range of incidence. The interpretation of the curves plotted in terms of $\bar{C}_L$ would have suggested a variable $m'_{w.eff}$ with incidence.

The difference between the two forms of trim curve slope arises from the non-linearity of the $C_L - \alpha$ characteristic of the aircraft which makes the assumption of eqn.2.19 invalid.

$$\left(\frac{d\bar{\eta}}{d\bar{\alpha}} = \frac{d\bar{\eta}}{dC_L} \cdot \frac{dC_L}{d\alpha}, \text{ i.e. } \frac{d\bar{\eta}}{d\alpha} \propto \frac{d\bar{\eta}}{dC_L}\right)$$

This statement can only be used if $dC_L/d\alpha$ is constant otherwise it is a function of incidence and the statement no longer holds.

In Ref.6 the lift characteristic of the aircraft is estimated under simulated power-on conditions from tunnel tests. Fig.7.6 shows that for fixed elevator angles the lift curve slope is a function of thrust coefficient T'_c, the slope increasing with T'_c. Since the tunnel tests were carried out at constant tunnel airspeed the thrust coefficient could be maintained constant and the incidence varied to produce the lift characteristic shown in fig.7.6. In flight the airspeed must be varied and so constant thrust coefficient cannot be maintained.

Since the engines were set at constant power, see section 4, the thrust would vary with forward speed and be related to power by the approximate relationship,

$$\eta P = TV$$

Thus as speed decreases at a given power setting the thrust will increase and the thrust coefficient will become a function of incidence,

$$T_c = k\frac{C_p}{V^3} \quad \text{and} \quad \alpha V^2 = \text{constant},$$

$$\text{thus} \quad T_c = f(\alpha, C_p)$$

From the flight trials, (performed at constant power), the thrust coefficient is low at low incidence and increases as incidence increases, Part II section 4 fig.3. Thus there will be a transfer of the "observed" C_L -α characteristic from the low T_c' value at low incidence to the high T_c' value at high incidence, fig.7.7. This transfer will tend to make the lift curve non-linear since the thrust coefficient is a function of α^n where $n > 1$. The lift curve slope will now be a function of incidence and power.

The C.G. of the aircraft will also have a bearing on the slope of the lift characteristic since the changing elevator angle to trim, $\bar{n}$, with incidence will produce a change in the tail lift relative to the wing lift. Fig.7.6 shows the lift curve slopes at constant thrust coefficient and elevator angle. If a constant thrust is considered then the change in elevator angle to trim with incidence will produce a different lift curve slope at forward and aft C.G.locations, fig.7.7 shows that an aft C.G. will tend to produce a greater value of overall lift curve slope than a forward C.G.

Taken together these two effects will produce an aircraft lift characteristic which will be a function of Power and C.G. and the generalisation used in eqn.2.19 is strictly invalid. These are not the only effects that will produce non-linearity of the lift characteristic. In section 6.1 it was seen that compressibility would cause non-linearity but this effect becomes more important as speed, and hence Mach number, increases. Aeroelasticity may also add to the general effect although

although there is no direct evidence in the case of the aircraft considered.

Fig.7.8 shows the comparison between the forward and aft C.G. lift characteristics at high and low powers. These are taken from the calculated incidences for given values of $\bar{C}_L$, table 7.3. There is a general trend towards an increasing slope as incidence increases, as expected under power, and the slope of the aft C.G. case is just greater than the forward C.G.case.

It should be mentioned that the thrust coefficient $T_c' = 0.44$ used in some of the tunnel tests is unrealistically high for comparison with the real aircraft. In flight at $C_L = 1.2$ this would correspond to a power of 280 T.H.P. and at $C_L = 0.2$ the power would have to be about 4,200 T.H.P. The installed maximum horse power was about 260 T.H.P. at sea level I.S.A. This emphasises the practical difficulty in making comparison between tunnel and flight data. Whereas the tunnel measurements can be assessed under constant speed airflow and variable incidence the same cannot be done in flight. Where power on characteristics are to be compared the incidence-speed relationship becomes critical for correct comparison.

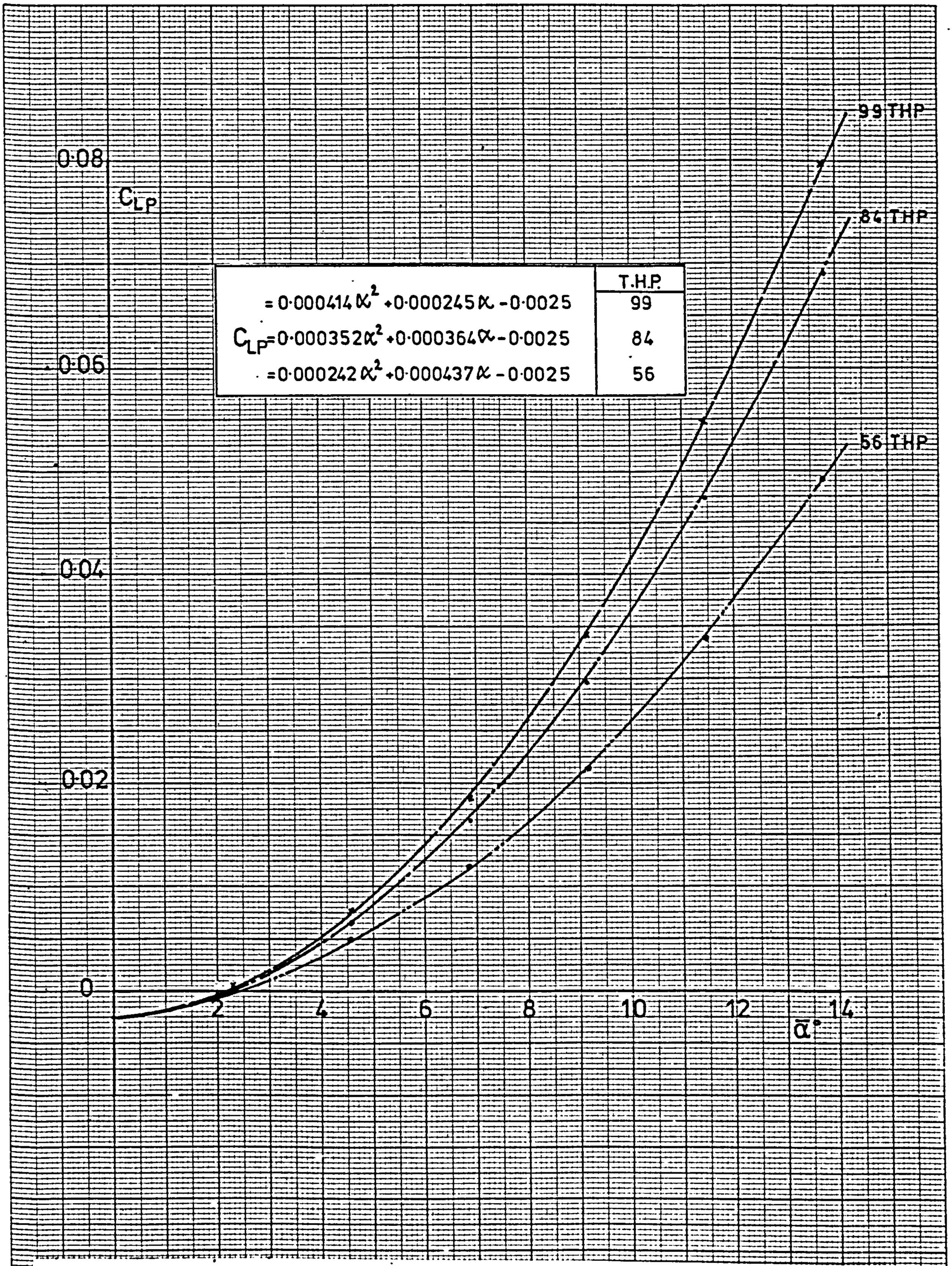

	T.H.P.
$= 0{\cdot}000414\,\bar{\alpha}^2 + 0{\cdot}000245\,\bar{\alpha} - 0{\cdot}0025$	99
$C_{LP} = 0{\cdot}000352\,\bar{\alpha}^2 + 0{\cdot}000364\,\bar{\alpha} - 0{\cdot}0025$	84
$= 0{\cdot}000242\,\bar{\alpha}^2 + 0{\cdot}000437\,\bar{\alpha} - 0{\cdot}0025$	56

FIG.7.1 Propeller Lift Contribution as a function of Power and Incidence

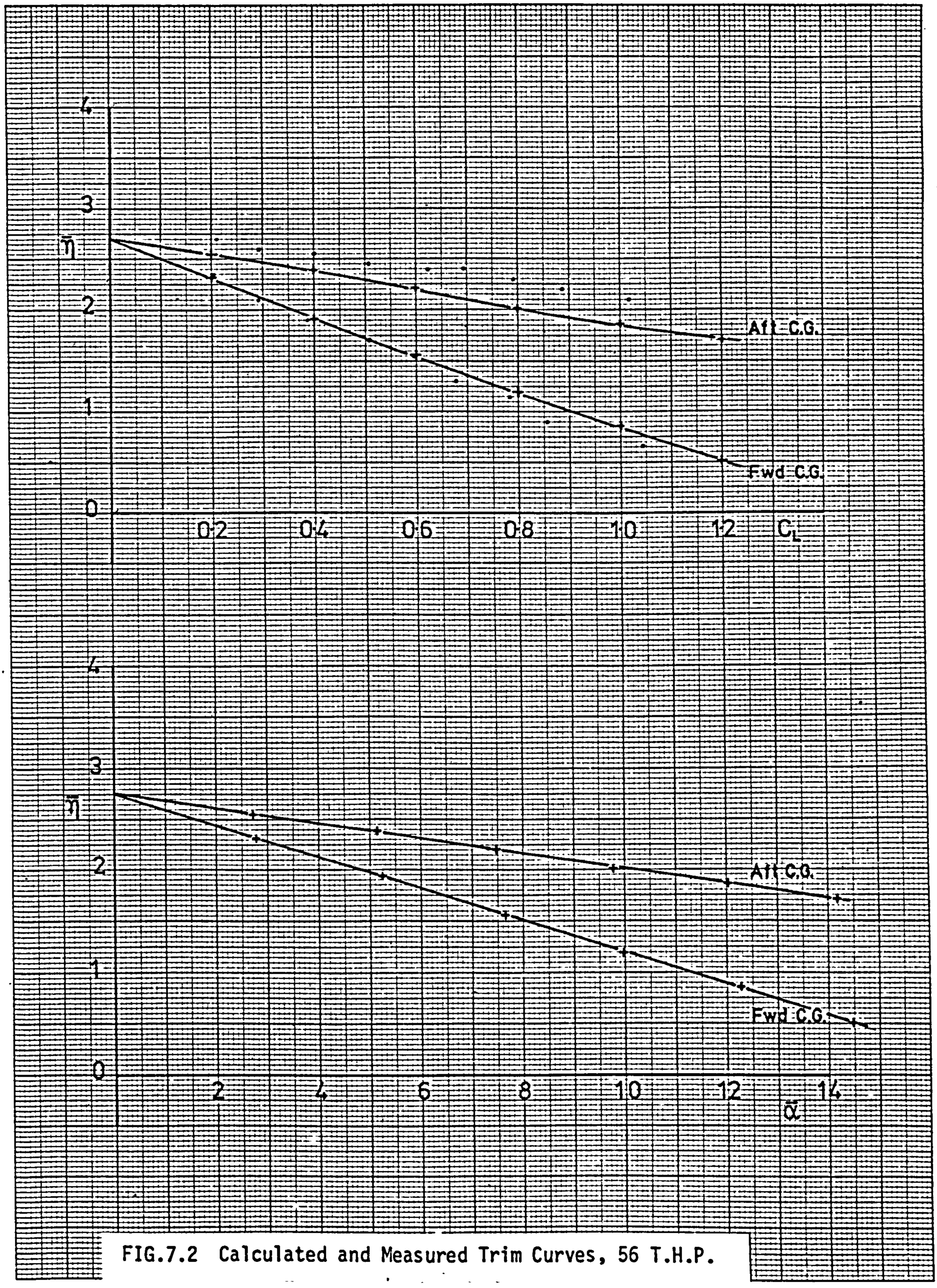

FIG.7.2 Calculated and Measured Trim Curves, 56 T.H.P.

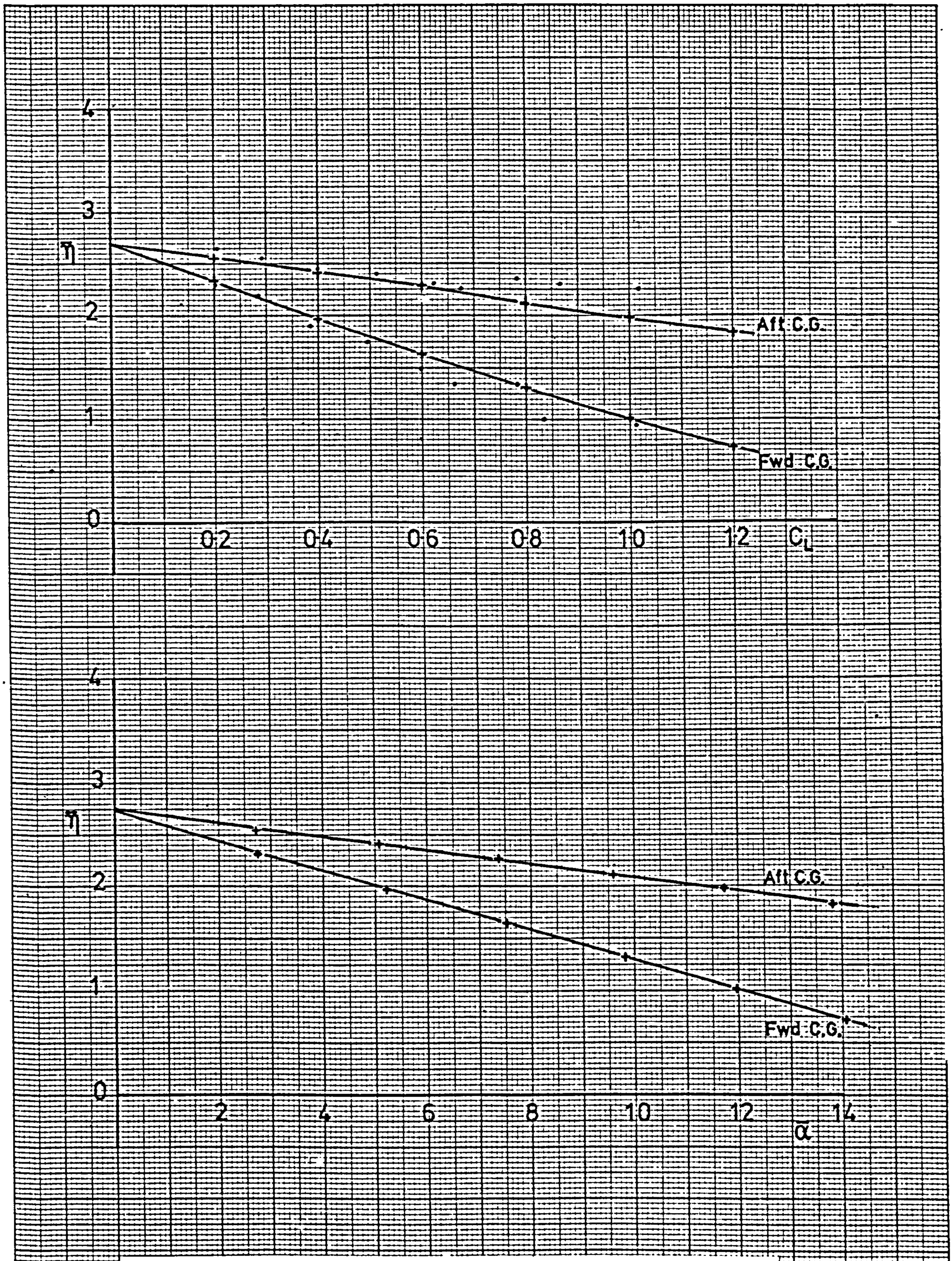

FIG.7.3 Calculated and Measured Trim Curves, 84 T.H.P.

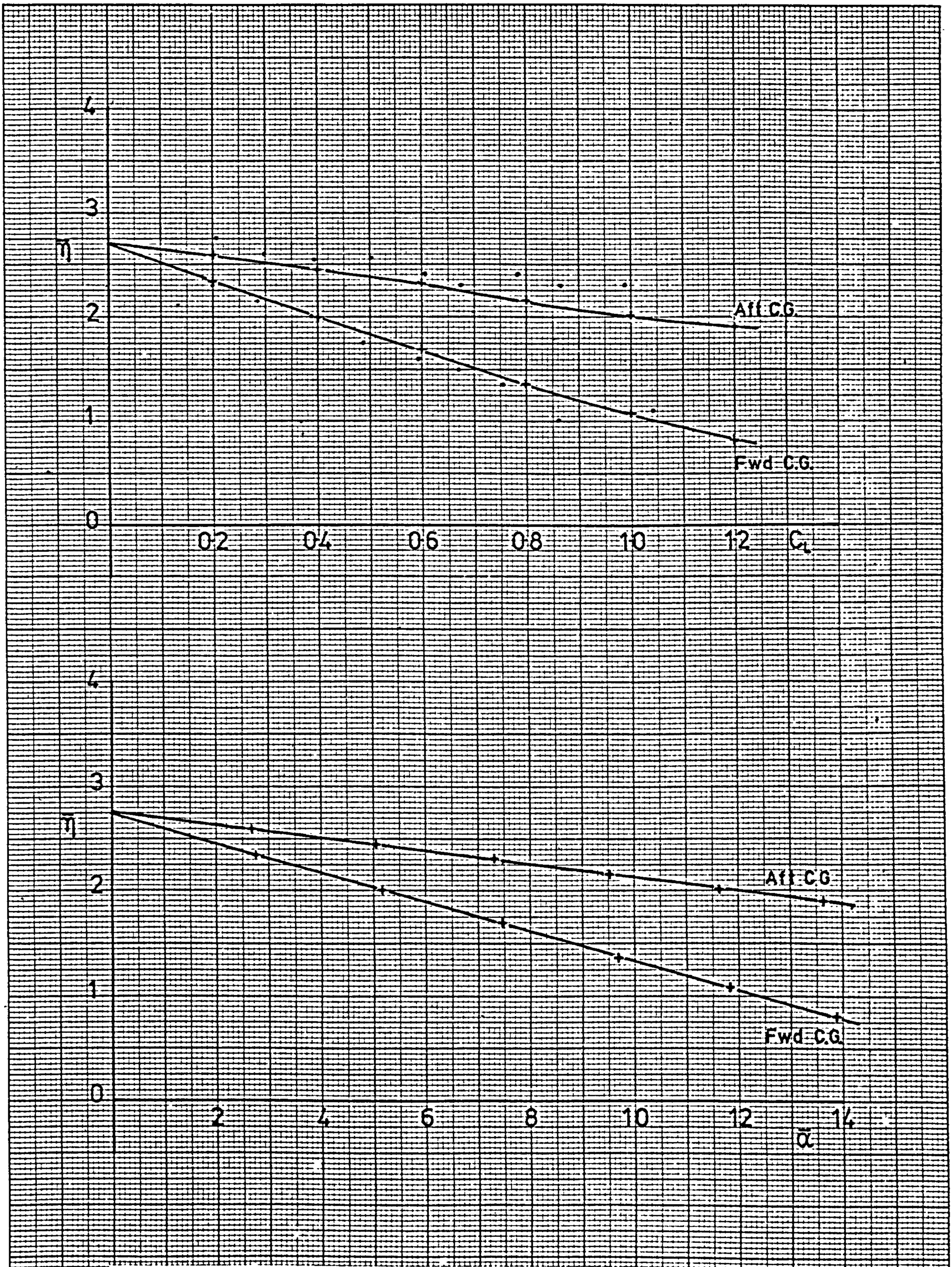

FIG.7.4 Calculated and Measured Trim Curves, 99 T.H.P.

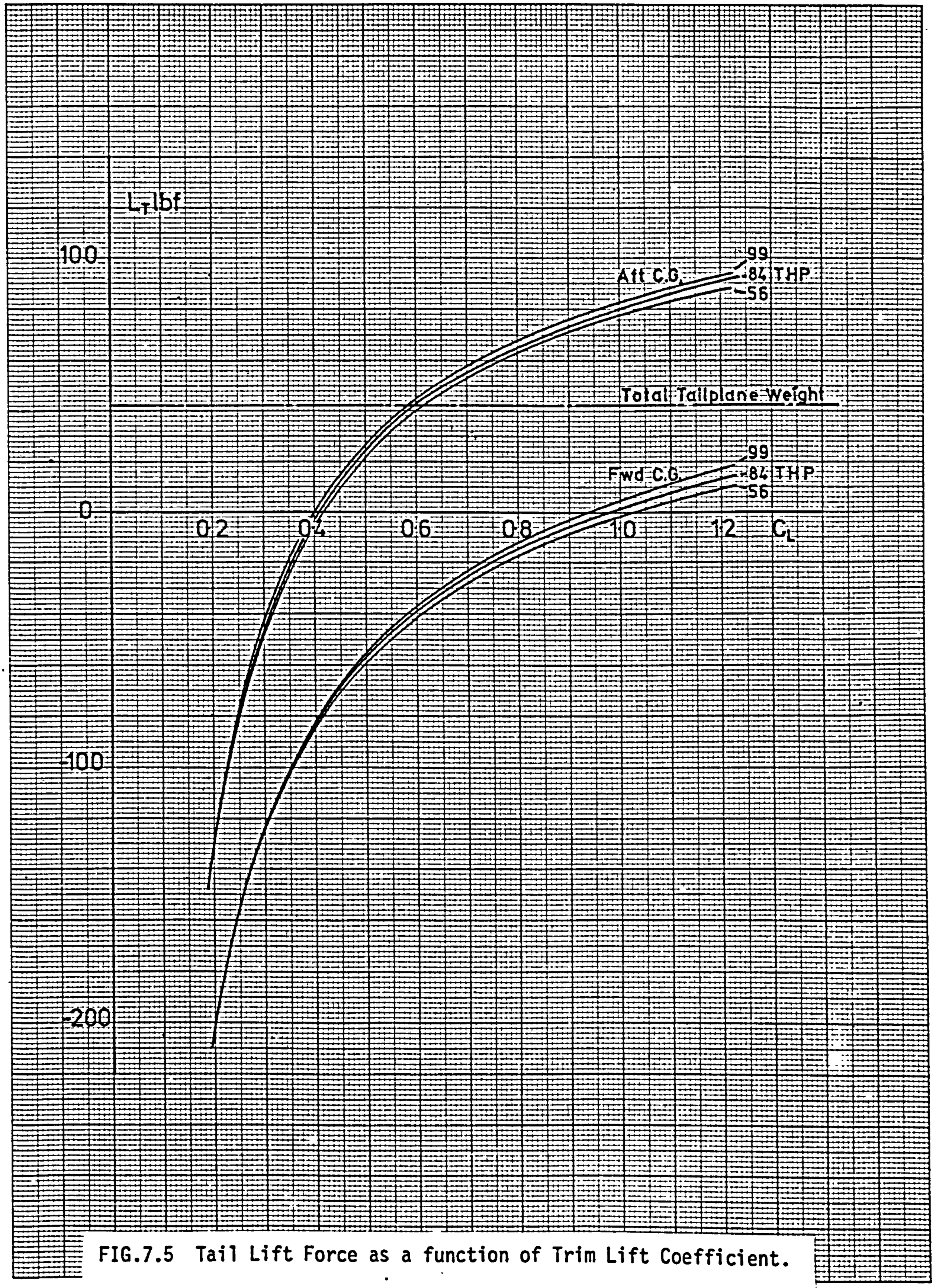

FIG.7.5 Tail Lift Force as a function of Trim Lift Coefficient.

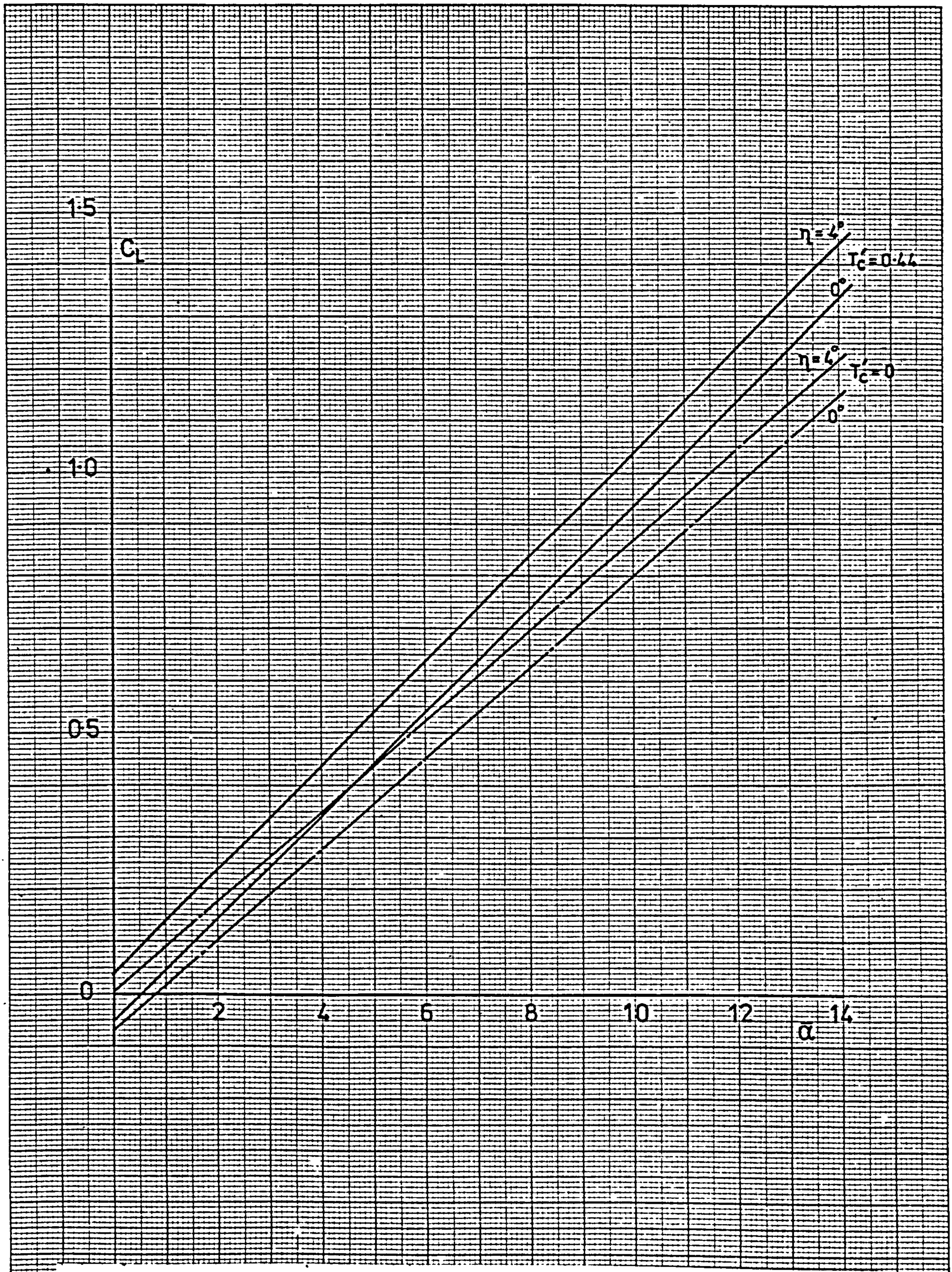

FIG.7.6 Theoretical Lift-Incidence Characteristic, from NASA TN-D 6800

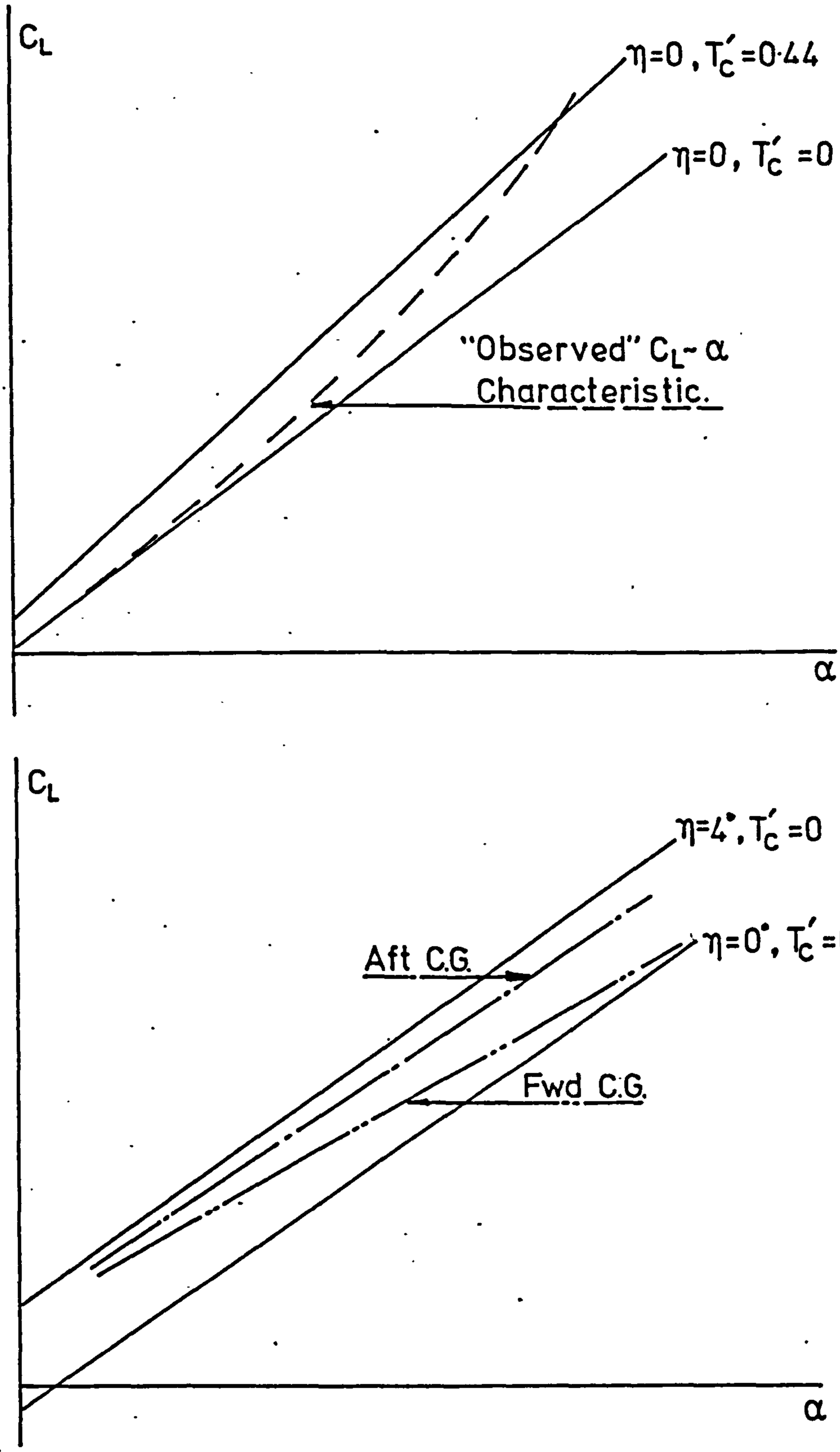

FIG.7.7 Effect of thrust and C.G. on Measured Lift Curve Slopes

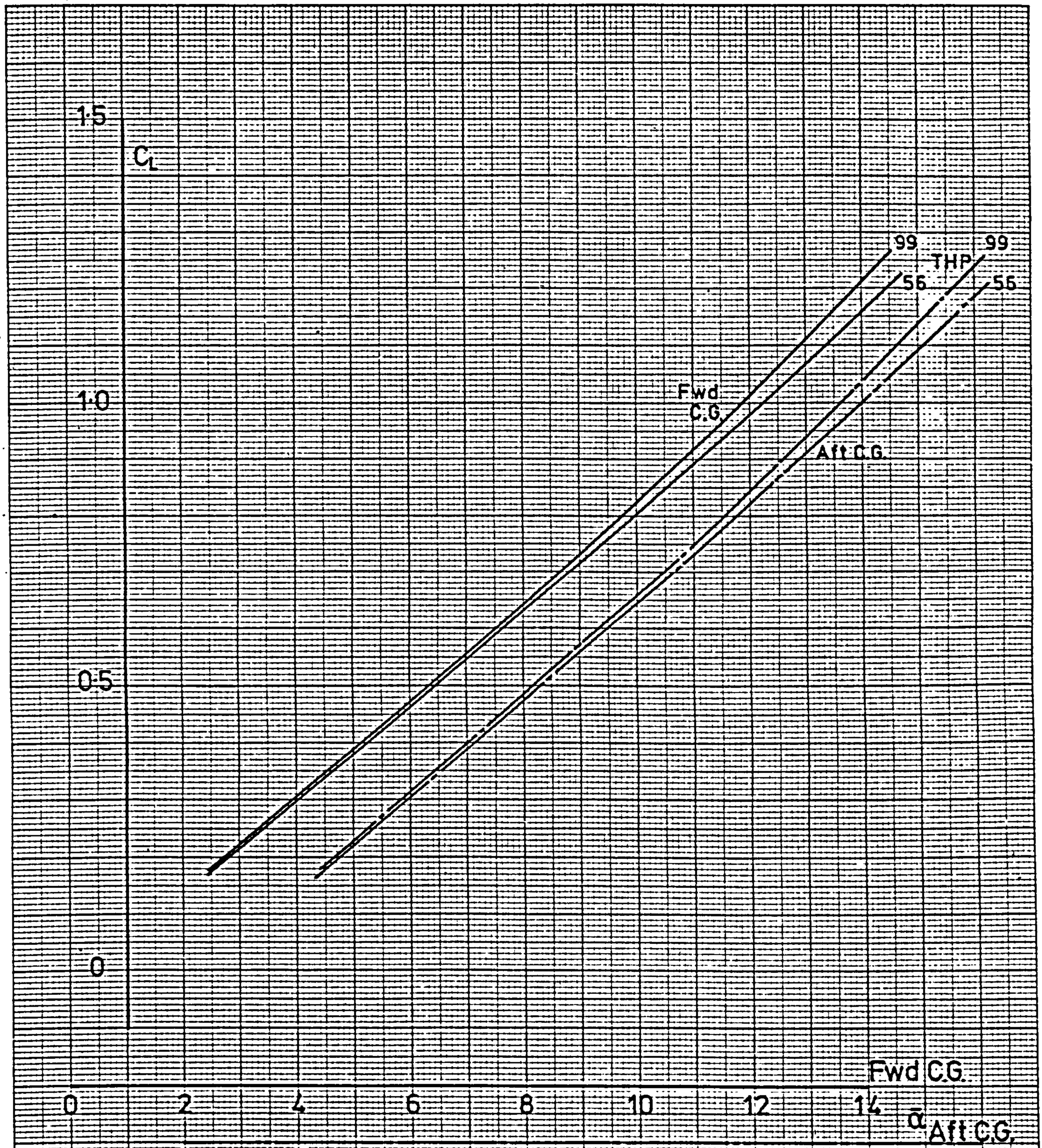

FIG.7.8 Calculated Lift Curve Slopes from Flight data

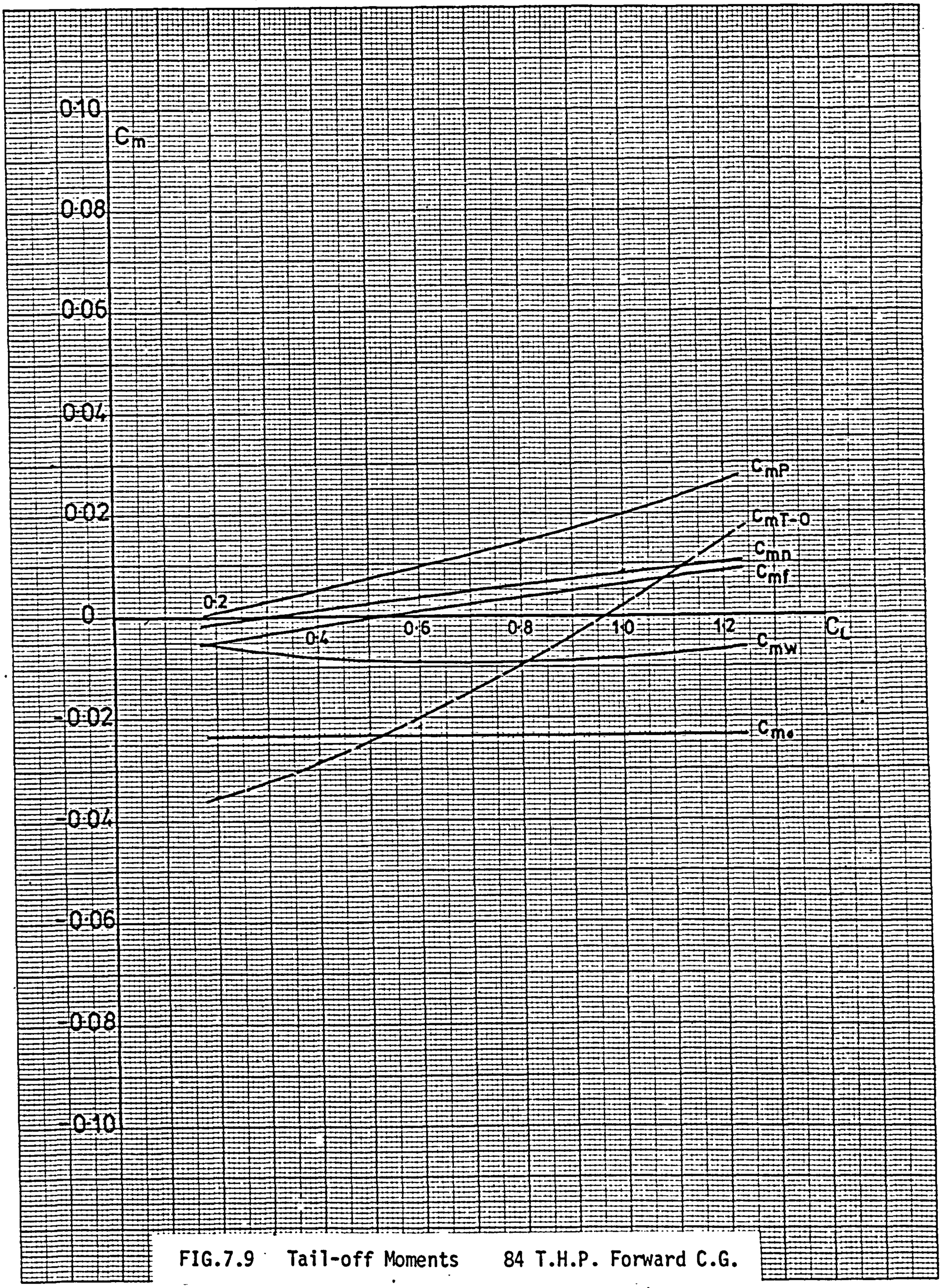

FIG.7.9 Tail-off Moments 84 T.H.P. Forward C.G.

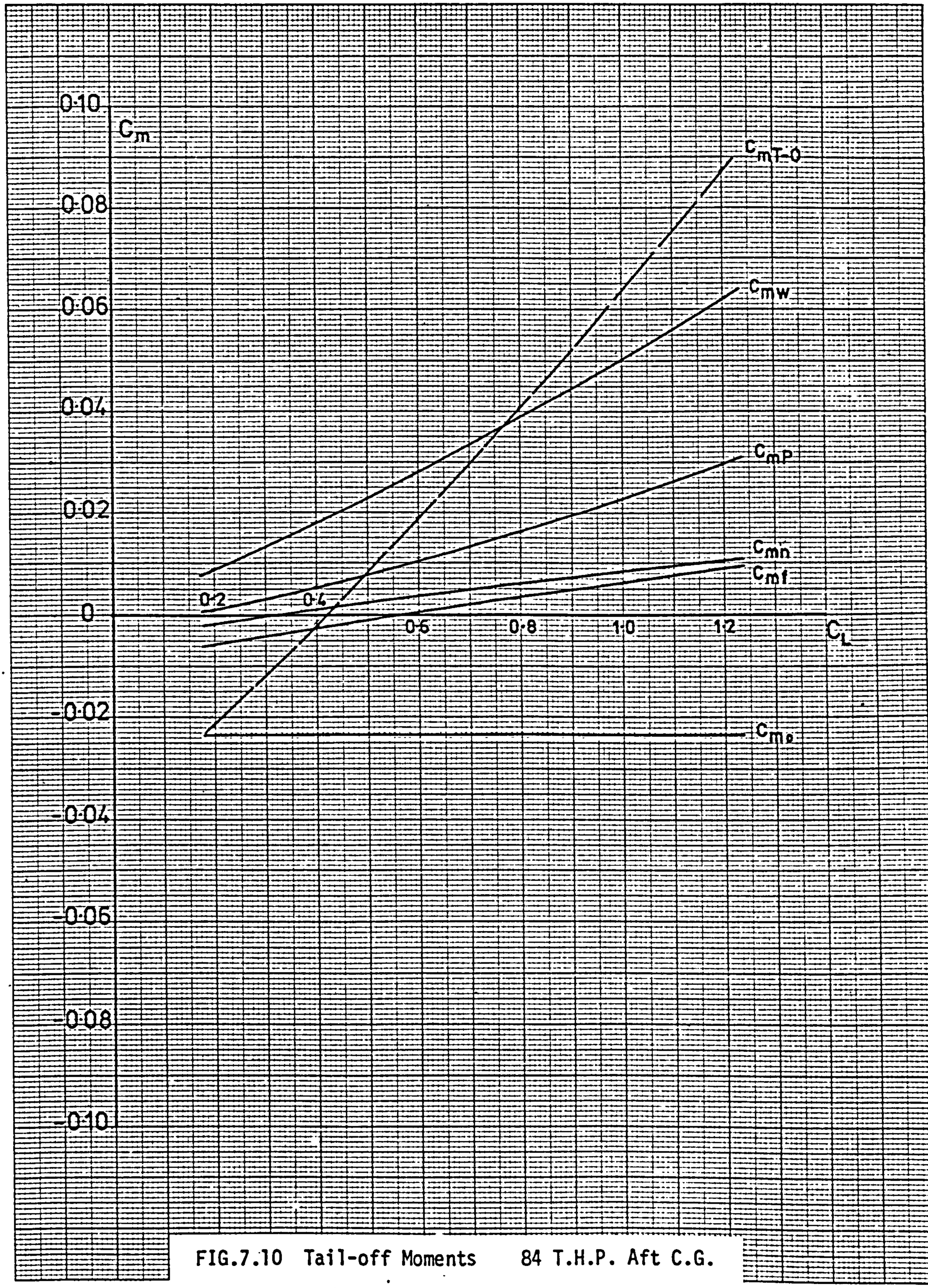

FIG.7.10 Tail-off Moments 84 T.H.P. Aft C.G.

		FORWARD C.G.								AFT C.G.					
$\bar{C}_L$	Power	0.2	0.4	0.6	0.8	1.0	1.2		Power	0.2	0.4	0.6	0.8	1.0	1.2
C_{L_f}	All	-.01477	-.01477	-.01477	-.01477	-.01477	-.01477		All	-.01477	-.01477	-.01477	-.01477	-.01477	-.01477
	56	-.00630	-.00593	-.00584	-.00582	-.00583	-.00584		56	-.00630	-.00592	-.00583	-.00581	-.00582	-.00577
C_{L_n}	84	-.00630	-.00590	-.00581	-.00581	-.00586	-.00586		84	-.00630	-.00590	-.00581	-.00580	-.00584	-.00584
	99	-.00630	-.00590	-.00582	-.00582	-.00587	-.00591		99	-.00630	-.00590	-.00582	-.00581	-.00585	-.00593
C_{L_P}	All	-.00250	-.00250	-.00250	-.00250	-.00250	-.00250		All	-.00250	-.00250	-.00250	-.00250	-.00250	-.00250
	56	-.07393	-.07549	-.07843	-.07989	-.08161	-.08151		56	-.07392	-.07527	-.07804	-.07879	-.08104	-.08094
C_{L_T}	84	-.07457	-.07767	-.08241	-.08456	-.08769	-.08940		84	-.07447	-.07715	-.08148	-.08312	-.08547	-.08675
(α_o, r_o)	99	-.07493	-.07866	-.08426	-.08699	-.09031	-.09318		99	-.07512	-.07827	-.08352	-.08556	-.08809	-.09154
	56	.04958	.04210	.03559	.02771	.02028	.01201		56	.05450	.05179	.05007	.04601	.04427	.04000
$C_{L_Y}(\bar{n})$	84	.05023	.04424	.03907	.03228	.02584	.01886		84	.05489	.05398	.05392	.05093	.04868	.04589
	99	.05070	.04547	.04139	.03445	.02846	.02208		99	.05602	.05543	.05601	.05343	.05130	.05044
	56	-.24792	-.45659	-.66595	-.87527	-1.08443	-1.29261		56	-.24299	-.44667	-.65107	-.85540	-1.05986	-1.26374
TOTAL-$\bar{C}_L$	84	-.24791	-.45660	-.66642	-.87536	-1.08498	-1.29367		84	-.24315	-.44634	-.65064	-.85526	-1.05965	-1.26397
	99	-.24780	-.45636	-.66596	-.87538	-1.08499	-1.29428		99	-.24267	-.44601	-.65060	-.85521	-1.06308	-1.26404

TABLE 7.1 Calculation of $\bar{\alpha}$, $\bar{C}_L$; $\bar{\alpha}$ independent terms

		FORWARD C.G.							AFT C.G.						
$\bar{C}_L$	Power	0.2	0.4	0.6	0.8	1.0	1.2		Power	0.2	0.4	0.6	0.8	1.0	1.2
	56	.07998	.07719	.07658	.07650	.07652	.07673		56	.08003	.07722	.07659	.07642	.07643	.07662
C_{L_w}	84	.08026	.07743	.07705	.07679	.07716	.07757		84	.08030	.07744	.07692	.07683	.07701	.07736
	99	.08041	.07762	.07718	.07725	.07755	.07803		99	.08044	.07761	.07715	.07710	.07736	.07777
C_{L_f}	All	.00211	.00211	.00211	.00211	.00211	.00211		All	.00211	.00211	.00211	.00211	.00211	.00211
	56	.00158	.00148	.00146	.00146	.00146	.00145		56	.00158	.00148	.00146	.00146	.00146	.00144
C_{L_n}	84	.00158	.00147	.00146	.00146	.00146	.00146		84	.00158	.00147	.00146	.00146	.00146	.00146
	99	.00158	.00147	.00146	.00146	.00147	.00147		99	.00158	.00147	.00146	.00146	.00146	.00148
	56	.00044	.00044	.00044	.00044	.00044	.00044		56	.00044	.00044	.00044	.00044	.00044	.00044
C_{L_P}	84	.00036	.00036	.00036	.00036	.00036	.00036		84	.00036	.00036	.00036	.00036	.00036	.00036
	99	.00025	.00025	.00025	.00025	.00025	.00025		99	.00025	.00025	.00025	.00025	.00025	.00025
	56	.00441	.00448	.00464	.00481	.00495	.00503		56	.00438	.00445	.00460	.00476	.00490	.00498
$C_{L_T}(\bar{\alpha})$	84	.00441	.00453	.00477	.00500	.00521	.00536		84	.00437	.00446	.00468	.00489	.00507	.00521
	99	.00442	.00457	.00486	.00512	.00534	.00554		99	.00429	.00447	.00473	.00497	.00518	.00537
	56	.08852	.08570	.08523	.08532	.08548	.08576		56	.08854	.08570	.08520	.08519	.08534	.08559
TOTAL	84	.08871	.08589	.08574	.08571	.08629	.08685		84	.08871	.08583	.08552	.08564	.08600	.08649
	99	.08877	.08602	.08586	.08619	.08672	.08740		99	.08867	.08591	.08570	.08589	.08636	.08698

TABLE 7.2 Calculation of $\bar{\alpha}$, $\bar{C}_L$. $\bar{\alpha}$ dependent terms

FORWARD C.G.

AFT C.G.

$\bar{C}_L$	Power	0.2	0.4	0.6	0.8	1.0	1.2		Power	0.2	0.4	0.6	0.8	1.0	1.2
$C_{Lp}(\bar{a}^2)$	56	.000242	.000242	.000242	.000242	.000242	.000242		56	.000242	.000242	.000242	.000242	.000242	.000242
	84	.000352	.000352	.000352	.000352	.000352	.000352		84	.000352	.000352	.000352	.000352	.000352	.000352
	99	.000414	.000414	.000414	.000414	.000414	.000414		99	.000414	.000414	.000414	.000414	.000414	.000414
$\bar{a}$	56	2.780	5.250	7.648	9.986	12.261	14.481		56	2.724	5.137	7.483	9.770	12.010	14.195
	84	2.764	5.205	7.539	9.817	11.987	14.091		84	2.712	5.094	7.384	9.607	11.756	13.835
	99	2.756	5.176	7.486	9.704	11.842	13.894		99	2.703	5.068	7.332	9.520	11.658	13.646

TABLE 7.3 Calculation of $\bar{a}$ and $\bar{C}_L$. $\bar{a}^2$ dependent terms

FORWARD C.G.

AFT C.G.

$\bar{C}_L$	Power	0.2	0.4	0.6	0.8	1.0	1.2		Power	0.2	0.4	0.6	0.8	1.0	1.2
$\bar{\eta}$	56	2.37	1.92	1.48	1.08	0.70	0.60		56	2.66	2.50	2.37	2.25	2.14	2.05
Measured	84	2.36	1.92	1.50	1.10	0.74	0.66		84	2.64	2.46	2.30	2.18	2.08	2.02
(smoothed)	99	2.40	1.96	1.55	1.17	0.83	0.55		99	2.70	2.55	2.44	2.34	2.24	2.16
$\bar{\eta}$	56	2.32	1.93	1.57	1.20	0.86	0.51		56	2.55	2.38	2.22	2.02	1.87	1.71
Calculated	84	2.33	1.97	1.64	1.32	1.02	0.73		84	2.55	2.42	2.29	2.12	1.98	1.83
	99	2.34	2.00	1.70	1.37	1.00	0.82		99	2.60	2.45	2.32	2.16	2.02	1.91

TABLE 7.4 Tailplane angle to trim, $\bar{\eta}$

		FORWARD C.G.							AFT C.G.						
$\bar{C}_L$	Power	0.2	0.4	0.6	0.8	1.0	1.2		Power	0.2	0.4	0.6	0.8	1.0	1.2
C_{m_w}	56	-.00558	-.00809	-.00932	-.00935	-.00824	-.00606		56	+.00899	.01823	.02839	.03936	.05108	.06352
	84	-.00558	-.00807	-.00935	-.00943	-.00852	-.00659		84	.00897	.01810	.02805	.03874	.05007	.06200
	99	-.00558	-.00806	-.00904	-.00952	-.00868	-.00694		99	.00895	.01803	.02790	.03843	.04976	.06120
C_{m_f}	56	-.00503	-.00213	+.00068	.00342	.00611	.00876		56	-.00578	-.00258	+.00051	.00354	.00651	.00944
	84	-.00505	-.00218	.00055	.00323	.00579	.00829		84	-.00580	-.00264	.00038	.00332	.00617	.00896
	99	-.00506	-.00222	.00049	.00309	.00561	.00805		99	-.00581	-.00268	.00031	.00321	.00604	.00870
C_{m_n}	56	-.00155	.00096	.00332	.00564	.00792	.01018		56	-.00182	+.00091	.00346	.00597	.00845	.01075
	84	-.00157	.00087	.00323	.00549	.00770	.00980		84	-.00183	.00080	.00336	.00580	.00816	.01049
	99	-.00157	.00088	.00322	.00543	.00755	.00964		99	-.00184	.00078	.00330	.00570	.00804	.01021
C_{m_p}	55	.00021	.00398	.00774	.01174	.01591	.02046		56	.00031	.00445	.00862	.01308	.01773	.02280
	84	.00046	.00488	.00953	.01465	.02024	.02619		84	.00063	.00553	.01075	.01650	.02275	.02940
	99	.00060	.00535	.01053	.01628	.02264	.02946		99	.00080	.00611	.01194	.01839	.02552	.03315
C_{mo}	All	-.02323	-.02323	-.02323	-.02323	-.02323	-.02323		All	-.02323	-.02323	-.02323	-.02323	-.02323	-.02323
C_{mp} (Direct)	All	-0	-.00006	-.00011	-.00016	-.00024	-.00036		All	- 0	-.00006	-.00011	-.00016	-.00024	-.00036
Total	56	-.03518	-.02856	-.02091	-.01193	-.00176	.00975		56	-.02154	-.00229	.01764	.03855	.06031	.08292
C_m	84	-.03522	-.02869	-.02117	-.00940	.00173	.01415		84	-.02126	-.00149	.01921	.04096	.06368	.08725
(Tail Off)	99	-.03523	-.02734	-.01850	-.00811	.00366	.01663		99	-.02113	-.00105	.02011	.04233	.06589	.08969

TABLE 7.5 Calculated Pitching Moment, tail off.

		FORWARD C.G.							AFT C.G.						
$\bar{C}_L$	Power	0.2	0.4	0.6	0.8	1.0	1.2		Power	0.2	0.4	0.6	0.8	1.0	1.2
	56	-.01209	-.00987	-.00735	-.00415	-.00064	.00334		56	-.00749	-.00062	.00645	.01372	.02161	.02975
C_{L_T}	84	-.01215	-.00985	-.00738	-.00320	.00060	.00499		84	-.00773	-.00045	.00700	.01479	.02281	.03122
	99	-.01205	-.00954	-.00649	-.00286	.00139	.00587		99	-.00750	-.00019	.00717	.01518	.02360	.03219
	56	-.03479	-.02837	.02102	.01169	.00150	-.00998		56	+.02122	.00196	-.01794	-.03840	-.06047	-.08307
C_{m_T}	84	-.03496	-.02831	.02111	.00900	-.00202	-.01464		84	.02189	.00149	-.01947	-.04137	-.06381	-.08715
	99	-.03468	-.02743	-.01857	00803	-.00425	-.01713		99	.02125	.00077	-.01994	-.04245	-.06601	-.08986
	56	-.00039	-.00019	.00011	-.00024	-.00027	-.00023		56	-.00031	-.0003	-.00029	-.00015	-.00010	-.00015
ΔC_m	84	-.00025	-.00037	-.00005	-.00040	-.00028	-.00049		84	.00063	0	.00026	.00040	-.00013	.0001
	99	-.00055	-.00008	.00006	.000078	.00060	.00050		99	.00012	-.00027	.00017	-.00012	-.00012	-.00017
	56	.006	.003	-.0016	.0036	.004	.003		56	.004	.005	.004	+.002	.002	.002
$\Delta\bar{n}$	84	.004	.006	.0001	.006	.004	.007		84	-.009	0	.003	.006	.002	-.0015
	99	.008	-.001	.001	.0012	.009	.007		99	-.0018	.004	-.002	.002	+.002	+.002
	56	-205	- 84	- 42	- 18	- 2	9		56	- 132	- 5	39	60	76	87
L_T lbf	84	-206	- 84	- 42	- 14	2	14		84	- 136	- 4	41	65	80	91
	99	-204	- 81	- 37	- 12	5	17		99	- 132	- 2	42	67	83	92

TABLE 7.5 (Concluded) Pitching Moment due to tail, and total

8. Aeroelasticity of the Fuselage

There are two possible sources of aeroelastic distortion which may affect the tailplane angle relative to the aircraft datum line. The first is a bending of the fuselage under the load imposed on it by the tail, the second is the local distortion of the structure around the tailplane mounting.

The fuselage bending can be estimated by considering the fuselage under load aft of the wing spar.

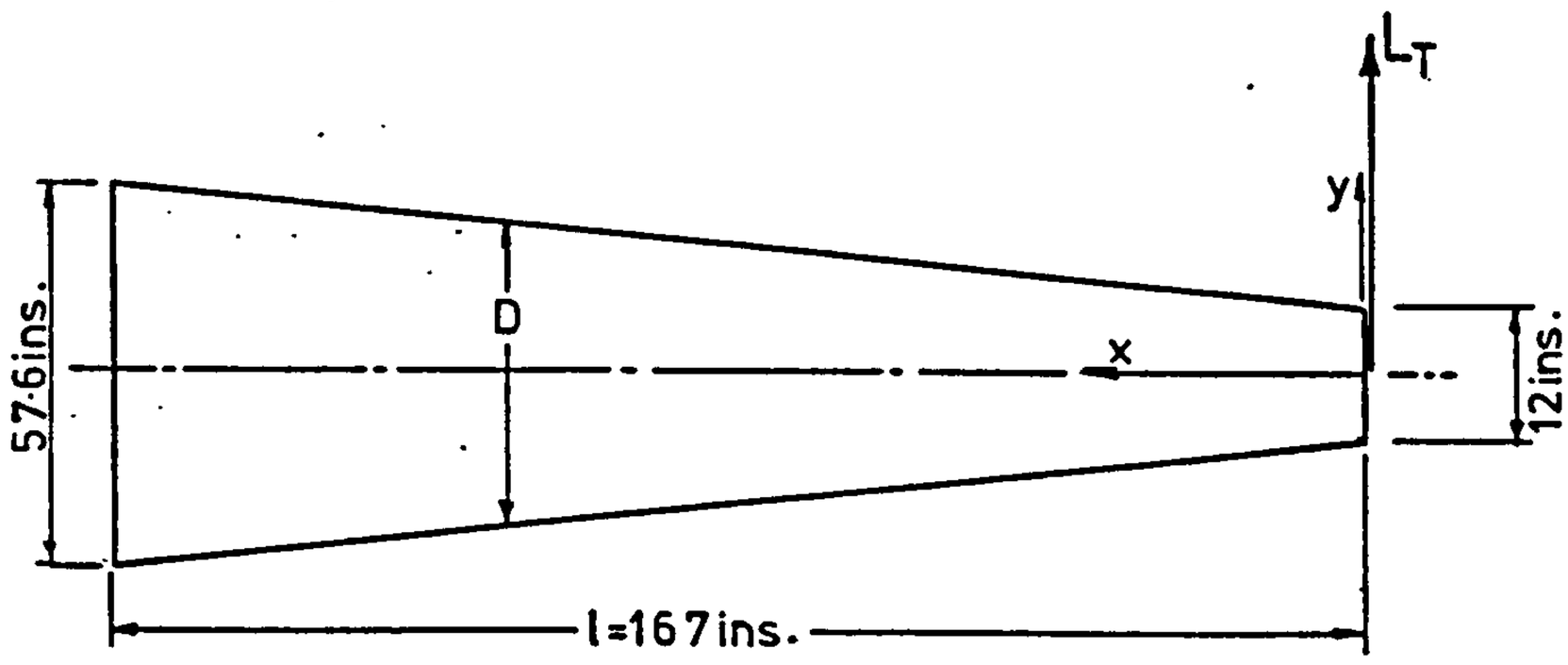

The fuselage is approximated to a thin walled circular cone tapering from 57.6 ins diameter at the wing spar to 12 ins diameter at the tail. The tail load acts normal to the cone axis and the hinge moment is taken out by the pilots control since the tailplane is all moving.

Taking the origin at the tail of the aircraft the slope of the cone axis will be given by

$$\frac{dy}{dx} = \frac{1}{E} \int_0^{\ell} \frac{M}{I} \, dx$$

where the moment $M = L_T x$

and the moment of inertia of the fuselage at station x,

$$I = \frac{\pi D^3 t}{8}$$

where t is the skin thickness, 20 g = 0.036 ins.

The diameter D varies with x and is given by

$$D = 0.273x + 12$$

The integral becomes

$$\frac{dy}{dx} = \frac{8L_T}{\pi tE} \int_0^{\ell} \frac{x\ dx}{(0.273x + 12)}$$

and when evaluated gives

$$\frac{dy}{dx} = 0.000142\ L_T \text{ degrees}$$

The maximum tail load is of the order of 200 lbf, see fig.7.5, thus the maximum tail slope will be of the order of 0.028 degrees under the most severe loading case. Since the fuselage has been assumed to be a thin walled circular cone it is likely that the slope will have been over-estimated. The stiffening effect of the stringers may reduce the deflection to an even smaller value. The estimated error is outside the limit of measurement of tailplane position.

The calibration of the tailplane transducer is performed on the ground under zero tailplane load conditions. In flight the tailplane lift becomes greater than its weight and the reversed static force may produce small local distortion of the structure and there may be some backlash in the tailplane hinge bearings due to wear and mechanical tolerance. It was seen in section 7 that when a positive tail lift occurred in excess of the tailplane weight there was a tendency for the tail position to shift about 0.2^0. Fig.8.1 shows the installation of the transducer on the aircraft and Fig.8.2 gives the relevant dimensions of the components. A deflection of 0.2^0 in control position corresponds to a potentiometer shaft travel of 0.02 ins, or 0.5mm, which is slightly less than the thickness of an adult human thumb nail. It is not unreasonable to suppose that reversal of tail lift loads could cause local structural distortions of this magnitude.

Without the original aircraft available for tests it is not possible to verify these estimates in practice. Also the backlash in the elevator tab system will be peculiar to the test aircraft and may be time dependent as wear and servicing take place.

FIG.8.1 Tailplane Position Transducer Installation

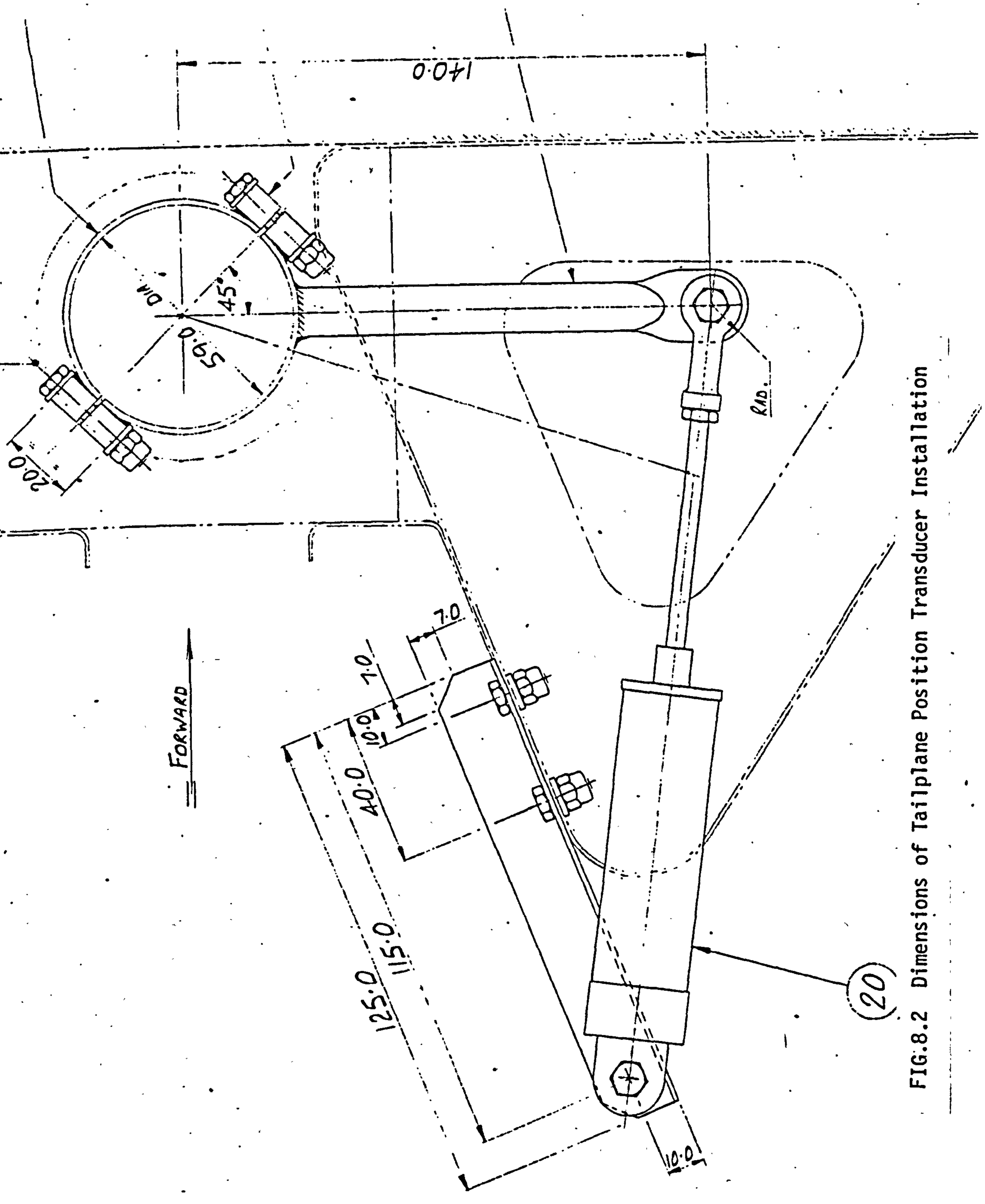

FIG.8.2 Dimensions of Tailplane Position Transducer Installation

9. Controls Free Static Stability

So far this analysis has only been applied to the controls fixed static stability, i.e. the static stability relating to control position to trim with incidence change. The parallel analysis relating to the control force to trim with incidence, controls free static stability, is fundamentally similar. The only difference in the analysis is that the tail lift is expressed in terms of hinge moment coefficient instead of control angle. This modifies the values of the tail lift parameters and the tail lift equation can now be expressed as

$$C_{L_T} = \bar{a}_1 \alpha_T + \frac{a_2}{b_2} C_H + \bar{a}_3 \beta \qquad (9.1)$$

where $\bar{a}_1 = a_1(1 - \frac{a_2 b_1}{b_2 a_1})$ and $\bar{a}_3 = a_3(1 - \frac{a_2 b_3}{b_2 a_3})$ (9.2)

The factor $(1 - \frac{a_2 b_1}{b_2 a_1})$ is known as the controls free factor.

Replacing the values of a_1 and a_3 with $\bar{a}_1$ and $\bar{a}_3$ and introducing a_2/b_2 instead of a_2 in the trim equations will enable the same form of analysis to be completed

Considerable difficulty was experienced in the measurement of the control forces necessary to find the elevator hinge moment and the data obtained was not of sufficiently good quality to justify a theoretical analysis. The reasons for the poor quality of the data have not been fully resolved but can be attributed in part to the very high level of friction in the control circuit. Fig.9.1 shows the measured control loads for increasing and decreasing load application and the calculated nose-down spring load under zero airload conditions. The applied loads vary by about 50% of the mean. These characteristics were measured on the ground and not in a flight environment which could cause further variation in the control friction due to temperature effects on cable tensions and lubricants.

The definition of the controls free stability criterion is important since the requirement for airworthiness considerations and that for static stability are not necessarily compatible. The controls free static stability is determined by the trim curve of elevator hinge

moment to trim against incidence, the slope of the curves giving the value of m_w under controls free conditions. The accepted limit of stability, $E_1 = 0$, is thus given by the trim curve slope being zero, point 1 curve A fig 9.2.

The airworthiness requirement, ref.4, is based on the pilot stick force, stating that, "... the stick force versus airspeed gradient must be positive.", (i.e. having a slope indicating stability, actually negative), fig.9.3. At the limit of stability therefore the stick force, P_η, will be constant with speed and when this is translated onto the C_H versus $\bar{\alpha}$ diagram it produces a fan of constant P_η lines radiating from the origin, fig.9.2. This implies that the limit of stability based on the airworthiness requirement is defined by the point of tangency between the trim curve and a constant P_η radial, point 2 curve A fig.9.2.

The only occasion when the two conditions are compatible is when the control force is zero at the point of tangency, point 3 , curve B, fig.9.2. This condition cannot be met for two C.G.loadings since there will always be a difference in control force to trim for a fixed tab setting at any given incidence. The out of trim force held in the measurement of the controls free static stability will therefore have an important bearing on the relationship between airworthiness requirement and static stability criterion.

The airworthiness test for static stability also makes the assumption that the lift curve slope is constant since the test is defined in terms of airspeed and not incidence. The slope of the trim curve will be a function of airspeed and therefore it will not be possible to deduce a value of the derivative m_w from the trim curve slope. This method of assessment of static stability is designed to show the handling quality of the aircraft rather than its static stability. It is not a non-dimensional method and is only intended as a test for handling acceptability and not as a means of measurement of the aerodynamic characteristics of the aircraft.

It has been shown that, in the case of aircraft considered, the effects of power are destabilising and this will be the case for all tractor propeller aircraft with the propeller forward of the C.G. The fuselage and nacelles will also contribute a destabilising effect. Unless these effects are estimated and included at the design stage the

the aircraft is likely to be less stable than intended and will require an increase in static stability to comply with the airworthiness requirements. Since the requirements for light aircraft only call for controls free static stability to be demonstrated compliance can normally be shown by modifying the control hinge moment characteristics by the use of springs, weights or geared tabs. These methods of correcting the controls free static stability are described in detail in ref.9, chapters 8 and 10. Although the controls free static stability may be made acceptable in this way the controls fixed static stability will remain very low. This gives the effect of a "pressure sensitive" control which maintains trim through control force rather than by control movement. Although this is not unacceptable in principle it may produce unpleasant handling characteristics to pilots of low experience. It is preferable to provide a positive controls fixed static stability so that the natural control feel in terms of force and movement is retained.

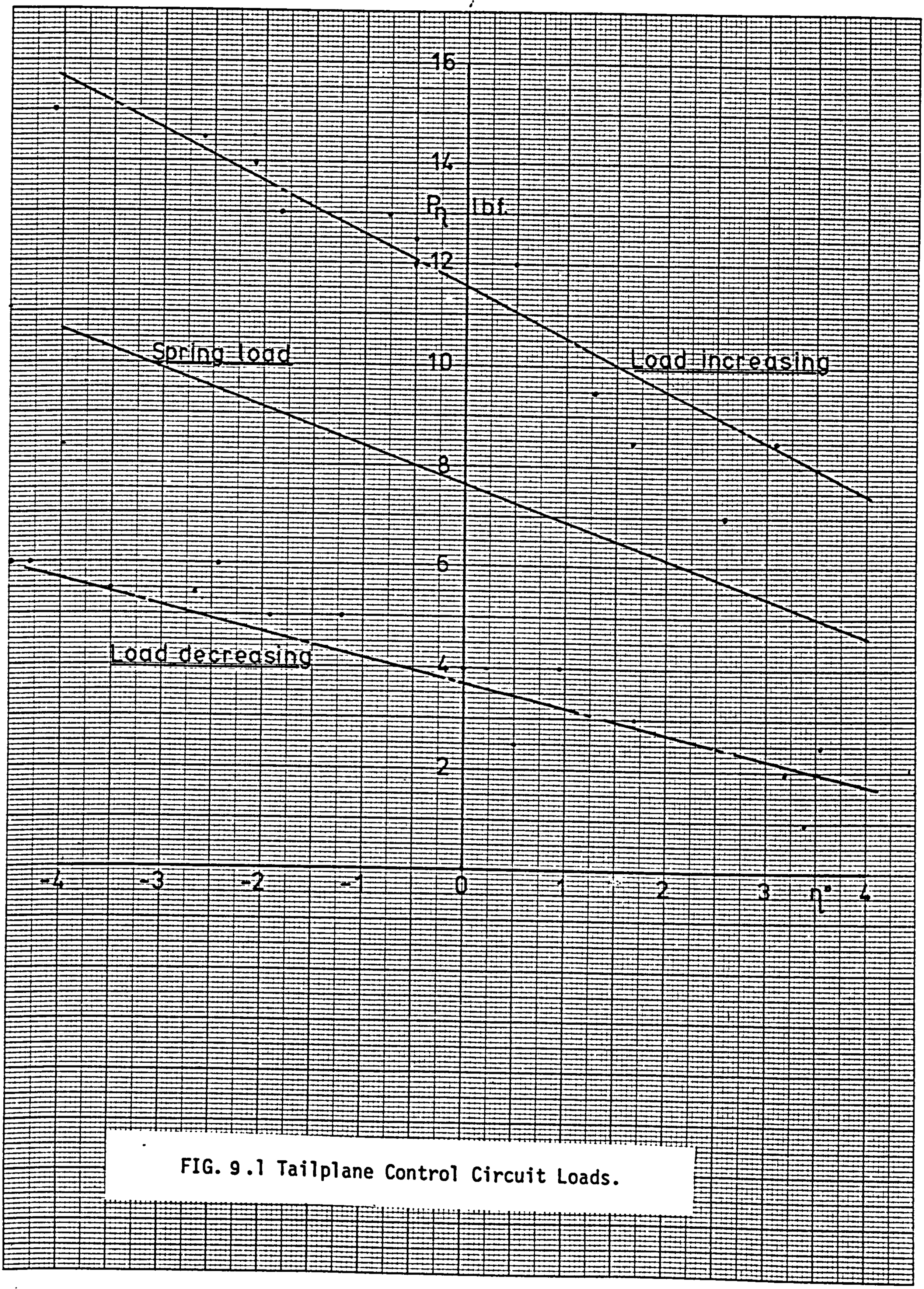

FIG. 9.1 Tailplane Control Circuit Loads.

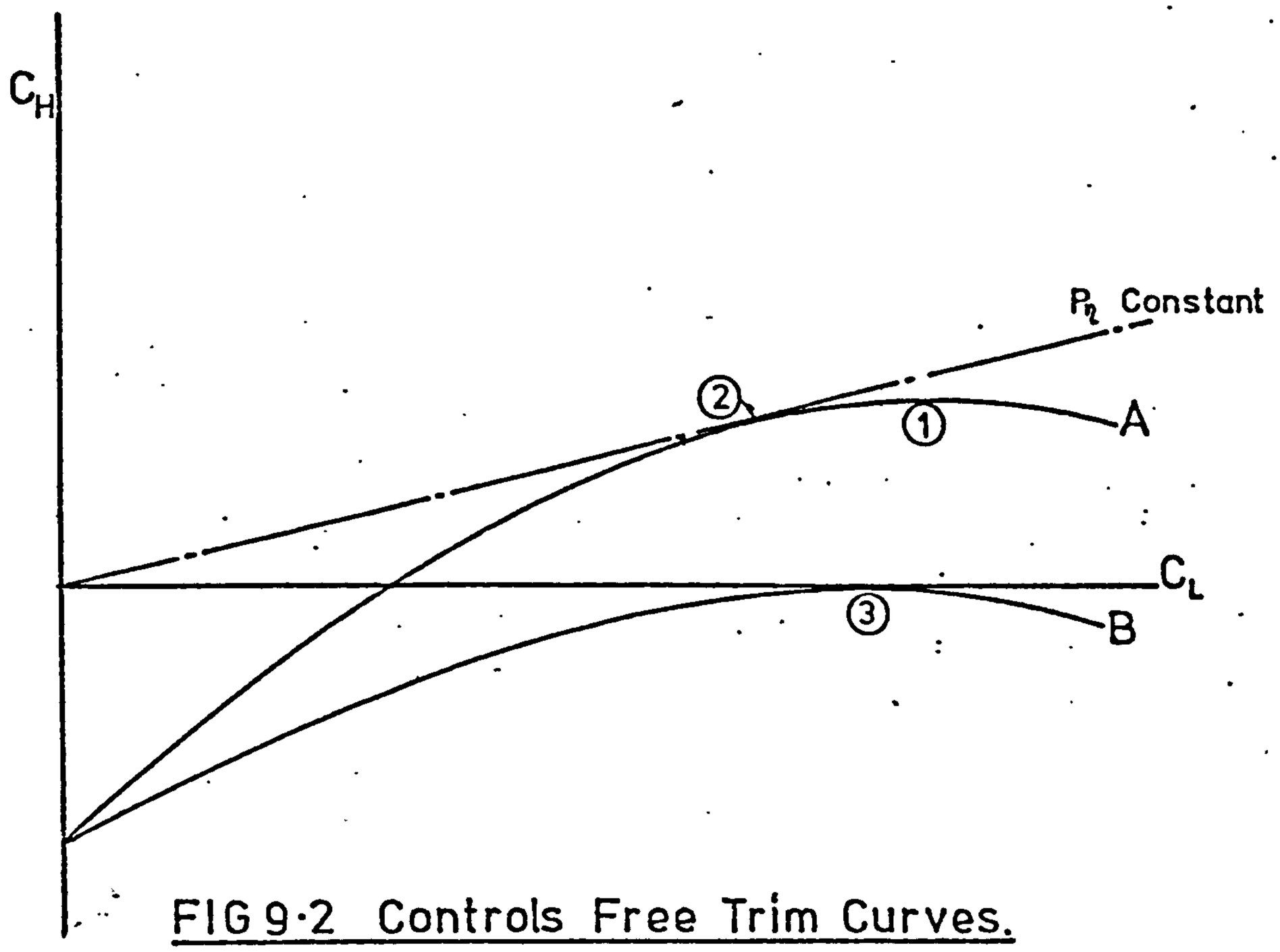

FIG 9·2 Controls Free Trim Curves.

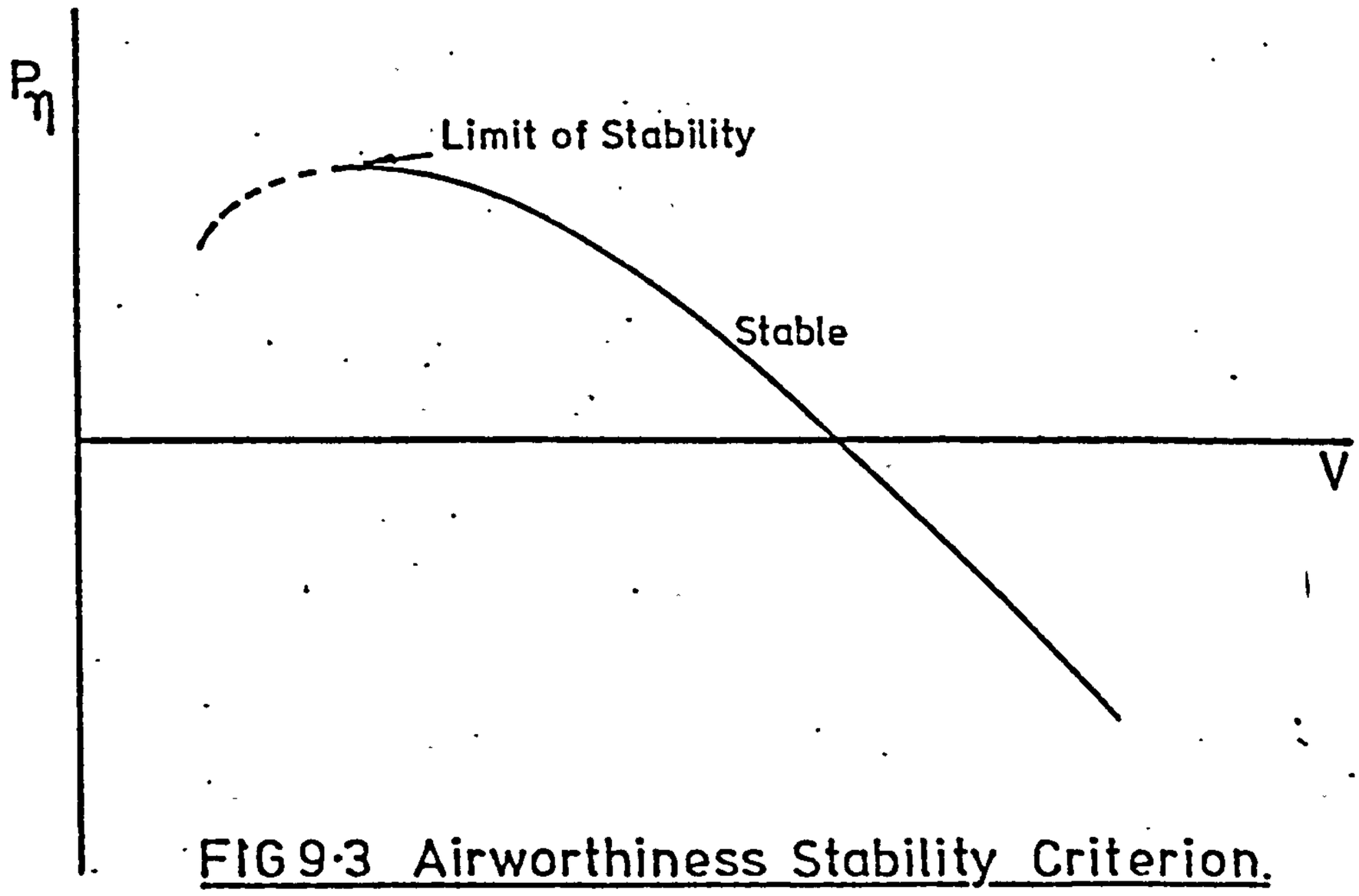

FIG 9·3 Airworthiness Stability Criterion.

10. Conclusions

Although the detailed analysis of the static stability trim curves relates to only one aircraft type some generalised conclusions can be drawn in addition to some conclusions which may be specific to aircraft type.

1. The original trim curves, $\bar{\eta}$ against C_L, showed a tendency towards a reduction in slope as speed decreased whereas the calculated curves, $\bar{\eta}$ against α, were linear. The difference is seen to arise from the assumption of a linear lift characteristic in the simple analysis of the aircraft. It has been shown that the lift curve slope is non-linear under the effects of power and C.G. location, thus the assumed proportionality between $d\bar{\eta}/d\bar{C}_L$ and $d\bar{\eta}/d\bar{\alpha}$ is not acceptable.

2. The simplifying assumptions of the linearised model led to a serious overestimation of the expected level of static stability. This was due mainly to the omission of the propeller normal force terms and slipstream interference effects, both of these were strongly destabilising. To a lesser extent the fuselage and nacelle also showed destabilising effects.

3. If the non-linear model of the aircraft is to be used then the full non-linear equations of trim must be solved. These will include the effects of compressibility, sect.6.1, aeroelasticity, sects.6.2 & 8, incidence, Part II sect.1, and Power, Part II, sects.2,3 & 4. The solution of the non-linear equations of trim has been shown to match the measured trim curve data very closely thus verifying that the methods developed to account for the discrepancies are acceptable.

4. As a consequence to 1, the trim curves drawn in terms of $\bar{C}_L$ are not valid. These should be drawn in terms of trim incidence, α, to determine the value of $d\bar{C}m/d\bar{\alpha}$ and hence $m'_{w.eff}$. Also since $m'_{w.eff}$ contains a speed dependent term, it is important to consider the data from the different C.G.locations at the same weight and power. This will make the data compatible for comparison and also for estimation of the neutral point. The calculated trim curves, $\bar{\eta}$ against $\bar{\alpha}$, are linear and the local slope is seen to be a function of C.G.position and engine

power setting. This indicates that under the conditions of constant weight and power the value of $m'_{w.eff}$ is independent of incidence.

Measurement of trim curve data for airworthiness purposes should take into account the effect of weight and power changes on the trim curve slope.

5. Generalised effects of power on static stability cannot be adequately estimated since the speed-incidence relationship needs to be known to determine the normal force and slipstream contributions. Also both contributions are affected by the airframe and are valid only for the aircraft considered. In particular the upwash field ahead of the wing contributes to the normal force and direct pitching moment produced by the propeller.

6. Although the general aeroelastic bending of the fuselage has been shown to be negligible in the case of the test aircraft local structural distortion and mechanical tolerance in bearings may produce significant errors in measured data. At the aft C.G. the elevator movement required to trim over the whole speed range was only ½ degree. Any systematic error due to loading of the tail may seriously distort the trim curve and the calibration of the transducer measuring the control position should include a check to see if it is sensitive to applied load at the tail.

7. The assessment of the longitudinal static stability from trim curves remains a very simple technique for the general assessment of the handling qualities of a light aircraft. It is capable of producing results in a short time and with the minimum of equipment and pilot skill. To produce reliable results however it is necessary to record more than the minimum data. To establish steady flight conditions in the trim requires a minimum of airspeed, altitude and normal acceleration to be recorded. Pitch attitude and pitch rate are also desireable. It has been shown to be preferable to draw the trim curves in terms of incidence rather than lift coefficient. If it is not possible to measure incidence directly then the lift incidence characteristic should be determined for the test conditions to correct the measured data to incidence terms for compatibility.

If the considerations of this thesis are borne in mind when planning a series of longitudinal handling trials then the prediction of the neutral points and limits of C.G. travel will be improved. This will help to eliminate any possible flight conditions of loading, power and speed that will lead to doubtful handling characteristics which may otherwise remain undetected.

References

1. ETKIN, B — Dynamics of Atmospheric Flight, Ch.6. Wiley, 1972

2. ESHELBY,M.E. — An Instrumentation system to measure the Stability Characteristics of Light Aircraft Cranfield Aero Memo No.101

3. BABISTER,A.W. — Aircraft Stability and Control Pergamon 1961

4. - — British Civil Airworthiness Requirements Section K, Chapter K2. C.A.A.

5. FISHER,L.R. — Approximate corrections for the effects of compressibility on the subsonic stability derivatives of swept wings NACA Tech Note 1854 (1949)

6. WOLOWICZ,C.H. & YANCEY,R.B. — Longitudinal Aerodynamic Characteristics of Light, Twin-Engined, Propeller-driven Airplanes NASA TN-D6800 1972

7. FINK,M.P. & FREEMAN,D.C. — Full-Scale Wind Tunnel Investigation of Static Longitudinal and Lateral Characteristics of a Light, Twin-Engine Airplane NASA TN-D4983 1969

8. - — Detail Specification for 10-320 series Engines Avco Lycoming Spec.No.2287-F 1966 Avco Lycoming Co. Williamsburg Pa, U.S.A.

9. IRVING,F.G. — An Introduction to the Longitudinal Static Stability of Low-Speed Aircraft. Pergamon Press 1966

CRANFIELD INSTITUTE OF TECHNOLOGY

Aerodynamics Division

College of Aeronautics

Ph.D. Thesis

M. E. ESHELBY.

A Non-Linear Analysis of the Longitudinal Static Stability of Light, Multi-Engined Aircraft

Part II

January 1979

CONTENTS

PART II

Section I

The Correction of Longitudinal Static Stability Trim Curves for Airframe Design

Abstract from Cranfield Report Aero No.30

CRANFIELD INSTITUTE OF TECHNOLOGY

The Correction of Longitudinal Static Stability Trim Curves for Airframe Design

(Abstract from Cranfield Report Aero No.30)

by

M. E. Eshelby

Aerodynamics Division

College of Aeronautics

SUMMARY

The longitudinal static stability of an aircraft is usually assessed by means of trim curves of elevator position and hinge moment against lift coefficient. From the simple, classical theory the trim curves should be linear but in practice it is common to find some curvature which indicates a variable level of static stability with incidence. The purpose of this report is to determine a method of predicting the degree of curvature which may be expected to occur due to the deviation of the design of the aircraft from the simplified model used in the theoretical analysis.

It is shown that by using easily estimated aerodynamic data and aircraft design parameters it is possible to determine correction functions which account for a very large proportion of the curvature of the measured trim curves. Use of these corrections at the design stage could predict the variation in aircraft handling qualities which could save later modifications to the control system. Alternatively the estimation of control parameters from the trim curve data can be considerably improved by first accounting for non-linearities in the measured data.

A sample analysis is applied to flight measured data to show the degree of correction which may be expected by this method.

CONTENTS

Notation

A	Aspect Ratio
a	Lift curve slope
C_L, C_D, C_m	Non-dimensional Force and Moment Coefficients (lift, drag, pitching moment respectively)
$\bar{c}$	Mean aerodynamic chord (m.a.c.)
D	Drag Force
e	N.A.C.A. span efficiency factor
$F(C_L)$	Stability factor, see eqn.27
h	C.G.position aft of L.E. of m.a.c.
h_o	Aerodynamic centre
L	Lift force
l_T	Tail arm
M	Pitching moment
p,q	Coordinates of drag force
S	Wing area
S_T	Tailplane area
$\bar{V}$	Tail volume coefficient
y	Height of tailplane above m.a.c.
z	Height of C.G. above m.a.c.
α	Incidence
ϵ	Downwash at the tail
η	Elevator angle
β	Elevator tab angle
η_T	Tailplane setting angle

Subscripts

o	Zero lift condition
1 2 3	Tailplane, elevator and tab respectively
C.G.	About the C.G.
i	Induced or lift dependent (drag)
M	Measured, or modified theory
S	Simple theory
T	Tail
W	Wing, or aircraft less tail
z	Lift independent (drag)

Correction of Trim Curves for Airframe Design

1. Development of the Pitching Moment Equation

The classical theory of longitudinal static stability assumes that the aircraft is of a very simple design and that the change of incidence with speed does not affect the pitching moment equation. In practice this is unlikely to be achieved and there will be incidence dependent effects on the pitching moment equation which will lead to a variable degree of static stability with speed.

The simple representation of the aircraft, fig.1a, considers only the pitching moment of the forces acting normal to the flight path and since all components of the aircraft are assumed to lie along the extended m.a.c. the pitching moment equation about the C.G. can be written as

$$M_{CG} = M_o + L_W(h - h_o)\bar{c} - L_T\left[l_T - (h - h_o)\bar{c}\right]$$

which can be expressed in coefficient terms in the form

$$C_{mCG} = C_{mo} + C_{LW}(h - h_o) - C_{LT}\frac{S_T}{S}\left[\frac{l_T}{\bar{c}} - (h - h_o)\right] \qquad (1)$$

Now the lift force of the complete aircraft, L, is given by

$$L = L_W + L_T$$

and thus

$$C_L = C_{LW} + C_{LT}\frac{S_T}{S}$$

hence, from (1)

$$C_{mCG} = C_{mo} + C_L(h - h_o) - \bar{V}\,C_{LT} \qquad (2)$$

where $\bar{V} = \frac{S_T l_T}{S\,\bar{c}}$, the tail volume coefficient.

Equation (2) represents the pitching moment equation in its simple form.

A more realistic model of the aircraft is shown in fig.1b; here the datum line is still the zero lift line through the aerodynamic centre of the wing but the centre of gravity is a distance $z\bar{c}$ above the datum and the tailplane a distance $y\bar{c}$ above the datum. The drag of the wing and tail can be considered to act at the aerodynamic centres of each respectively and the drag of the fuselage, together with any interference

drag acts at a point $p\bar{c}$ aft of the leading edge of the m.a.c. and $q\bar{c}$ above the m.a.c. As the incidence increases, fig.1c, the moment arms of the forces about the C.G. vary and the pitching moment equation will be modified. The effect of each force can be assessed and included in the general pitching moment equation.

1.1 Moment of the Lift Force L_W about the C.G.

From fig.2. the moment arm of the lift force of the aircraft less tail about the C.G. is given by A'C where

$$A'C = \{(h - h_o)\cos\alpha + z\sin\alpha\}\,\bar{c} \qquad (3)$$

and the pitching moment about the C.G. in coefficient terms will be given by

$$C_{mCG} = C_{LW}\{(h - h_o)\cos\alpha + z\sin\alpha\} \qquad (4)$$

1.2 Moment of the Tail LiftForce L_T about the C.G.

From fig.3 the moment arm of the tail lift force about the C.G., GC is given by

$$GC = -[\{l_T - (h - h_o)\bar{c}\}\cos\alpha + (y - z)\bar{c}\sin\alpha] \qquad (5)$$

thus the pitching moment about the C.G. will be

$$C_{mCG} = -C_{LT}\frac{S_I}{S}\left[\left\{\frac{l_I}{\bar{c}} - (h - h_o)\right\}\cos\alpha + (y - z)\sin\alpha\right] \qquad (6)$$

1.3 Moment of Wing Drag about the C.G.

The wing drag can be considered to be represented by a lift independent drag D_{ow} and a lift dependent or vortex drag, D_{iw}, both acting through the aerodynamic centre of the wing. From Fig.4 the moment arm CO is given by

$$CO = \{(h - h_o)\sin\alpha - z\cos\alpha\}\,\bar{c} \qquad (7)$$

and the pitching moment about the C.G. is given by

$$C_{mCG} = C_{DW}\{(h - h_o)\sin\alpha - z\cos\alpha\} \qquad (8)$$

1.4 Moment of the tail drag about the C.G.

From fig.3 the moment arm GD of the tail drag about the C.G. can be expressed as

$$GD = -\{l_T - (h - h_o)\,\bar{c}\}\sin\alpha + (y - z)\,\bar{c}\cos\alpha \qquad (9)$$

and the moment of the drag force about the C.G. thus becomes

$$C_{mCG} = -C_{DT}\frac{S_I}{S}\left[\left\{\frac{l_I}{\bar{c}} - (h - h_o)\right\}\sin\alpha - (y - z)\cos\alpha\right] \qquad (10)$$

1.5 Moment of the Fuselage drag about the C.G.

The residual drag D_Z of the aircraft is lift independent and can be mainly attributed to fuselage profile drag and interference drag which can be assumed to act at a point $p\bar{c}$ aft and $q\bar{c}$ above the leading edge of the mean aerodynamic chord, fig 5. The moment arm QT is given by

$$QT = \{(q - z)\cos\alpha + (h - p)\sin\alpha\}\,\bar{c} \qquad (11)$$

and the moment of the drag D_Z is given by

$$C_{mCG} = C_{DZ}\{(q - z)\cos\alpha + (h - p)\sin\alpha\} \qquad (12)$$

2. The Modified Pitching Moment Equation

By adding the pitching moment contributions from section 1 the modified pitching moment equation is given by

$$\begin{aligned} C_{mCG} = {} & C_{mo} + C_{LW}\{(h - h_o)\cos\alpha + z\sin\alpha\} \\ & - C_{LT}\frac{S_I}{S}\left[\left\{\frac{l_I}{\bar{c}} - (h - h_o)\right\}\cos\alpha + (y - z)\sin\alpha\right] \\ & + C_{DW}\{(h - h_o)\sin\alpha - z\cos\alpha\} \\ & - C_{DT}\frac{S_I}{S}\left[\left\{\frac{l_I}{\bar{c}} - (h - h_o)\right\}\sin\alpha - (y - z)\cos\alpha\right] \\ & + C_{DZ}\{(q - z)\cos\alpha + (h - p)\sin\alpha\} \end{aligned} \qquad (13)$$

Now in terms of the complete aircraft the force coefficients can be expressed as

$$C_L = C_{LW} + C_{LT}\frac{S_I}{S} \qquad (14)$$

and $$C_D = C_{DW} + C_{DT}\frac{S_I}{S} + C_{DZ}$$

thus from 13, separating the terms in $(h - h_o)$ and z,

$$C_{mCG} = C_{mo} + (h - h_o)\{ C_L\cos\alpha + C_D\sin\alpha \} + z\{ C_L\sin\alpha - C_D\cos\alpha\}$$
$$- \bar{V}\{ C_{LT}\left[\cos\alpha + \frac{\bar{c}y}{l_T}\sin\alpha\right] + C_{DT}\left[\sin\alpha - \frac{\bar{c}y}{l_T}\cos\alpha\right]\}$$
$$+ C_{DZ}\{ q\cos\alpha + (h_o - p)\sin\alpha\} \qquad (15)$$

Here C_L and C_D are the flight measured lift and drag coefficients respectively and C_{LT} and C_{DT} are the tail lift and drag coefficients. C_{DZ} is the drag due to the fuselage and interference. Eqn.15 can be compared with eqn.2 to show the additional terms due to drag and incidence.

Writing C_{LT} and C_{DT} in the form

$$C_{LT} = C_{LTo} + \frac{dC_{LT}}{d\alpha}.\alpha \qquad (16)$$

and
$$C_{DT} = C_{DTo} + \frac{dC_{DT}}{d\alpha}.\alpha \qquad (17)$$

where subscript o refers to the zero lift incidence condition,

Letting

$$\bar{A} = \cos\alpha + \frac{\bar{c}y}{l_T}\sin\alpha$$
$$\text{and} \quad \bar{B} = \sin\alpha - \frac{\bar{c}y}{l_T}\cos\alpha \qquad (18)$$

such that $-\bar{B} = \frac{d\bar{A}}{d\alpha}$ and $\bar{A} = \frac{d\bar{B}}{d\alpha}$,

$$\text{then} \quad \frac{d}{d\alpha}(\bar{A}C_{LT}) = -C_{LT}\bar{B} + \frac{dC_{LT}}{d\alpha}\bar{A} \qquad (19)$$

$$\text{and} \quad \frac{d}{d\alpha}(\bar{B}C_{DT}) = C_{DT}\bar{A} + \frac{dC_{DT}}{d\alpha}\bar{B}. \qquad (20)$$

Differentiating (15) with respect to α gives the static stability criterion $\left[dC_m/d\alpha\right]_M$, where subscript M refers to the modified theory,

$$\left[\frac{dC_m}{d\alpha}\right]_M = (h-h_o)\left\{ -C_L\sin\alpha + C_D\cos\alpha + \frac{dC_L}{d\alpha}\cos\alpha + \frac{dC_D}{d\alpha}\sin\alpha \right\}$$
$$+ z\left\{ C_L\cos\alpha + C_D\sin\alpha + \frac{dC_L}{d\alpha}\sin\alpha - \frac{dC_D}{d\alpha}\cos\alpha \right\}$$
$$- \bar{V}\left\{ - C_{LTo}\bar{B} + C_{DTo}\bar{A} + \frac{dC_{LT}}{d\alpha}(\bar{A} - \bar{B}\alpha) + \frac{dC_{DT}}{d\alpha}(\bar{B} + \bar{A}\alpha)\right\}$$
$$+ C_{DZ}\{ - q\sin\alpha + (h_o - p)\cos\alpha\} \qquad (21)$$

Assuming the drag of the aircraft and each lift producing component to be of the form.

$$C_D = C_{Do} + \frac{C_L^2}{\pi Ae} \tag{22}$$

where C_{DO} is the zero lift drag and e is the span efficiency factor, (21) can be written as

$$\left[\frac{dC_m}{d\alpha}\right]_M = (h - h_o)\left\{ -C_L \sin\alpha + C_D\cos\alpha + a\cos\alpha + \frac{2aC_L}{\pi Ae}\sin\alpha\right\}$$

$$+ z\left\{ C_L\cos\alpha + C_D\sin\alpha + a\sin\alpha - \frac{2aC_L}{\pi Ae}\cos\alpha \right\}$$

$$- \bar{V}\left\{ -\bar{B}C_{LTo} + \bar{A}C_{DTo} + \frac{dC_{LT}}{d\alpha}\left[(\bar{A} - \bar{B}\alpha) + \frac{2C_{LT}}{(\pi Ae)_T}(\bar{B} + \bar{A}\alpha)\right]\right\}$$

$$+ C_{DZ}\{-q\sin\alpha + (h_o - p)\cos\alpha\} \tag{23}$$

In the linear region of the C_L - α relationship the incidence can be expressed as

$$\alpha = C_L/a \tag{24}$$

where α is measured from the zero lift incidence.

Expressing sin α and cos α in series form and using eqn (24) gives

$$\text{Sin } \alpha = \frac{C_L}{a} - \frac{C_L^3}{6a^3} + \frac{C_L^5}{120a^5} - \cdots\cdots\cdots$$

$$\text{and} \quad \text{Cos } \alpha = 1 - \frac{C_L^2}{2a^2} + \frac{C_L^4}{24a^4} - \cdots\cdots\cdots \tag{25}$$

Hence eqn (23) can be written in terms of the flight lift coefficient using (22) and (25), neglecting terms above $\frac{C_L^3}{a^3}$

$$\left[\frac{dC_m}{d\alpha}\right]_M = (h - h_o)\left\{ (a + C_{Do}) + C_L^2\left(\frac{3}{\pi Ae} - \frac{3}{2a} - \frac{C_{Do}}{2a^2}\right) + C_L^4\left(\frac{5}{24a^3} - \frac{5}{6a^2\pi Ae}\right)\right\}$$

$$+ z\left\{ C_L\left(2 + \frac{C_{Do}}{a} - \frac{2a}{\pi Ae}\right) + C_L^3\left(\frac{2}{a\pi Ae} - \frac{2}{3a^2} - \frac{C_{Do}}{6a^3}\right) + C_L^5\left(\frac{1}{6a^3\pi Ae}\right)\right\}$$

$$- \bar{V}\left\{ C_{LTo}\left[-\frac{C_L}{a} + \frac{C_L^3}{6a^3} + \frac{\bar{c}y}{l_T}\left(1 - \frac{C_L^2}{2a^2}\right)\right] + C_{DTo}\left[1 - \frac{C_L^2}{2a^2} + \frac{\bar{c}y}{l_T}\left(\frac{C_L}{a} - \frac{C_L^3}{6a^3}\right)\right]\right.$$

$$\left. + \frac{dC_{LT}}{d\alpha}\left[1 - \frac{3C_L^2}{2a^2} + \frac{\bar{c}y}{l_T}\left(\frac{2C_L}{a} - \frac{2}{3}\frac{C_L^3}{a^3}\right)\right] + \frac{2C_{LT}}{(\pi Ae)_T}\left[\left(\frac{2C_L}{a} - \frac{2C_L^3}{3a^3} - \frac{\bar{c}y}{l_T}\left(1 - \frac{C_L^2}{a^2}\right)\right)\right]\right\}$$

$$+ C_{DZ}\left\{-q\left(\frac{C_L}{a} - \frac{C_L^3}{6a^3}\right) + (h_o - p)\left(1 - \frac{C_L^2}{2a^2}\right)\right\} \tag{26}$$

For convenience (26) can be written in the form

$$\left[\frac{dC_m}{d\alpha}\right]_M = a(h - h_o)\, F_1(C_L) + z\, F_2(C_L) + C_{DZ}\, F_3(C_L)$$

$$- \bar{V}\left\{\frac{dC_{LT}}{d\alpha}\left[F_4(C_L) + C_{LT}\, F_5(C_L)\right] + C_{LTo}\, F_6(C_L) + C_{DTo}\, F_7(C_L)\right\} \qquad (27)$$

where $F_1(C_L) = 1 + \frac{C_{Do}}{a} + C_L{}^2\left(\frac{3}{a\pi Ae} - \frac{3}{2a^2} - \frac{C_{Do}}{2a^3}\right) + C_L{}^4\left(\frac{5}{24a^4} - \frac{5}{6a^3\pi Ae}\right)$

$$F_2(C_L) = C_L\left(2 + \frac{C_{Do}}{a} - \frac{2a}{\pi Ae}\right) + C_L{}^3\left(\frac{2}{a\pi Ae} - \frac{2}{3a^2} - \frac{C_{Do}}{6a^3}\right) + \frac{C_L{}^5}{6a^3\pi Ae}$$

$$F_3(C_L) = -q\left(\frac{C_L}{a} - \frac{C_L{}^3}{6a^3}\right) + (h_o - p)\left(1 - \frac{C_L{}^2}{2a^2}\right)$$

$$F_4(C_L) = 1 - \frac{3C_L{}^2}{2a^2} + \frac{\bar{c}y}{l_T}\left(\frac{2C_L}{a} - \frac{2C_L{}^3}{3a^3}\right)$$

$$F_5(C_L) = \frac{2}{(\pi Ae)_T}\left[\frac{2C_L}{a} - \frac{2C_L{}^3}{3a^3} - \frac{\bar{c}y}{l_T}\left(1 - \frac{C_L{}^2}{a^2}\right)\right]$$

$$F_6(C_L) = -\frac{C_L}{a} + \frac{C_L{}^3}{6a^3} - \frac{\bar{c}y}{l_T}\left(1 - \frac{C_L{}^2}{2a^2}\right)$$

and $$F_7(C_L) = 1 - \frac{C_L{}^2}{2a^2} + \frac{\bar{c}y}{l_T}\left(\frac{C_L}{a} - \frac{C_L{}^3}{6a^3}\right)$$

Eqn.(27) now represents the static stability equation for the complete aircraft and can be compared with the simple version derived by differentiating eqn.(2) with respect to α.

$$\left[\frac{dC_m}{d\alpha}\right]_S = a(h - h_o) - \bar{V}\frac{dC_{LT}}{d\alpha} \qquad (28)$$

The difference between the full expression, eqn (27), and the simple expression, eqn (28), can be accounted for by defining a correction $\Delta\left[\frac{dC_m}{d\alpha}\right]_S$ to the simple expression, thus

$$\left[\frac{dC_m}{d\alpha}\right]_S + \Delta\left[\frac{dC_m}{d\alpha}\right]_S = \left[\frac{dC_m}{d\alpha}\right]_M \qquad (29)$$

From eqns (27), (28) and (29) the correction is given by

$$\Delta\left[\frac{dC_m}{d\alpha}\right]_S = a(h - h_o)[F_1(C_L) - 1] + z\,F_2(C_L) + C_{DZ}\,F_3(C_L) \qquad (30)$$
$$- \bar{V}\left\{\frac{dC_{LT}}{d\alpha}\left[(F_4(C_L) - 1) + C_{LT}F_5(C_L)\right] + C_{LTo}F_6(C_L) + C_{DTo}F_7(CL)\right\}$$

Each of these functions depends only on flight lift coefficient and constant aircraft parameters and so each can be evaluated for the aircraft in a given configuration

3. Correction of Trim Curve Slopes

Since the trim curve slope is normally used as a measure of the aircraft static stability the correction function should be written as a correction to the trim curve slope $\frac{d\bar{\eta}}{dC_L}$ of the aircraft.

Assuming that the tail lift can be written in the form

$$C_{LT} = a_1\alpha_T + a_2 n + a_3\beta \qquad (31)$$

and using eqn (16) this can be expressed as

$$C_{LT} = (a_1\alpha_{To} + a_2 n_o + a_3\beta_o) + (a_1\frac{d\alpha T}{d\alpha} + a_2\frac{dn}{d\alpha} + a_3\frac{d\beta}{d\alpha})\alpha \qquad (32)$$

From eqn (2) when the aircraft is in trim, $C_{mCG} = 0$, the elevator angle to trim $\bar{\eta}$ is given by

$$\bar{V}a_2\bar{\eta} = C_{mo} + C_L(h - h_o) - \bar{V}\left[a_1\alpha_T + a_3\beta\right] \qquad (33)$$

For a constant trim tab angle, β, the trim curve slope $\frac{d\bar{\eta}}{dC_L}$ is given by

$$\bar{V}a_2 a\left[\frac{d\bar{\eta}}{dC_L}\right]_S = a(h - h_o) - \bar{V}a_1\frac{d\alpha I}{d\alpha} \qquad (34)$$

Substituting for C_{LT} from eqn (32) in eqn (15) and performing a similar analysis for the full pitching moment equation gives, for the same conditions,

$$\bar{V}a_2 a\, F_4(C_L)\left[\frac{d\bar{n}}{dC_L}\right]_M = a(h - h_o)F_1(C_L) + z\, F_2(C_L) + C_{DZ}\, F_3(C_L) \qquad (35)$$
$$- \bar{V}\left\{a_1\frac{d\alpha_T}{d\alpha}\left[F_4(C_L) + C_{LT}F_5(C_L)\right] + C_{LTo}F_6(C_L) + C_{DTo}F_7(C_L)\right\}$$

The trim curve slope correction $\Delta\left[\frac{d\bar{n}}{dC_L}\right]_S$ can be defined as

$$\therefore \Delta\left[\frac{d\bar{n}}{dC_L}\right]_S = \left[\frac{d\bar{n}}{dC_L}\right]_M - \left[\frac{d\bar{n}}{dC_L}\right]_S \qquad (36)$$

and therefore from eqns (34) and (35) this is given by

$$\Delta\left[\frac{d\bar{n}}{dC_L}\right]_S = \frac{1}{\bar{V}a_2 a}\left\{a(h - h_o)\left[\frac{F_1(C_L)}{F_4(C_L)} - 1\right] + z\,\frac{F_2(C_L)}{F_4(C_L)} + C_{DZ}\,\frac{F_3(C_L)}{F_4(C_L)}\right.$$
$$\left. - \bar{V}\left[a_1\frac{d\alpha_T}{d\alpha}\cdot C_{LT}\,\frac{F_5(C_L)}{F_4(C_L)} + C_{LTo}\,\frac{F_6(C_L)}{F_4(C_L)} + C_{DTo}\,\frac{F_7(C_L)}{F_4(C_L)}\right]\right\} \qquad (37)$$

Equation (37) represents a full correction to the simple pitching moment equation to account for the deviation of the real aircraft from the simplified theoretical model. It can be seen that each element of the correction is separately assessed and applied, therefore each can be considered on its merits for a particular aircraft configuration and applied if it is significantly large.

The stability factors, $F_1(C_L)$ to $F_7(C_L)$, defined in eqn (27) can be evaluated for a particular aircraft; they are shown in table 1 for the Piper Twin Comanche. From the stability factors the correction functions developed in eqn (37) can be formed; the values for these are shown in table 2. When the correction functions are applied to the appropriate aircraft parameters then the trim curve corrections can be evaluated, table 3.

The position of the longitudinal and vertical C.G. is calculated from the basic aircraft empty weight and C.G. and the particular test loading, see appendix A1. The longitudinal C.G. correction showed a

slight stabilising effect tending to a maximum at a C_L of about 0.8 whereas the vertical C.G. correction gave a substantial destabilisation with respect to the simple theory.

The fuselage drag, C_{DZ}, assessed from the drag estimates of ref.1., was assumed to act through a point at quarter chord on the axis of the equivalent body of revolution. The correction produced by the fuselage drag was a small destabilising effect in the case considered and it is unlikely that the drag of a conventional aircraft will be large enough to cause a substantial correction to the trim curve slope. Although a trim change may occur due to the increment in drag of a configuration change, for example extention of the landing gear, the magnitude of the drag increment and the shift of centre of drag will not in general cause more than a second order correction.

The corrections to the trim curve slope due to the tail are estimated from the lift and drag of the tail at zero flight-lift incidence. Since the corrections due to the tail are usually small it is sufficient to assume that the zero flight-lift condition corresponds to the zero lift wing incidence for the purposes of estimation. From ref 1 the zero lift incidence relative to the aircraft body datum was -3.11^{o} and the zero lift tailplane trim setting from the measured trim curves was 2.81^{o}, thus the zero lift tail incidence was -0.3^{o} and the zero lift tail lift coefficient, C_{LTo}, can now be estimated. Using the data of ref 1 the corresponding value of zero lift tail drag coefficient C_{DTo}, can also be estimated. The corrections due to the zero lift values of C_{LT} and C_{DT} are very small and probably negligible for all conventional aircraft although high mounted tail designs could make them significant. The correction due to the tail lift, which arises from the induced tail drag, is estimated from the local tail incidence, α_T, and the tail trim setting, $\bar{n}$,

$$C_{LT} = a_1\alpha_T + a_2(\bar{n} - \alpha_o)$$

which can be written

$$C_{LT} = a_1\frac{C_L}{a}(1 - \frac{d\epsilon}{d\alpha}) + a_1 n_T + a_2(\bar{n} + \alpha_o)$$

Thus the values of C_{LT} can be reasonably estimated through the range of lift coefficient for each C.G.condition.

The overall correction due to the tail is small in the case considered, accounting for about 10% of the total correction at the most, but for an aircraft with a large tail or a high mounted tail this could become more significant.

3.1 Application of the corrections to the measured trim curves

The measured trim curves of the aircraft are shown in fig 6. These were measured under constant power conditions at a moderate engine output and were chosen because of the general absence of high power effects and for the close approximation to level flight during the test runs.

The trim curves as measured show a general reduction in slope as C_L increases indicating a steady loss of static stability, this is seen in the curves of slope, $d\bar{n}/dC_L$, against C_L. When the correction for the airframe design is included from table 3 the variation of trim curve slope is considerably reduced and the values of the slopes after correction are close to constants as predicted by the simple theory. In the aft C.G. case the correction is very nearly complete reducing the variation in slope over the interval C_L = 0.2 to 1.2 from 0.45^o to about 0.05^o. At forward C.G. the correction reduces the slope variation from 0.6^o to less than 0.15^o over the same interval, although this is not as complete a correction as the aft C.G. case it is a considerable improvement in approximation to the theoretical prediction.

4. Conclusions

The extended analysis of the aircraft model has provided correction functions to the measured trim curve slopes which have been shown to account for most of the curvature found in a sample of measured trim curves. Although the correction reduces the curvature to relatively small values it leaves a small residual variation in slope which may be due to power and slipstream effects. In general it can be concluded that application of the correction functions to the simple, classical theory will reasonably predict the variation in slope which may be expected to be found in the measurement of the trim curves.

It is evident that the correction due to the vertical offset of the C.G. from the m.a.c. provides the major contribution and for a first estimate only this need be considered. If however the aircraft is of an unusual design or has a high mounted tail then the other terms in the extended pitching moment equation could become significant.

The corrections can also be applied to the controls free trim curves by the addition of the elevator hinge moment parameter b_2 in eqns (35) and (37). In the case considered the controls free data was not of sufficiently reliable quality for purpose of proving the correction formula.

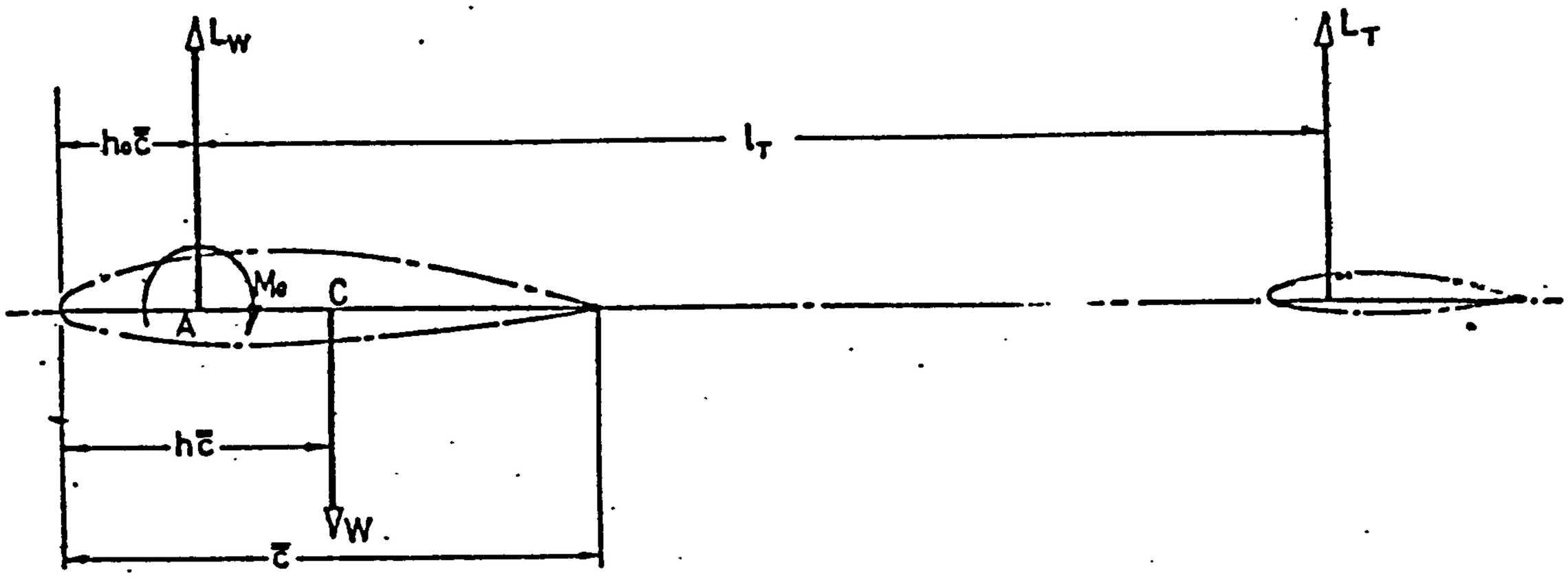

Fig 1a Simplified Model of the Aircraft

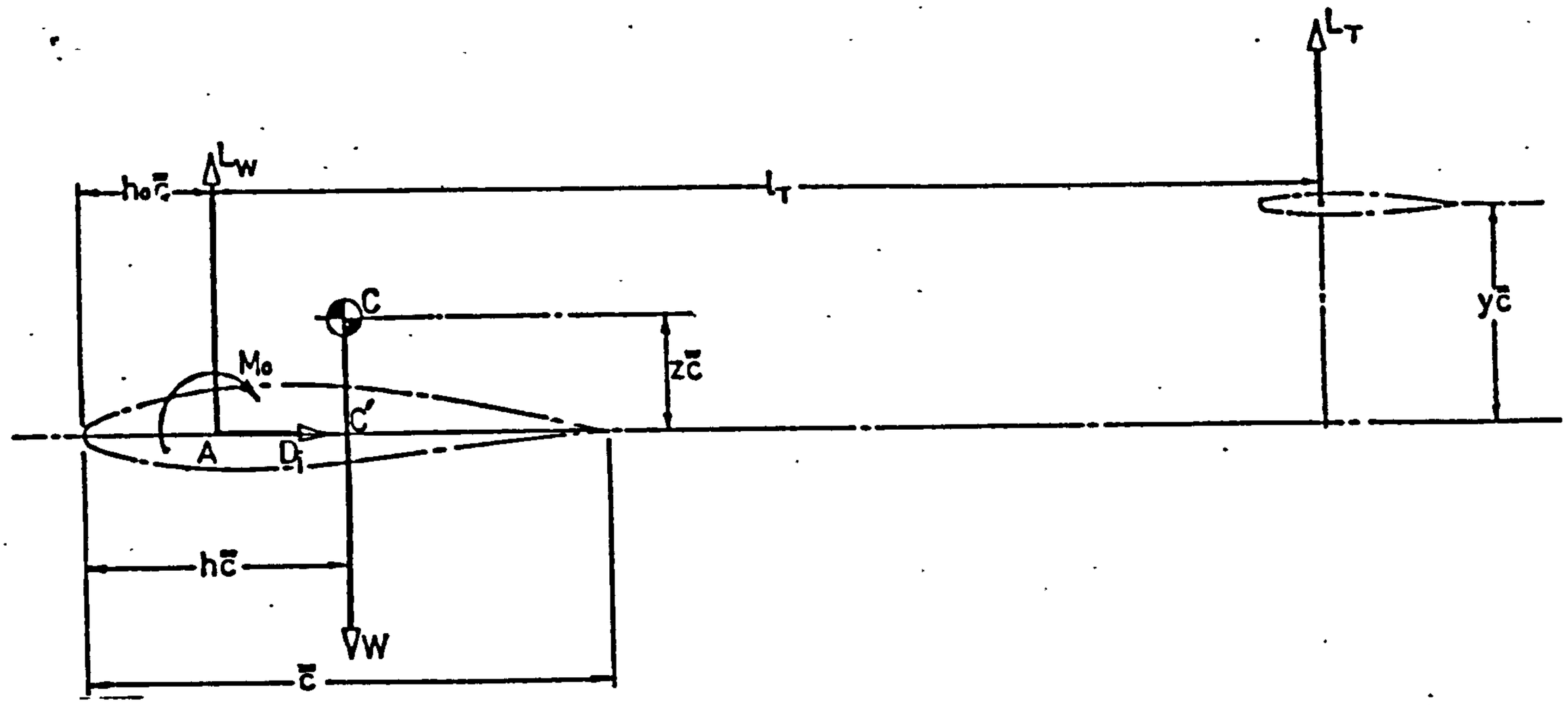

Fig 1b Extended Model of the Aircraft, Zero Incidence

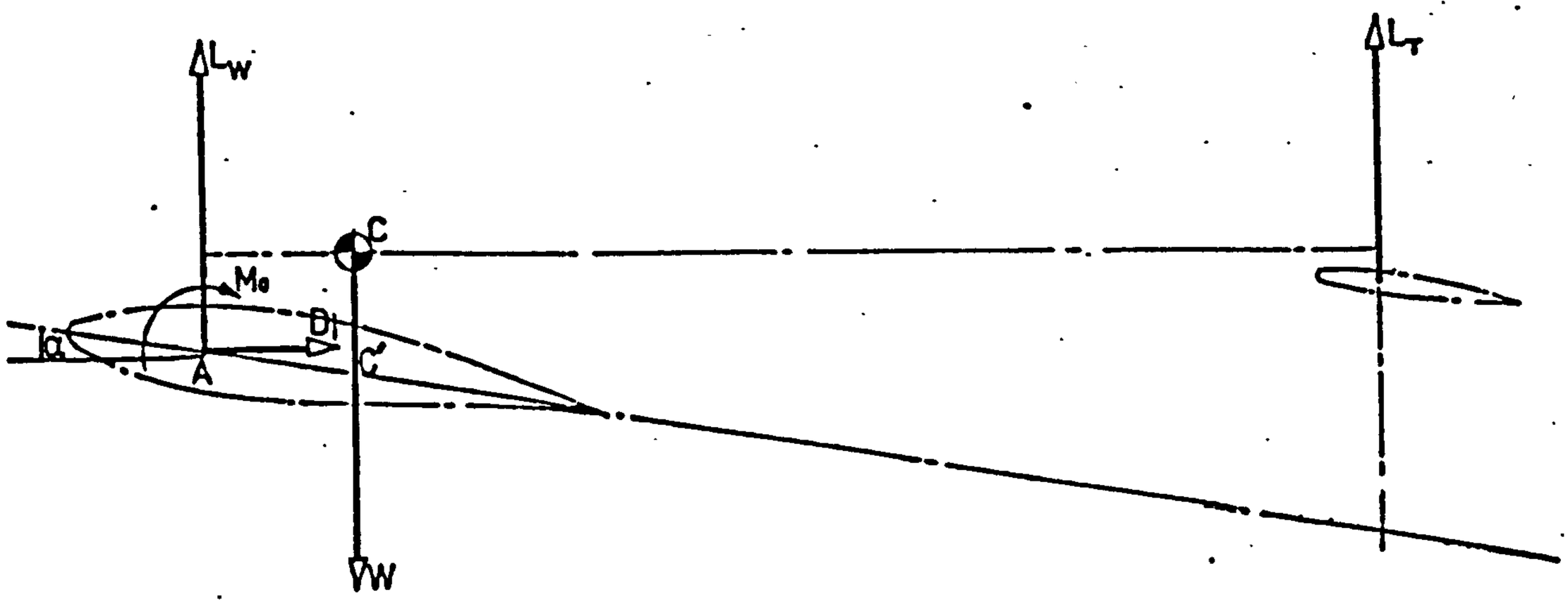

Fig 1c Extended Model of the Aircraft, High Incidence

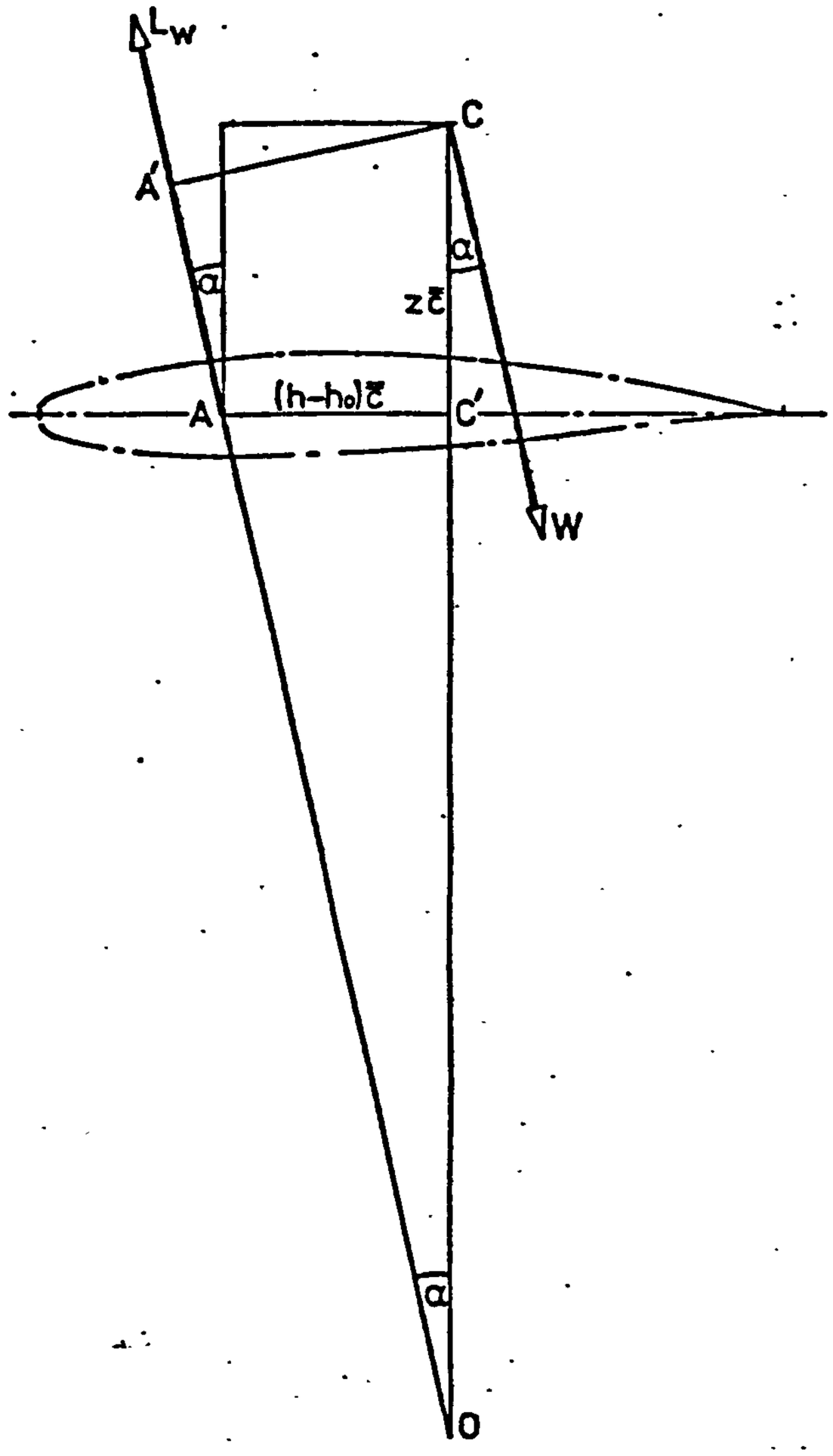

Fig 2 Moment of the Wing Lift Force about the C.G.

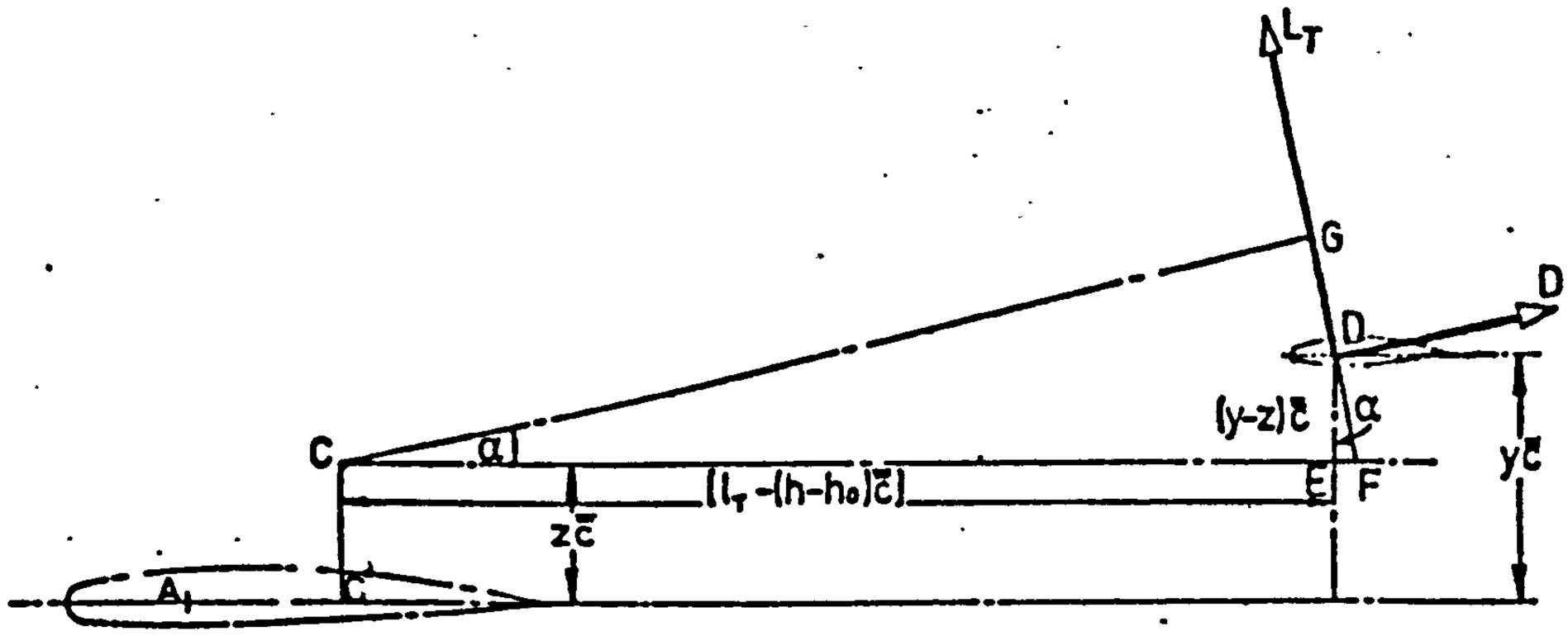

Fig 3 Moment of the Tail Lift and Drag Forces about the C.G.

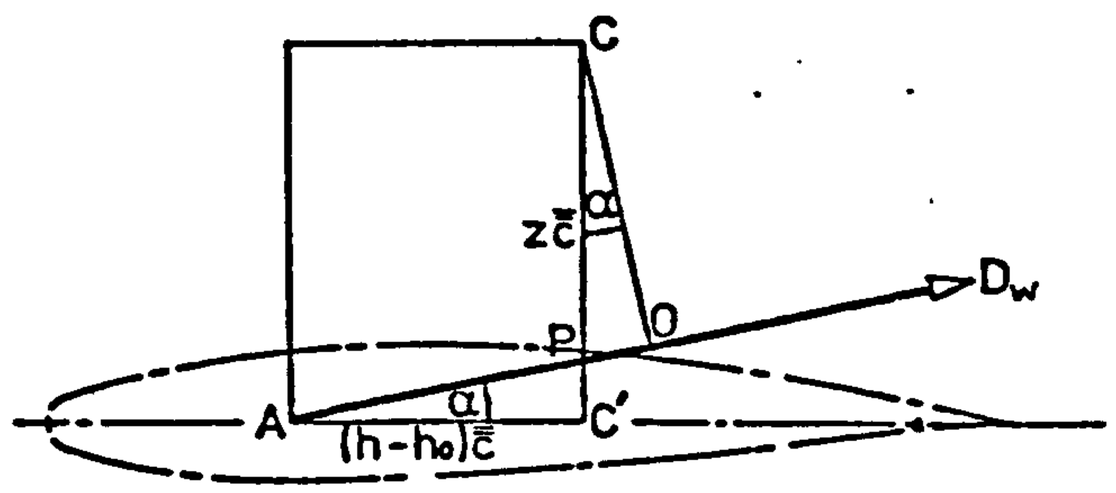

Fig 4 Moment of the Wing Drag about the C.G.

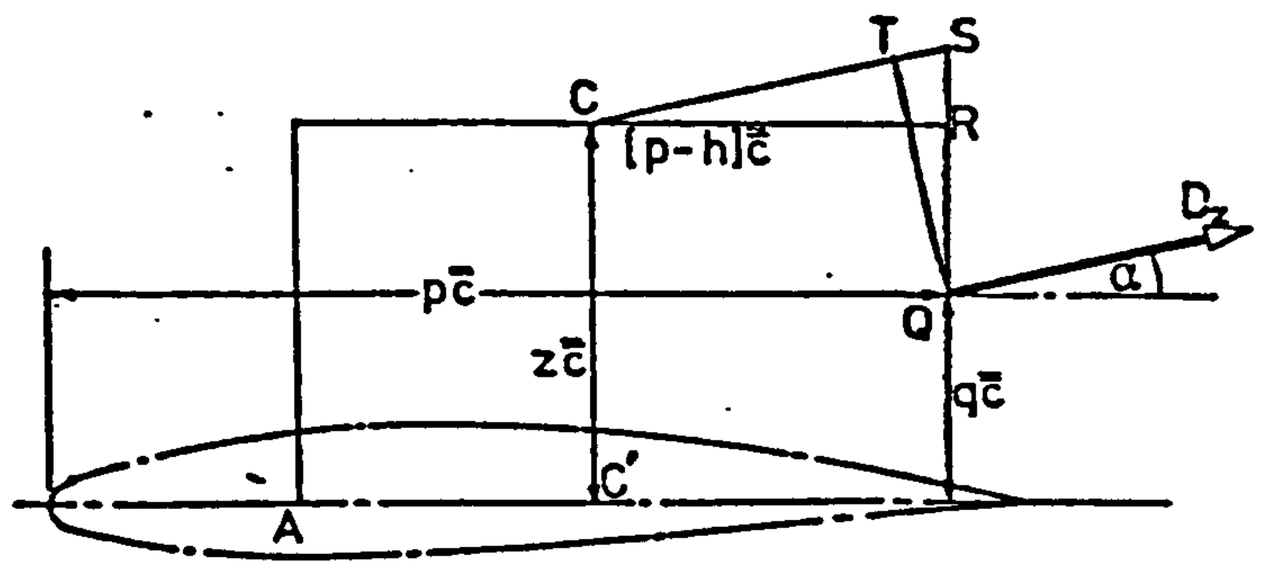

Fig 5 Moment of the Fuselage and Interference Drag about the C.G.

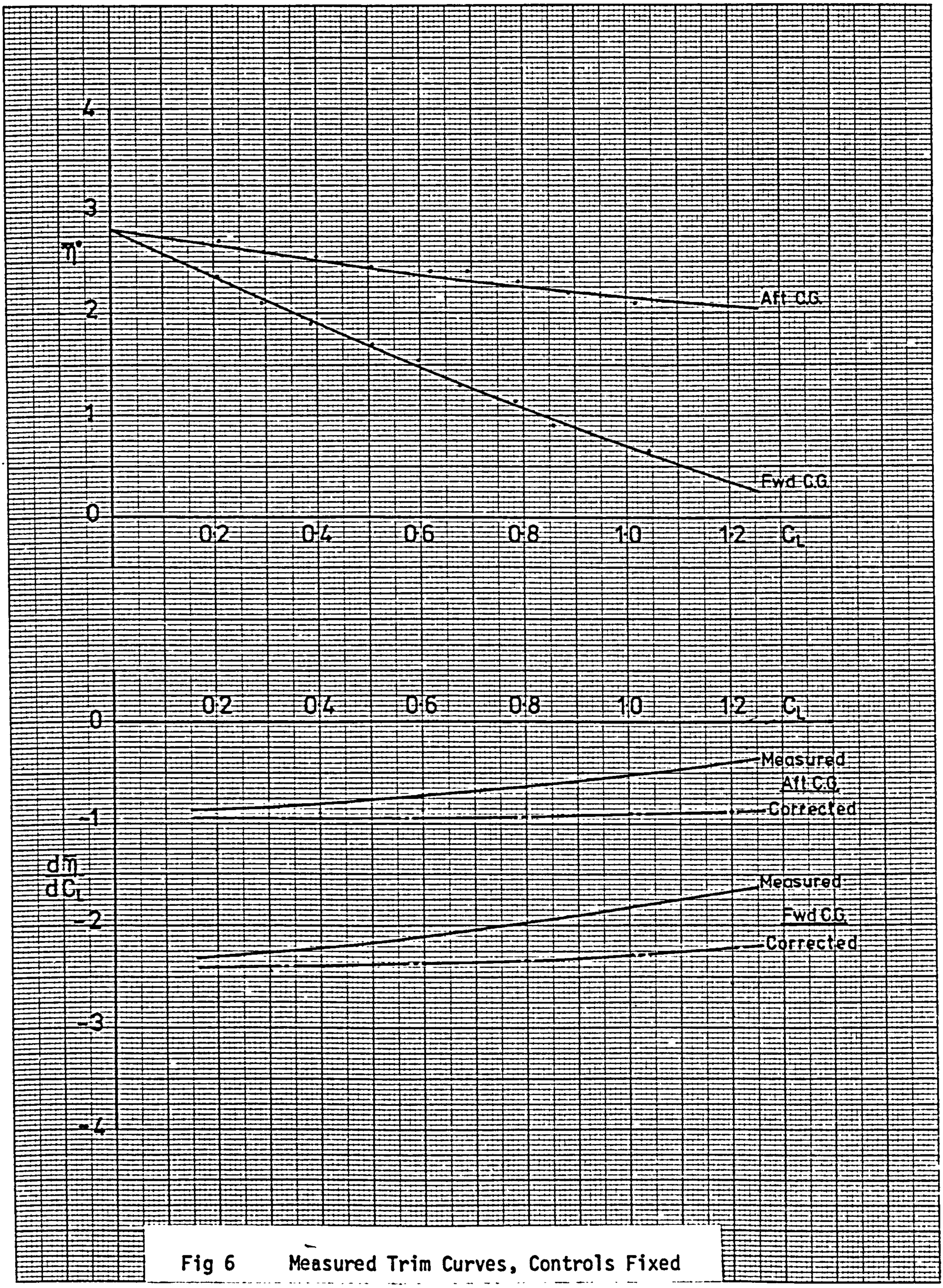

Fig 6 Measured Trim Curves, Controls Fixed

	C_L						
Stability factor	0	0.2	0.4	0.6	0.8	1.0	1.2
$F_1(C_L)$	1.0048	1.0039	1.0012	0.9968	0.9905	0.9825	0.9780
$F_2(C_L)$	0	0.2749	0.5498	0.8246	1.0991	1.3733	1.6472
$F_3(C_L)$	.4125	.4025	.3918	.3806	.3687	.3562	.3431
$F_4(C_L)$	1	1.0076	1.0104	1.0083	1.0012	0.9893	0.9724
$F_5(C_L)$	-0.0167	-0.0060	0.0048	0.0155	0.0262	0.03677	0.0473
$F_6(C_L)$	-0.1250	-0.1689	-0.2045	-0.2438	-0.2827	-0.3212	-0.3591
$F_7(C_L)$	1	0.9942	0.9868	0.9777	0.9671	0.9548	0.9409

TABLE 1 Stability Factors

	C_L						
Correction Function	0	0.2	0.4	0.6	0.8	1.0	1.2
$[F_1(C_L)/F_4(C_L)- 1]$	0.0048	-0.0037	-0.0091	-0.0114	-0.0107	-0.0069	-0.0058
$F_2(C_L)/F_4(C_L)$	0	0.2728	0.5441	0.8178	1.0978	1.3882	1.6940
$F_3(C_L)/F_4(C_L)$	.4125	.3995	.3878	.3775	.3683	.3601	.3528
$F_5(C_L)/F_4(C_L)$	-0.0167	-0.0060	0.0048	0.0154	0.0262	0.0372	0.0486
$F_6(C_L)/F_4(C_L)$	-0.1250	-0.1676	-0.2024	-0.2418	-0.2824	-0.3247	-0.3693
$F_7(C_L)/F_4(C_L)$	1	0.9867	0.9766	0.9697	0.9659	0.9651	0.9676

TABLE 2 Stability Correction Functions

Trim Curve Slope Correction due to	C_L 0	0.2	0.4	0.6	0.8	1.0	1.2
Fwd C.G. $(h - h_o)$	0.0051	-0.0040	-0.0098	-0.0123	-0.0115	-0.0074	0.0063
z	0	0.0910	0.1826	0.2744	0.3684	0.4659	0.5685
$a_1 \frac{d\alpha_T}{d\alpha} C_{LT}$	-0.0013	0	-0.0006	-0.0038	-0.0102	-0.0202	-0.0394
Aft C.G. $(h - h_o)$	0.0105	-0.0080	-0.0199	-0.0249	-0.0234	-0.0150	0.0127
z	0	0.0827	0.1650	0.2479	0.3329	0.4208	0.5136
$a_1 \frac{d\alpha_T}{d\alpha} C_{LT}$	-0.0013	0.0007	-0.0018	-0.0094	-0.0230	-0.0432	-0.0687
C_{DZ}	0.0219	0.0234	0.025	0.0266	0.0284	0.0302	0.0323
C_{LTo}	-0.0047	-0.0063	-0.0076	-0.0091	-0.0106	-0.0121	-0.0138
C_{DTo}	-0.0150	-0.0145	-0.0148	-0.0146	-0.0146	-0.0146	-0.0146
Fwd C.G. Total	0.0060	0.0896	0.1748	0.2612	0.3499	0.4418	0.5393
Aft C.G. Total	0.0114	0.0780	0.1459	0.2165	0.2897	0.3661	0.4615

TABLE 3 Corrections to Trim Curve Slopes, deg/C_L

References

1. WOLOWICZ C.H. & YANCEY R.B. — Longitudinal Aerodynamic Characteristics of Light, Twin-Engine, Propeller-Driven Airplanes. NASA TN-D 6800 1972

APPENDIX A

AIRCRAFT DATA AND FLIGHT LOADINGS

1. Piper Twin Comanche 'A' Series

This is a light twin-engined aircraft extensively used in flying training establishments, by private owners and air taxi firms. It represents a very typical modern aircraft available for use by pilots of all levels of experience.

The aircraft used in the trials was a standard production model powered by 2-160 H.P. Lycoming 10-360-C engines. The instrumentation system installed for the test purposes was designed to have as little effect as possible on the exterior of the aircraft so that the handling characterisitcs would not be affected in any way. Ref.3. describes the instrumentation system in detail.

The loading conditions associated with the trial cases were:

	Weight	Horizontal C.G.	Vertical C.G.
Forward C.G.	3392 lb	17.36% $\bar{c}$	9.94% $\bar{c}$
Aft C.G.	3519 lb	23.95% $\bar{c}$	8.98% $\bar{c}$

The salient dimensions of the aircraft are shown in Table A1 and the outline G.A. in Fig.A1.

Wing

Section	NACA 64_2A215 (modified)
Area	178 ft^2
Span	35.98 ft
Mean aerodynamic chord	4.958 ft
Aspect ratio	7.28
Dehedral angle	5^o-00'
Incidence (root)	2^o-00'
Twist	0^o
Taper ratio	0.513

Tailplane

Section	NACA 0008
Area	32.50 ft^2
Span	12.50 ft
Mean aerodynamic chord	2.70 ft
Aspect ratio	4.8
Taper ratio	0.515

Tailplane Tab

Area	5.0 ft^2
Span	9.9 ft
Chord (% of local tail-plane chord)	18% $\bar{c}_T$

Tail Arm 14.40 ft

TABLE A1

Twin Comanche-Dimensions and Data

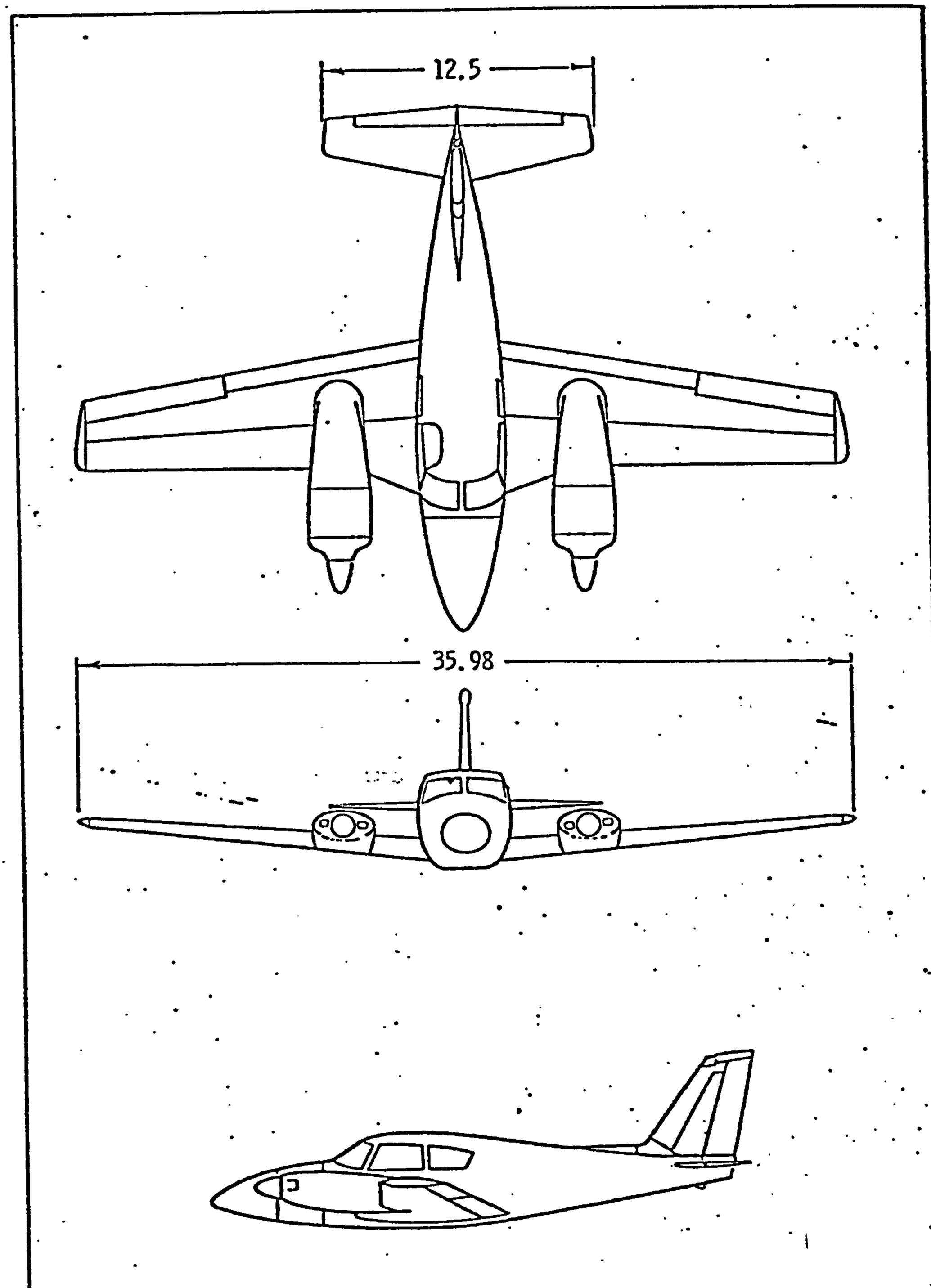

FIG. A1. PIPER TWIN COMANCHE.

PART II

Section 2

The Effect of Propeller Slipstream on Longitudinal Static Stability Trim Curves

Cranfield Report Aero No.32 (Issue 2).

Cranfield Report Aero No. 32
June 1976 Issue 2

CRANFIELD INSTITUTE OF TECHNOLOGY

THE EFFECT OF PROPELLER SLIPSTREAM ON LONGITUDINAL STATIC STABILITY TRIM CURVES

by

M.E. ESHELBY

Aerodynamics Division
College of Aeronautics

SUMMARY

The high energy slipstream from a propeller may interfere with other parts of the aircraft and cause additional terms to arise in the pitching moment equation. These terms will modify the trim curves causing non-linearities to occur. This report analyses the effect of slipstream interference as it is likely to occur on a twin-engined light aircraft. The slipstream interference with the wing and nacelle is considered separately from the interference with the tail for convenience and to make the application of the estimation method more general.

The prediction of the slipstream behaviour is calculated by a computer programme and compared with flight measurements made on the test aircraft. The comparison shows that the programme is providing a reasonable simulation.

The distortion of the trim curves is calculated in terms of a correction to the trim curve slope estimated from the simple theory of static stability and shows that the wing and nacelle interference is generally destabilising. The interference at the tail is also destabilising and the overall effect of the slipstream is seen to be a general destabilisation which is proportional to power and increases at high values of incidence.

CONTENTS

NOTATION

A	Aspect Ratio, Propeller Disc Area
a	Lift curve slope of aircraft
a_1, a_2, a_3	Lift curve slopes of tailplane, elevator, tab respectively
b	Wing span
b_1, b_2, b_3	Hinge moment parameters of tailplane, elevator, tab respectively
C_L	Lift coefficient
C_m	Pitching moment coefficient
$\bar{c}$	Mean aerodynamic chord (m.a.c.)
D	Propeller Diameter
e	NACA span efficiency factor
F_T, F_{T_2}, F_T'	Tail effectiveness parameters (see eqns 15, 30, 32)
F_1, F_2, F_3	Stability factors (eqn.A.16)
f, g, k	General coordinates
H_o, H_1	Freestream total head
h	Position of CG aft of L.E. of m.a.c.
h_o	Position of aerodynamic centre aft of L.E. of m.a.c.
K, K_1	General constants (eqns.11 and 21)
k_ε	Downwash factor
L	Lift force
l_T	Tail arm
M	Pitching moment
P	Power
p, p_o	Static pressures
q	Total pressures, $\frac{1}{2}\rho V^2$
r	Radius
S	Wing area
u, v, w	General velocities
V	True airspeed
$\bar{V}$	Tail volume coefficient
ΔV, v	Incremental velocities

W	Weight
x, y, z	General position coordinates
Z_C	Propeller normal force coefficient
α	Incidence
β	Control tab angle
ε	Downwash angle
η	Elevator angle, propeller efficiency
θ, ψ, ϕ	General angles
ν	Vortex induced velocities
ρ	Air density
σ	Relative density
Γ	Circulation
η_T	Tail setting angle
Δ	Incremental change or error

Subscripts

A	Aerodynamic
P	Due to Power
O	Reference; or zero power
S	Due to Slipstream
w	Wing
n	Nacelle
T	Tail

THE EFFECT OF PROPELLER SLIPSTREAM ON LONGITUDINAL STATIC STABILITY

1. Introduction

The influence of the propeller slipstream on the static stability of the aircraft arises mainly from two effects. Firstly there will be an interference between the slipstream and the wing and nacelle which will modify the lift equation and also cause a direct pitching effect. Secondly there may be a part of the tailplane immersed in the high energy slipstream which will modify the tail lift and require a change in elevator angle to maintain longitudinal trim.

Although both these effects contribute to the pitching moment equation they will be treated separately as independent effects for convenience. This will make the corrections simpler and their application more general.

To analyse the effect of the propeller slipstream knowledge of three characteristics is required,

a) the slipstream velocity relative to freestream

b) the locus of the slipstream aft of the propeller

and c) the extent of the tail immersion in the slipstream

In the flight trials measurements were taken relating to slipstream energy but the measurements were limited to a single velocity sample taken just forward of the leading edge of the tailplane at half span. This showed clearly that there was a strong interference but it also indicated that the degree of interference varied with flight conditions.

To investigate the observed effects it was found necessary to simulate the observed slipstream characteristics by computing a simplified model of the aircraft in flight with engines running. The programme and its development is described in Appendix I.

2. Instrumentation of the Aircraft for the Measurement of Slipstream Energy Characteristics

The aircraft used in the trials was a Piper Twin Comanche 'A' series instrumented for the recording of in flight data for handling trials, Ref 1 describes the instrumentation in detail.

To detect the slipstream a pitot head was installed on the tailplane behind the propeller. The pitot was a ¼" O.D.tube attached to the lower skin of the tailplane and projecting approximately 6" forward of the leading edge along the chord line of the tail. It was stationed at half semi-span on the starboard side of the tailplane. A nylon tube led directly into the aircraft to a differential pressure gauge mounted in the cabin.

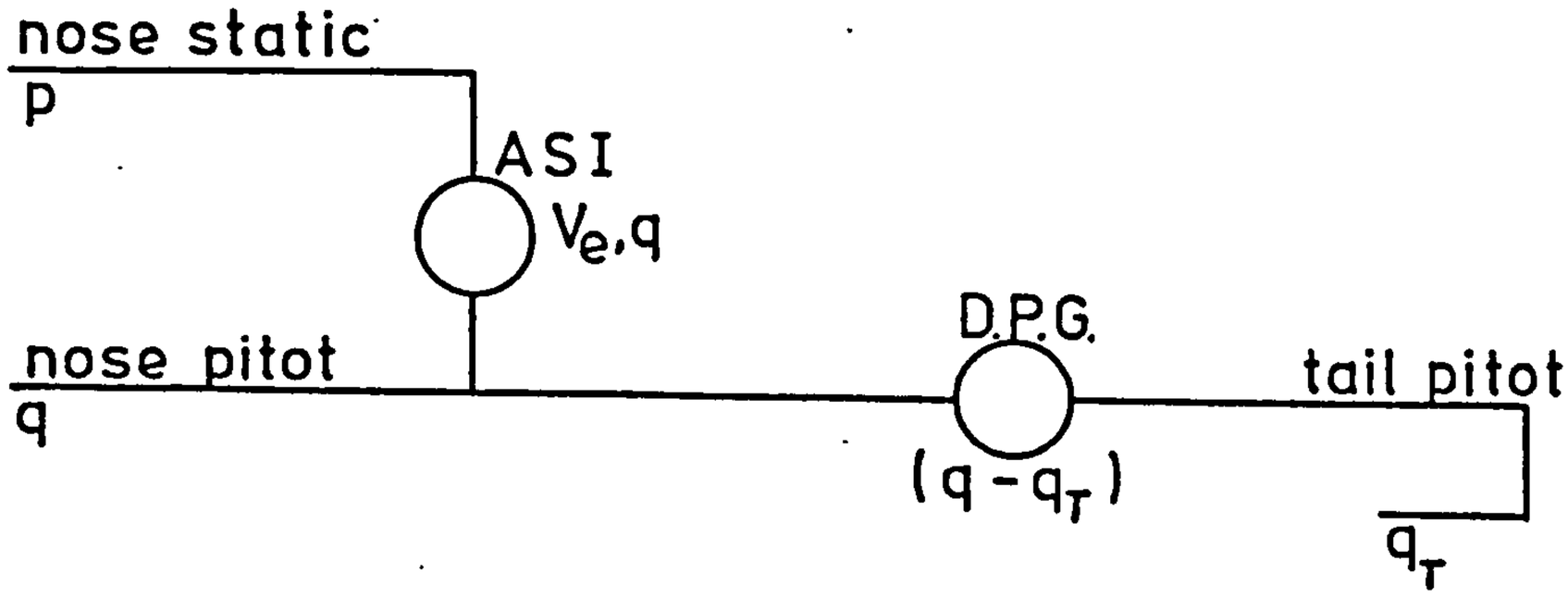

FIG 1 Pitot-Static System

The reference dynamic pressure was taken from a nose boom mounted pitot-static head which had been previously calibrated, Ref.2.

From the airspeed indicator the equivalent airspeed, and hence dynamic head, of the free stream could be found. This was compared with the dynamic head error between the reference and tail systems to give the slipstream energy factor q_T/q.

Let $\Delta q = q - q_T$ be the pressure measured by the differential pressure gauge, q_T is then given by

$$q_T = q - (q - q_T) = q - \Delta q$$

hence, knowing q from the A.S.I. the slipstream energy factor is given by

$$\frac{q_T}{q} = \frac{q - \Delta q}{q}$$

The position of the tail pitot was chosen to give a best average coverage of the slipstream. Unfortunately there was no time for any development flying and only one pitot tube could be considered for installation therefore a mid span was accepted giving a compromise between the ideal situation in the slipstream and the most strongly affected area of the tail.

3. Calculation of Slipstream Energy Factor q_T/q

Using the momentum theory of the propeller and assuming the propeller to be replaced by an actuator disc the slipstream velocity

behind the propeller can be estimated.

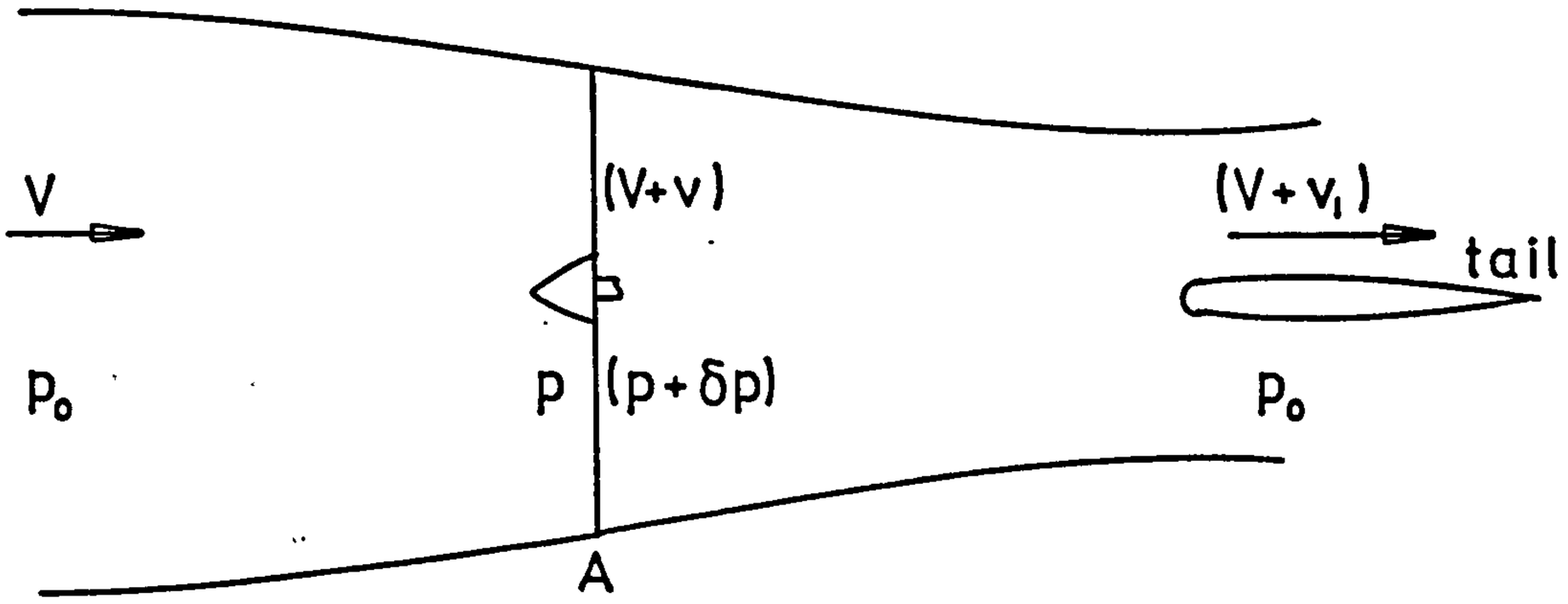

FIG 2 Propeller Momentum Theory

Let the actuator disc, area A, be in a free stream velocity V at a pressure p_0. The flow is accelerated into the propeller and passes the disc at a speed (V + v), behind the disc where the pressure has recovered to the free stream static pressure p_0 the velocity is $(V + v_1)$.

Ahead of the actuator disc the total head of the flow is H_0 and

$$H_0 = p_0 + \tfrac{1}{2}\rho V^2 = p + \tfrac{1}{2}\rho(V + v)^2$$

Behind the actuator disc the total head of the flow is H_1 and

$$H_1 = p + \delta p + \tfrac{1}{2}\rho(V + v)^2 = p_0 + \tfrac{1}{2}\rho(V + v_1)^2$$

therefore the differential pressure across the actuator disc is

$$\delta p = H_1 - H_0 = \rho(V + \tfrac{1}{2}v_1)v_1 \qquad (1)$$

The thrust is given by the momentum change hence

$$T = A\rho(V + v)v_1 \qquad (2)$$

and since $T = A\delta p$

$$\delta p = \rho(V + v)v_1 \qquad (3)$$

Comparing (1) and (3) gives

$$v = \tfrac{1}{2}v_1$$

hence (2) becomes

$$T = A\rho(V + \tfrac{1}{2}v_1)v_1 \qquad (4)$$

The thrust power, ηP, is given by

$$\eta P = TV$$

and from (4)

$$\eta P = A\rho(V + \tfrac{1}{2}v_1)Vv_1,$$

where η is the propeller efficiency and P the B.H.P. output of the engines thus

$$\frac{\eta P}{AqV} = \left[2 + \frac{v_1}{V}\right]\frac{v_1}{V} \qquad (5)$$

where $q = \tfrac{1}{2}\rho V^2$

If the tail is immersed in the slipstream then the dynamic head q_T will be given by

$$q_T = \tfrac{1}{2}\rho(V + v_1)^2$$

and the slipstream energy factor q_T/q will be

$$\frac{q_T}{q} = \frac{\tfrac{1}{2}\rho(V + v_1)^2}{\tfrac{1}{2}\rho V^2} = 1 + \left[2 + \frac{v_1}{V}\right]\frac{v_1}{V} \qquad (6)$$

thus from (5) and (6)

$$\frac{q_T}{q} = 1 + \frac{\eta P}{AqV} \qquad (7)$$

or
$$q_T - q = \Delta q = \frac{\eta P}{AV} = \frac{\sigma^{\frac{1}{2}}\eta P}{AV_e} \qquad (8)$$

therefore the increment in slipstream velocity at the tail is inversely proportional to speed at constant thrust power.

Substituting for qV in terms of C_L in (7) gives

$$\frac{q_T}{q} = 1 + \frac{\eta P}{A}(\tfrac{1}{2}\rho)^{\frac{1}{2}}\left(\frac{S}{W}\right)^{3/2} C_L^{\,3/2} \qquad (9)$$

and for constant power, weight and altitude (9) can be expressed as

$$\frac{q_T}{q} = 1 + KC_L^{\,3/2} \qquad (10)$$

where $K = \frac{\sigma^{\frac{1}{2}}\eta P}{A}\left[\left(\frac{S}{W}\right)^3 \frac{\rho_0}{2}\right]^{\frac{1}{2}}$ (11)

The value of K is seen to be a function of engine power, airspeed altitude and weight. However, for most purposes at constant engine power setting and altitude it can be regarded as a constant since the weight will not vary significantly with time and the change in propeller efficiency with speed is not usually large, particularly in the case of a constant speed propeller.

4. Comparison of Calculated and Observed Slipstream

The slipstream energy factor, calculated from equation (9) and allowing for variation of propeller efficiency with airspeed, can be compared with the measured values of the slipstream energy from the tailplane mounted pitot head, Ref.3. Measurements were made at five power settings from throttles closed to maximum continuous cruise power at two C.G. positions. It was found that there was a very different characteristic from between the forward and aft C.G. slipstream energy factors as C_L increased.

Consider the aft C.G. characteristic, Figs. 3 to 7. At the higher power settings there is a very close agreement between the theoretical and measured slipstream energy factors, this can be seen in figs. 5 and 7. At a power setting of 15"/2400 r.p.m.* the tail appears to be immersed in the slipstream and both theory and measurement show the same form throughout the range of C_L.

At maximum cruise power 24"/2400 r.p.m. the theory and measurement again agree closely up to a C_L of approximately 0.75 above which the slipstream energy factor rapidly diminishes to unity. This would appear to be caused by the tailplane moving out of the high energy slipstream. At a power setting of 20"/2400 r.p.m. the slipstream energy factor at low C_L (less than 0.45) and at higher C_L (above 0.75) corresponds very closely to the calculated value but in between there is a flat spot in which q_T/q is almost unity, this covers the range of C_L between 0.5 and 0.7. There were no attempts in the limited flight trial to investigate this flat spot other than to repeat the readings to prove its existence. It is considered that it is most likely to be caused by the wake of the wing passing over the pitot region, although it is not clear why this should not appear in the other slipstream profiles.

At the lower power settings 10"/2400 r.p.m. the propeller is seen to be idling at the high speeds and only begins to produce thrust at C_L values higher than 0.6. At C_L of 0.9 and above the theoretical and observed effects are in very close agreement.

---

* Power settings given in this form refer to a manifold pressure in inches of mercury and an engine rotational speed.

With throttles closed the windmilling propeller is seen to absorb energy from the freestream with a maximum energy loss at about $C_L = 0.7$. No simulation of the windmilling case was calculated.

Comparison of the observed forward and aft C.G. slipstream energy profiles shows a very marked difference in the characteristics. At all power conditions the forward C.G. characteristic initially behaves normally at C_L values of up to about 0.4 after which energy factor decreases to approximately unity at about $C_L = 0.6$, this state remains down to $C_L = 0.8$ after which energy is lost still further and q_T/q decreases to about 0.85. This form of characteristic is similar for all power conditions.

No positive reason has been found for this behaviour and the programme for simulation of the slipstream (App.1.) showed that the tail lift force change due to the C.G. shift made very little difference to the predicted slipstream position. It is felt that the effect is more likely to occur from differences in the flight techniques used in the two C.G.loading cases. Different pilots were used to fly the forward and aft C.G. flights to minimise the aircraft weight change due to the carriage of ballast. It has since been noted that their methods of trimming out small angles of sideslip are not identical. Since it is known that a power induced sideforce exists in the case of a propeller driven aircraft (Refs 4 & 5) and that the sideforce is a function of speed and power, then at all flight conditions with power there must be a sideforce on the aircraft which will have to be trimmed out with the use of either rudder deflection or a small degree of bank angle, or a combination of both. The individual piloting methods may result in differences in the degree of sideslip angle between the flights at each C.G.condition. Such differences may be sufficient to sweep the low energy slipstream core inwards towards the fuselage and into the region around the tailplane pitot installation. A considerably extended series of trials and a more comprehensive instrumentation system would have to be provided to investigate this effect in detail to establish the cause of the apparent C.G. influence on slipstream energy factor.

5. The Effect of the Slipstream on the Lift of the Tail

The effect of the propeller slipstream on the tail is to increase the energy of the flow over a part of the tailplane. This will modify the lift at a given tail incidence. Also the power will cause the downwash to be modified and these two effects will alter the total lift produced by the tailplane. The lift coefficient of the tailplane is given by the equation

$$C_{LT} = a_1\alpha_T + a_2 n + a_3\beta \qquad 12.$$

and thus the lift force in the free stream would be given by

$$L_T = qS_T C_{LT} \qquad 13.$$

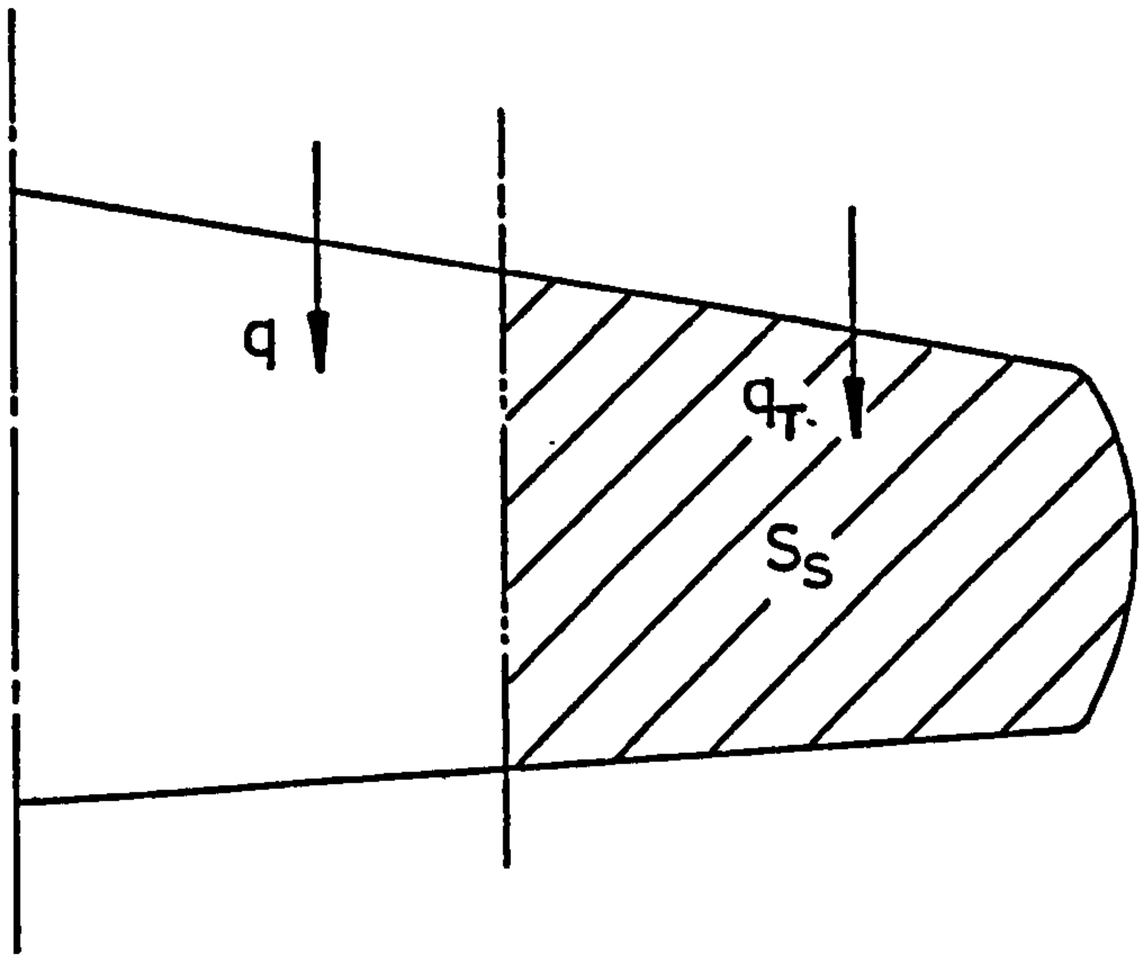

Let the area of the tailplane in the slipstream be S_s, the lift force of the tail can be expressed under these conditions as

$$L_T = \left\{ q(S_T - S_s) + qS_s \right\} C_{LT}$$

or
$$L_T = qS_T \left\{ 1 + \left[\frac{q_T}{q} - 1 \right] \frac{S_s}{S_T} \right\} C_{LT} \qquad 14.$$

The tail effectiveness is therefore increased by a factor F_T, where

$$F_T = 1 + \left[\frac{q_T}{q} - 1 \right] \frac{S_s}{S_T} \qquad 15.$$

The downwash will be increased by a small amount, $\Delta\varepsilon$, to the power on value ε_p. This increase can be considered to be proportional to power, see App.1., giving

$$\varepsilon_p = \varepsilon_o + \Delta\varepsilon \qquad 16.$$

Since it is assumed that downwash in the absence of power is proportional to incidence the power on downwash increment can be approximated to

$$\Delta\varepsilon = \frac{C_L}{a} \frac{d\varepsilon_o}{d\alpha} \left(\frac{\varepsilon_p}{\varepsilon_o} - 1 \right) = k_\varepsilon C_L \qquad 17.$$

where k_ε is a constant for a given engine power.

A comparison can now be made between the elevator angle to trim in the presence of the slipstream ($\bar{\eta}$) and the elevator angle which would be required to trim under the same conditions with no

slipstream effect present, $(\bar{\eta} + \Delta\bar{\eta})$

The lift force would be the same in each case and thus from 14, 15, 12 and 16, equating the expressions for the tail lift force gives

$$L_T = qS_TF_T \left\{ a_1(\alpha - \varepsilon_p + \eta_T) + a_2\bar{\eta} + a_3\beta \right\}$$

$$= qS_T \left\{ a_1(\alpha - \varepsilon_o + \eta_T) + a_2(\bar{\eta} + \Delta\bar{\eta}) + a_3\beta \right\} \qquad 18.$$

where η_T is the tail setting angle relative to wing zero lift line. Separating the elevator angle correction $\Delta\bar{\eta}$ gives

$$qS_Ta_2\Delta\bar{\eta} = qS_T(F_T - 1)C_{LT} - qS_TF_Ta_1k_\varepsilon C_L \qquad 19.$$

and the power on tail lift will now be given by C_{LTP}, where

$$C_{LTP} = C_{LT} + a_2\Delta\eta = F_T \left\{ C_{LT} - a_1k_\varepsilon C_L \right\} \qquad 20.$$

From equations 10, 11, and 15, F_T is seen to be a function of C_L for specified power conditions together with the immersed area of the tail. F_T can therefore be considered to be of the form

$$F_T = 1 + K_1C_L^{3/2} \qquad 21.$$

where $K_1 = K\frac{S_S}{S_T}$ using equation 10.

It should however be noted that $\frac{S_S}{S_T}$ is also a function of incidence and that the full expression for F_T is more complex than that indicated in equation 21.

6. The Effect of Slipstream at the Tail on Measured Static Stability Trim Curves

Consider the pitching moment equation of the aircraft, defined in the classical manner, without slipstream.

$$C_{mCG} = C_{mo} + C_L(h - h_o) - \bar{V} \left\{ a_1\alpha_T + a_2\eta + a_3\beta \right\} \qquad 22.$$

Now in steady level trimmed flight $C_{mCG} = 0$ and the elevator angle to trim, $\bar{\eta}_o$, can be expressed as

$$\bar{V}a_2\bar{\eta}_o = C_{mo} + C_L(h - h_o) - \bar{V} \left\{ a_1\alpha_T + a_3\beta \right\} \qquad 23.$$

The tab setting angle, β, can be considered constant in the controls fixed analysis, thus differentiating 23 with respect to C_L gives

$$\frac{d\bar{\eta}_o}{dC_L} = \frac{(h - h_o)}{\bar{V}a_2} - \frac{a_1}{aa_2}\left(1 - \frac{d\varepsilon}{d\alpha}\right) \qquad 24.$$

where $\frac{d\bar{n}_o}{dC_L}$ is the slope of the elevator trim curve in the absence of slipstream effects of power.

If the tail of the aircraft is partly immersed in the slipstream the tail lift coefficient will be modified to account for the increased slipstream energy and downwash and the modified tail lift coefficient, $C_{L_{TP}}$, can be included in the pitching moment equation giving, from eqn. 20,

$$C_{mCG} = C_{mo} + C_L(h - h_o) - \bar{V}F_T \left\{ C_{LT} - a_1 k_\varepsilon C_L \right\} \quad 25.$$

The tail lift coefficient C_{LT} can be considered to be of the form

$$C_{LT} = C_{LTo} + C_L \cdot \frac{dC_{LT}}{dC_L} \quad 26.$$

where C_{LTo} is the constant element necessary to trim at $C_L = 0$,

thus $$C_{LTo} = \frac{C_{mo}}{\bar{V}} = a_1 n_T + a_2 \bar{n}_o + a_3 \beta_o \quad 27.$$

where n_T is the tailplane setting angle relative to the wing zero lift line and $\bar{n}_o$ and β_o the elevator and tab settings to trim at $C_L = 0$

Separating the elevator angle to trim with power on from equation 25. gives

$$\bar{V}F_T a_2 \bar{n}_p = C_{mo} + C_L(h - h_o) + \bar{V}F_T a_1 k_\varepsilon C_L - \bar{V}F_T \{ a_1 \alpha_T + a_3 \beta \} \quad 28.$$

For small changes of aircraft incidence the elevator angle to trim can be considered to be of the form

$$\bar{n}_p = \bar{n}_o + C_L \cdot \frac{d\bar{n}_p}{dC_L} \quad 29.$$

and the differentiation of the function $F_T\bar{n}_p$ with respect to C_L can be expressed as

$$\frac{d}{dC_L}(F_T\bar{n}_p) = (F_T + C_L F_T') \frac{d\bar{n}_p}{dC_L} + F_T'\bar{n}_o \quad 30.$$

where $$F_T' = \frac{dF_T}{dC_L}$$

Similarly from equation 26. the derivative of C_{LT} can be expressed as

$$\frac{d}{dC_L}(F_T C_{LT}) = (F_T + C_L F_T') \frac{dC_{LT}}{dC_L} + F_T' C_{LTo} \quad 31.$$

Differentiating eqn.28 with respect to C_L and using the results of eqns 30 and 31, with β constant gives

$$F_{T_2}\,\bar{V}a_2\,\frac{d\bar{n}_p}{dC_L} = (h - h_o) + \bar{V}a_1 k_\varepsilon F_{T2} - \bar{V}\,F_{T_2}\,\frac{a_1}{a}\left(1 - \frac{d\varepsilon}{d\alpha}\right) - \bar{V}C_{LTo}F_T' \qquad 32.$$

where $F_{T_2} = (F_T + C_L F_T')$

The trim curve slope, power on, is given by

$$\frac{d\bar{n}_p}{dC_L} = \frac{(h - h_o)}{\bar{V}a_2}\,\frac{1}{F_{T_2}} + \frac{a_1 k_\varepsilon}{a_2} - \frac{C_{LTo}\,F_T'}{a_2\,F_{T_2}} - \frac{a_1}{aa_2}\left(1 - \frac{d\varepsilon}{d\alpha}\right) \qquad 33.$$

Comparing equations 33 and 24 gives the correction to the trim curve slope due to slipstream at the tailplane, $\Delta\left[\frac{d\bar{n}_p}{dC_L}\right]$, as

$$\Delta\left[\frac{d\bar{n}_p}{dC_L}\right] = \frac{d\bar{n}_p}{dC_L} - \frac{d\bar{n}_o}{dC_L} = \frac{(h - h_o)}{\bar{V}a_2}\left[\frac{1}{F_{T_2}} - 1\right] + \frac{a_1 k\varepsilon}{a_2} - \frac{C_{LTo}\,F_T'}{a_2\,F_{T_2}} \qquad 34.$$

This represents the additional propeller contribution to the trim curve slope due to the influence of the propeller slipstream on the tail of the aircraft.

6.1 Evaluation of the Contribution of the Slipstream at the Tail to the Trim Curve Slope

The correction to the trim curve slope can be seen to comprise three parts, the downwash correction which is a constant within the limits of the experimental evidence, the tail lift correction which is dependent on C_{LT_θ} and is small and the C.G.position, h. The latter corrections are functions of the slipstream energy at the tail and depend on F_T.

The only measurements which were taken relating to the slipstream concerned a single velocity sample. This enabled a check to be made on the estimation of the slipstream energy factor, section 3, which showed a very close agreement between the theoretical estimate of the energy factor and the measured value at the aft C.G. loading. The discrepancy between the slipstream energies measured at forward C.G. and aft C.G. is not explained satisfactorily by the programme which was developed to simulate the slipstream characteristics of this particular aircraft (Appendix A.1.) In section 4 it was considered that it was probably caused by sideslip and not by C.G. shift as is at first apparent and the predicted values are accepted for this analysis.

The calculation of the factor F_T was made using the computed values of tailplane immersion and slipstream energy factor from Appendix A.1. From this the values of F_T' and F_{T2} were found and combined to form the functions F_T'/F_{T2} and $(1/F_{T2} - 1)$, Table 1, which are used to give the corrections to the trim curve slope, eqn.34.

The contribution due to C_{LT_0} is similar for both C.G. locations and will generally only vary significantly with C.G. if there is a large effect of tail lift on slipstream position. Table 3a and 3b show that it is small and has a destabilising effect with respect to the basic aircraft diminishing with increase in C_L.

The contribution due to the C.G. position increases with C_L and is stabilising. The aft C.G. produces a greater effect than the forward C.G. and increasing power increases the contribution.

The downwash contribution is determined from the calculated flow field at the tail, Appendix A.1., since no direct measurements of the flow direction at the tail were made.

The programme calculates the induced velocities at points in the slipstream at a plane through the slipstream just ahead of the tail. From the induced velocities and the slipstream velocity a flow vector relative to the freestream can be calculated to represent the downwash field 0.5ft ahead of the tailplane, APP A1 figs A 16 to A 19. Three positions in the slipstream are considered, on the upper edge (u), the centre (o) and the lower edge (l). Due to the tail lift force the predicted flow vector is distorted when the point under consideration passes close to the tailplane leading edge. Away from this area of local distortion an average downwash field vector can be assumed.

It is not possible to find the downwash rate $d\varepsilon/d\alpha$ from the calculated data since it is not based on a single point relative to the wing but on a filament of flow emanating from a point remote from the wing and passing through the general slipstream region. Figs.A 16 to A 19 do not therefore represent a truly continuous state. The figures can be used to estimate the effect of power on downwash rate by assuming the relationship of Eqn.16 in the form

$$\Delta\varepsilon = \varepsilon_0\left(\frac{\varepsilon p}{\varepsilon 0} - 1\right)$$

The values found from the programme are given in table 2 and a mean value is accepted for each power and C.G. combination as a first order correction.

This gives a correction to the trim curve slope due to downwash variation with power which is constant with C_L but varies in magnitude with power and C.G. The corrections are shown in Tables 3a and 3b and are destabilising.

The overall correction due to slipstream at the tail is shown in tables 3a and 3b. At forward C.G. this is seen to be a general destabilisation decreasing with increase in C_L, the decrease being more marked at higher powers. At aft C.G. there is a destabilisation at low C_L decreasing as C_L increases and becoming a stabilisation at high power conditions.

7. Wing and Nacelle contribution to the Pitching Moment Equation due to Slipstream Interference

The whole of the engine nacelle and a section of the wing aft of the propeller will be subject to a local flow which has been modified by the increased momentum due to power and also in direction due to the propeller normal force and thrust, fig.8. The estimate of the slipstream interference can be made by finding the incremental velocity and local incidence and using these to determine the increment in lift produced by the wing and nacelle. The incremental lift will produce a moment about the C.G. which will modify the pitching moment equation and hence the static stability. There are two effects of the slipstream which must be considered, these are, firstly, an increment in the direct pitching moment and, secondly, an increment in lift.

The direct increment in pitching moment from the wing and nacelle due to slipstream can be added to the basic pitching moment equation, eqn.22. as an additional term ΔC_{mwn}. This arises from the increment in lift due to velocity and incidence over the nacelle and the portion of the wing immersed in the slipstream. Both lift increments act at some distance from the C.G. and thus produce pitching moments.

The incremental lift will add to the total lift of the aircraft so that the total lift, L, can be considered to be the sum of the aerodynamic lift due to incidence, L_A, and incremental slipstream lift, ΔL_{wn}

$$L = L_A + \Delta L_{wm} \qquad 35.$$

Since only the overall lift, L, can be measured in flight a correction must be made to the flight lift coefficient to allow the slipstream contribution to be separated from the incidence dependent lift. In coefficient form this can be expressed as

$$C_{LA} = C_L - \Delta C_{Lwn} \qquad 36.$$

Including the additional terms in the pitching moment equation, 22, gives

$$C_{mCG} = C_{mo} + (C_L - \Delta C_{Lwn})(h - h_o) + \Delta C_{mwn}$$

$$- \bar{V}\left\{\frac{a_1}{a}(C_L - \Delta C_{Lwn})(1 - \frac{d\varepsilon}{d\alpha}) + a_1 n_T + a_2 \bar{n}_s + a_3\beta\right\} \quad 37$$

which now represents the pitching moment equation of the aircraft including the wing and nacelle slipstream interference effects.

In steady trimmed flight $C_{mCG} = 0$ and the elevator angle to trim, $\bar{n}_s$, can be extracted from the pitching moment equation

$$\bar{V}a_2\bar{n}_s = C_{mo} + (C_L - \Delta C_{Lwn})(h-h_o) + \Delta C_{mwn} - \bar{V}\left\{\frac{a_1}{a}(C_L - \Delta C_{Lwn})(1-\frac{d\varepsilon}{d\alpha}) + a_1\eta_T + a_3\beta\right\} \quad 38.$$

Assuming the trim tab to be fixed, β = constant, the trim curve slope can be found by differentiating 38. with respect to C_L, giving

$$\frac{d\bar{n}_s}{dC_L} = \left\{1 - \frac{d}{dC_L}(\Delta C_{Lwn})\right\}\left[\frac{(h-h_o)}{\bar{V}a_2} - \frac{a_1}{aa_2}(1-\frac{d\varepsilon}{d\alpha})\right] + \frac{1}{\bar{V}a_2}\frac{d}{dC_L}(\Delta C_{mwn}) \quad 39.$$

Comparing the trim curve slopes with and without slipstream effects, eqns 22 and 39, gives a correction to the basic power off case to account for the effects of power. The correction, $\Delta(\frac{d\bar{n}_s}{dC_L})$ is defined as,

$$\Delta(\frac{d\bar{n}_s}{dC_L}) = (\frac{d\bar{n}_s}{dC_L}) - (\frac{d\bar{n}_o}{dC_L})$$

and is given by

$$\Delta(\frac{d\bar{n}_s}{dC_L}) = -\frac{d}{dC_L}(\Delta C_{Lwn})\cdot\frac{d\bar{n}_o}{dC_L} + \frac{1}{\bar{V}a_2}\frac{d}{dC_L}(\Delta C_{mwn}) \quad 40$$

This now represents the correction to the trim curve slope, controls fixed, due to the wing and nacelle slipstream interference effects.

7.1 Contribution to the Pitching Moment due to the Wing

The slipstream effect of power on the immersed portion of the wing can be considered to be due to two sources, firstly the increased local velocity of the airflow and secondly the change in local angle of incidence at the wing. These effects produce an increment in the lift force generated by the wing which can be expressed, using Fig.8, as

$$L_W + \Delta L_W = \tfrac{1}{2}\rho V^2(S-Si)a\alpha + \tfrac{1}{2}\rho(V + \Delta V)^2 Si\ a(\alpha + \Delta\alpha) \qquad (41)$$

Thus the incremental lift coefficient ΔC_{LW} can be written

$$\Delta C_{LW} = C_{LW}\frac{Si}{S}\left[\ 2\frac{\Delta V}{V} + \frac{\Delta\alpha}{\alpha}\right] \qquad (42)$$

neglecting second order quantities.

From eqn (5) the incremental velocity, v_1, in the airflow of the fully developed slipstream is given approximately by

$$\frac{v_1}{V} = \frac{1}{2}\ \frac{\eta P}{AqV} \qquad (43)$$

Assuming that the slipstream is 20% developed over the wing region the velocity increment in eqn (^{42}) can be approximated by

$$\frac{\Delta V}{V} = \frac{1.2\ \ \eta P}{4AqV} \qquad (44)$$

or, from eqn.(11)

$$\frac{\Delta V}{V} = \frac{0.3\ \ \sigma^{\frac{1}{2}}\ \eta P}{A}\left[\left(\frac{S}{W}\right)^3\ \ \frac{\rho_o}{2}\right]^{\frac{1}{2}}\quad C_L{}^{3/2} \qquad (45)$$

where ηP is the thrust horse power

The local change of incidence behind the propeller is a function of the propeller downwash due to the propeller normal force and the increase in velocity arising from the increased momentum due to thrust. An approximation to the flow direction behind the propeller can be made by assuming that the propeller imparts its momentum change to the airflow through the disc in the direction of flight and that the normal force is produced by a momentum change normal to the propeller axis.

From Fig.9 resolving the undisturbed flow into components parallel to and normal to the axis of the propeller gives

$$\begin{aligned} &\text{axially,} && V\cos(\alpha - \phi) \\ &\text{and normally} && V\sin(\alpha - \phi) \end{aligned} \qquad (46)$$

where α is the incidence relative to the wing zero lift line and ϕ is the angle between the wing zero lift line and the propeller axis.

The outflow from the propeller will have a velocity $V + \Delta V$, from eqn (45), and, if the normal component is assumed to be unaffected by the propeller then the component of the propeller outflow will be

$$\begin{aligned} &\text{axially} && (V + \Delta V) \cos (\alpha - \phi) \\ &\text{and normally} && V \sin (\alpha - \phi) \end{aligned} \qquad (47)$$

In addition there will be a downwash produced by the propeller normal force. An average value of the downwash can be estimated from the normal force coefficient, Z_c, by the momentum theory,

$$\tfrac{1}{2}\rho V^2 D^2 Z_c = \dot{m}\, \upsilon = \frac{\pi D^2}{4}\, \rho V \upsilon \qquad (48)$$

where υ is the downwash velocity due to the normal force generated by the propeller, hence υ is given by

$$\upsilon = \frac{2VZ_c}{\pi} \qquad (49)$$

The flow direction behind the propeller, $\alpha' - \phi$, will therefore be given by

$$\tan (\alpha' - \phi) = \frac{V \sin (\alpha-\phi) - \upsilon}{(V+\Delta V)\cos(\alpha-\phi)} \qquad (50)$$

Although such an estimate is only approximate it will serve to provide a value of $\frac{\Delta\alpha}{\alpha}$ for use in the assessment of ΔC_L in eqn (42)

The moment of the lift increment due to slipstream about the C.G. is given by, (eqn 4 ref 6).

$$\Delta C_{mCG} = \Delta C_{Lw} \left\{ (h - k) \cos \alpha + z \sin \alpha \right\} \qquad (51)$$

since the lift force acts at the centre of pressure of that part of the wing immersed in the slipstream which can be assumed to be a distance $k\bar{c}$ behind the leading edge of the mean aerodynamic chord.

From ref 7 the centre of pressure of the immersed portion of the wing is at $0.244\bar{c}$ and the extent of the wing immersion in the slipstream can be estimated by projecting the propeller disc aft at the slipstream exit angle α' to determine the intersection between the slipstream boundary and the wing, see fig 8.

The calculated values of the incremental lift due to slipstream, ΔC_{Lw}, are shown in table 4 for an average aircraft weight between the forward and aft C.G. cases. The incremental lift increases with incidence since the slipstream momentum arises from the velocity increment of a smaller mass flow rate, the effect being proportional to the thrust power.

The moment produced by the wing lift, ΔC_{mw}, is shown in table 5 for both forward and aft C.G.cases. At the forward C.G. the moment is nose down (negative) since the centre of lift of the immersed part of the wing is aft of the C.G. The moment produced is small but increases with C_L and is approximately proportional to power. At aft C.G. the centre of lift and C.G. are very close and only a very small nose up moment is produced.

7.2 Contribution to the pitching moment due to the nacelle

The flow over the nacelle will be generally complicated by its close proximity to the propeller, also since the nacelle also acts as a cooling air duct to the engine there may be substantial forces due to the internal flow. Insufficient data is available in the case considered to make a reasonable estimate of the duct forces.

From ref 7 the lift curve slope of the nacelle is 0.094 per radian (based on a wing area of 178 ft^2) assuming that the nacelle is replaced by an equivalent body of revolution. By similar analysis to the wing incremental lift due to the power the nacelle incremental lift will be

$$\Delta C_{Ln} = N\, C_{Ln} \left\{ \frac{2\Delta V}{V} + \frac{\Delta\alpha}{\alpha} \right\} \qquad (52)$$

where N is the number of nacelles

The values of ΔV and $\Delta\alpha$ may not however be the same as those in the case of the wing since the development of the slipstream will be very much less complete, an incremental velocity of half the fully developed slipstream velocity can be assumed since the nacelle leading edge is close to the propeller disc. The average downwash velocity can be assumed to be the same as that used for the wing since the distance from the propeller to the wing is less than I diameter.

The moment of the incremental lift due to the slipstream acting on the nacelle is given by

$$\Delta C_{mCG} = \Delta C_{Ln} \{ (h + f) \cos \alpha + (z - g) \sin \alpha \} \qquad 53.$$

where f and g are the co-ordinates of the centre of lift of the nacelle, assumed to be at quarter chord on the centre line of the equivalent body of revolution, fig.8.

The nacelle lift due to slipstream is very small and does not become significant until higher incidences are reached, Table 4 shows the incremental lift, ΔC_{Ln}. The pitching moment due to the nacelle, ΔCmn, is however more significant and at higher incidence is of the same order of magnitude as that produced by the slipstream over the wing, this is shown in table 5.

The combined wing-nacelle lift contribution due to slipstream, ΔC_{Lwn}, is very small at low incidence but as incidence increases it becomes significant and at the higher powers it may account for 10% of the total lift. From Table 4 and fig.10 it can be seen that the lift contribution and its rate of change with C_L are both approximately proportional to power.

The combined wing-nacelle pitching moment, ΔC_{mwn}, is shown in Table 5 and fig.11. At forward C.G. the pitching moment increment is almost zero, there being only a very small residual moment which tends to be negative. Its rate of change with C_L is also small and negative at low incidence, which is a stabilising effect, but becoming positive, or destabilising, at high incidence. At aft C.G. the pitching moment increases at higher incidences and its rate of change with C_L becomes significantly large and destabilising. This effect is also proportional to power.

7.3 Corrections to the Trim Curve Slope due to Slipstream - Wing-Nacelle Interference

The influence of the increment in lift on the trim curve slope is proportional to the simple theory static margin, eqn.40, and is destabilising to a statically stable aircraft. The magnitude of the effect is shown in Table 6.

From fig.11 and eqn.40 it can be seen that the rate of change of slipstream induced pitching moment with C_L is a linear function of C_L and the correction will be proportional to it. At low incidences the contribution is stabilising due to the small negative lift generated by the nacelles but as incidence increases the effect becomes destabilising.

The overall effect is to produce a general destabilisation with respect to the aircraft without power, the effect becoming more significant as C_L increases. There is little difference between the magnitude of the total corrections at forward and aft C.G., see Tables 6a and 6b.

8. Total Correction to the Trim Curve Slope for Slipstream Effects.

By considering the slipstream interference at the wing and nacelle and at the tail separately it has been possible to demonstrate the effects of the slipstream on the static stability of the aircraft.

The wing-nacelle interference arises from the difference between the slipstream and freestream velocities and also the local flow direction change which may occur. These effects become more severe as incidence increases at constant power. Table 7 shows the magnitude of the correction.

The interference at the tail is a function of the tail load necessary to trim the aircraft and incidence. Table 7 shows that this produces a destabilising effect which decreases with incidence.

The sum of these corrections gives an overall destabilisation effect which has a minimum magnitude at about $C_L = 0.6$. At low incidence the tail effects are dominant and at high incidence the slipstream-wing-nacelle effects become increasingly important. Figs.12 to 14 show the total correction applied to the trim curve slopes taken from measured flight data. The measured slopes, power on, show a trend towards destabilisation as incidence increases. After correction for slipstream effects the slope curves are seen to be shifted to a generally greater slope, indicating increased overall static stability, and to be more constant with C_L which indicates that some of the incidence dependent destabilisation has been accounted for.

9. Conclusions

Within the limits of the estimation, and insofar as these can be verified by flight measurement, the corrections show that the slipstream effects are destabilising under all normal flight conditions and that the destabilisation tends to increase with increasing incidence and power. By considering the origins of the destabilisation it is seen that the direct pitching moment and the downwash increment at the tail are the destabilising contributions whereas the wing-nacelle lift contribution and the slipstream energy factor at the tail are stabilising. If the destabilising effect of power on static stability is to be minimised it is necessary to consider the nacelle lift due to slipstream interference, to reduce the direct pitching moment, and to place the tailplane as far as possible away from the direct influence of the slipstream so that the downwash effect is minimised.

Since so little reliable information concerning the slipstream location is available it is difficult to make specific recommendations to reduce this effect. It may however be possible to determine whether or not the tail is moving out of the slipstream region as incidence increases and whether any sudden change of slipstream influence is likely to give rise to inconsistent handling qualities or short period, self induced oscillations.

Only controls fixed static stability data has been considered here, but the general results can be extended to the controls free trim curves.

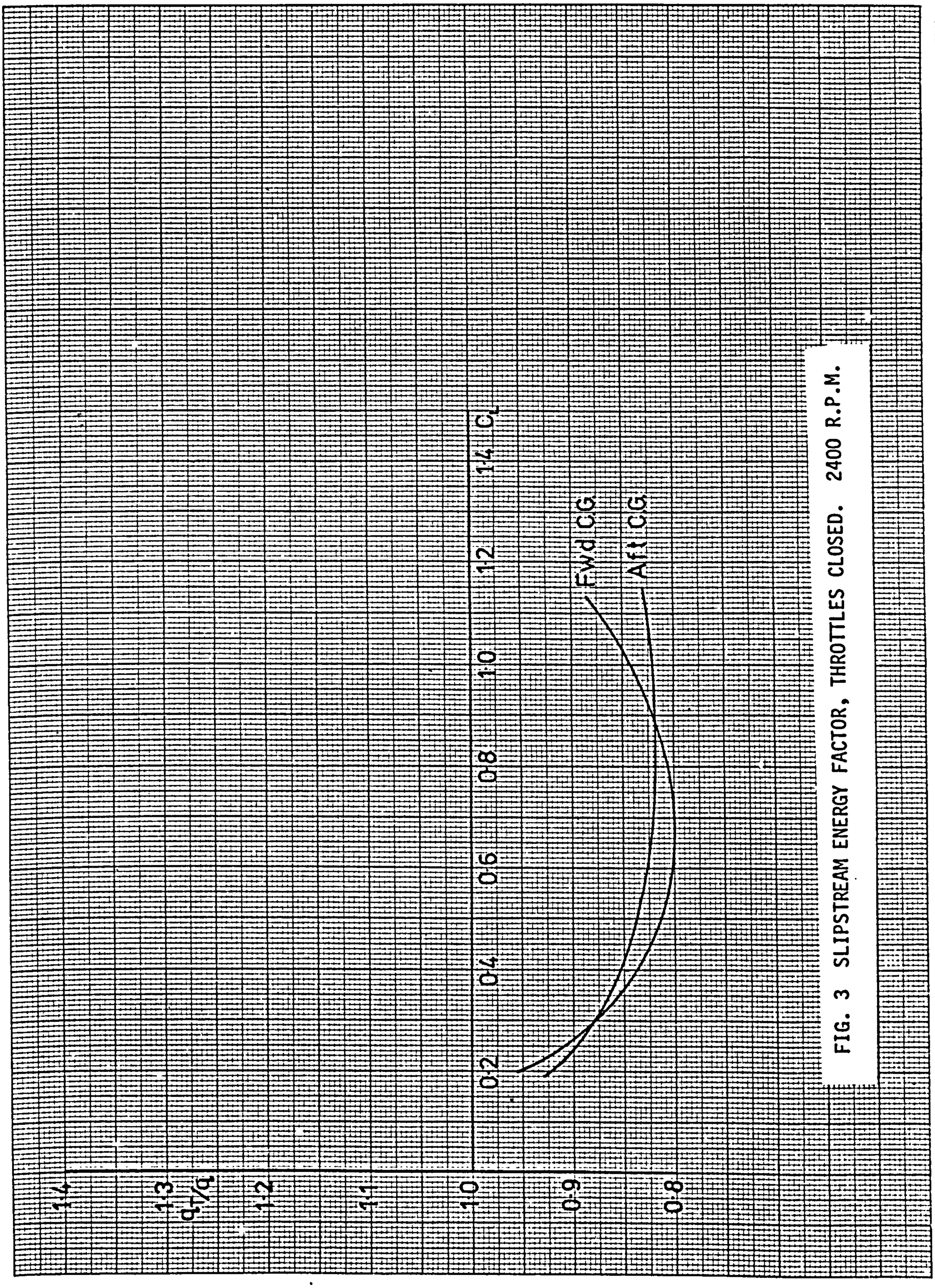
1·4
1·3
1·2
1·1
1·0
0·9
0·8
qT/q
1·2
1·4 CL
Fwd C.G
Aft C.G
0·6
0·8
1·0
0·4
0·2
FIG. 3 SLIPSTREAM ENERGY FACTOR, THROTTLES CLOSED. 2400 R.P.M.

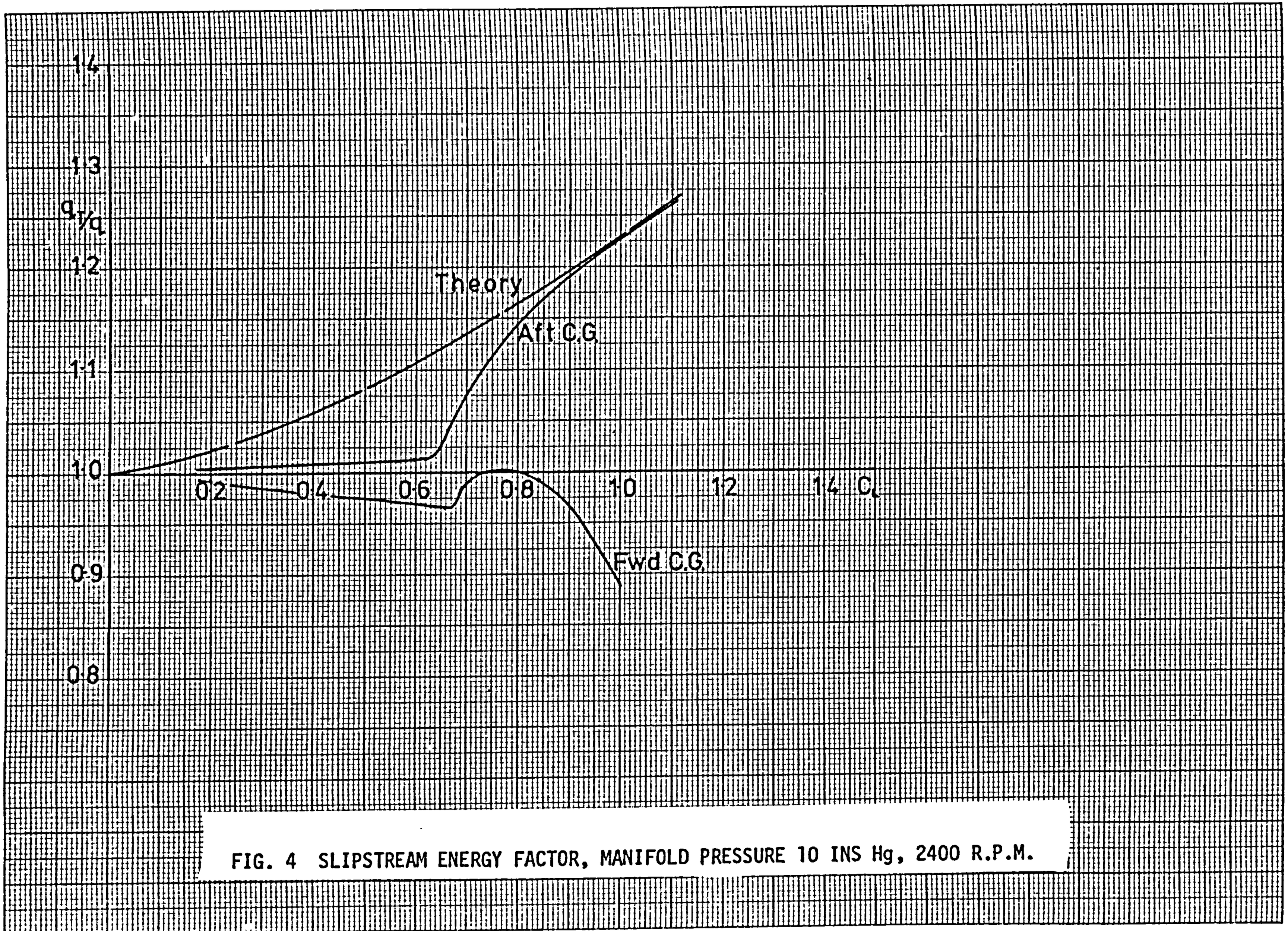

FIG. 4 SLIPSTREAM ENERGY FACTOR, MANIFOLD PRESSURE 10 INS Hg, 2400 R.P.M.

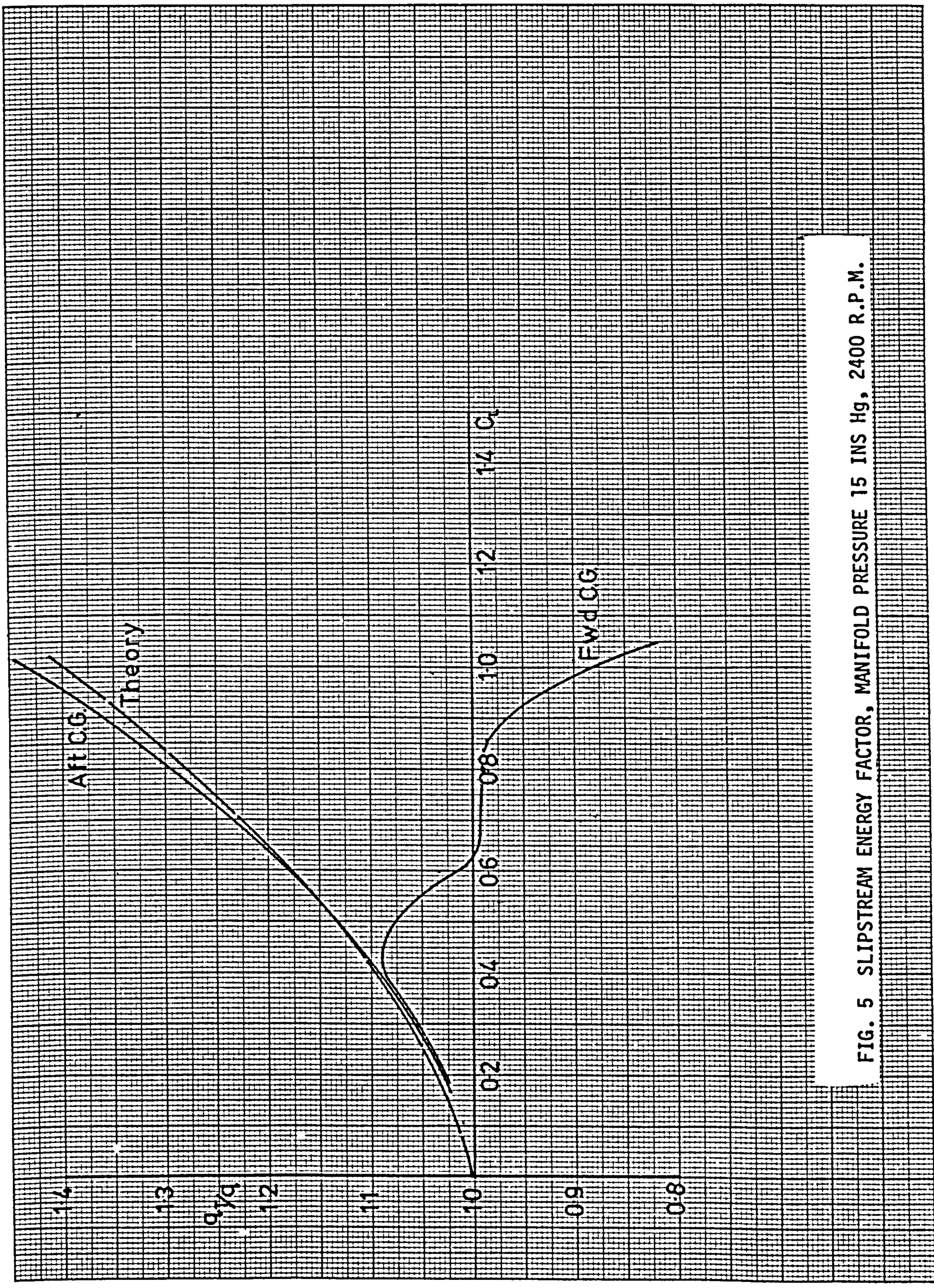

FIG. 5 SLIPSTREAM ENERGY FACTOR, MANIFOLD PRESSURE 15 INS Hg, 2400 R.P.M.

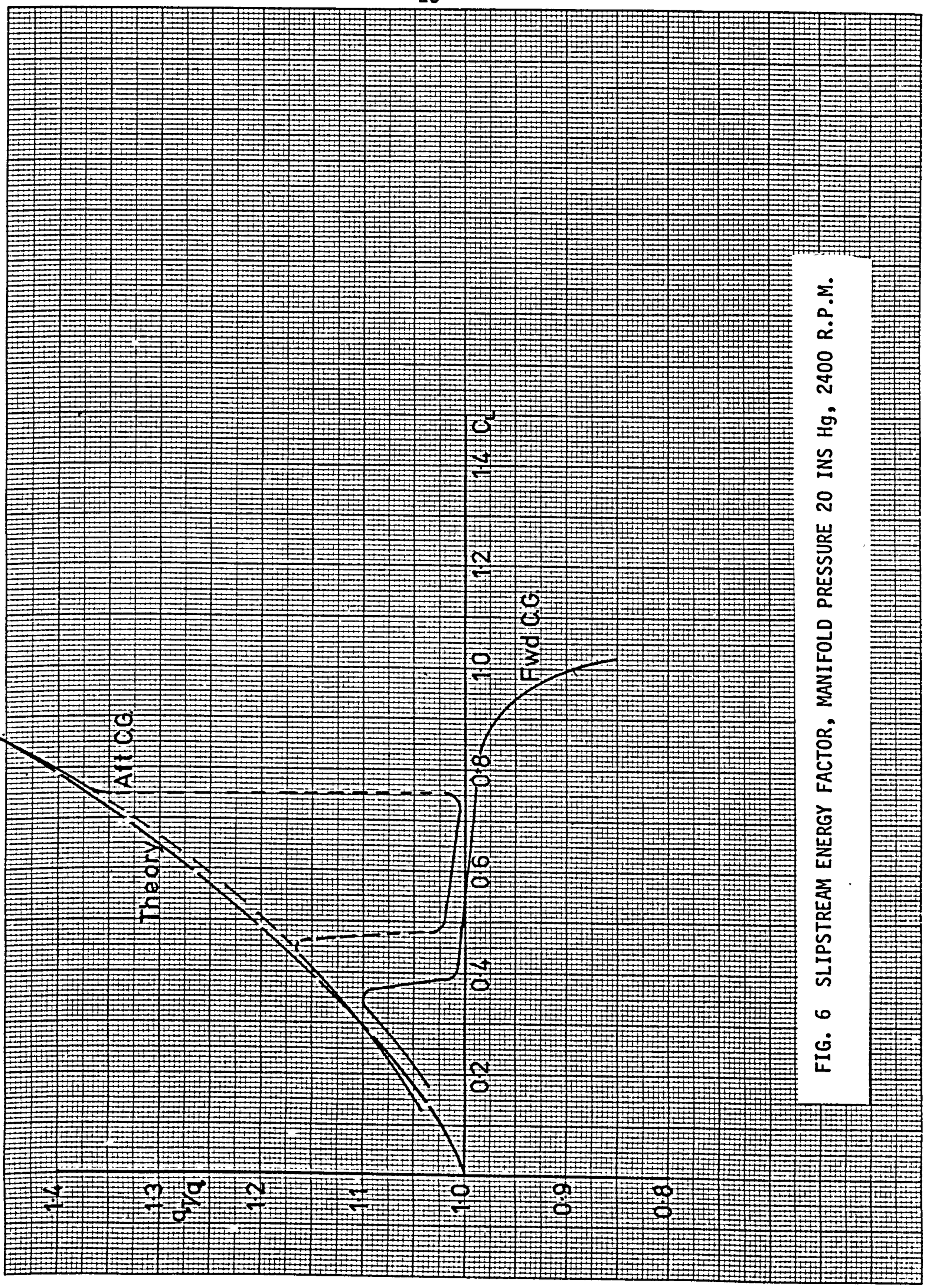
q/q
1·4
1·3
1·2
1·1
1·0
0·9
0·8
Theory
Attcc.
C.G.
1·2
1·4
0·4
0·6
0·8
1·0
Fwd C.G.
0·2
FIG. 6 SLIPSTREAM ENERGY FACTOR, MANIFOLD PRESSURE 20 INS Hg, 2400 R.P.M.

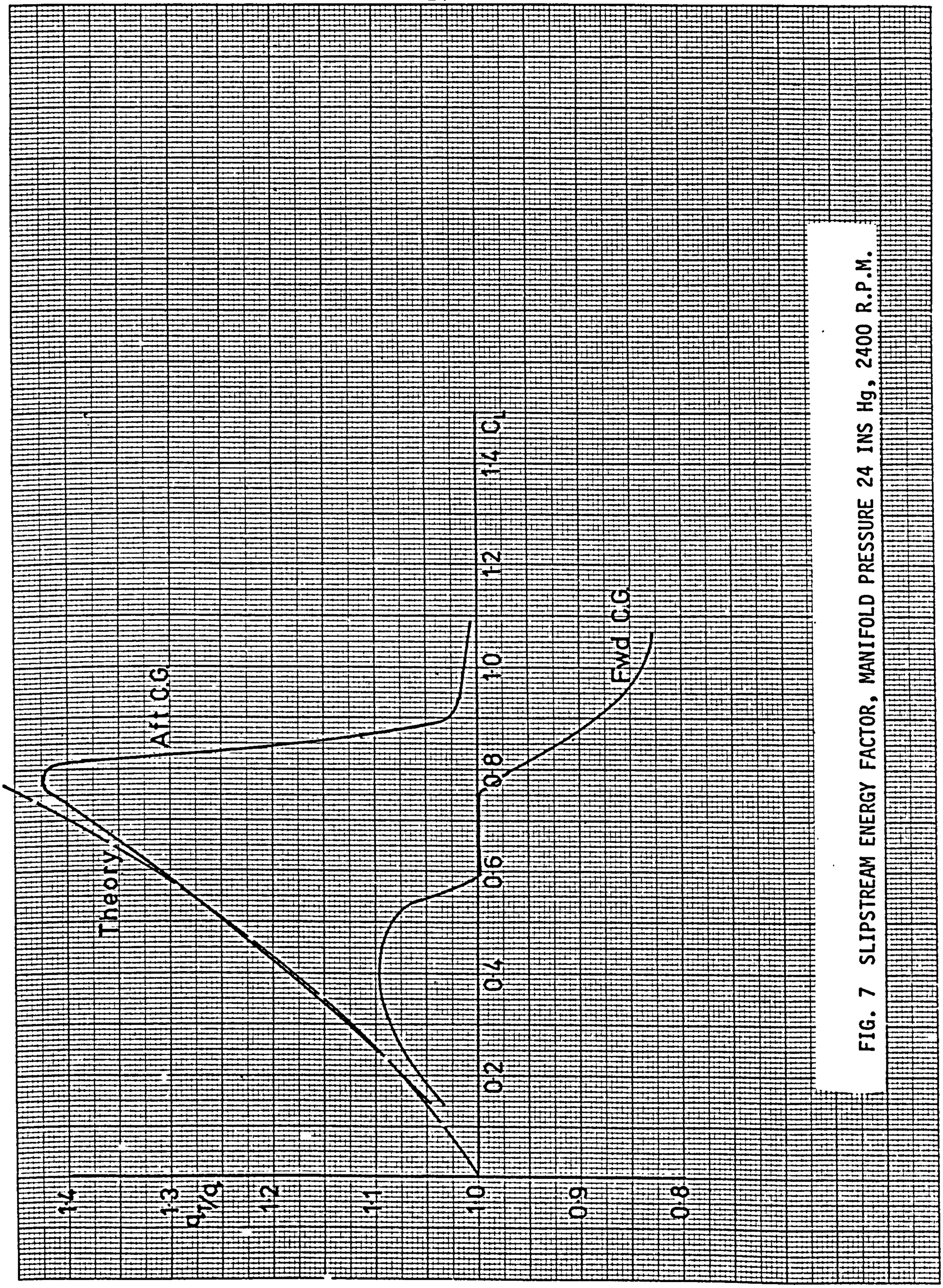

FIG. 7 SLIPSTREAM ENERGY FACTOR, MANIFOLD PRESSURE 24 INS Hg, 2400 R.P.M.

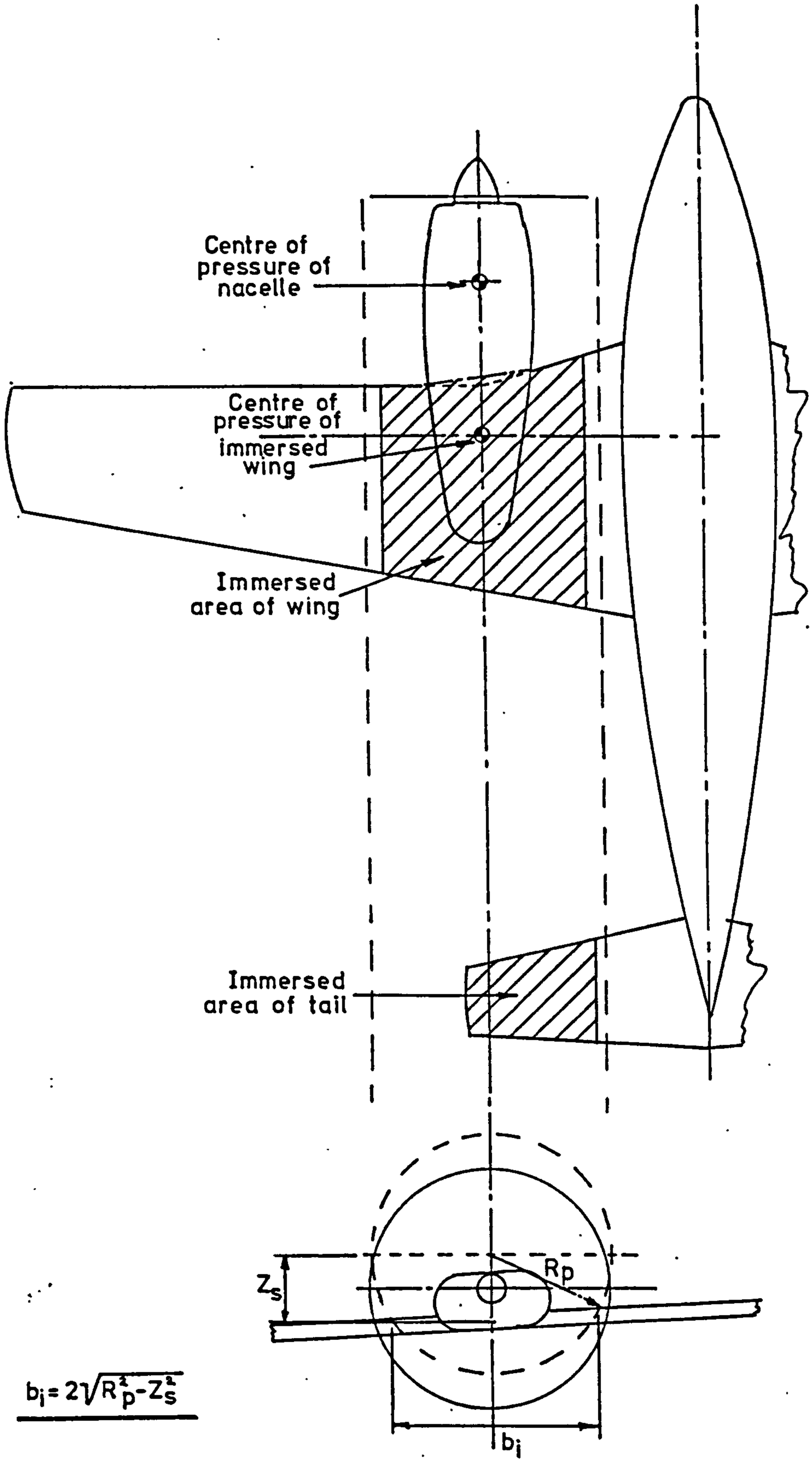

$b_i = 2\sqrt{R_p^2 - Z_s^2}$

FIG 8 Propeller Slipstream Interference.

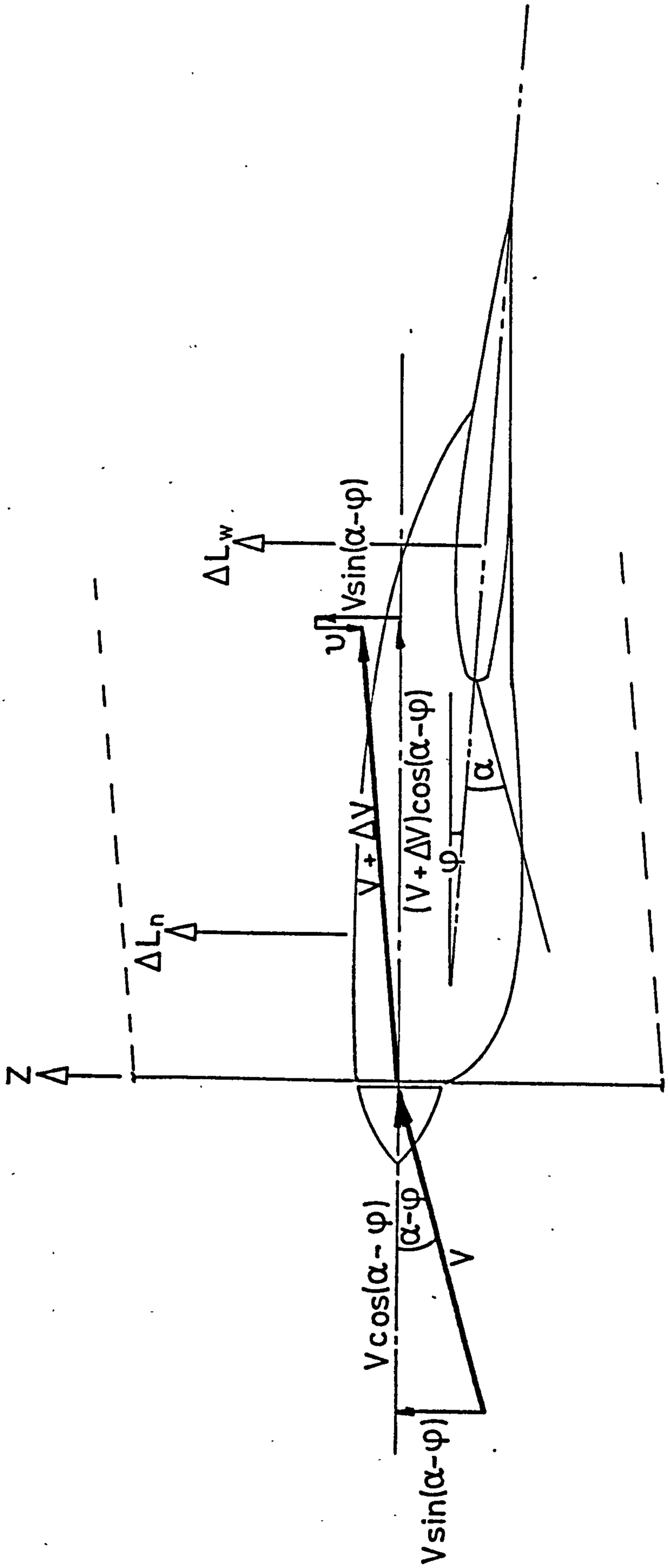

FIG. 9 Propeller Slipstream in Wing-Nacelle Region.

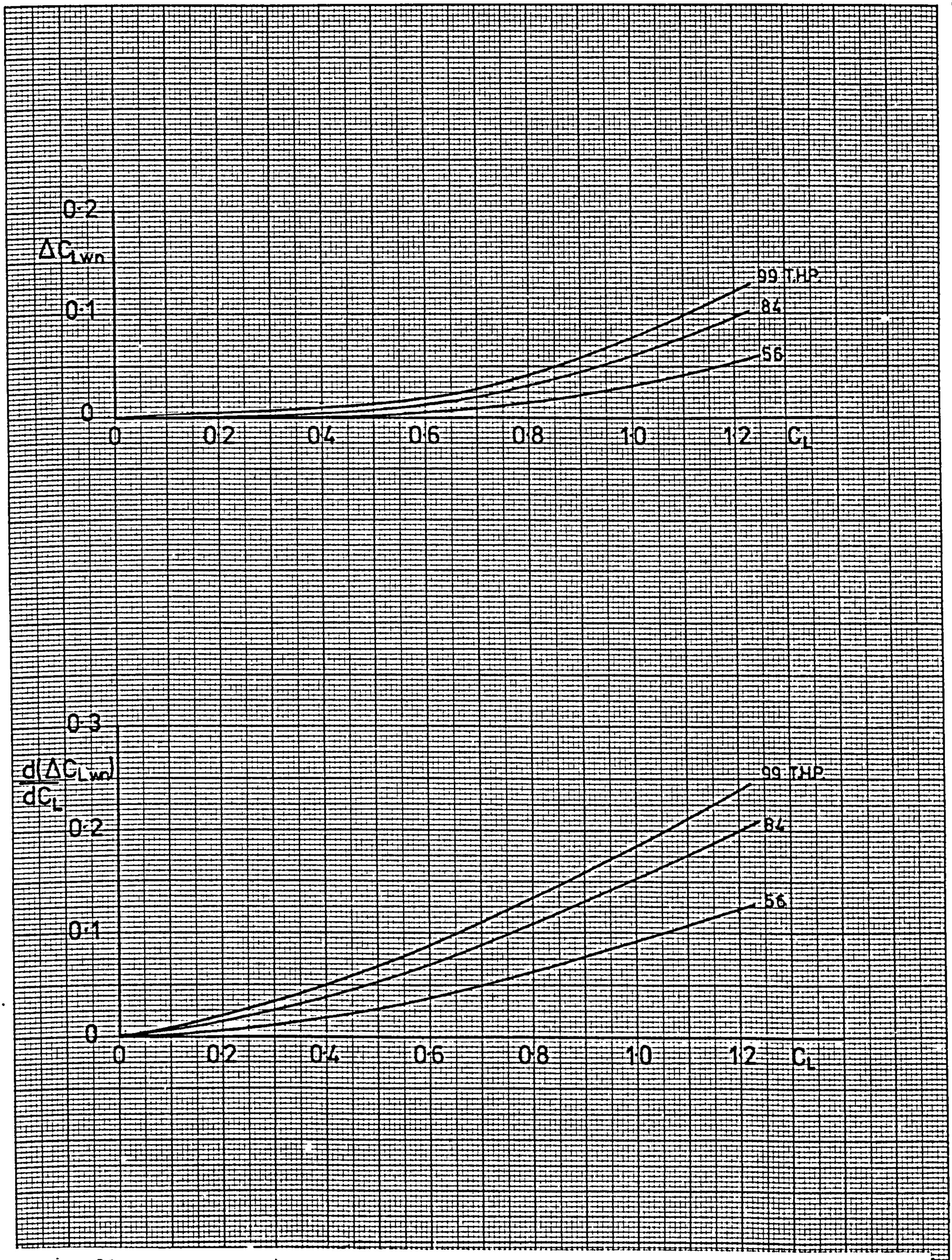

FIG. 10. Lift Increment due to Slipstream Interference with Wing and Nacelle

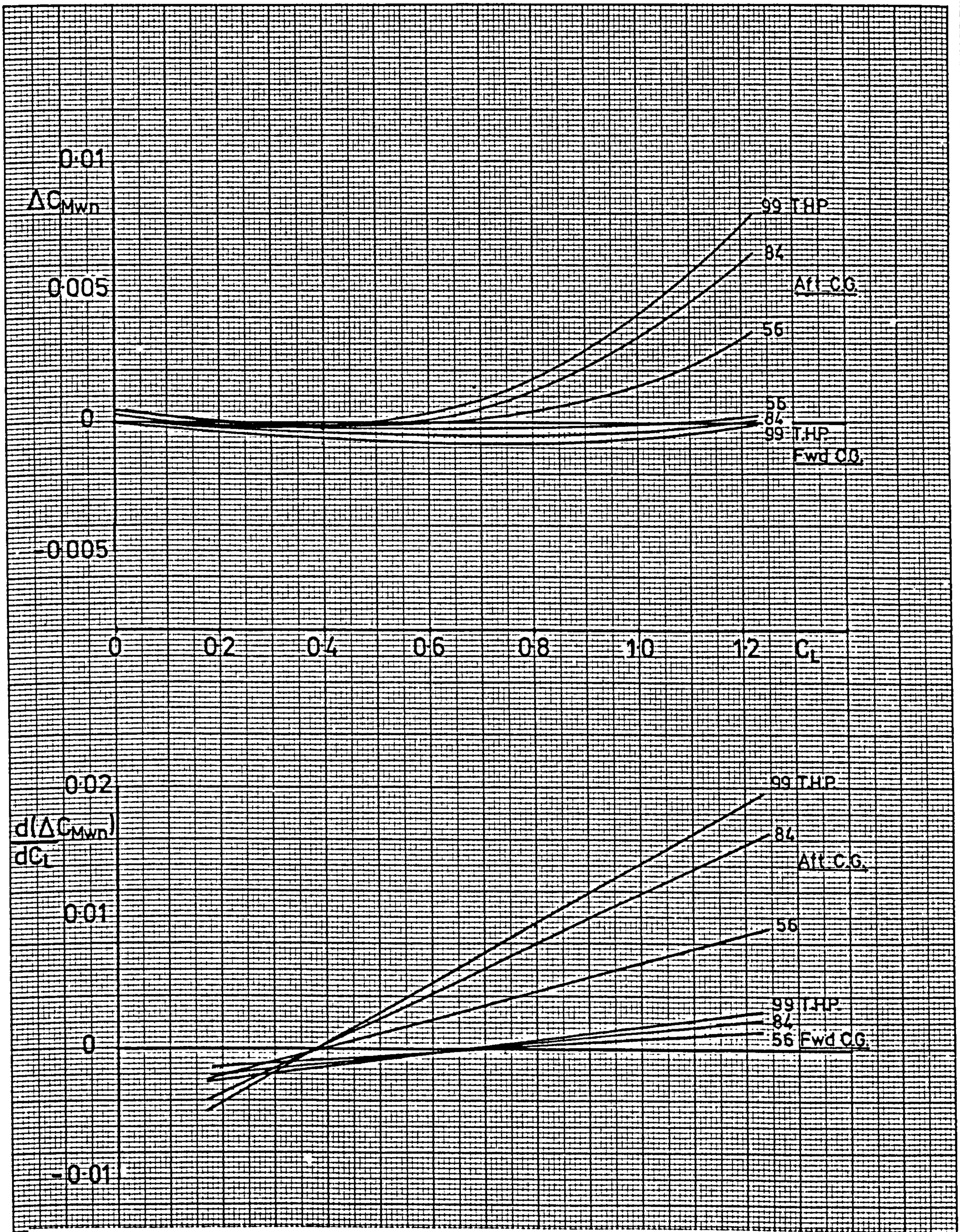

FIG.11. Pitching Moment Movement due to Slipstream Interference with Wing and Nacelle.

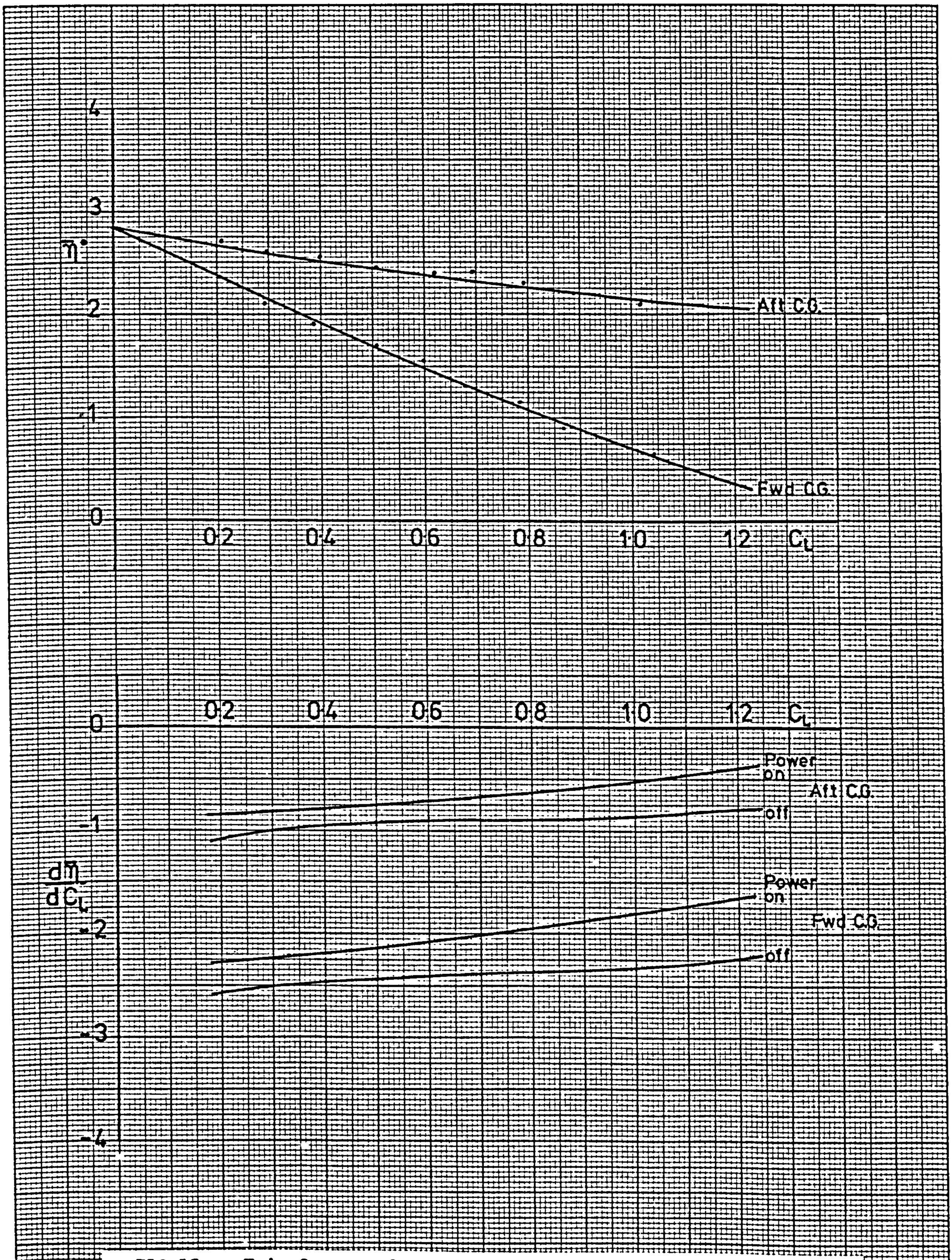

FIG.12. Trim Curves, Controls Fixed 56 T.H.P. (15"/2400 RPM)

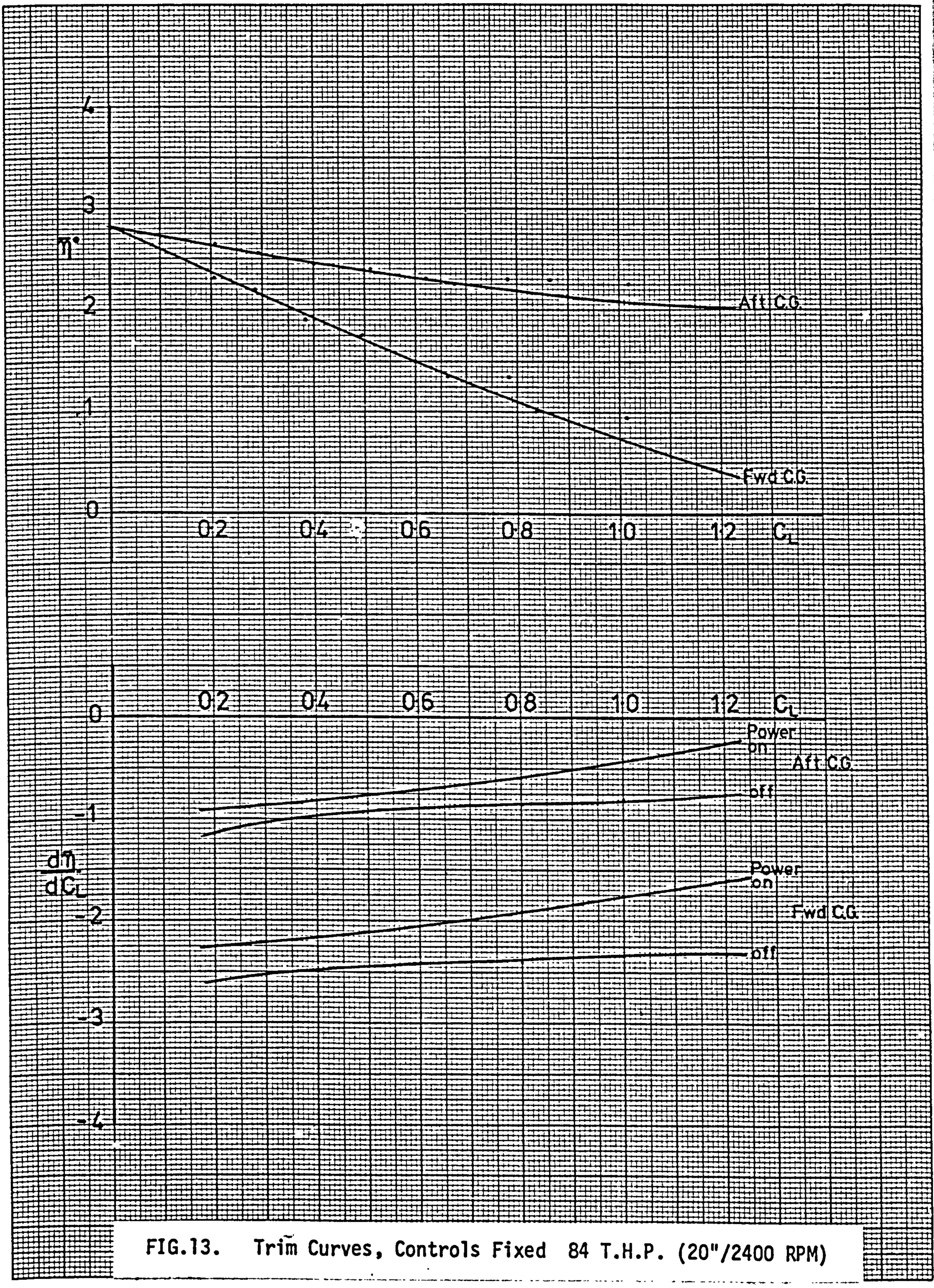

FIG.13. Trim Curves, Controls Fixed 84 T.H.P. (20"/2400 RPM)

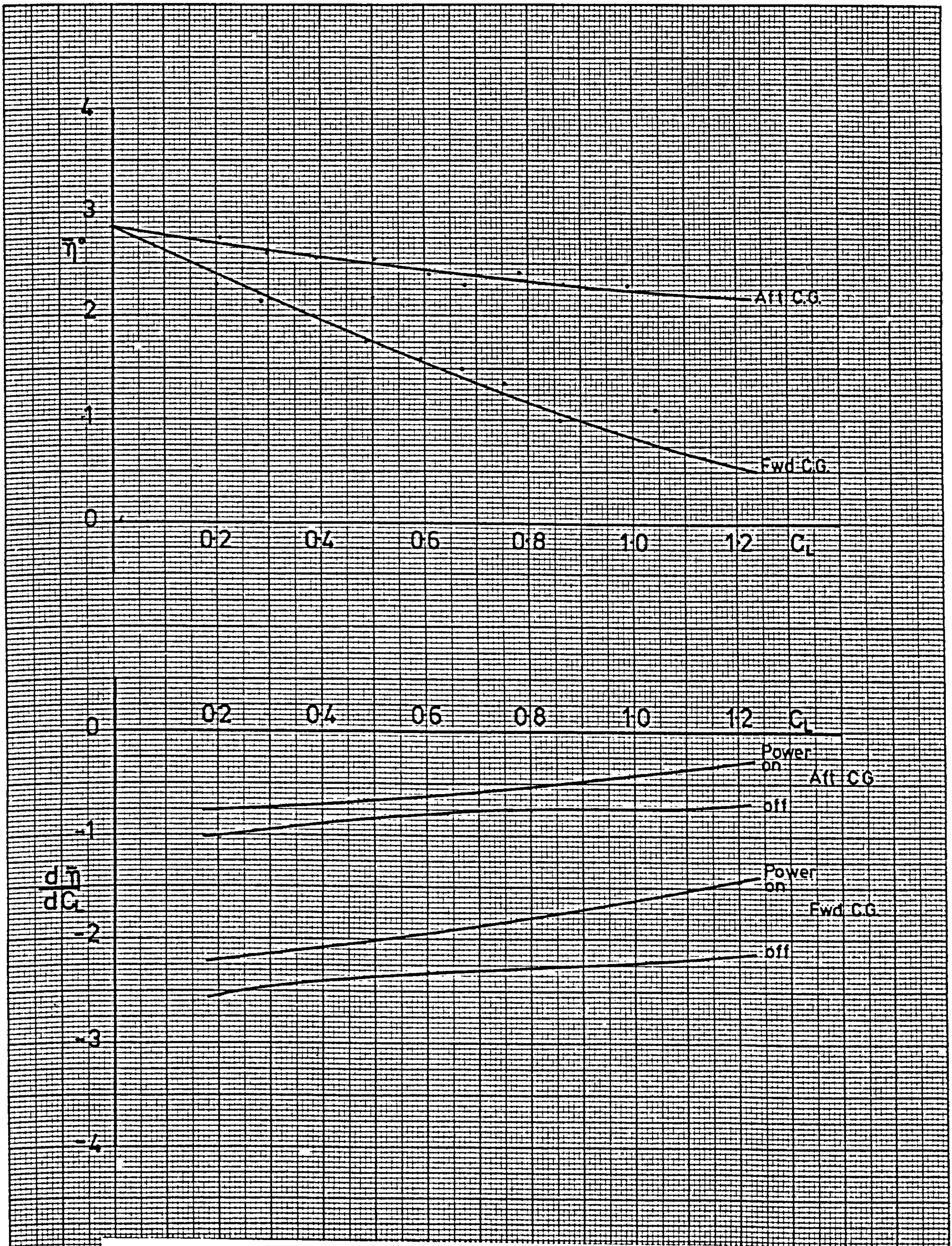

FIG.14. Trim Curves, Controls Fixed 99 T.H.P. (24"/2400 RPM)

Slipstream Function		C_L					
	Power	0.2	0.4	0.6	0.8	1.0	1.2
F_T	56	1.019	1.056	1.099	1.112	1.147	1.149
	84	1.027	1.082	1.151	1.175	1.216	1.230
	99	1.036	1.097	1.178	1.210	1.260	1.299
F_T'	56	0.133	0.172	0.135	0.050	0.015	0.013
	84	0.225	0.288	0.250	0.136	0.088	0.080
	99	0.260	0.334	0.295	0.217	0.200	0.197
F_{T_2}	56	1.046	1.125	1.180	1.152	1.162	1.165
	84	1.072	1.197	1.301	1.284	1.304	1.310
	99	1.088	1.230	1.355	1.387	1.460	1.535
F_T'/F_{T_2}	56	0.127	0.153	0.114	0.043	0.013	0.011
	84	0.210	0.241	0.192	0.106	0.067	0.061
	99	0.239	0.272	0.221	0.156	0.137	0.128
$(1/F_{T_2} - 1)$	56	-0.081	-0.187	-0.262	-0.279	-0.315	-0.348
	84	-0.067	-0.164	-0.231	-0.221	-0.233	-0.237
	99	-0.044	-0.111	-0.152	-0.132	-0.139	-0.142

TABLE 1. Slipstream Functions, Tailplane Interference Effect

$(\frac{\epsilon_p}{\epsilon_o} - 1)$	Power	C_L						Mean
		0.2	0.4	0.6	0.8	1.0	1.2	
Fwd C.G.	56	0.025	0.080	0.110	0.115	0.105	0.083	0.106
	84	0.035	0.096	0.130	0.135	0.130	0.097	0.117
	99	0.038	0.100	0.131	0.133	0.131	0.098	0.119
Aft C.G.	56	0.040	0.100	0.125	0.125	0.115	0.087	0.110
	84	0.060	0.120	0.144	0.144	0.132	0.102	0.128
	99	0.067	0.132	0.147	0.147	0.142	0.107	0.135

TABLE 2. Downwash Rate Factor $(\frac{\epsilon_p}{\epsilon_o} - 1)$

$\Delta \frac{d\bar{n}}{dC_L}_p$ due to:-	Power	C_L					
		0.2	0.4	0.6	0.8	1.0	1.2
$(h - h_o)$	56	-0.047	-0.119	-0.182	-0.142	-0.149	-0.152
	84	-0.072	-0.176	-0.248	-0.237	-0.250	-0.254
	99	-0.087	-0.200	-0.281	-0.299	-0.338	-0.374
C_{LTo}	56	0.008	0.010	0.007	0.003	0.001	0
	84	0.013	0.015	0.012	0.006	0.004	0.004
	99	0.015	0.017	0.014	0.010	0.009	0.008
k_ε	56	0.365	0.365	0.365	0.365	0.365	0.365
	84	0.401	0.401	0.401	0.401	0.401	0.401
	99	0.408	0.408	0.408	0.408	0.408	0.408
TOTAL	56	0.326	0.256	0.190	0.226	0.217	0.213
	84	0.342	0.240	0.165	0.170	0.155	0.151
	99	0.336	0.225	0.141	0.119	0.079	0.042

TABLE 3a. Correction to Trim Curve Slope due to Slipstream at the Tail, Forward C.G.

$\Delta \frac{d\bar{\eta}}{dC_L}$ p due to:-	Power	C_L					
		0.2	0.4	0.6	0.8	1.0	1.2
$(h - h_o)$	56	-0.096	-0.243	-0.332	-0.288	-0.304	-0.310
	84	-0.146	-0.358	-0.505	-0.483	-0.509	-0.518
	99	-0.177	-0.408	-0.573	-0.610	-0.688	-0.761
C_{LTo}	56	0.008	0.010	0.007	0.003	0.001	0
	84	0.013	0.015	0.012	0.006	0.004	0.004
	99	0.015	0.017	0.014	0.010	0.009	0.008
k_ε	56	0.380	0.380	0.380	0.380	0.380	0.380
	84	0.437	0.437	0.437	0.437	0.437	0.437
	99	0.466	0.466	0.466	0.466	0.466	0.466
TOTAL	56	0.292	0.147	0.055	0.095	0.077	0.070
	84	0.304	0.094	-0.056	-0.040	-0.068	-0.077
	99	0.304	0.075	-0.093	-0.134	-0.213	-0.287

TABLE 3b Correction to Trim Curve Slope due to Slipstream at the Tail, Aft C.G.

		C_L					
	POWER	0.2	0.4	0.6	0.8	1.0	1.2
ΔC_{Lw}	56	0.0025	0.0020	0.0058	0.0155	0.0303	0.0512
	84	0.0035	0.0055	0.0136	0.0304	0.0561	0.0925
	99	0.0041	0.0146	0.0182	0.0392	0.0706	0.1153
ΔC_{Ln}	56	0.0001	-0.0002	-0.0002	0.0004	0.0015	0.0035
	84	0.0002	-0.0001	0.0002	0.0014	0.0035	0.0069
	99	0.0002	0	0.0005	0.0020	0.0046	0.0088
ΔC_{Lwn}	56	0.0026	0.0018	0.0056	0.0159	0.0318	0.0547
	84	0.0037	0.0054	0.0138	0.0318	0.0596	0.0994
	99	0.0043	0.0146	0.0187	0.0412	0.0752	0.1241

TABLE 4. Increment in Lift due to Slipstream from Wing and Nacelle

		C_L					
	POWER	0.2	0.4	0.6	0.8	1.0	1.2
ΔC_{mw}	56	-0.0002	-0.0001	-0.0003	-0.0008	-0.0015	-0.0023
	84	-0.0002	-0.0003	-0.0008	-0.0016	-0.0028	-0.0041
	99	-0.0003	-0.0009	-0.0011	-0.0021	-0.0035	-0.0052
ΔC_{mn}	56	0.0001	-0.0002	-0.0002	0.0002	0.0009	0.0020
	84	0.0001	0	0.0001	0.0008	0.0021	0.0041
	99	0.0001	0	0.0003	0.0012	0.0027	0.0050
ΔC_{mwn}	56	-0.0001	-0.0003	-0.0005	-0.0006	-0.0006	-0.0003
	84	-0.0001	-0.0003	-0.0007	-0.0008	-0.0007	-0.0000
	99	-0.0002	-0.0009	-0.0007	-0.0009	-0.0008	-0.0002

5a . Forward C.G.

TABLE 5. Increment in Pitching Moment due to Slipstream from Wing and Nacelle

		C_L					
	POWER	0.2	0.4	0.6	0.8	1.0	1.2
ΔC_{mw}	56	0	0	0	0.0002	0.0004	0.0009
	84	0	0	0.0001	0.0003	0.0007	0.0016
	99	0	0	0.0001	0.0004	0.0009	0.0020
ΔC_{mn}	56	0.0001	-0.0002	-0.0002	0.0002	0.0010	0.0023
	84	0.0001	-0.0001	0.0001	0.0009	0.0023	0.0045
	99	0.0001	0	0.0003	0.0013	0.0030	0.0056
ΔC_{mwn}	56	0.0001	-0.0002	-0.0002	0.0004	0.0014	0.0032
	84	0.0001	-0.0001	0.0002	0.0012	0.0030	0.0061
	99	0.0001	0	0.0004	0.0017	0.0039	0.0076

5b. Aft C.G.

TABLE 5 Increment in Pitching Moment due to Slipstream from Wing & Nacelle

$\Delta\left[\frac{d\bar{\eta}_s}{dC_L}\right]$ due to	Power	C_L					
		0.2	0.4	0.6	0.8	1.0	1.2
ΔC_{Lwn}	56	0.0159	0.0477	0.1007	0.1643	0.2438	0.3259
	84	0.0397	0.1060	0.1855	0.2862	0.4054	0.5300
	99	0.0530	0.1325	0.2332	0.3551	0.4902	0.6333
ΔC_{mwn}	56	-0.0236	-0.0135	-0.0067	0.0034	0.0118	0.0203
	84	-0.0338	-0.0203	-0.0068	0.0068	0.0203	0.0338
	99	-0.0405	-0.0236	-0.0051	0.0118	0.0304	0.0473
TOTAL	56	-0.0077	0.0342	0.0940	0.1677	0.2556	0.3462
	84	0.0059	0.0857	0.1787	0.2930	0.4257	0.5638
	99	0.0125	0.1089	0.2281	0.3433	0.5206	0.6806

TABLE 6a Correction to Trim Curve Slopes due to Slipstream-Wing-Nacelle Interference

Forward C.G.

$\Delta\left[\frac{d\bar{n}_s}{dC_L}\right]$ due to	Power	C_L					
		0.2	0.4	0.6	0.8	1.0	1.2
ΔC_{Lwn}	56	0.0092	0.0277	0.0585	0.0954	0.1416	0.1894
	84	0.0231	0.0616	0.1078	0.1663	0.2356	0.3080
	99	0.0308	0.0770	0.1355	0.2063	0.2849	0.3680
ΔC_{mwn}	56	-0.0338	0.0017	0.0388	0.0743	0.1115	0.1470
	84	-0.0608	0.0034	0.0676	0.1317	0.1959	0.2610
	99	-0.0693	0.0084	0.0861	0.1621	0.2399	0.3176
TOTAL	56	-0.0245	0.0294	0.0973	0.1697	0.2531	0.3364
	84	-0.0377	0.0650	0.1754	0.2980	0.4315	0.5690
	99	-0.0385	0.0854	0.2216	0.3684	0.5248	0.6856

TABLE 6b. Correction to Trim Curve Slopes due to Slipstream-Wing-Nacelle Interference

Aft. C.G.

Correction due to	Power	C_L					
		0.2	0.4	0.6	0.8	1.0	1.2
Slipstream-Wing-Nacelle Interference	56	-0.0077	0.0342	0.0940	0.1677	0.2556	0.3462
	84	0.0059	0.0857	0.1787	0.2930	0.4257	0.5638
	99	0.0125	0.1089	0.2281	0.3433	0.5206	0.6806
Slipstream-Tail Interference	56	0.3260	0.2560	0.1900	0.2260	0.2170	0.2130
	84	0.3420	0.2400	0.1650	0.1700	0.1550	0.1510
	99	0.3360	0.2250	0.1410	0.1190	0.0790	0.0420
TOTAL	56	0.3183	0.2902	0.2840	0.3937	0.4726	0.5592
	84	0.3479	0.3257	0.3437	0.4630	0.5807	0.7148
	99	0.3485	0.3339	0.3691	0.4623	0.5996	0.7226

TABLE 7a Total Correction to Trim Curve Slopes due to Slipstream Interference, Forward C.G.

Correction due to	Power	C_L					
		0.2	0.4	0.6	0.8	1.0	1.2
Slipstream-Wing-Nacelle Interference	56	-0.0245	0.0294	0.0973	0.1697	0.2531	0.3364
	84	-0.0377	0.0650	0.1754	0.2980	0.4315	0.5690
	99	-0.0385	0.0854	0.2216	0.3684	0.5248	0.6856
Slipstream-Tail Interference	56	0.2920	0.1470	0.0550	0.0950	0.0770	0.0700
	84	0.3040	0.0940	-0.0560	-0.0400	-0.0680	-0.0770
	99	0.3040	0.0750	-0.0930	-0.1340	-0.2130	-0.2870
TOTAL	56	0.2675	0.1764	0.1523	0.2647	0.3301	0.4064
	84	0.2663	0.1590	0.1194	0.2580	0.3635	0.4920
	99	0.2655	0.1595	0.1286	0.2344	0.3118	0.3986

TABLE 7b. Total Correction to Trim Curve Slopes due to Slipstream Interference, Aft C.G.

REFERENCES

Ref.1 ESHELBY, M.E. An Instrumentation System to Measure the Stability Characteristics of Light Aircraft. Cranfield Aero Memo No. 101 1972

Ref.2 ESHELBY, M.E. A Comparative Assessment of Three Methods of Measurement of Pressure Error Corrections. Cranfield Report Aero No. 11 1972

Ref.3 ESHELBY, M.E. An Investigation of the Slipstream Effects of Power on Logitudinal Static Stability. Cranfield Aero Memo No.148 1974

Ref.4 HARRIS, H.T. Slipstream Induced Sideslip on a Dove Aircraft in Trimmed Flight. Dept. of Aero. M.Sc Thesis, Cranfield 1971

Ref.5 GOULTER, S.V. A Wind Tunnel Investigation of Propeller Slipstream Effects on a Twin Engined Aircraft. Dept. of Aero. M.Sc Thesis, Cranfield 1972

Ref.6 ESHELBY, M.E. Incidence Related Distortion of Low Speed Longitudinal Static Stability Trim Curves. Cranfield Report Aero No. 30 1975 (Abstract - Section I Part II

Ref.7. WOLOWICZ,C.H. & YANCEY, R.B. Longitudinal Aerodynamic Characteristics of Light, Twin-Engined, Propeller-driven Airplanes. NASA TN-6800 1972

Ref.8. ESHELBY,M.E. An Analysis of the Force System of a Propeller. Cranfield Report Aero No.33. 1977.

APPENDIX A.1

A COMPUTER PROGRAMME FOR THE SIMULATION OF THE PROPELLER SLIPSTREAM CHARACTERISTICS OF A TWIN ENGINED AIRCRAFT

A.1 Introduction

To determine the degree of interference between a propeller slipstream and the tailplane of an aircraft a computer programme has been developed to simulate the flow path of a fluid filament issuing from a point on the propeller disc in the presence of the aircraft wing, fuselage and tail. This entails calculating the instantaneous velocities at a point on the fluid filament and the direction of the flow at that point. The flow is allowed to travel a short distance in the calculated direction to a new point at which the process is repeated to delineate the path of the slipstream filament and its eventual position with respect to the tailplane. By selecting points on the perimeter of the propeller disc an approximation to the position of the slipstream relative to the tail can be made. This will indicate the degree of slipstream-tailplane interference and also the amount of distortion of the slipstream section shape at the tail location.

The method of analysis is based on the principles used by Silverstein and Katzoff et al. (Refs. A.1 and A.2), with reference to later developments (Refs. A.3, A.5). It is assumed that the various components of the aircraft are independent and mutual interference is neglected, each providing flow perturbations which can be considered additive.

The lifting surfaces are replaced by simple bound vortices at the quarter chord line with fully rolled up trailing vortices from the tips. This simplified lifting system is considered adequate for the purpose of this exercise and a comparison between flat and fully rolled up trailing vortex systems when used to calculate the downwash is given in Refs. A.1 and A.3. The propeller slipstream is represented by an incremental velocity calculated by the actuator disc theory (Ref. A.6 and section 3). It is assumed that the inflow factor at the disc is half that of the developed slipstream at the tail and that a linear velocity gradient exists between them. No propeller slipstream rotation is included. The increases slipstream velocity over the wing will produce an increase in load lift and consequently increase the downwash behind the wing in the slipstream region. This local lift is represented by a bound vortex system at the wing quarter chord line aft of the propeller, the calculation of the vortex being a function of the engine power, Ref. A.4.

The gross downwash will be the sum of the downwash components due to the wing, tail and power effects at any point under the influence of the vortex systems. There will also be a further disturbance to the flow from the fuselage displacement and the total disturbances can be summed into components in the flight direction and normal to the

flight direction laterally and vertically. Since the aircraft components are assumed to be independent the effect of each variable can be found in isolation enabling the causes of the slipstream distortion to be isolated and quantified.

A.2 Analysis of Bound Vortex System

The Bound Vortex systems are each treated by the Biot-Savart vortex element theory to give the induced velocity components at a point, P, at a distance r from the vortex line, (Ref. A.6).

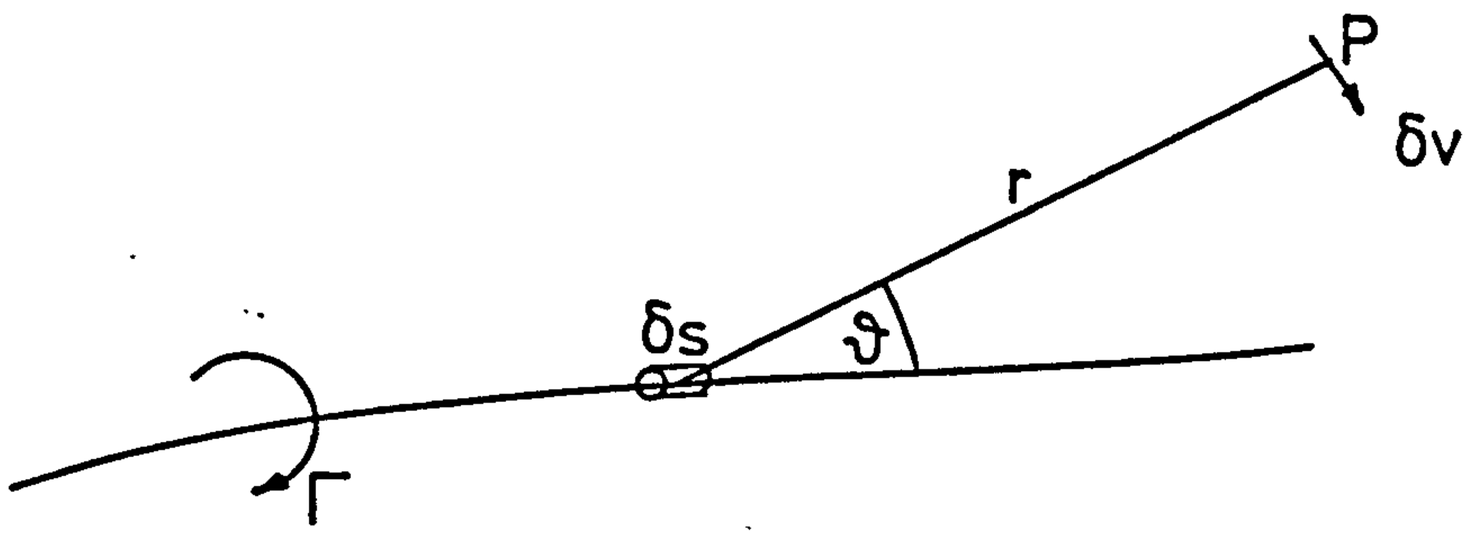

FIG A1

The induced velocity component δv due to a small element δs of a line vortex strength Γ is given by

$$\delta v = \frac{\Gamma}{4\pi r^2} \delta s \sin \theta \qquad A.1$$

Integrating A.1 along a straight line vortex of finite length AB gives

$$v = \frac{\Gamma}{4\pi h} (\cos \theta_1 + \cos \theta_2) \qquad A.2$$

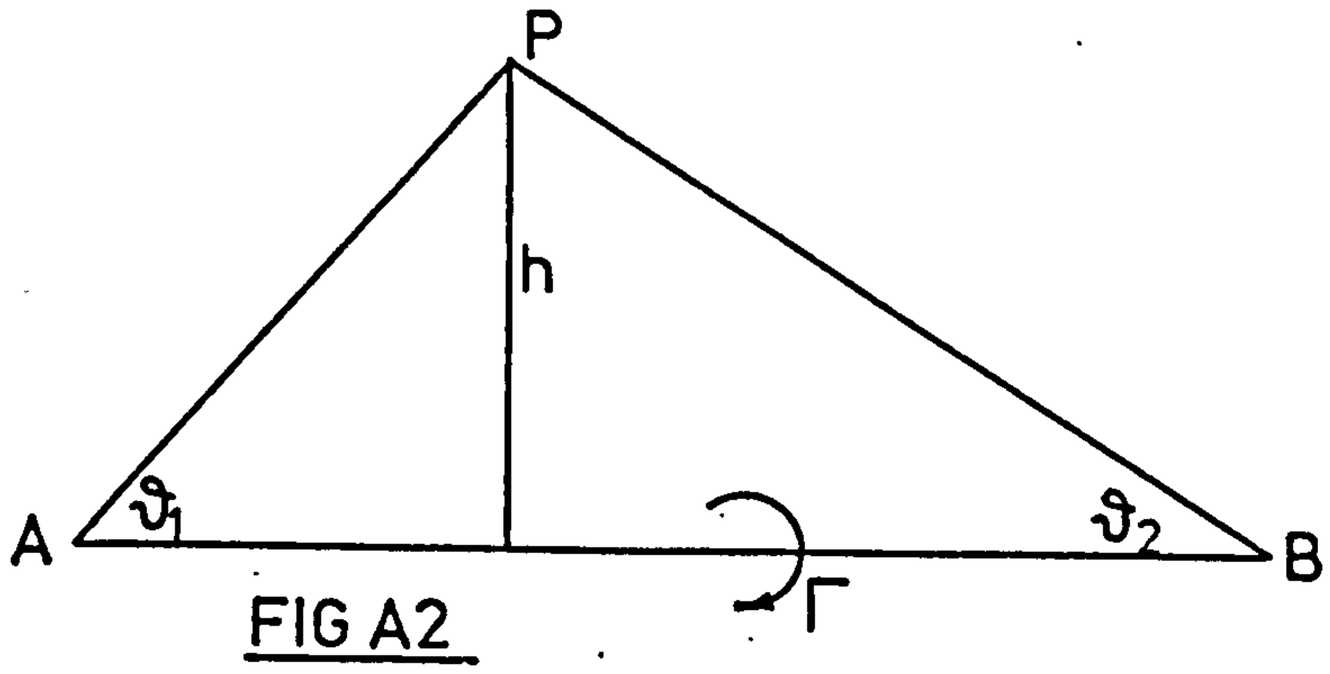

FIG A2

The aircraft is referred to a system of axes centred at the mid point of the wing lifting line vortex, O, and aligned with the Ox axis in the direction of flight, Oy to starboard and Oz downwards perpendicular to Ox and Oy. The trailing vortices are assumed to trail in the direction of flight. Although these axes are used for the calculation of the slipstream filament locus the positions of the tail and propeller with respect to the origin of the axis system is based on the body axes of the aircraft aligned to the wing zero lift incidence. This implies that the starting point, the co-ordinates of the point on the propeller disc relative to the body axes, have to be converted to the wind axes before calculation of the locus commences. When the filament has reached the tail the co-ordinates are re-converted to body axes relative to the tail pitot position.

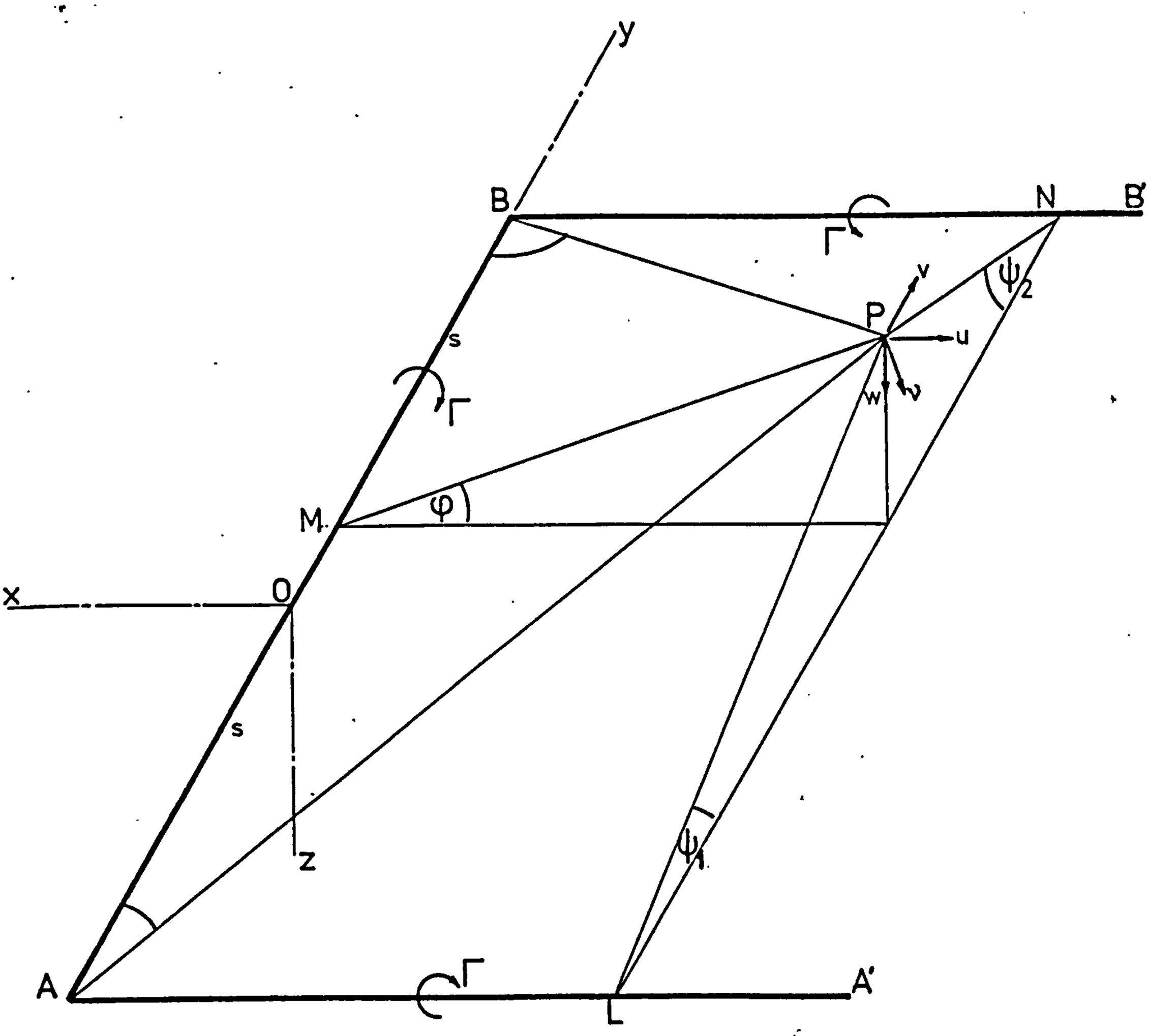

FIG. A3.

Considering a horseshoe vortex A'ABB' of strength Γ the three elements of the vortex can be assumed to act separately on the general point P, Fig. A.3.

The velocity contribution from the line vortex AB of the length 2s will be

$$= \frac{\Gamma}{4\pi MP} (\cos PAO + \cos PBO)$$

$$= \frac{\Gamma}{4\pi(x^2 + z^2)^{\frac{1}{2}}} \left[\frac{(y + s)}{(x^2 + z^2 + (y + s)^2)^{\frac{1}{2}}} \right.$$

$$\left. - \frac{(y - s)}{(x^2 + z^2 + (y - s)^2)^{\frac{1}{2}}} \right] \qquad A.3$$

and the components of ν along the axes Ox, Oy and Oz will be u_1, $_1$ and w_1 respectively, given by

$$u_1 = -\nu_1 \sin\phi = -\frac{\nu_1 z}{(x^2 + z^2)^{\frac{1}{2}}}$$

$$\nu_1 = 0 \qquad A.4$$

$$w_1 = \nu_1 \cos\phi = \frac{\nu_1 x}{(x^2 + z^2)^{\frac{1}{2}}}$$

Similarly the contribution due to the semi infinite trailing vortex AA' will be

$$\nu_2 = \frac{\Gamma}{4\pi PL} (1 + \cos PAA')$$

$$= \frac{\Gamma}{4\pi(z^2 + (y + s)^2)^{\frac{1}{2}}} \left[1 + \frac{x}{(x^2 + z^2 + (y + s)^2)^{\frac{1}{2}}} \right] \qquad A.5$$

and the components along the co-ordinate axes will be given by

$$u_2 = 0$$

$$\nu_2 = \nu_2 \sin\psi_1 \qquad A.6$$

$$w_2 = \nu_2 \cos\psi_1$$

Similarly the contribution due to the semi infinite trailing vortex BB' will be

$$u_3 = 0$$
$$v_3 = -\nu_2 \sin \psi_2 \qquad \text{A.7}$$
$$w_3 = -\nu_3 \cos \psi_2$$

The total components of the velocity at P are thus given from A.4, A.6 and A.7 by

$$u = u_1$$
$$v = v_2 + v_3$$
$$w = w_1 + w_2 + w_3$$

This process can be used for each horseshoe vortex system and the sum of the velocity components at the point P from all the vortex systems gives the overall incremental velocity component at that point from the aircraft model.

A.2.1 Representation of the Wing

The wing is assumed to have a basic span loading due to its incidence to the free stream of L/2s lbf/ft. From the lift equation for a line vortex in steady flow the circulation Γ is given by

$$\Gamma = \frac{L}{2s\rho V} \qquad \text{A.8}$$

where V is the free stream velocity.

The wing is thus replaced by a single line vortex of strength Γ at the quarter chord line.

A.2.2 Representation of the Tail

The tail is treated in the same way as the wing, being replaced by a single line vortex at quarter chord.. The vortex strength Γ_T being calculated from the tail lift and span and free stream velocity as in equation A.8. The estimation of the tail lift force is considered in section A.3.

A.2.3 Representation of the Propeller Slipstream

The slipstream velocity is calculated from the actuator disc theory. Since flight measurement showed that the slipstream was fully developed by the time it reaches the tail, a linear variation in the outflow factor is assumed between the propeller disc and the tail. The outflow factor is calculated from the approximation to the slipstream energy factor at the tail q_T/q (Refs. A.6 and section 3), which gives

$$\frac{q_T}{q} = (1 + K C_L^{3/2}) \qquad A.9$$

The increased velocity over the wing behind the propeller will produce an increase in local lift which can be represented by a horseshoe vortex system superimposed on the wing vortex system (Ref. A.4). Assuming that the propeller does not alter the local flow direction but only increases its velocity the incident airflow then the expression for the increase in local lift per unit span ΔL can be written in the form

$$L + \Delta L = \tfrac{1}{2}\rho(V + \Delta V)^2 \bar{c} a \alpha \qquad A.10$$

and expanding the R.H.S.

$$L + \Delta L = \tfrac{1}{2}\rho(V^2 + 2V\Delta V + \Delta V^2)\bar{c} a \alpha$$

neglecting second order powers of ΔV gives

$$\Delta L = \rho V \Delta V \bar{c} a \alpha \qquad A.11$$

Now by the lifting line theory the same increase can be written in the form

$$L + \Delta L = \rho V(\Gamma + \Delta\Gamma) \qquad A.12$$

hence from A.11 and A.12

$$\Delta\Gamma = \Delta V \bar{c} a \alpha = \Delta V \bar{c} C_L \qquad A.13$$

Thus the additional vortex system on the wing behind the propeller will have a circulation $\Delta\Gamma$ and cover a span equal to the propeller slipstream diameter at the wing.

From equation 10 the velocity ratio at the tail to free stream is give by

$$\frac{V_T}{V} = (1 + K C_L^{3/2})^{\frac{1}{2}}$$

hence ΔV is given by the approximation

$$\Delta V = V_T - V \doteq V(\tfrac{1}{2}KC_L^{3/2})$$

Since the outflow factor at the tail is twice that at the propeller disc the value of ΔV at the wing is given by

$$\Delta V = V(\tfrac{1}{2}K\,C_L^{3/2})\tfrac{1}{2}\ \frac{x}{(x + \ell_T)} \qquad \text{A.14}$$

where x is the distance between the propeller disc and the wing lifting line and ℓ_T is the tail arm between the aerodynamic centres.

A.3 Estimation of Tail Load

The tailplane load required to trim the aircraft in steady flight is the sum of the loads required to balance the aerodynamic moment and the engine thrust moment. Each may be treated separately and assumed to be independent in the first order approximation.

i) Aerodynamic Moment Contribution

Using the pitching moment equation for the aircraft developed in Ref. A.8, (equation (15)) to include the effect of the vertical offset of the C.G. and tailplane from the mean aerodynamic chord the tail lift can be expressed in the reduced form,

$$C_{LT} = \{C_{mo} + (h - h_o)F_1 + zF_2\}\ \frac{1}{\bar{V}F_3} \qquad \text{A.15}$$

where $$C_{LT} = L_T/\tfrac{1}{2}\rho_o V_e^2 S_T \qquad \text{A.16}$$

and $$F_1 = C_L \cos\alpha + C_D \sin\alpha$$

$$F_2 = C_L \sin\alpha - C_D \cos\alpha$$

and $$F_3 = \mathrm{Cos}\ \alpha + \frac{\bar{c}y}{I_T} \sin\alpha$$

where α = incidence

l_T = tail arm

z = C.G.height above m.a.c.

and $y\bar{\bar{c}}$ = Height of tail above m.a.c.

From the lift equation for the complete aircraft

$$\tfrac{1}{2}\rho_o V_e^2 = W/SC_L \qquad \text{A.17}$$

thus from A.15, A.16 and A.17

$$L_T = \frac{WS_T}{\bar{V}SF_3C_L}\{C_{mo} + (h - h_o)F_1 + zF_2\} \qquad \text{A.18}$$

from Ref. A.7 $C_{mo} = -0.0463$

and from Ref. A.8 $h_o = 0.110\bar{c}$ and $\bar{V} = 0.530$

Equation A.18 thus gives the tail load to balance the aerodynamic moment.

ii) Direct Thrust Moment

The pitching moment produced by the propeller in the sum of two moments, one due to the direct thurst along the propeller axis and the other due to the normal force generated by the angle of incidence of the propeller due to the slipstream. The normal force can be estimated using the methods described in Refs. A.9 and A.10, and the propeller pitching moment can thus be approximated by the polynomial

$$C_{mp} = -C_L^{1.3} P(0.2 - z) \times 10^{-3} \qquad \text{A.19}$$

where z is the vertical C.G. expressed as a fraction of $\bar{c}$ above the m.a.c.

The tail load due to the engine thrust is given by

$$L_T = -C_L^{0.3} P(0.2 - z) \frac{WS_T}{\bar{V}S} \times 10^{-3} \qquad \text{A.20}$$

The total tail load is the sum of the tail lift forces from equations A.18 and A.20, these are shown in Fig. A.4

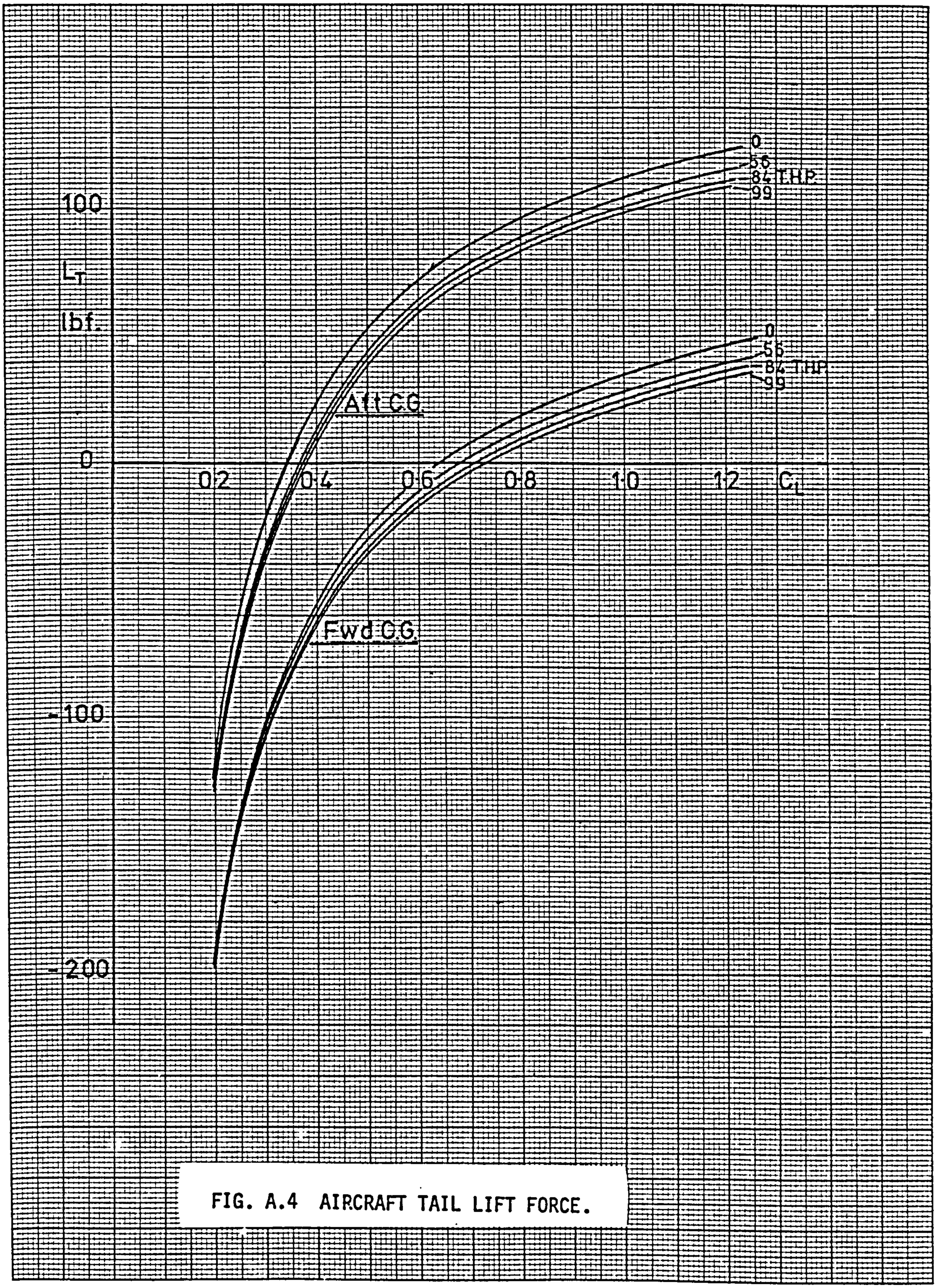

FIG. A.4 AIRCRAFT TAIL LIFT FORCE.

A.4 Estimation of the Fuselage Effect

The fuselage produces a blockage to the airflow and causes flow disturbance which will tend to distort the shape of the propeller slipstream as it passes the fuselage region. To estimate the extent of the fuselage effect it is necessary to be able to represent the fuselage by a relationship between its cross section area and its length. Since the fuselage is of a complex shape it is not possible to present this relationship easily. A reasonable approximation can be made by replacing the fuselage by a body of revolution based on the NACA 4-digit series aerofoils. The length of the body is chosen to be greater than the fuselage to allow for the blunted rear fuselage and the boundary layer of 15% and length of 27 ft. was found to closely agree with the aircraft. The body of revolution was set at -3^{o} (nose down) to the fuselage datum line with the nose points coincident to obtain the best possible fit. A comparison between the bodies is shown in Fig. A.5.

The thickness envelope of the NACA 0015 aerofoil is given by the equation

$$\pm y = \frac{t}{0.20}\{0.2969x^{\frac{1}{2}} - 0.1260x - 0.3516x^2 + 0.2843x^3 - 0.1015x^4\}$$

where $x\bar{c}$ is the length aft of the leading edge

$y\bar{c}$ is the thickness ordinate = fuselage radius r

$t\bar{c}$ is the maximum thickness

and $\bar{c}$ is the chord length

In calculating the fuselage displacement effect on the slipstream an axisymmetric continuity equation is used.

At any fuselage section with a radius r the cross section area is given by

$$A = \pi r^2$$

and the rate of change of area with radius is

$$dA = 2\pi r\, dr$$

Thus the volume change dv, per unit length $d\ell$ is

$$dv = 2\pi r\, dr\, d\ell$$

At some radius R outside the fuselage $(R > r)$ the volume change per unit length will similarly be

$$dV = 2\pi R dR d\ell$$

but by the law of continuity

$$dv = dV$$

thus the displacement of a particle at some radius R from the centre of the fuselage due to the change in fuselage area between two stations will be

$$dR = \frac{r}{R}\, dr ,$$

which is compatible with slender body axial flow constraints.

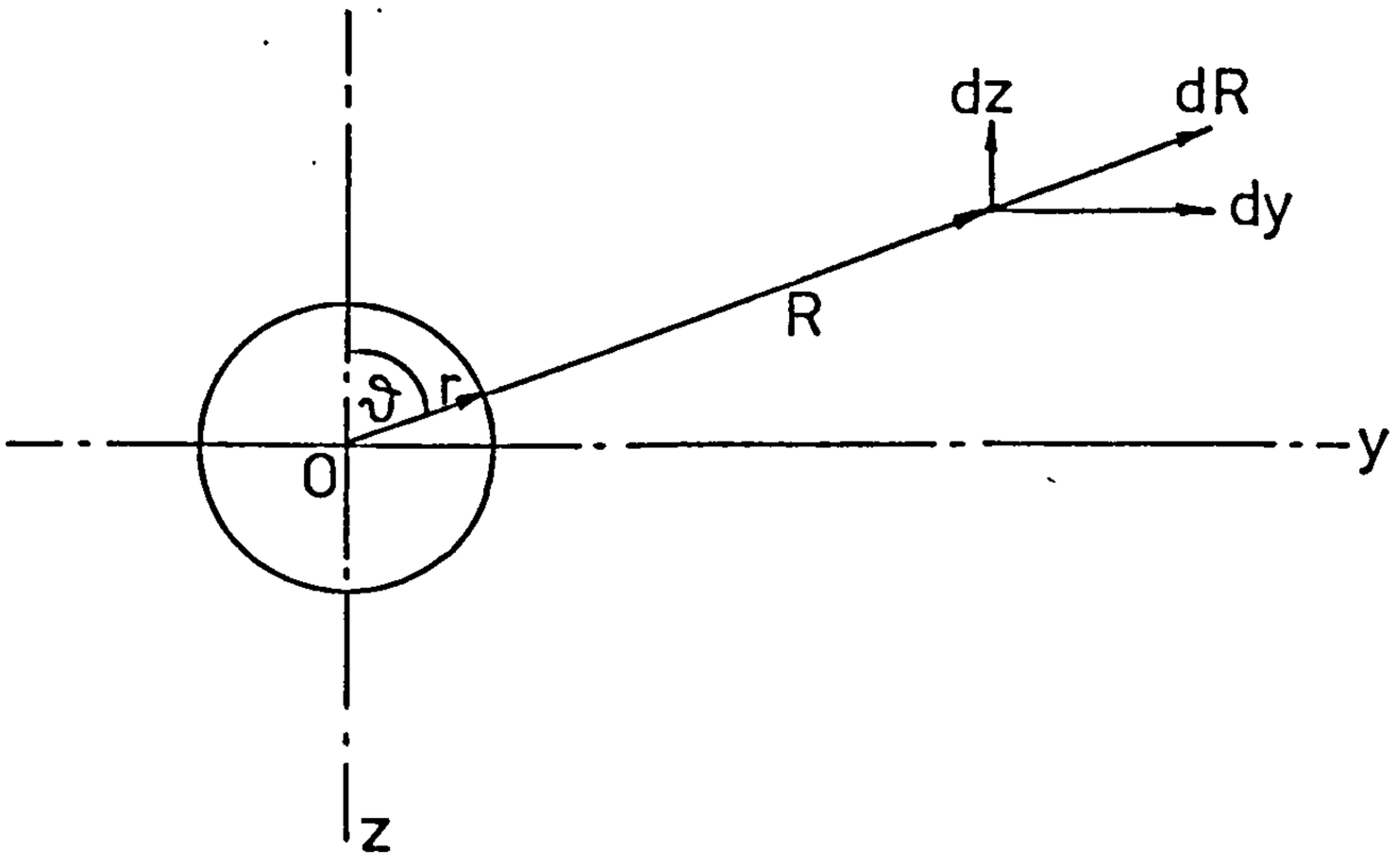

The components of displacement will be

$$dY = dR \sin \phi$$

and $$dZ = dR \cos \phi$$

where $$\phi = \tan^{-1}(Y/Z)$$

In calculating the fuselage displacement the value of dr is found by comparing the current value of fuselage radius r with the previously calculated value to give the fuselage section change per unit length. The value of the displacement components dy and dZ can then be calculated and used to modify the slipstream filament positions.

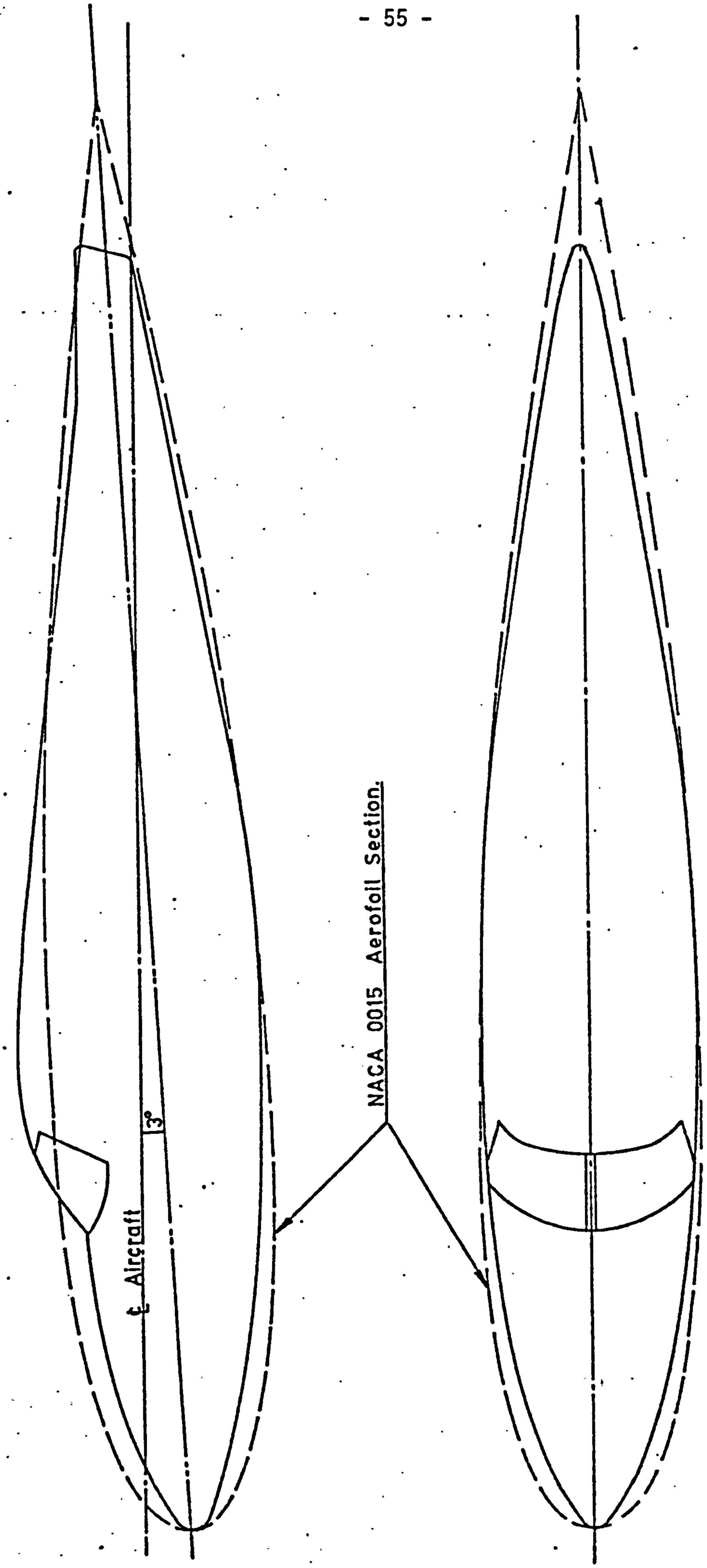

FIG A5 Comparison of Fuselage with NACA 0015 Section Body of Revolution.

A.5 Propeller Slipstream Contraction

As the slipstream velocity varies along the efflux from the propeller disc to reach its fully developed velocity there will be a change in the slipstream diameter. This arises from the law of conservation of mass which states that in the absence of mixing of the high energy flow from the propeller with the lower energy freestream

$$\rho AV = \text{constant}$$

Using the notation of section 3 and letting A_1 be the area of the fully developed slipstream then

$$\rho A(V + v) = \rho A_1(V + v_1) \qquad A.21$$

and letting $v = aV$, it can be seen that by using equations 2 and 3

$$2v = v_1$$

thus

$$A(1 + a) = A_1(1 + 2a) \qquad A.22$$

or expressed as diameters

$$\frac{D_1^2}{D^2} = \frac{A_1}{A} = \frac{1 + a}{1 + 2a}$$

giving

$$\frac{D_1}{D} = \left(\frac{1 + a}{1 + 2a}\right)^{\frac{1}{2}} \doteq 1 - \tfrac{1}{2}a \qquad A.23$$

Now the slipstream energy factor $\frac{q_T}{q} = (1 + 2a)$

hence $\left(\frac{q_T}{q}\right)^{-\frac{1}{4}} = (1 + 2a)^{-\frac{1}{4}} \doteq 1 - \tfrac{1}{2}a \qquad A.24$

and from A.23 and A.24

$$\frac{D_1}{D} \doteq \left(\frac{q_T}{q}\right)^{-\frac{1}{4}} \qquad A.25$$

The value of q_T/q referred to in equation A.25 is the theoretical value of the slipstream energy factor, not necessarily the measured value since this may be modified by local flow disturbances.

The relationship between slipstream contraction and energy factor is shown in Fig. A.6. Since for all measured values of the slipstream energy factor considered the contraction is less than 10% and considering that substantial shape distortion of the slipstream is evident this effect is not considered significant enough to include in the general programme.

A.6 The Slipstream Simulation Programme

The programme was developed specifically for the Piper Twin Comanche used in the trials leading up to the analysis of power effects on aircraft handling qualities. It could, however, be converted to be applicable to any aircraft by changing the constants to suit the geometric properties of the aircraft considered.

The input data is kept to the minimum level concerning only the parameters that have a direct effect on the longitudinal stability trim curves, C.G., weight and power, since the object of the exercise is to find the effect of changes of each variable in isolation and to compare with the flight conditions of the trials. Fig. A.7 shows the flow diagram of the programme and Table A.1 lists the programme stages. The language is Hewlett Packard Basic 2000 B.

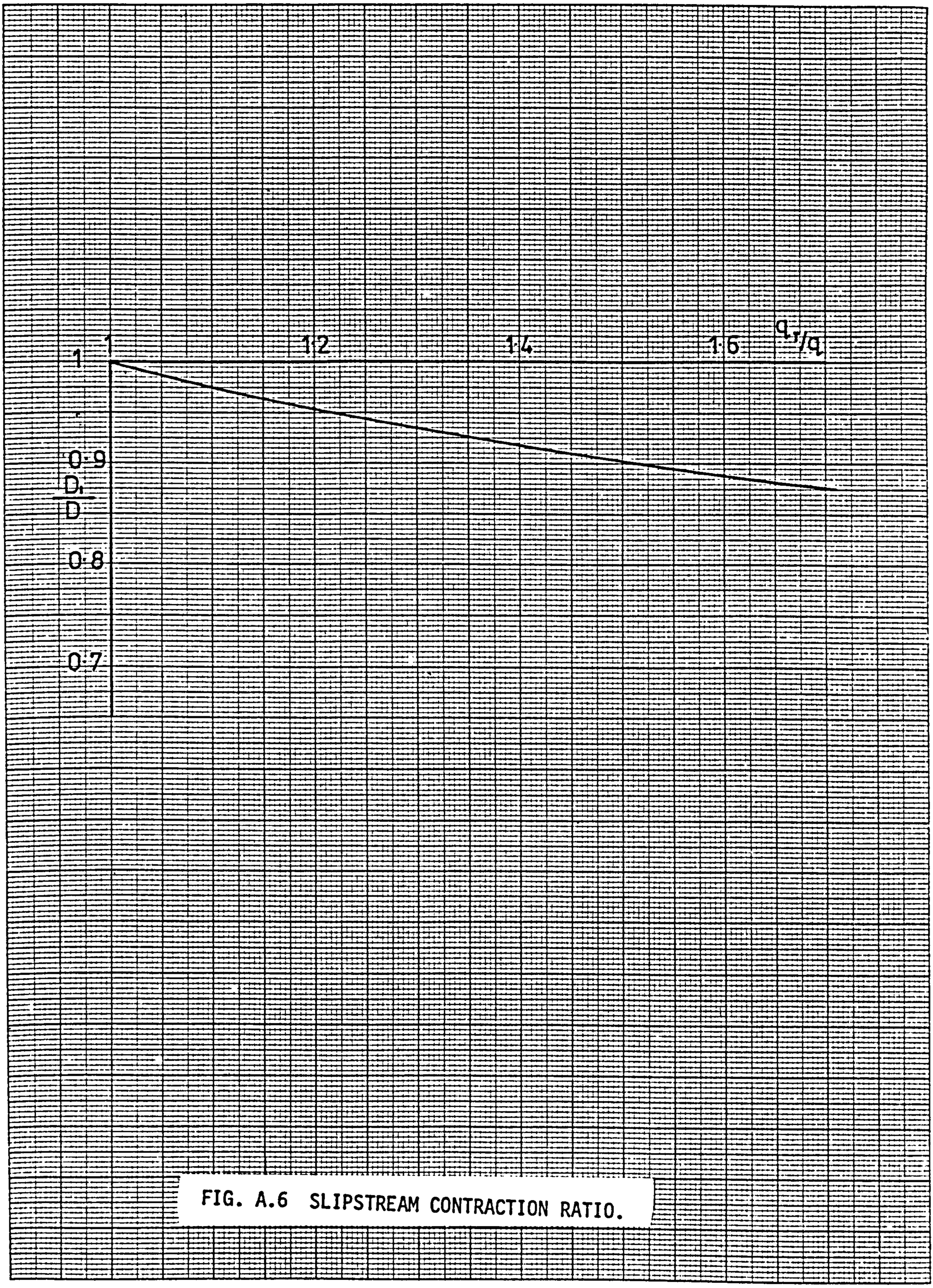

FIG. A.6 SLIPSTREAM CONTRACTION RATIO.

A.7 PROGRAMME OPERATION

The programme is written to allow the sequential calculation of a slipstream filament from each of a series of points, defined by co-ordinates X, Y, Z, with respect to the origin of the body axis system. The variables in the calculation are the aircraft loading conditions, weight (L), horizontal C.G. (H) and vertical C.G.(H1), and the thrust horse power (P) developed by the engine-propeller combination. The calculations are performed at values of C_L from 0.2 to 1.2 at intervals of 0.2.

The programme begins by printing its title and requesting weight and C.G. data. On receiving the data L, H, H1 the weight L is inspected, if L = 0 then the programme terminates, (this is the only way to terminate the programme). The weight and C.G. data is printed as a title and the power requested. The power is prefixed by a marker, θ, which is normally given the value of 0. If θ is given the value 1 then on completion of the data series the programme will return to line 20 to request a new weight and C.G. input.

Following the power input the programme reads the first data case from the stored data (line 1360 et seq.), sets C_L = 0.2 and proceeds to calculate the constants and initial conditions. A marker K is set to zero and the calculation of the induced velocities, directions and displacements at the starting point carried out, the marker is increased by 0.05 inspected to check that K < 1, if this is so then the slipstream filament is extended along the local flow vector by 1/20th of the distance between the starting point and the tail. The iteration continues until K > 1 when the output is printed. The output contains the slipstream filament co-ordinates with respect to the tail and its velocity and direction. Other data is also printed to check the proper running of the programme.

After printing the output C_L is increased by 0.2 and the process repeated until C_L = 1.2. the starting co-ordinate date (Z,Y,Z) is preceded by a marker J which is normally given the value 0. A value J = 1 denotes the last data case and returns the programme to the next power data input. After input of the new power data the starting co-ordinate data is restored for the next sequence.

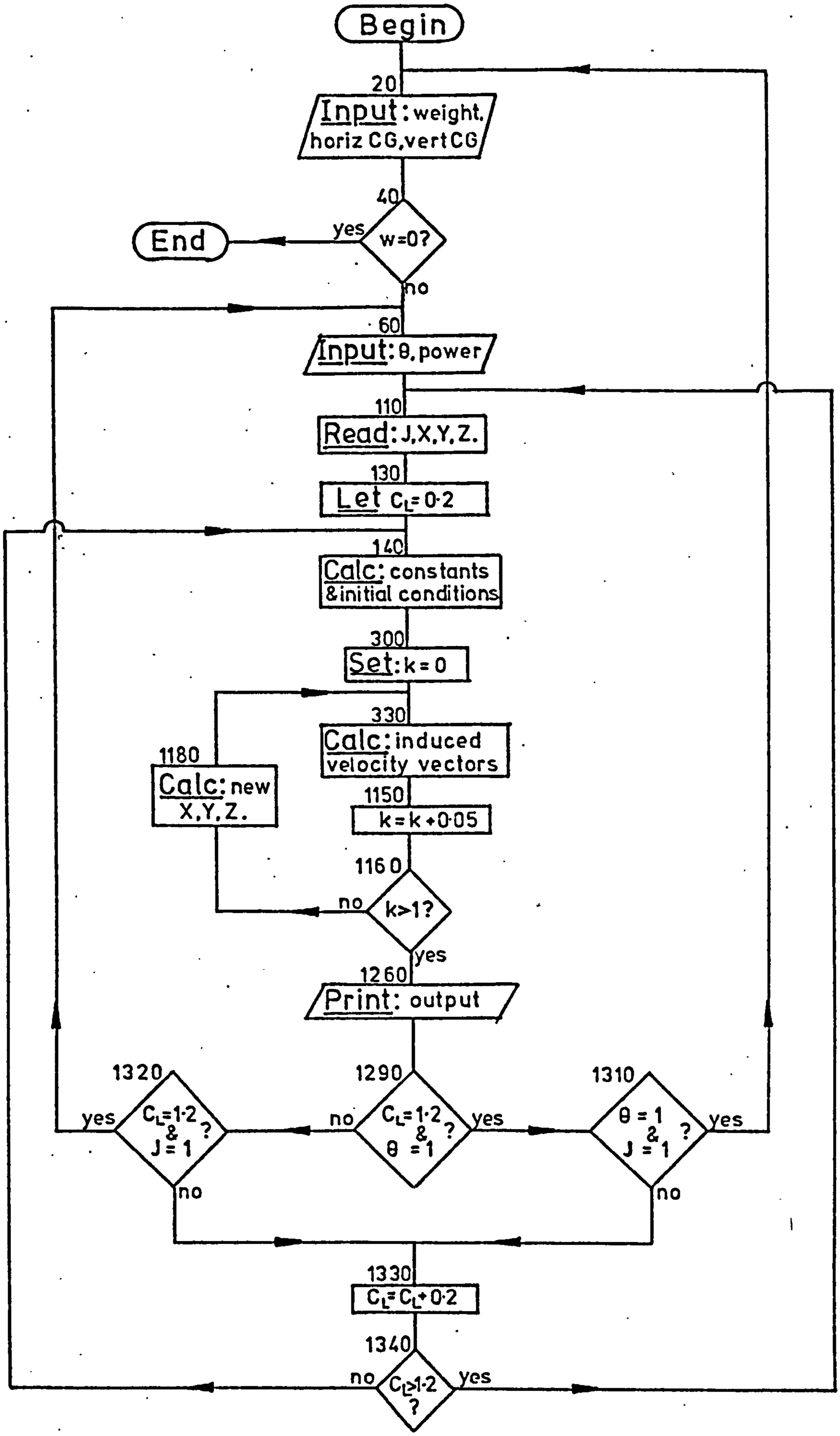

FIG. A7. SLIPSTREAM SIMULATION PROGRAMME FLOW DIAGRAM

Table A1

SLIPSTREAM SIMULATION PROGRAMME

```
10   PRINT "SLIPSTREAM SIMULATION PROGRAMME "
20   PRINT "INPUT WEIGHT AND C.G."
30   INPUT L,H,H1
40   IF L=0 THEN 1450
50   PRINT "WEIGHT";L;"HORIZ.C.G.";H;"VERT.C.G.";H1
60   INPUT O,P
70   PRINT "L          L2          P          C          E          Z          V"
80   PRINT "QT/Q        F          Y          EO        E/EO        L3        L4"
90   PRINT
100   RESTORE
110   READ J,X,Y,Z
120   PRINT X,Y,Z
130   LET C=.2
140   VO=SQR(5.4835*L/C)
150   EO=C/5
160   X1=X*COS(EO)+Z*SIN(EO)
170   Y1=Y
180   Z1=Z*COS(EO)-X*SIN(EO)
190   X2=(X+13)*COS(EO)+(Z+2.4)*SIN(EO)
200   Y2=Y
210   Z2=(Z+2.4)*COS(EO)-(X+13)*SIN(EO)
220   F1=C-.0074*C↑3
230   F2=.137*C*C+.00126*C↑4
240   F3=1+.024*C
250   L3=(F1*(H-.11)-.0463+H1*F2)*L*.344/(C*F3)
260   L4=-3.445E-04*L*P*(.2-H1)*(C↑.3)
270   L2=L3+L4
280   A=739.31*P*(C/L)↑1.5
290   D=X2/20
300   LET K=0
310   V=VO*SQR(1+A*(1+K))
320   REM FUSELAGE DISPLACEMENT EFFECT
330   X5=X1*COS(EO-.122)+(Z1+.8)*SIN(EO-.122)
340   Y5=Y
350   Z5=(Z1+.8)*COS(EO-.122)-X1*SIN(EO-.122)
360   M=(9-X5)/27
370   R1=.75*(.2969*SQR(M)-.126*M-.3516*M*M+.2843*M↑3-.1015*M↑4)*27
380   IF K=0 THEN 440
390   R2=SQR(Y5*Y5+Z5*Z5)
400   Q=ATN(Y5/Z5)
410   Z6=R1*(R1-R3)*COS(Q)/R2
420   Y6=R1*(R1-R3)*SIN(Q)/R2
430   GOTO 450
440   Z6=Y6=0
450   R3=R1
```

```
460   REM WING INDUCED VELOCITIES
470   T1=(13.55*(L-L2)/V0)/12.566
480   B1=X1*X1+Z1*Z1
490   B2=SQR(X1*X1+Z1*Z1+(Y1+18)↑2)
500   B3=SQR(X1*X1+Z1*Z1+(Y1-18)↑2)
510   B4=Z1*Z1+(Y1+18)↑2
520   B5=Z1*Z1+(Y1-18)↑2
530   B6=(1/B1)*((Y1+18)/B2-(Y1-18)/B3)
540   B7=(1/B5)*(1+X1/B3)
550   B8=(1/B4)*(1+X1/B2)
560   U1=-T1*Z1*B6
570   W1=T1*X1*B6
580   IF X1>0 THEN 640
590   V2=-T1*Z1*B7
600   W2=-T1*(Y1-18)*B7
610   V3=T1*Z1*B8
620   W3=T1*(Y1+18)*B8
630   GOTO 650
640   V2=V3=W2=W3=0
650   REM PROPELLER VORTEX INDUCED VELOCITIES
660   T3=(4.958*C*V0*SQR(1.35*A))/12.566
670   C1=X1*X1+Z1*Z1
680   C2=SQR(X1*X1+Z1*Z1+(Y1+2.75)↑2)
690   C3=SQR(X1*X1+Z1*Z1+(Y1+8.75)↑2)
700   C4=Z1*Z1+(Y1+2.75)↑2
710   C5=Z1*Z1+(Y1+8.75)↑2
720   C6=(1/C1)*((Y1+2.75)/C2-(Y1+8.75)/C3)
730   C7=(1/C5)*(1+X1/C3)
740   C8=(1/C4)*(1+X1/C2)
750   U5=-T3*Z1*C6
760   W5=T3*X1*C6
770   IF X1>0 THEN 830
780   V5=-T3*Z1*C7
790   W5=-T3*(Y1+8.75)*C7
800   V6=T3*Z1*C8
810   W6=T3*(Y1+2.75)*C8
820   GOTO 840
830   V5=W5=V6=W6=0
840   G1=X1*X1+Z1*Z1
850   G2=SQR(X1*X1+Z1*Z1+(Y1-2.75)↑2)
860   G3=SQR(X1*X1+Z1*Z1+(Y1-8.75)↑2)
870   G4=Z1*Z1+(Y1-2.75)↑2
880   G5=Z1*Z1+(Y1-8.75)↑2
890   G6=(1/G1)*((Y1-2.75)/G2-(Y1-8.75)/G3)
900   G7=(1/G5)*(1+X1/G3)
910   G8=(1/G4)*(1+X1/G2)
920   U7=-T3*Z1*G6
930   W0=T3*X1*G6
940   IF X1>0 THEN 1000
950   V7=-T3*Z1*G7
960   W7=-T3*(Y1-8.75)*G7
970   V8=T3*Z1*G8
980   W8=T3*(Y1-2.75)*G8
990   GOTO 1010
1000   V7=V8=W7=W8=0
```

```
1010  REM TAIL INDUCED VELOCITIES
1020  T2=(39.02*L2/V0)/12.566
1030  D1=(X2+1.2)↑2+Z2*Z2
1040  D2=SQR((X2+1.2)↑2+Z2*Z2+(Y2+6.25)↑2)
1050  D3=SQR((X2+1.2)↑2+Z2*Z2+(Y2-6.25)↑2)
1060  D4=(1/D1)*((Y2+6.25)/D2-(Y2-6.25)/D3)
1070  U4=-T2*Z2*D4
1080  W4=T2*(X2+1.2)*D4
1090  REM TOTAL INDUCED VELOCITIES
1100  U9=U1+U4+U5+U7+V
1110  V9=V2+V3+V5+V6+V7+V8
1120  W9=W1+W2+W3+W4+W5+W6+W7+W8+W0
1130  E=ATN(W9/U9)
1140  F=ATN(V9/U9)
1150  K=K+.05
1160  IF K <= 1 THEN 1180
1170  IF K>1 THEN 1250
1180  X1=X1-D
1190  Y1=Y1-D*TAN(F)-Y6
1200  Z1=Z1-D*TAN(E)-Z6
1210  X2=X2-D
1220  Y2=Y2-D*TAN(F)-Y6
1230  Z2=Z2-D*TAN(E)-Z6
1240  GOTO 310
1250  Z3=Z2*COS(E0)+X2*SIN(E0)
1260  PRINT L;L2;P;C;E*57.296;Z3;V
1270  PRINT (V/V0)↑2;F*57.296;Y1;E0*57.296;E/E0;L3;L4
1280  PRINT
1290  IF C=1.2 AND 0=1 THEN 1310
1300  GOTO 1320
1310  IF 0=1 AND J=1 THEN 20
1320  IF C=1.2 AND J=1 THEN 60
1330  LET C=C+.2
1340  IF C>1.2 THEN 110
1350  IF C <= 1.2 THEN 140
1360  DATA 0,6,-5.75,-.6
1370  DATA 0,6,-5.75,-3.6
1380  DATA 0,6,-3.63,-2.72
1390  DATA 0,6,-2.75,-.6
1400  DATA 0,6,-3.63,1.52
1410  DATA 0,6,-5.75,2.4
1420  DATA 0,6,-7.87,1.52
1430  DATA 0,6,-8.75,-.6
1440  DATA 1,6,-7.87,-2.72
1450  END
```

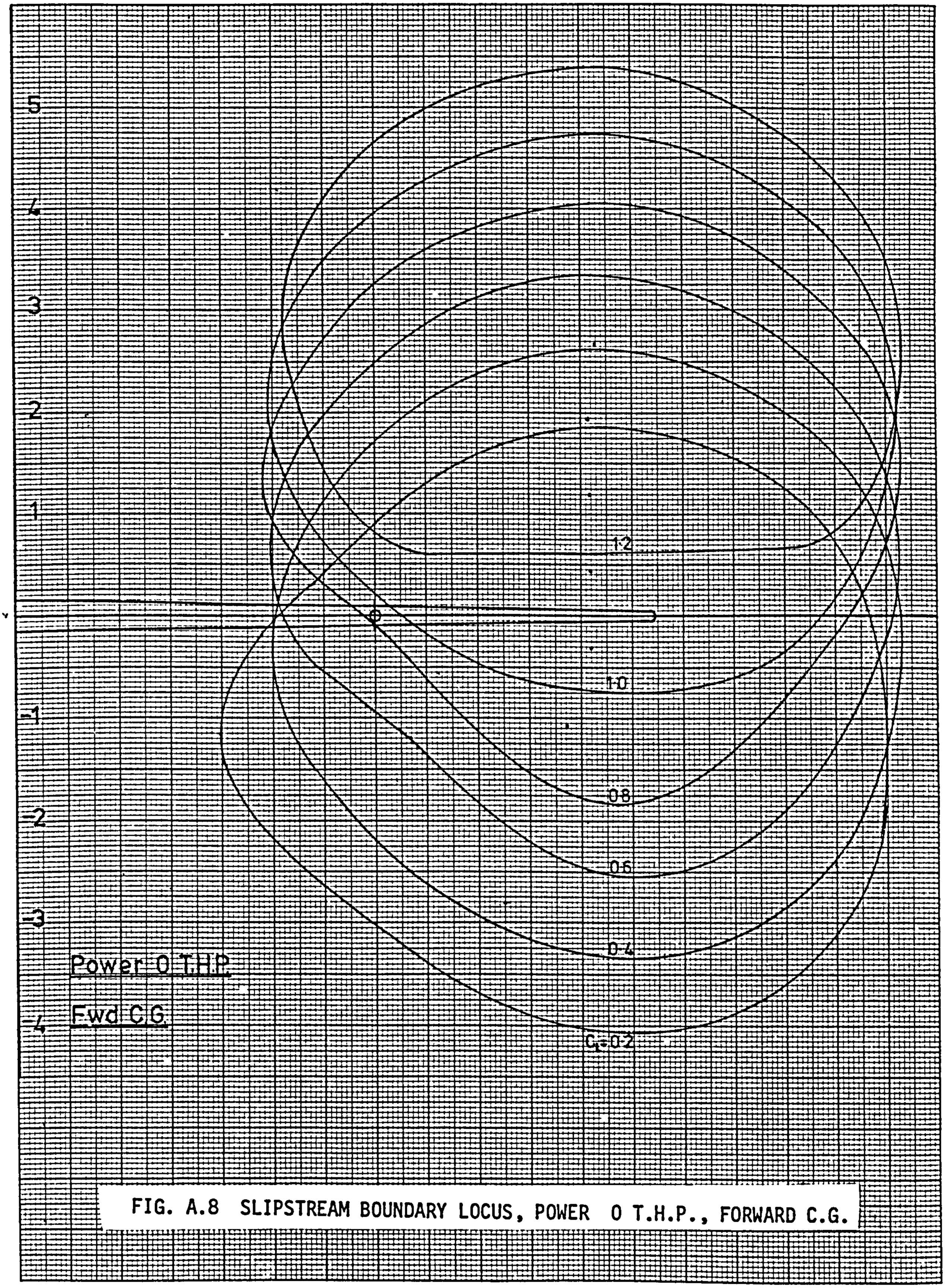

FIG. A.8 SLIPSTREAM BOUNDARY LOCUS, POWER 0 T.H.P., FORWARD C.G.

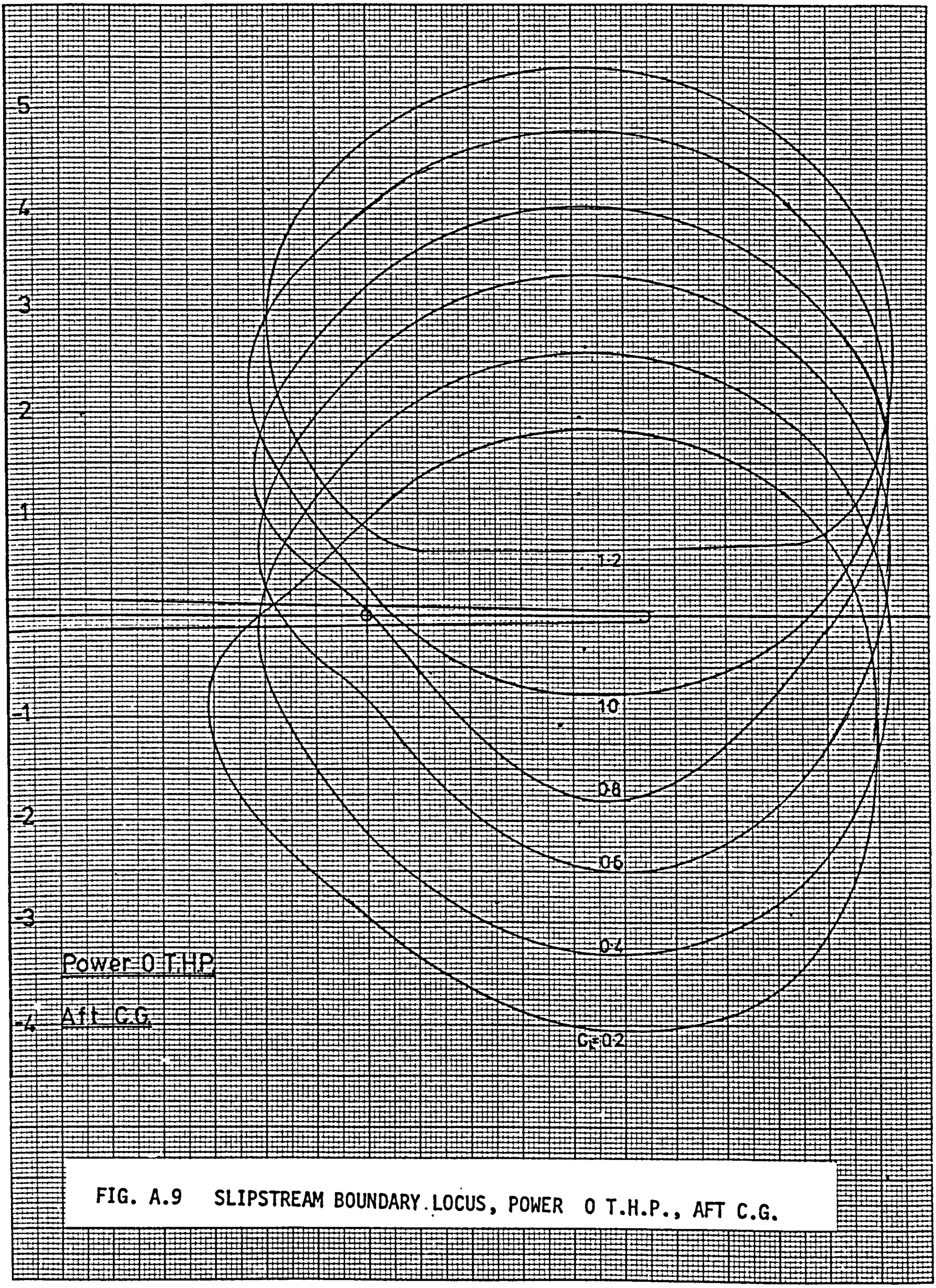

FIG. A.9 SLIPSTREAM BOUNDARY LOCUS, POWER 0 T.H.P., AFT C.G.

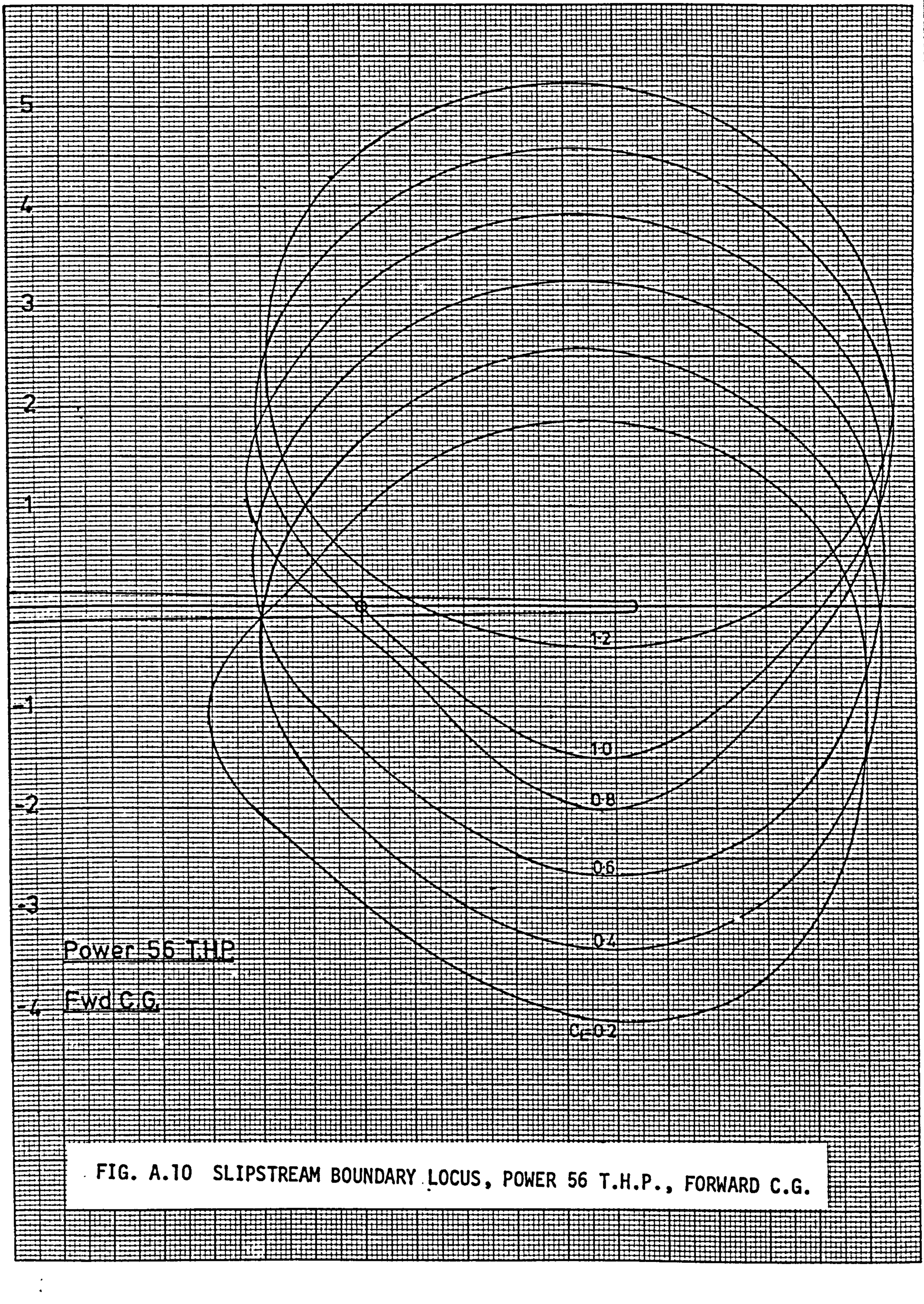

FIG. A.10 SLIPSTREAM BOUNDARY LOCUS, POWER 56 T.H.P., FORWARD C.G.

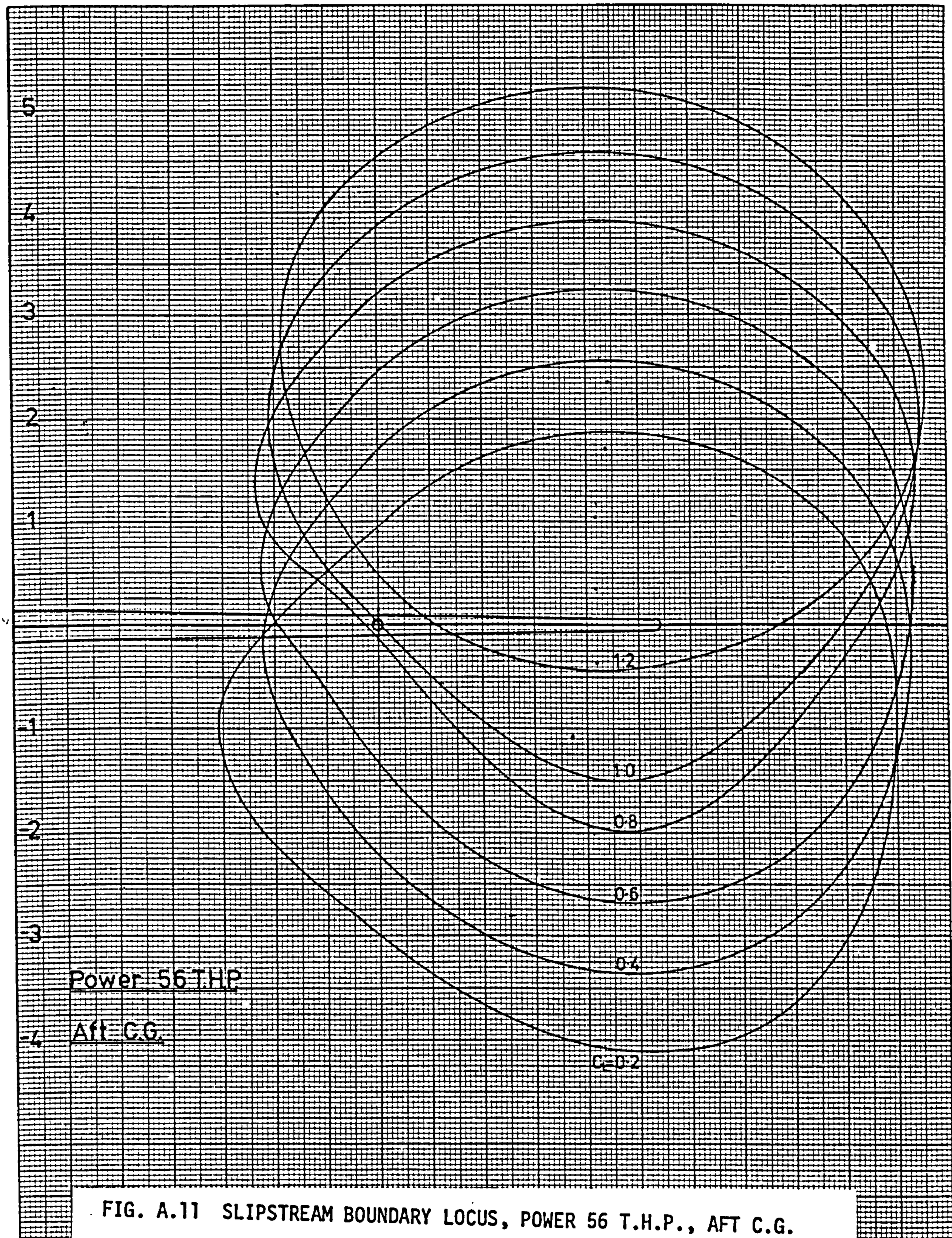

FIG. A.11 SLIPSTREAM BOUNDARY LOCUS, POWER 56 T.H.P., AFT C.G.

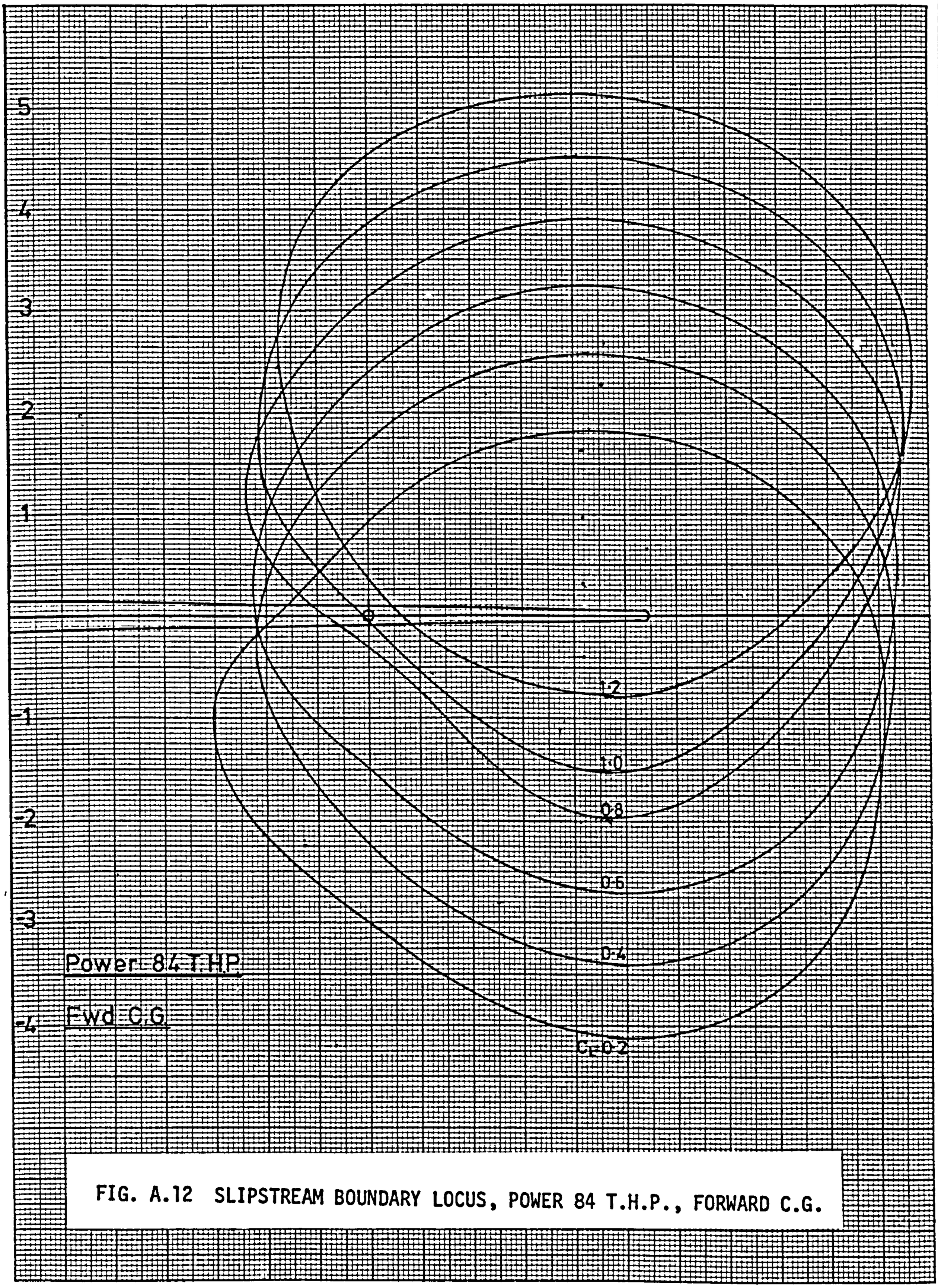

FIG. A.12 SLIPSTREAM BOUNDARY LOCUS, POWER 84 T.H.P., FORWARD C.G.

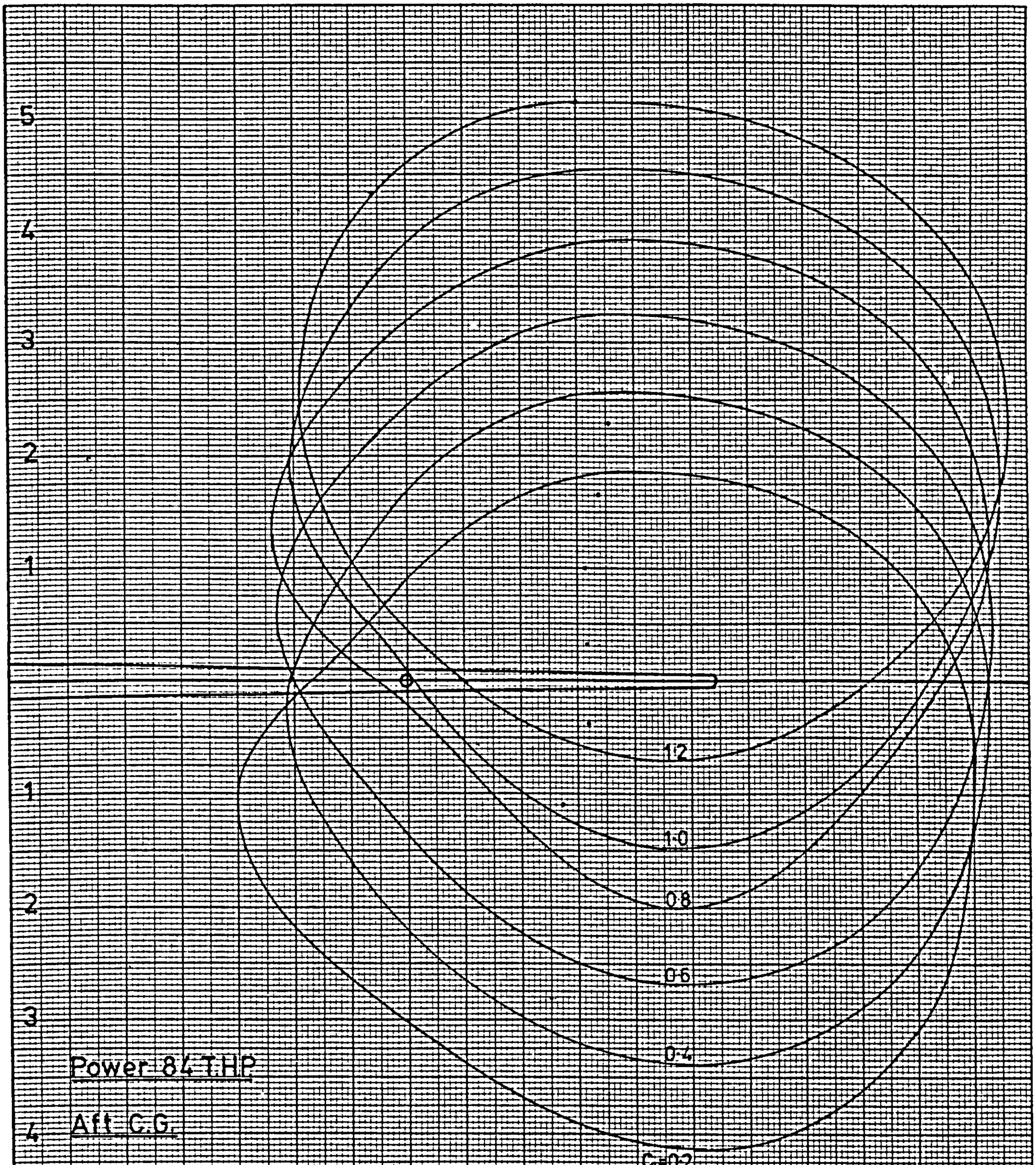

FIG. A.13 SLIPSTREAM BOUNDARY LOCUS, POWER 84 T.H.P., AFT C.G.

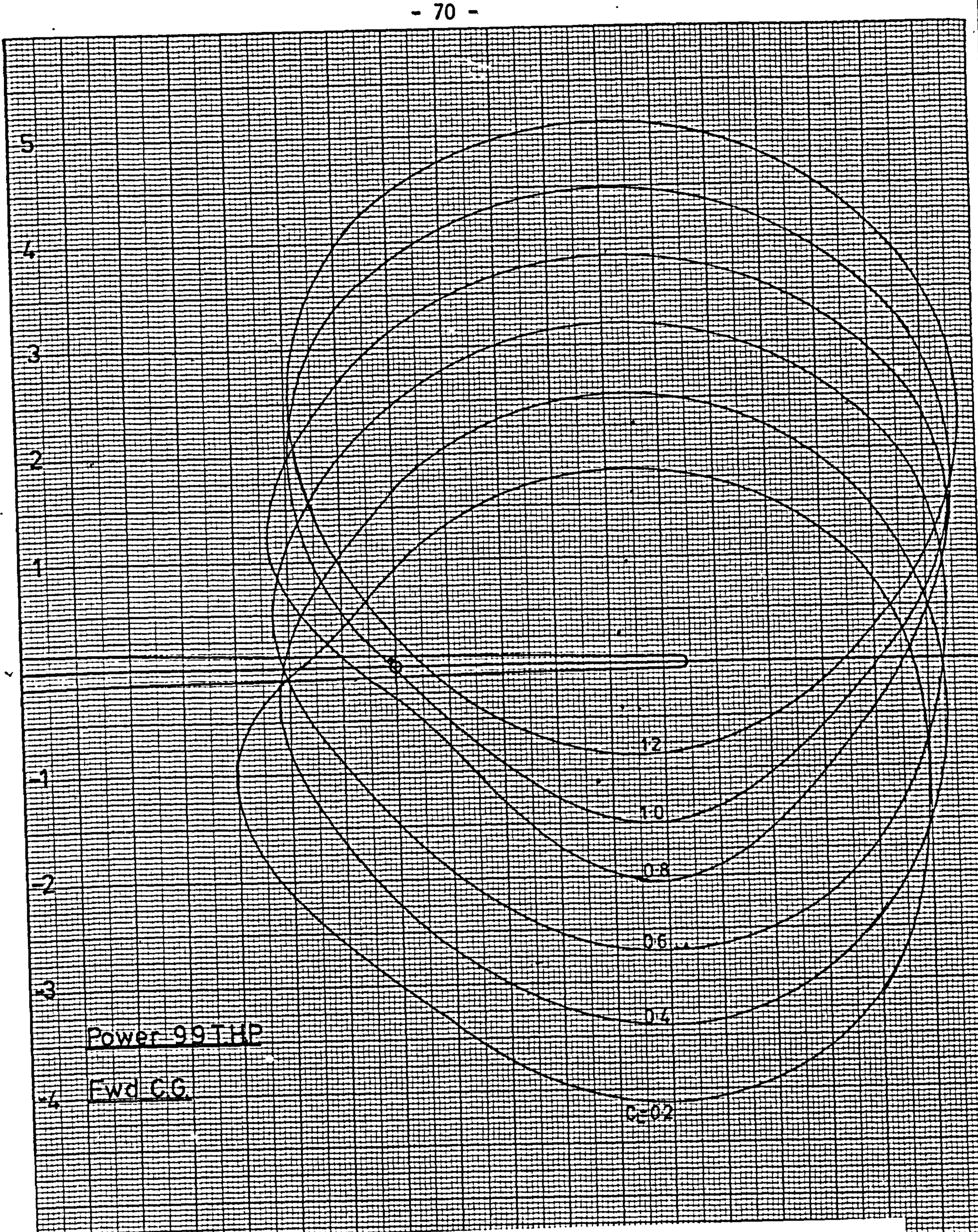

FIG. A.14 SLIPSTREAM BOUNDARY LOCUS, POWER 99 T.H.P., FORWARD C.G.

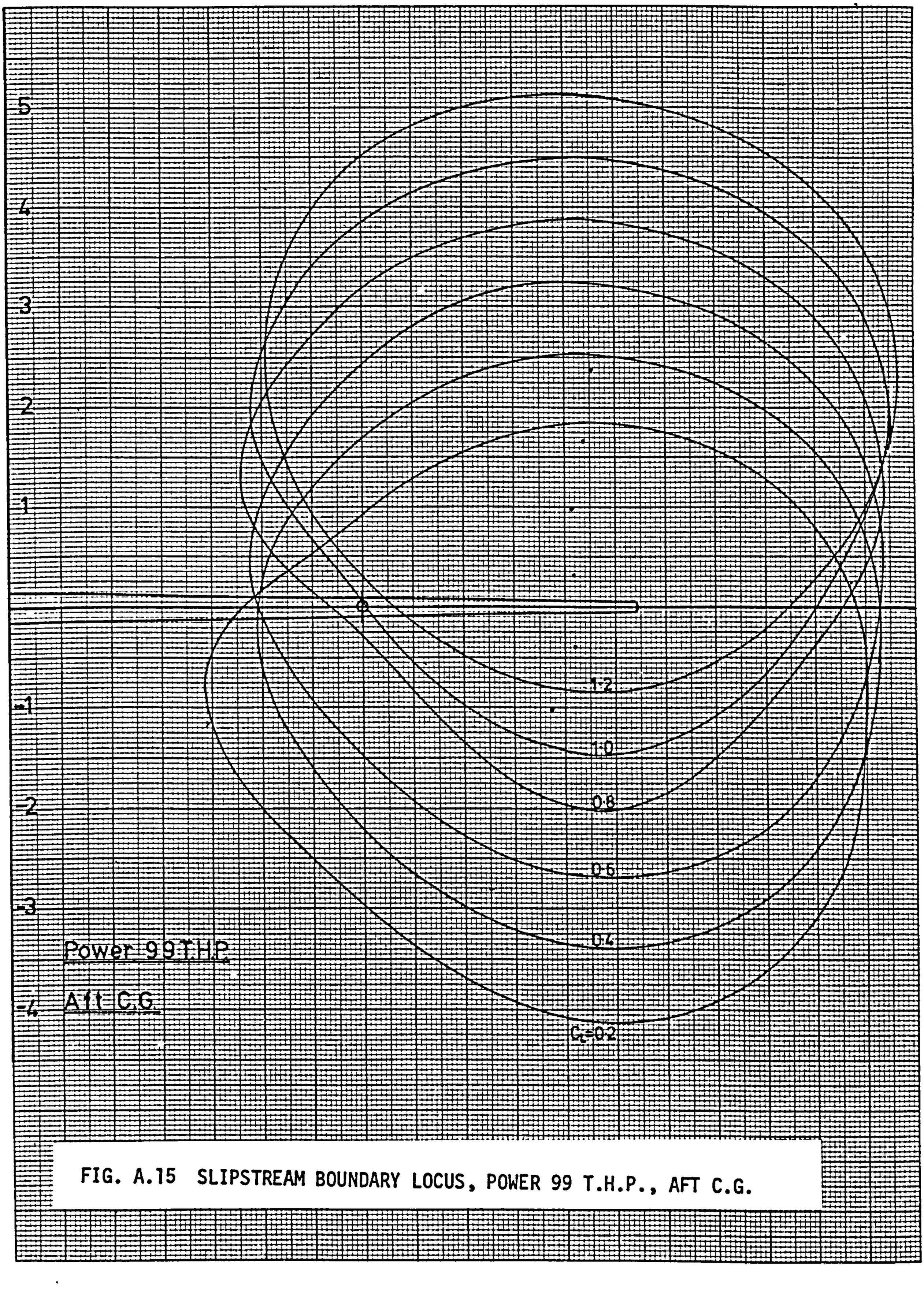

FIG. A.15 SLIPSTREAM BOUNDARY LOCUS, POWER 99 T.H.P., AFT C.G.

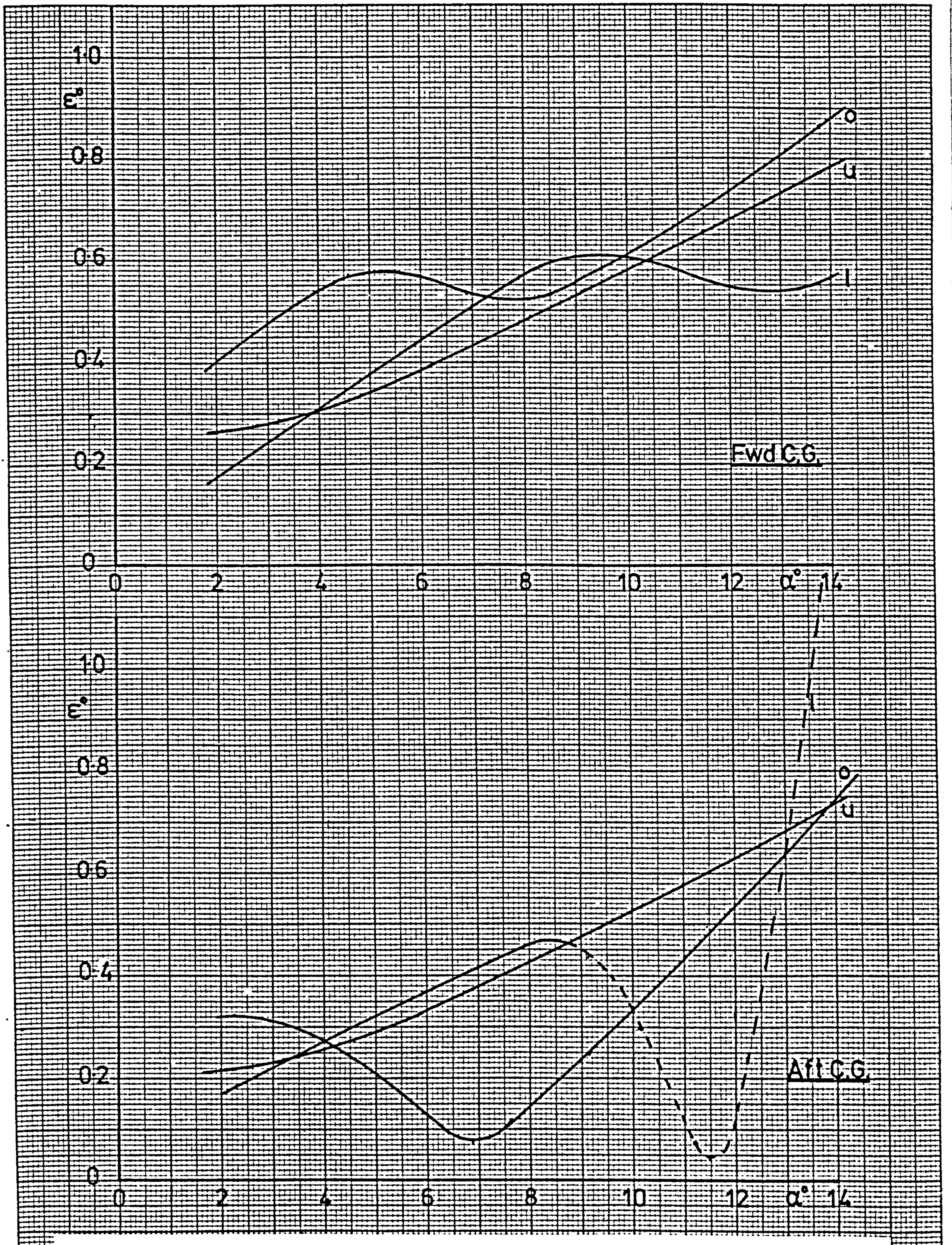

FIG. A.16 Calculated Downwash in the Slipstream at the Tail, zero power.

FIG.A:17 Calculated Downwash in the Slipstream at the Tail, 56 T.H.P.

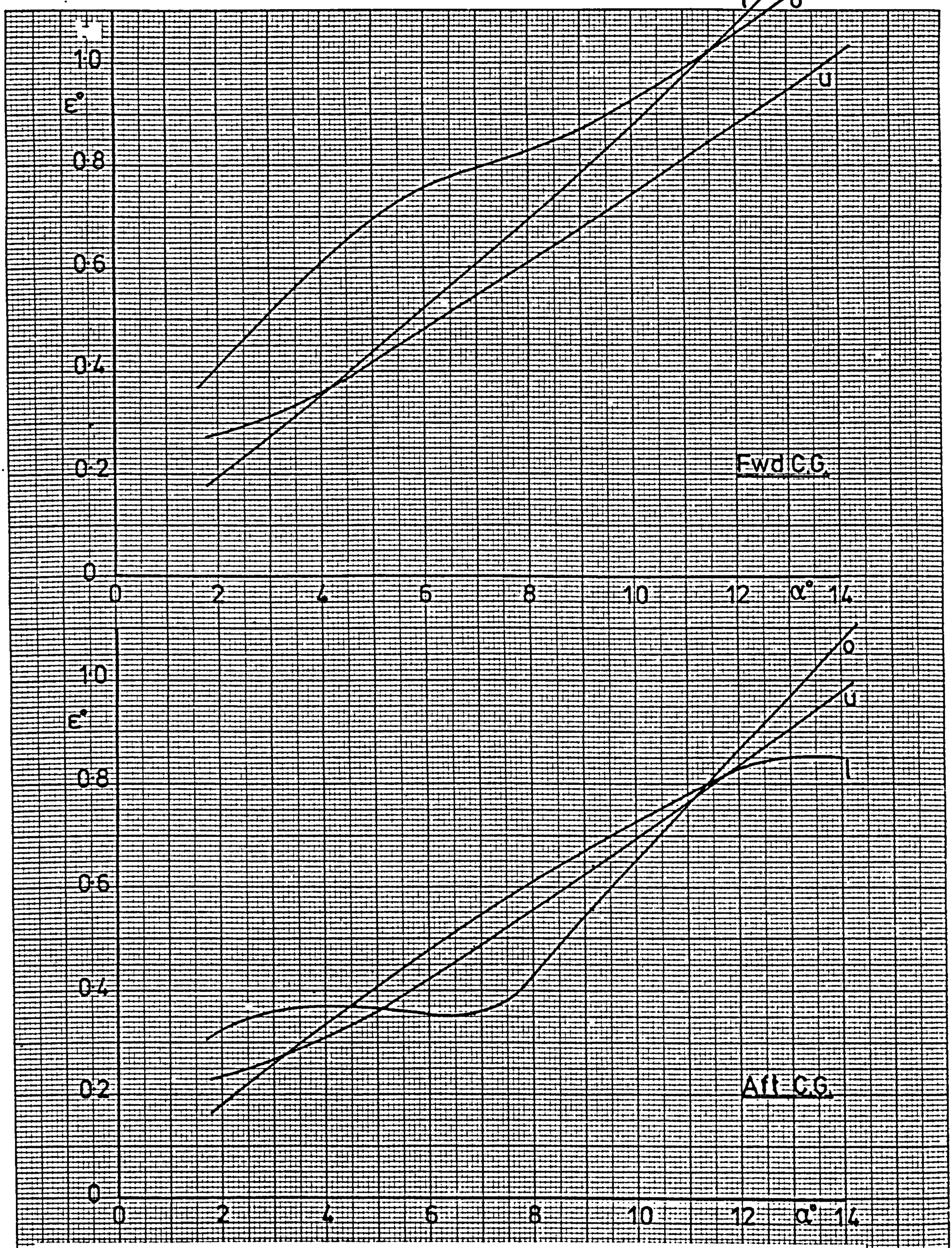

FIG.A.18 Calculated Downwash in the Slipstream at the Tail, 84 T.H.P.

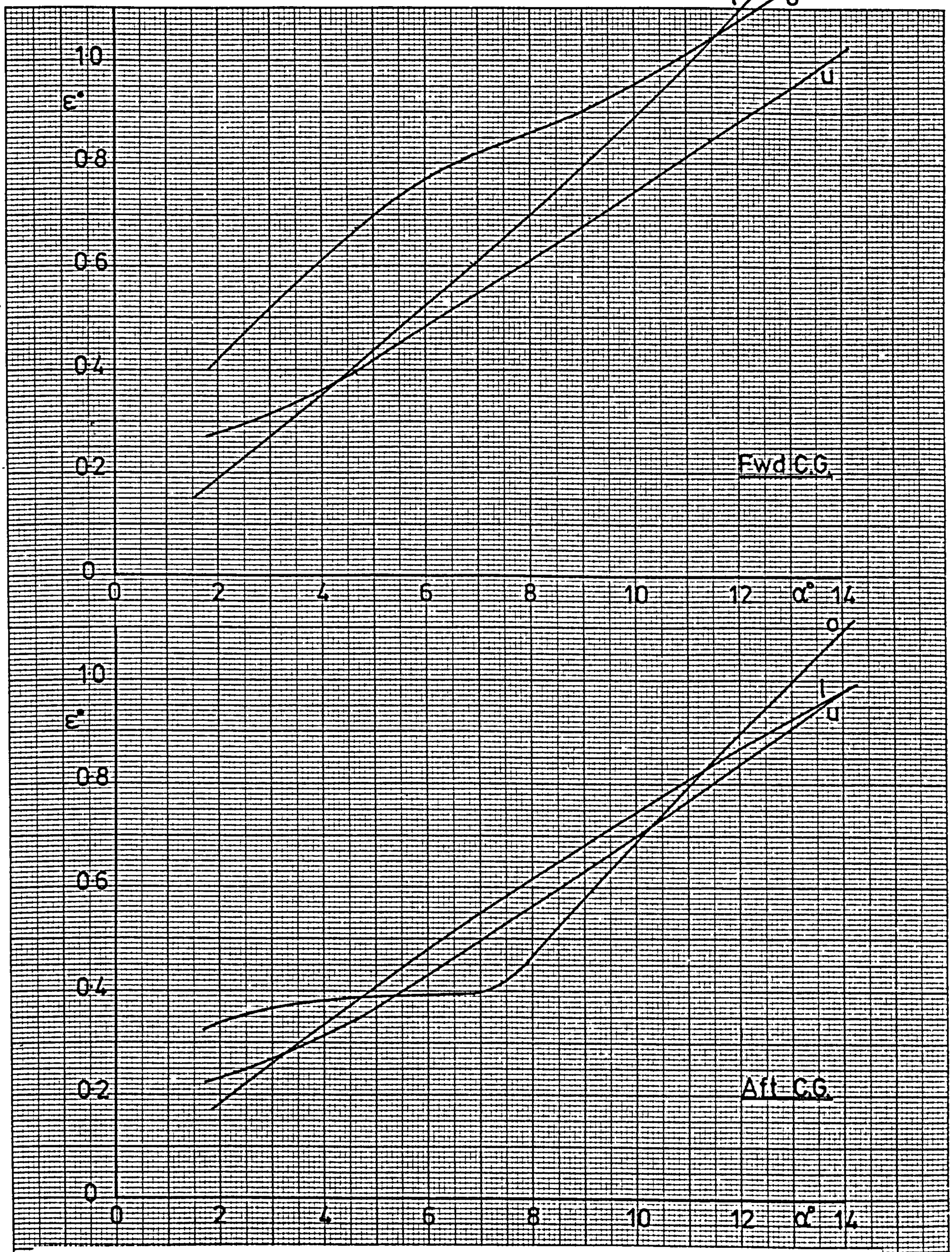

FIG.A.19 Calculated Downwash in the Slipstream at the Tail, 99 T.H.P.

A.8. Discussion

Although the programme has some simplifying assumptions that reduce the aircraft model to a very basic level it does predict with a reasonable degree of accuracy the value of the slipstream measurements made in the flight trials. It is also very significant that the boundary of the slipstream predicted by the programme appears to correspond to that found by the flight measurements. Due to the very limited flight data available it would not be advisable to draw too many conclusions from the comparison of the data but what can be compared would substantiate that the programme is adequately predicting the slipstream locus. In view of these observations it is considered that a more sophisticated programme probably would not significantly improve the prediction, and could lose its flexibility of application.

REFERENCES - APPENDIX A

A.1 Silverstein A, Katzoff S and Bullivant W K — Downwash and Wake Behind Plain and Flapped Airfoils. NACA Report No 651, 1939

A.2 Silverstein A and Katzoff S — Design Charts for Predicting Downwash Angles and Wake Characteristics behind Plain and Flapped Wings. NACA Report No 648, 1939

A.3 Decker J L — Prediction of Downwash at Various Angles of Attack for Arbitary Tail Locations. Aeronautical Engineering Review, Vol 15, No 8, 1956

A.4 Rethorst S — Lift on a Wing in a Propeller Slipstream as Related to Low Speed Flight. Aeronautical Engineering Review, Vol 15, No 10, 1956

A.5 Donovan A F and Lawrence H R — Aerodynamic Components of Aircraft at High Speeds (High Speed Aerodynamics and Jet Propulsion, Vol VII). Princeton University Press, 1957

A.6 Glauert H — The Elements of Aerofoil and Airscrew Theory. C.U.P. 2nd Edition, 1959

A.7 Wolowicz C H and Yancey R B — Longitudinal Aerodynamic Characteristics of Light Twin Engined, Propeller Driven Airplanes. NASA TN D-6800

A.8 Eshelby M E — Incidence Related Distortion of Low Speed Longitudinal Static Stability Twin Curves. Cranfield Report Aero No 30

A.9	Ribner H S	Fomulas for Propeller in Yaw and Charts of the Sideforce Derivatives NACA Report No 819, 1945
A.10	Ribner H S	Propellers in Yaw NACA Report No 820, 1945

PART II

Section 3

An Analysis of the Force System of a Propeller

Cranfield Report Aero No.33

Cranfield Report Aero No. 33
April, 1977.

CRANFIELD INSTITUTE OF TECHNOLOGY

An Analysis of the Force System of a Propeller

by

M.E. ESHELBY

Aerodynamics Division
College of Aeronautics

Summary

The handling qualities of a propeller driven aircraft may be significantly influenced by the forces generated by the propeller. Little information is however available on the magnitude of the forces and moments produced by the propeller about axes normal to the propeller axis, and what is available is generally of an arbitrary nature. This paper analyses the propeller operation by the strip theory relating the propeller operation to aircraft flight conditions of variable incidence with speed. Propeller performance is produced for a specific case of an aircraft - engine - propeller combination which shows characteristics of the performance, as functions of power and flight conditions which can be used to predict the power effects of propellers on the aircraft handling qualities.

Contents

NOTATION

A	Propeller disc area, Aspect Ratio
a	Axial interference factor, v/V
a'	Angular Velocity interference factor
a_x	lift curve slope, station x
B	Number of Blades
b	local blade chord
b_o	maximum blade chord
C_D	Drag coefficient $D/\frac{1}{2}\rho V_\beta^2 bdr$
C_L	Lift coefficient $L/\frac{1}{2}\rho V_\beta^2 bdr$
C_M	Pitching Moment coefficient $M/\rho n^2 D^5$
C_N	Yawing Moment coefficient $Y/\rho n^2 D^5$
C_P	Power coefficient $P/\rho n^3 D^5$
C_Q	Torque coefficient $Q/\rho n^2 D^5$
C_T	Thrust coefficient $T/\rho n^2 D^4$
C_Y	Side force coefficient $Y/\rho n^2 D^4$
C_Z	Normal force coefficient $Z/\rho n^2 D^4$
c	propeller blade element chord
D	Propeller diameter, Drag Force
e	NASA span efficiency factor
H	Total Head of flow
J	Advance ratio V/nD
K	Propeller efficiency constant (eqn.56)
L	Lift force
M	Pitching moment
N	Yawing moment
P	Engine Shaft Power
p	pressure
Q	Engine Torque

r	Propeller blade element radius
T	Thrust
t	Propeller blade element thickness
V	True airspeed
u,v	velocity components
x	Propeller blade element station 2r/D
Y	Side force
Z	Normal force
α	Incidence
β	Blade setting angle, pitch angle
γ	Flight path angle, separation drag factor.
θ	Blade angular position, fig.
ϕ	Airflow vector, blade helix angle
ρ	air density

Subscripts

β	Propeller blade
i	induced
P	Propeller
x	Propeller blade element, radius x
z	Profile
o	sea level, I.S.A., reference.

AN ANALYSIS OF THE FORCE SYSTEM OF A PROPELLER

1. INTRODUCTION

The purpose of a propeller is to convert rotational shaft power into useful thrust power by acting on a fluid surrounding the propeller. This process can be broadly analysed by the momentum theory of the propeller which reduces the propeller to a basic actuator disc by means of which the airflow through the disc experiences a change of momentum; this theory only predicts a thrust force in terms of speed and power.

In practice a propeller produces not only thrust in its axial direction but also forces along and moments about axes normal to the propeller axis of rotation; these forces arise from the inclination of the propeller axis to the incident airstream. Previous analysis of the propeller operating in this mode have tended towards a factor to be applied to the thrust force and a projected propeller disc area (Ribner, refs 1 & 2) or have considered the propeller "fin effect" in which the propeller is assumed to produce forces which can be analysed in a similar manner to a lifting surface at the propeller, (Priestley, ref.3). A theory is required which will be more general and relate to the aircraft-powerplant combination. In all but a very few cases the powerplant is rigidly fixed to the airframe and so there will be a fixed relationship between the aircraft incidence and the propeller incidence relative to the airflow direction. Since the aircraft incidence is a function of forward speed (or more strictly C_L) there will be a relationship between the normal force generated by the propeller and the advance ratio; this can now be used to find the secondary relationship between the propeller normal force and the aircraft flight condition.

Normally the only propeller variables known are the aircraft forward speed, the rotational speed of the engine and its shaft horse power and some geometric data for the propeller. With so little information it will be necessary to analyse the propeller operation in a relative sense comparing estimated performance with some measured quantity and using the broad results from the momentum theory as a reasonable approximation where necessary. The propeller can be analysed by the Strip Theory assuming or estimating the strip sectional data where necessary. The method is well established, ref.4, etc, but modern computing techniques enable a more rigorous treatment to be attempted and iteration between computed and measured values to be used to determine the propeller operation relative to the flight conditions of the aircraft. Borst et al, ref.5, summarises the technology of present day propeller design and considers the theoretical strip analysis which forms the basis of the theory of this report.

2. THE GENERAL ANALYSIS OF THE PROPELLER

The propeller blade element can be considered to act as an aerofoil in a flow with a velocity given by the sum of the rotational speed of the blade element and the axial velocity of the flow into the propeller. Since the propeller is doing work on the airstream it will modify the flow vector relative to the blade element giving rise to an increment in the effective forward speed of the blade; this increment is known as the displacement velocity and is defined as the velocity of the screw surface in the direction of its axis, (ref.5). It arises from the combination of the increase of the axial momentum of the flow through the propeller disc due to the thrust and the angular momentum imposed on the propeller slipstream due to the propeller torque reaction.

The displacement velocity will vary over the blade span since the thrust and torque components vary along the blade. The momentum theory can however be used to provide a reliable average value of the inflow factor at the propeller disc (the axial interference) and an average angular momentum can be calculated from the gross shaft power delivered to the propeller and used to give an estimate of the rotational interference factor. Using the average values of the interference factors will enable a good estimate to be made of the displacement velocity at any blade element.

2.1 Axial Interference Factor, a.

Using the momentum theory of the propeller the propeller is represented by an actuator disc of area A in a free stream of velocity V and pressure p_o. The flow is accelerated into the propeller disc and passes the disc at a speed $(V + v)$, behind the disc where the pressure has recovered to the free stream static pressure p_o the velocity is $(V + v_1)$, fig.1.

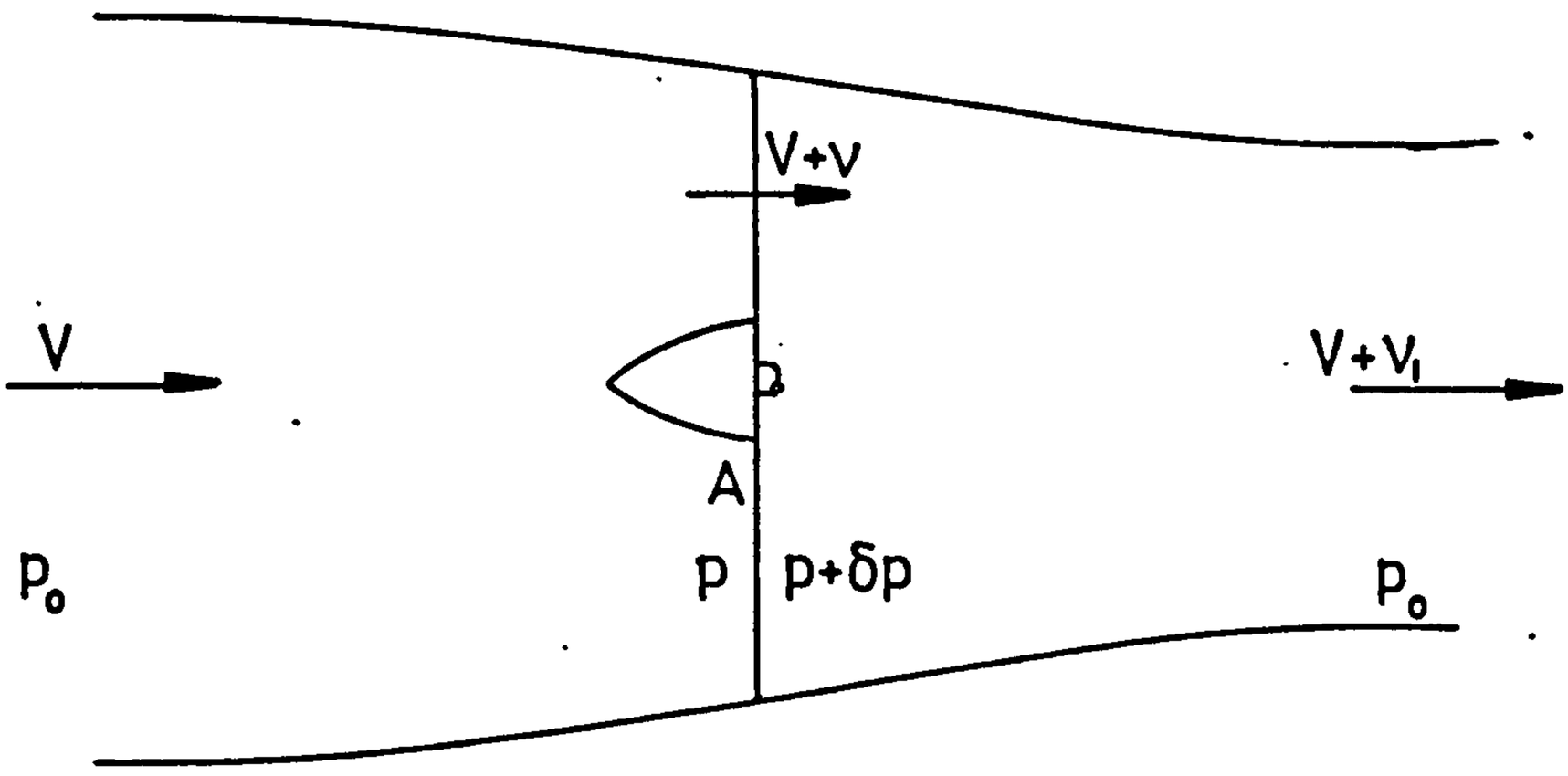

FIG 1.

Ahead of the propeller the total head of the flow is H_0 and,

$$H_0 = p_0 + \tfrac{1}{2}\rho V^2 = p + \tfrac{1}{2}\rho(V + v)^2$$

and behind the propeller the total head of the flow is H_1 and,

$$H_1 = p + \delta p + \tfrac{1}{2}\rho(V + v)^2 = p_0 + \tfrac{1}{2}\rho(V + v_1)^2$$

Therefore the differential pressure across the actuator disc is

$$\delta p = H_1 - H_0 = \rho(V + \tfrac{1}{2}v_1)v_1 \qquad (1)$$

The thrust, T, is given by the momentum change, thus

$$T = A\rho(V + v)v_1 \qquad (2)$$

and since $T = A\delta p$

$$\delta p = \rho(V + v)v_1 \qquad (3)$$

Comparing (1) and (3) gives

$$v = \tfrac{1}{2}v_1 \qquad (4)$$

Using (2) and (4) the thrust can be expressed in the form

$$T = A\rho(V + v)2v$$

The incremental velocity v represents the inflow interference velocity and can be written in the form

$$v = aV \qquad (5)$$

where a is the inflow interference factor.

Hence the thrust can be expressed as

$$T = 2A\rho V(1 + a)aV \qquad (6)$$

and the velocity of the airflow at the propeller disc is $V(1 + a)$.

From the definition of propeller efficiency,

$$\eta P = TV$$

where η is the propeller efficiency.

Hence (6) can be written in terms of power in the form

$$\eta P = 2A\rho V^3(1 + a)a$$

writing the power in coefficient form, $C_p = P/\rho n^3 D^5$ gives

$$nC_p = 2A\frac{\rho V^3}{\rho n^3 D^5}(1 + a)a = \tfrac{1}{2}\pi J^3(1 + a)a \qquad (7)$$

where J is the propeller tip advance ratio based on aircraft forward speed, see fig.3.

Solving (7) for a gives the approximate solution,

$$a = 2\frac{nC_p}{\pi J^3} \qquad (8)$$

The axial inflow factor, a, is thus a function of the propeller efficiency, η. In the calculation of a it is therefore necessary to estimate an initial value of η and to use an iterative procedure to find a.

2.2 Angular Velocity Interference Factor, a′.

The torque reaction of the propeller on the airstream will cause a rotation of the propeller slipstream about the propeller axis in the direction of the propeller rotation. This rotation is partly due to the system of trailing vortices shed by the blade and partly due to the circulation around the blade. The trailing vortices will produce an angular velocity ω to the flow in the plane of the propeller, and the circulation about the blade will give rise to an equal and opposite angular velocity in the inflow and the outflow. The sum of these components must be zero in the inflow since no rotation is possible until the flow has reached the vortex system generated by the propeller. It follows that the angular velocity of the developed outflow must be 2ω and that the rotational interference flow, which is due only to the system of trailing vortices, will have an angular velocity ω. The angular velocity interference factor, a′, can therefore be regarded as an apparent loss of propeller angular velocity, thus if the propeller angular velocity is Ω the effective rotational speed will be $\Omega - \omega$. Defining a′ as

$$\omega = \Omega a'$$

then the effective rotational speed of the propeller will be

$$\Omega(1 - a') \qquad (9)$$

The magnitude of the angular velocity interference factor can be estimated by considering the torque reaction of the propeller on the flow through the propeller disc.

Consider a small element of the propeller δr at radius r. The torque of the element, dQ, will produce a momentum change in the flow through the annular segment of the propeller disc given by

$$dQ = \dot{m}v.r \tag{10}$$

where $\dot{m}$ is the mass flow and v the induced velocity normal to the flow direction.

Thus (10) becomes, for the developed slipstream,

$$dQ = \{2\pi r\, dr.\rho V(1 + a)\}\{2\omega r\}r \tag{11}$$

from (9) $\omega = \Omega a' = 2\pi n a'$, where n is the propeller speed, and putting $x = 2r/D$, (11) becomes

$$dQ = \tfrac{1}{2}\pi^2 \rho V(1 + a) n a' D^4 x^3 dx \tag{12}$$

Now the shaft power P is given by

$$P = 2\pi n Q$$

and defining the power coefficient C_p to be $P/\rho n^3 D^5$ equation (12) becomes

$$dC_p = \pi^3 V(1 + a)a' \frac{\rho n^2 D^4}{\rho n^3 D^5} x^3 dx \tag{13}$$

Since the measurements of airspeed and propeller rotational speed are related to the aircraft and not to propeller blade conditions the propeller tip advance ratio J can be defined as

$$J = \frac{V}{nD} \tag{14}$$

thus (13) becomes

$$dC_p = \pi^3 J(1 + a)a' x^3 dx \tag{15}$$

Assuming a and a' to be constants over the disc area the power coefficient C_p can be found by integrating over the propeller disc radius

$$C_p = \pi^3 J(1 + a)a' \int_0^1 x^3 dx$$

giving $$C_p = \frac{\pi^3}{4} J(1 + a)a'$$

Thus the angular velocity interference factor a' is given by

$$a' = \frac{4C_p}{\pi^3 J(1 + a)} \tag{16}$$

This represents an average value for the angular velocity inflow factor over the propeller disc which can be calculated from the measured flight parameters.

2.3 Velocity Vector at the Propeller

Using the interference factors developed in sections 2.1 and 2.2 the Velocity vectors at the propeller can be calculated.

From Fig.2 the apparent wind angle ϕ_o to the propeller is given by

$$\tan \phi_o = \frac{V}{\pi n D x} \qquad (17)$$

whilst the actual wind angle ϕ_x, relative to the blade element at radius x is given by

$$\tan \phi_x = \frac{V(1 + a)}{\pi n D x(1 - a')} \qquad (18)$$

The velocity component of the propeller blade element can now be defined as

$$V_\beta = \frac{V(1 + a)}{\sin \phi_x} \qquad (19)$$

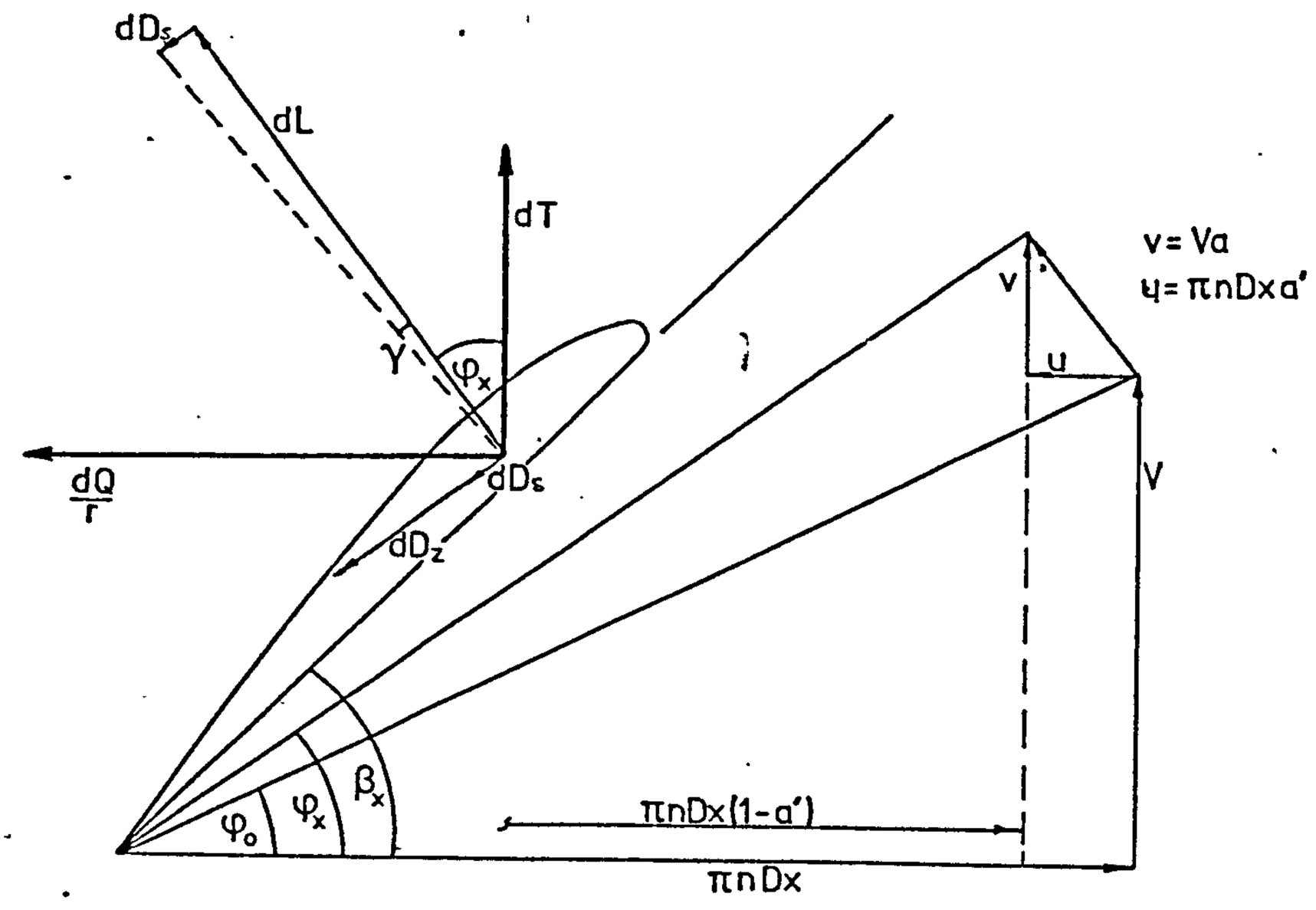

FIG.2. Propeller Blade Element Force and Velocity Diagram.

It should be noted that from equations (8) and (16) the values of the interference factors a and a′ are average values for the propeller and do not follow the blade loading profile or any asymmetry in loading which may arise from the incidence of the propeller to the local flow direction.

2.4 Resolution of Blade Element Forces

From Fig.2 the relative incidence between the airflow and the propeller blade is the difference between the blade element pitch angle β_x and the airflow vector ϕ_x. Thus the blade element, width δr, at radius x (where $x = 2r/D$) will be at an incidence α_x given by

$$\alpha_x = \beta_x - \phi_x \tag{20}$$

The blade element produces a lift force dL normal to the flow direction and a streamwise drag force dD which will be composed of a viscous drag or profile drag of the blade element and lift dependent separation drag component, see section 2.6. The total drag force can therefore be considered to be of the form

$$dD = dD_z + \gamma dL \tag{21}$$

where γ is a separation drag factor.

Resolving the blade element forces into a forward component, dT, (thrust) and a torque component dQ/r gives,

$$dT = B\{dL \cos \phi_x - dD \sin \phi_x\}$$

or

$$dT = B\{dL(\cos \phi_x - \gamma \sin \phi_x) - dD_z \sin \phi_x\} \tag{22}$$

and

$$\frac{dQ}{r} = B\{dL \sin \phi_x + dD_z \cos \phi_x\}$$

or

$$\frac{dQ}{r} = B\{dL(\sin \phi_x + \gamma \cos \phi_x) + dD_z \cos \phi_x\} \tag{23}$$

where B is the number of propeller blades.

Now the lift component is given by

$$dL = \tfrac{1}{2}\rho V_\beta^2 C_{L_x} b dr$$

and the profile drag similarly by

$$dD = \tfrac{1}{2}\rho V_\beta^2 C_{D_z} b dr$$

thus (22) and (23) become

$$dT = B\tfrac{1}{2}\rho V_\beta^2 b dr\{C_{L_X}(\cos\phi_X - \gamma\sin\phi_X) - C_{D_Z}\sin\phi_X\} \quad (24)$$

and

$$dQ = B\tfrac{1}{2}\rho V_\beta^2 b r dr\{C_{L_X}(\sin\phi_X + \gamma\cos\phi_X) + C_{D_Z}\cos\phi_X\} \quad (25)$$

Substituting $x = 2r/D$, putting the blade chord in terms of maximum chord $b = (b/b_o)b_o$, and substituting for V_β from equation (19) gives

$$dT = \frac{Bb_o}{4}\rho V^2(1+a)^2\frac{Ddx}{\sin^2\phi_X}\left\{\frac{b}{b_o}C_{L_X}(\cos\phi_X - \gamma\sin\phi_X) - \frac{b}{b_o}C_{D_Z}\sin\phi_X\right\} \quad (26)$$

and

$$dQ = \frac{Bb_o}{8}\rho V^2(1+a)^2\frac{D^2 x\,dx}{\sin^2\phi_X}\left\{\frac{b}{b_o}C_{L_X}(\sin\phi_X + \gamma\cos\phi_X) + \frac{b}{b_o}C_{D_Z}\cos\phi_X\right\} \quad (27)$$

Now the advance ratio J is given by

$$J = V/nD$$

and defining the thrust and torque coefficients from Fig.3 as

$$C_T = T/\rho n^2 D^4$$

and $$C_Q = Q/\rho n^2 D^5$$

equations (26) and (27) become,

$$\frac{dC_T}{dx} = \frac{b_o B}{4D}J^2(1+a)^2\left\{\frac{b}{b_o}C_{L_X}(\cos\phi_X - \gamma\sin\phi_X) - \frac{b}{b_o}C_{D_Z}\sin\phi_X\right\}\frac{1}{\sin^2\phi_X} \quad (28)$$

and

$$\frac{dC_Q}{dx} = \tfrac{1}{2}\frac{b_o B}{4D} J^2(1 + a)^2 x\left\{\frac{b}{b_o} C_{L_x} (\sin \phi_x + \gamma \cos \phi_x)\right.$$

$$\left. + \frac{b}{b_o} C_{D_z} \cos \phi_x\right\} \frac{1}{\sin^2 \phi_x} \qquad (29)$$

These expressions for the blade element thrust and torque components are completely general and can be integrated over the propeller disc to give the gross thrust and torque coefficients.

2.5 Forces Acting on the Blade Element at Incidence to the Airflow

The expression for wind angle, ϕ_x, relative to the blade element, equation (18), applies only to flow which is parallel to the propeller axis. In flight the propeller will generally be at some incidence to the free stream and therefore a component of the forward speed will act in the plane of the propeller and will combine with the rotational velocity to produce a periodic variation of incidence as the propeller rotates. From Fig.4 it can be seen that for the blade angular position θ the instantaneous axial velocity of a blade element at radius x will be,

$$V' = V(1 + a) \cos \alpha_p \qquad (30)$$

Where α_p is the propeller axis incidence to the local flow.

The instantaneous rotational velocity will be

$$V'_x = \pi n D x(1 - a') + V(1 + a) \sin \alpha_p \sin \theta \qquad (31)$$

Thus from (30) and (31) the instantaneous value of ϕ_x will become ϕ'_x given by

$$\tan \phi'_x = \frac{V(1 + a) \cos \alpha_p}{\pi n D x(1 - a') + V(1 + a) \sin \alpha_p \sin \theta} \qquad (32)$$

Using (30) and (32) the expressions for thrust and torque coefficients (28) and (29) repsectively become

$$\frac{dC_T}{dx} = \frac{b_o B}{4D} J^2(1 + a)^2\left\{\frac{b}{b_o} C_{L_x} (\cos \phi'_x - \gamma \sin \phi'_x)\right.$$

$$\left. - \frac{b}{b_o} C_{D_z} \sin \phi'_x\right\} \frac{\cos^2 \alpha_p}{\sin^2 \phi'_x} \qquad (33)$$

and

$$\frac{dC_Q}{dx} = \frac{b_o B}{4D} J^2 (1 + a)^2 x \left\{ \frac{b}{b_o} C_{L_x} (\sin \phi'_x + \gamma \cos \phi'_x) + \frac{b}{b_o} C_{D_z} \cos \phi'_x \right\} \frac{\cos^2 \alpha_p}{\sin^2 \phi'_x} \quad (34)$$

Both $\frac{dC_T}{dx}$ and $\frac{dC_Q}{dx}$ now have periodic variations which will cause an asymmetric loading over the propeller disc. Integrating the disc loading may produce forces which act in the plane of the disc and moments about axes normal to the propeller axis.

The torque force component $\frac{dQ}{r}$ of the element dr can be resolved into forces normal to the propeller axis, fig.4, these being

the normal force $\quad dZ = \frac{dQ}{r} \sin \theta \quad (35)$

and the side force $\quad dY = \frac{dQ}{r} \cos \theta \quad (36)$

Similarly the thrust component dT of the blade element will produce moments about the horizontal and vertical axes of the propeller disc, these being respectively,

the pitching moment $\quad dM = r\, dT \cos \theta \quad (37)$

and the yawing moment $\quad dN = r\, dT \sin \theta \quad (38)$

The magnitude of these forces and moments can be established by integrating over the propeller disc, thus for example, the normal force will be given by

$$Z = \frac{1}{2\pi} \int_0^1 \int_0^{2\pi} \frac{dQ}{r} \sin \theta \; dx \, d\theta$$

Before the integration can be performed it is necessary to define the propeller blade characteristics of lift and drag. From equations (35) and (36) it can be seen that there are three functions to be considered, these are

(a) the blade element lift characteristic $\frac{b}{b_o} C_{L_x}$

(b) the blade element profile drag characteristic $\frac{b}{b_o} C_{D_z}$

and (c) the induced drag coefficient γ.

Since the blade element forces are a function of local incidence, equation (20), the blade twist is also required as a function of spanwise position.

As these functions are all individual characteristics of the particular propeller considered the integral can only be performed for that one propeller type. Other propellers will require a change of characteristic.

2.6 Definition of Propeller Characteristics

The propeller blade characteristics are based on the manufacturers propeller data and in this example conform to the Hartzell Blade ref. 7663 which was used in corresponding flight trials, ref.7.

2.6.1 Blade Lift Characteristic

From equations (33) and (34) the lift contribution of the propeller blade element is provided by the term $\frac{b}{b_o} C_{L_x}$, and this can be expressed in terms of a local lift curve slope, a_x and incidence, equation (20), thus

$$\frac{b}{b_o} C_{L_x} = \frac{b}{b_o} a_x \alpha_x \qquad (39)$$

Since the blade thickness varies along the span the section lift curve slope will also vary along the blade span, an estimate can however be made by using the approximation for the lift curve slope of a two dimensional aerofoil,

$$a_x = 1.8\pi \left(1 + 0.8 \frac{t}{c}\right) \qquad (40)$$

where t/c is the thickness-chord ratio of the aerofoil, and assuming that the variation of lift curve slope along the blade is determined only by the thickness function.

The lift effectiveness of the blade element will also be a function of blade chord and therefore the effective lifting power can be described as $\frac{b}{b_o} a_x$ at any section. Using the blade chord thickness data from ref.7, the spanwise lift profile can be estimated. This is represented by a polynomial as a function of blade spanwise position x, in the form,

$$\frac{b}{b_o} a_x = (30.25 - (10x - 4.5)^2)^{\frac{1}{2}} + 0.7 \qquad (41)$$

and shown in fig.5.

The thickness chord profile of the blade with span can be approximated by the function

$$\frac{t}{c} = \frac{0.08}{x} \tag{46}$$

and is shown in fig.6. Thus using (46) in (45) the profile drag can be expressed as

$$C_{D_z} = 2C_{D_f} \quad 1 + 0.12x^{-1} + 0.00512x^{-4} \tag{47}$$

The profile drag characteristic of the blade is defined as $\frac{b}{b_o} C_{D_z}$ at any section and thus using (47) and the blade chord data the profile drag characteristic can be expressed as

$$\frac{b}{b_o} C_{D_z} = 0.004\ (2 - 1.35x) \tag{48}$$

In addition to the profile drag the blade section will produce a separation drag which is a function of section lift. From ref.9 the drag of an aerofoil section of the type used for a propeller blade is seen to increase as a function of lift,

$$C_{D_s} = \gamma\, C_{L_s}^2 \tag{49}$$

where C_{D_s} is the separation drag coefficient,

C_{L_s} the section lift coefficient, and

γ the separation drag factor.

Since the blade section thickness affects the separation factor the value of γ will increase towards the root of the blade. A simple approximation to the separation drag can be made to allow for this by assuming a constant value of γ and that the separation drag is proportional to the section lift coefficient,

$$\gamma = \frac{C_{D_s}}{C_{L_s}} = 0.033 \tag{50}$$

2.7 Propeller Efficiency

The propeller efficiency, η, is defined as the ratio of the work output to the work input, thus

$$\eta = \frac{TV}{P} \tag{51}$$

or in coefficient terms

$$\eta = J \frac{C_T}{C_P} = \frac{J}{2\pi} \cdot \frac{C_T}{C_Q} \tag{52}$$

It can be shown from Ref.10 that the ideal efficiency, η_i, can be expressed as

$$\eta_i = \frac{1 - a'}{1 + a} \tag{53}$$

this is however never achieved in practice since the profile drag of the propeller is not represented, neither is the thrust uniformly distributed across the propeller disc. The actual efficiency will be a function of the engine power and the propeller operation condition, which determines a and a', and can be found from equation (52). Since however the efficiency is needed to determine a and a' there must be an iterative process to calculate an efficiency which will satisfy the estimation of thrust and torque coefficients in terms of the overall propeller performance estimated by the momentum theory. To achieve this the ideal efficiency is factored by an estimate of the propeller efficiency with the blade drag, the estimated efficiency η_e then becomes

$$\eta_e = K \frac{(1 - a')}{(1 + a)} \tag{54}$$

After calculation of the propeller thrust and torque the efficiency calculated by equation (52) can be compared with η_e and K corrected to give an improved estimate until the required match of overall and calculated performance is achieved.

The value of K is a function of the wind vector ϕ_χ and the overall drag-lift ratio, Γ, of the blade element and can be expressed for the blade element as, (ref.10),

$$K = \frac{\tan \phi_x}{\tan (\phi_x + \Gamma)} \tag{55}$$

Since both ϕ_x and Γ will vary over the blade it is not possible to determine a value of K which would be acceptable for the blade and an estimation must be used followed by an iterative procedure to establish a working value of K for any particular operating condition.

2.8 Calculation of Propeller Forces

By the momentum theory of the propeller the thrust, T, produced by the propeller is given by

$$\eta P = TV \tag{56}$$

where P is the shaft power delivered to the propeller
η is the propeller efficiency, and
V the true airspeed

In coefficient form (56) can be expressed as

$$\eta C_p = JC_T \tag{57}$$

Also the power and torque coefficients are related, thus

$$C_p = 2\pi C_Q \tag{58}$$

Thus if the power input is known, and the propeller efficiency is known then the propeller gross thrust and torque can be found from (57) and (58).

The thrust and torque coefficients can also be calculated by integrating equations (33) and (34) over the propeller disc area. This involves a double integral, first calculating the blade loading by integrating along the blade and secondly integrating a revolution of the blade round the propeller disc. Since the loading will depend on blade incidence and the calculated inflow factors these parameters will have to be either estimated or calculated from estimated data. Having calculated C_T and C_Q by the integration the value of one of these can be compared with the value from the momentum theory, if these are not similar a correction can be made to the principle variable, which is the blade incidence, and an iterative process followed until a convergence is achieved. The gross thrust is the most convenient parameter to use for the iteration.

When the thrusts calculated by each method agree within specified limits the propeller efficiency based on the integrated thrust and torque can be calculated from (5) and compared with the initial estimate. Correction can then be made to the efficiency and the process repeated until the thrust and torque coefficients calculated by the momentum theory and the blade element theory agree, this state

defines the force system over the propeller disc and enables the normal forces and moments to be calculated.

Now that the disc loading is established the normal forces and moments can be found by integrating the components of the thrust and torque forces defined in equations (37) to (40) over the propeller disc.

3. DETERMINATION OF THE PROPELLER OPERATING CONDITIONS

Since the propeller is rigidly fixed to the aircraft the operating conditions of the propeller will be determined by the flight conditions of the aircraft and the engine power which can be regarded as independantly variable.

The shaft power delivered to the propeller can be found from the engine operating conditions, normally manifold inlet pressure and rotational speed together with the pressure and temperature of the atmosphere at the test altitude. The engine manufacturers guaranteed performance charts are usually adequate for this purpose.

The flight conditions of the aircraft will determine the operating conditions of the propeller in terms of the incident airflow to the propeller disc. The two parameters required, airspeed and propeller incidence, αp, are determined by the aircraft weight W and lift coefficient C_L. the lift equation for the aircraft is given by,

$$L = W \cos \gamma = \tfrac{1}{2}\rho V^2 S\, C_L \qquad (59)$$

If the flight path angle γ is small (say less than 10^0) then the effect of γ is negligible and the lift can be assumed equal to the aircraft weight, therefore by specifying the weight and C_L the airspeed is determined by equation (59).

For airspeeds above the stall region the $C_L - \alpha$ curve is usually linear and therefore the value of C_L determines the incidence of the wing zero lift line with respect to the airflow. Since the propeller is considered rigidly fixed to the airframe the aircraft incidence also determines the propeller incidence αp, this is given by,

$$\alpha_p = \alpha - \delta_p + \varepsilon_p \qquad (60)$$

where δ_p is the propeller setting angle with respect to the wing zero lift line, and ε_p is the upwash at the propeller due to the wing circulation, Γ.

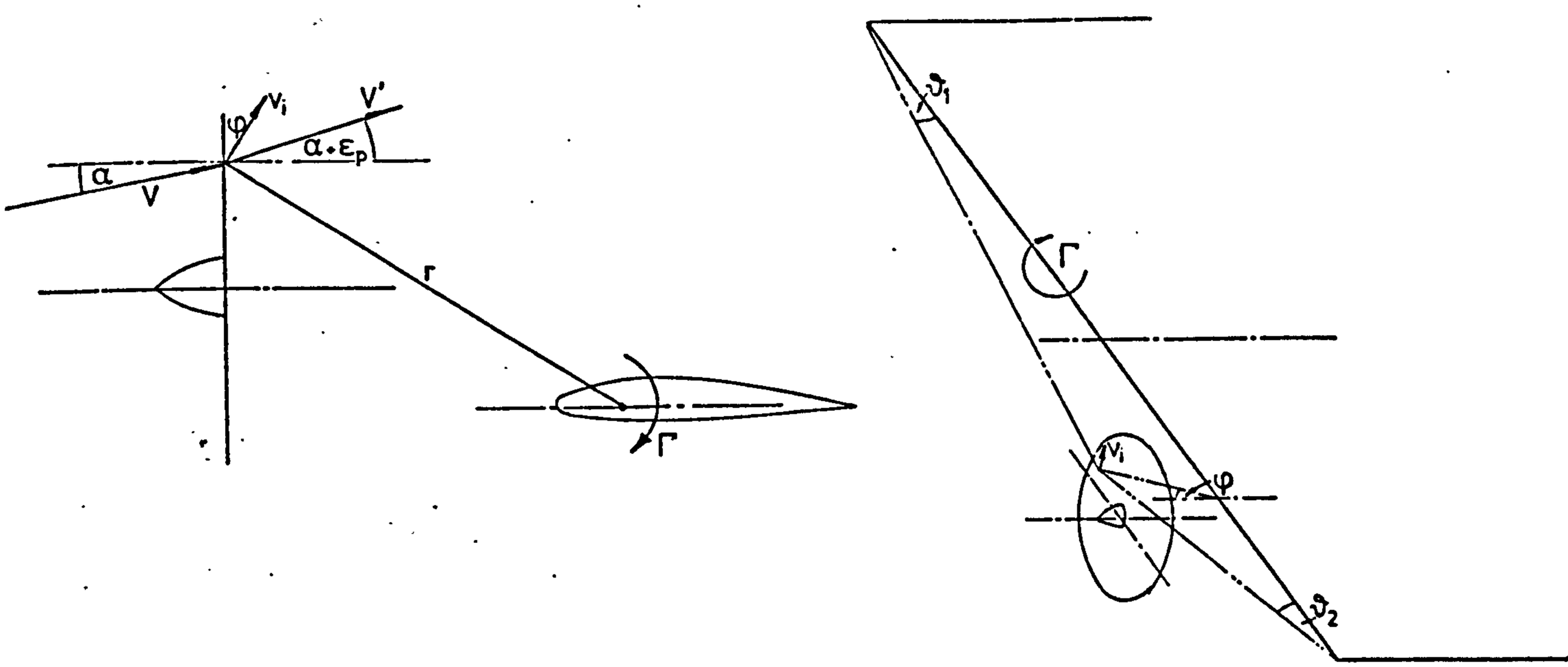

FIG 2a Induced Velocity at the Propeller due to the Wing.

The upwash is due to the circulation generated by the wing and can be approximated by assuming that the wing can be replaced by a simple bound vortex of strength r at the quarter chord given by

$$r = \frac{L}{\rho V s} \tag{61}$$

From Fig.2a it can be seen that the induced upward velocity, v_i, at a point on the propeller is given by

$$v_i = \frac{r}{4\pi r}(\cos\theta_1 + \cos\theta_2) \tag{62}$$

and so from (61) and (62)

$$v_i = \frac{L}{4\pi\rho s V r}(\cos\theta_1 + \cos\theta_2) \tag{63}$$

The addition of the forward velocity and induced velocity vectors gives the resultant flow direction

$$\alpha + \varepsilon_p = \tan^{-1}\left[\frac{v_i \cos\phi + V \sin\alpha}{v_i \sin\phi + V \cos\alpha}\right] \qquad (64)$$

and velocity

$$V' = \left\{(V \sin\alpha + v_i \cos\phi)^2 + (V \cos\alpha + v_i \sin\phi)^2\right\}^{\frac{1}{2}}$$

which can be reduced to

$$V' = V\left\{1 + (\frac{v_i}{V})^2 + 2\frac{v_i}{V}\sin(\alpha + \phi)\right\}^{\frac{1}{2}}$$

Neglecting the second order terms this is approximately

$$V' = V\left\{1 + \frac{v_i}{V}\sin(\alpha + \phi)\right\}$$

and the resultant velocity can be considered to be given by

$$V' = V(1 + a_w) \qquad (65)$$

where $a_w = \frac{v_i}{V}\sin(\alpha + \phi)$

This can be combined with the propeller inflow factor, a, from equation (8) and the total inflow factor at the point on the propeller disc now becomes

$$(1 + a + a_w) \qquad (66)$$

(neglecting second order terms).

Equations (64) and (66) now provide the flow vector at each blade element. This will vary over the propeller disc, since the upwash field is a function of the distance from the line vortex of the wing, causing an asymmetric inflow vector field and a consequent variation of blade loading with the blade angular position θ.

The propeller operating conditions can therefore be specified by the engine shaft power, aircraft weight and flight lift coefficient.

The examples of the calculated propeller performance discussed in section 4 are based on a Piper Twin Comanche 'A' series aircraft which was used for handling trials. The aircraft and its instrumentation are fully discussed in Ref.11.

The basic aerodynamic charactertistics of the aircraft were measured and agreed well with the theoretically derived data of Ref.13. In particular the lift-curve slope, $dC_L/d\alpha$, was measured to be 5 per radian with power for level flight, this corresponds to a theoretical value of 5.09 per radian, (Ref.13). The measured value was accepted for the individual aircraft used in the flight trials.

The handling trials consisted of a series of steady speed trims throughout the aircraft speed range at constant engine power. Several engine power settings were used corresponding to flight conditions from flight idle to maximum continuous power. The particular flight conditions used for the calculations corresponded to an aircraft weight of 3392 lb and lift coefficients from 0.2 to 1.2 at intervals of 0.2. The engine powers corresponded to the throttle settings used in the measurement of each set of trim curves. At low power settings the engine output was not always sufficient to maintain the required engine speed which was governed to 2400 rpm, under these conditions the propeller is not operating normally and therefore caculation of the performance is not reliable.

The computer programme used for the calculation of the performance is described in Appendix A1.

4. CALCULATED PROPELLER PERFORMANCE

The propeller performance calculated by the programme (APP A1) is based on a constant engine shaft horse power delivered to the propeller through a range of flight lift coefficients. The most convenient form of data presentation is therefore in terms of curves performance at constant power coefficient with the propeller advance ratio as the speed variable. The force and moment coefficients produced by the propeller, and defined in fig.3, can be considered separately.

4.1 Thrust Coefficient, C_T

From equation (54) the thrust coefficient is related to the power coefficient by the expression

$$\eta C_p = J\, C_T$$

therefore the curve of C_T against J for a constant C_p will have a hyperbolic form, assuming constant propeller efficiency. This is the case with the calculated values of C_T from the programme. The variation of propeller efficiency with J causes a slight distortion of the curves but the hyperbolic form is still apparent, fig.6a.

At all powers there is evidence of a decrease in propeller efficiency at low advance ratios which will tend to decrease the slope of the curves and preventing them from tending to infinity as the advance ratio approaches zero.

4.2 Normal Force Coefficient, C_Z

The normal force coefficient, which arises from the integration of the torque force component of the blade element, is seen to be primarily a function of incidence since it increases from zero at an advance ratio corresponding to a zero propeller incidence, fig.6b. The increase is approximately proportional to incidence but a slight inflection is present at $J \doteq 0.8$, this is due to the resolution of the thrust and drag components of each blade element into the torque force. Since the thrust and drag components sum to give the torque the thrust will dominate at low advance ratios where the thrust coefficient increases more rapidly as advance ratio decreases.

The increase in C_Z is approximately proportional to power coefficient and on extrapolating to a zero power condition it is seen that a line is produced which predicts a normal force existing at zero power. This force arises from the drag component of the blade element developed as the propeller absorbs energy from the airstream in a windmilling condition. It is significant that a normal force can be expected to be produced by a propeller at incidence to the airflow under any power condition.

4.3 Yawing Moment Coefficient, C_N

The yawing moment coefficient is also seen to be primarily a function of incidence, but since it arises from the integration of the thrust about the propeller normal axis and the thrust characteristic is relatively smooth, fig.6a, the yawing moment does not show any inflection in its form. It is notable however that C_N increases rapidly as J decreases leading to high values as the stall region is approached, fig.6c.

The yawing moment is proportional to power and, as in the case of the normal force, when extrapolated to zero power a residual moment is seen to be produced implying that asymmetric behaviour can be expected at all powers when the propeller is at incidence to the local flow.

4.4 Pitching Moment and Sideforce Coefficients, C_M, C_Y

By symmetry these should be zero but due to the asymmetry caused by the wing circulation flow over the propeller disc small values of both coefficients are seen to occur, Fig.6d and e. The sideforce coefficient is almost constant with advance ratio whilst the pitching moment coefficient increased in magnitude slightly as advance ratio decreases. These coefficients are solely due to wing circulation and when test cases were run with T zero both C_M and C_Y were very small, of the order 10^{-5}, this being the magnitude of the rounding error of the integration procedure.

4.5 Propeller Efficiency, η

The propeller efficiency is calculated in the programme as a part of the matching process between the integrated propeller performance and the momentum theory. The four computed curves showing the efficiency against advance ratio, fig.7, indicate that the maximum efficiency is a function of advance ratio and power coefficient and tends to a lower advance ratio as C_p decreases. At low advance ratios the efficiency decreases rapidly which is to be expected since the interference factors a and a' are increasing, equations (53) and (54). At high speeds and low power conditions the efficiency is reduced because of the high proportion of power required to overcome the torque relative to that available to produce thrust.

From the calculated efficiency curves a general efficiency characteristic can be constructed, fig.7a. This shows a typical "rolling surface" characteristic of a variable pitch propeller. The maxima of each constant power line shows a progressive increase with power and advance ratio to a maximum around 86%. At low advance ratios the efficiency tends to decrease with power to about 70%, within the limits of the calculated data.

4.6 Propeller Blade Angle, β

The programme calculates the blade tip incidence required to produce the thrust force and this is seen to be a function of the advance ratio, fig.8.

At low powers the blade angle required is roughly proportional to the advance ratio, a slight inflection is probably due to the propeller efficiency effects. As the power coefficient increases the blade angle required also increases as expected, but the proportional relationship with advance ratio is only evident at high speed. At low speeds the inflow factor increases the local flow velocity and a larger blade angle is required to produce positive incidence, this can be seen at $C_p = 0.065$ where the blade angle is almost constant with advance ratio.

5. CONCLUSIONS AND DISCUSSION

The study of the propeller at incidence to the airflow has shown that a considerable normal force and yawing moment can be expected to occur and that they are related to the aircraft incidence and engine power. Also it is seen that when the calculated data is extrapolated to a zero power condition there will be residual normal force and yawing moment which are not small. Since the programme was not developed to calculate negative thrusts the effects of a windmilling propeller cannot be surmised.

In particular it is seen that the normal force tends to increase more rapidly as the aircraft speed decreases, which in the case of a conventional aircraft, will tend to produce a nose up or destabilising pitching moment causing a divergence to the stall. As the aircraft C.G. moves aft destabilising the aircraft the propeller moment arm is increased leading to a more severe propeller moment destabilisation. If the estimation of the propeller normal force is omitted from the longitudinal static stability equations then the estimated static margins could be very much in error.

Since the yawing moment also increases as aircraft speed decreases there will be a maximum asymmetric flight case at low speeds and high power conditions leading to difficult handling qualities at the stall. Such effects are well known in twin engined aircraft and has led to the introduction of counter-rotating engines. Although this reduces the asymmetric effects of the propellers it does not affect the normal forces produced by the incidence to the local flow.

The calculated propeller performance is based on a specified aircraft-engine-propeller combination but other aircraft and power-plants could be analysed by the adaptation of the programme to the aircraft and propeller characteristics concerned. The programme does not include the effects of the wing induced velocity at the propeller since in the case concerned the propeller was ahead of the wing leading edge by about one chord length. If the propeller was close to the wing it would be necessary to include the induced flow field in the calculation of the blade element incidence.

The programme has only been developed to consider the effects of incidence on the propeller, whereas in general flight sideslip will also occur and will, by the same reasoning, produce a sideforce and a pitching moment. It is this sideforce which gives rise to the so called propeller fin effect. The sideslip could be included in the programme by adding a further term in equation (32) to account for the cyclic variation of ϕ'_x with sideslip as the propeller rotates. Alternatively the incidence and sideslip angles could be combined and the gross forces and moments calculated. The forces and moments could then be resolved into components along and about the normal and lateral axes.

Since the aircraft on which the calculated performance is based is no longer available for flight trials it is not possible to verify the results of the programme experimentally. The calculated values of the normal force do, however, appear to be compatible with the observed flight behaviour when used to correct the errors due to power between estimated and measured stability characteristics, ref.12. A further study including flight trials will be necessary to absolutely verify the programme effectiveness.

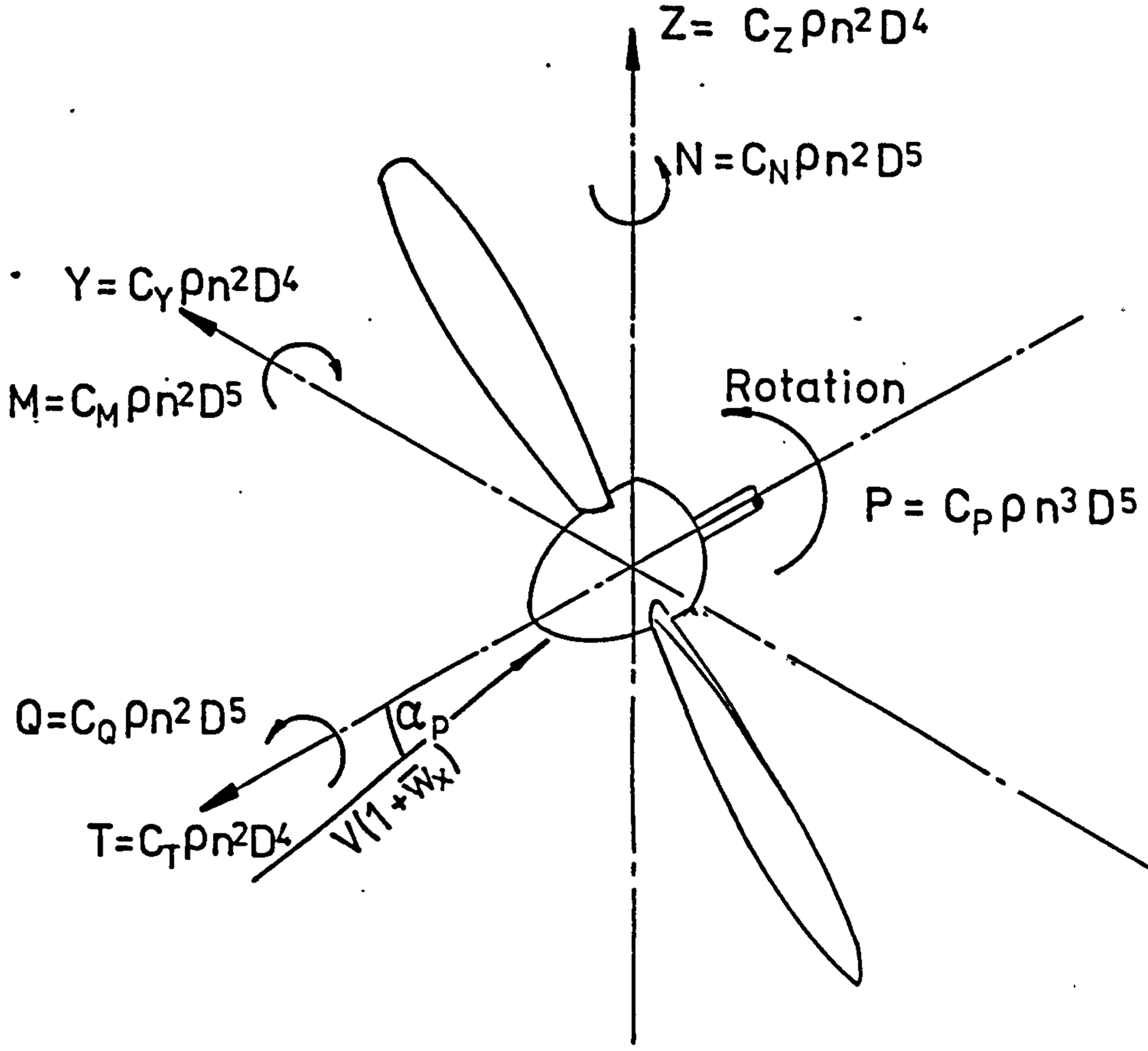

T = Thrust

Y = Side Force

Z = Normal Force

n = Propeller Speed (R.P.S.)

D = Propeller Diameter

ρ = Air Density

Q = Torque (Shaft)

M = Pitching Moment

N = Yawing Moment

P = Power

FIG.3 PROPELLER FORCE AND MOMENT NOTATION.

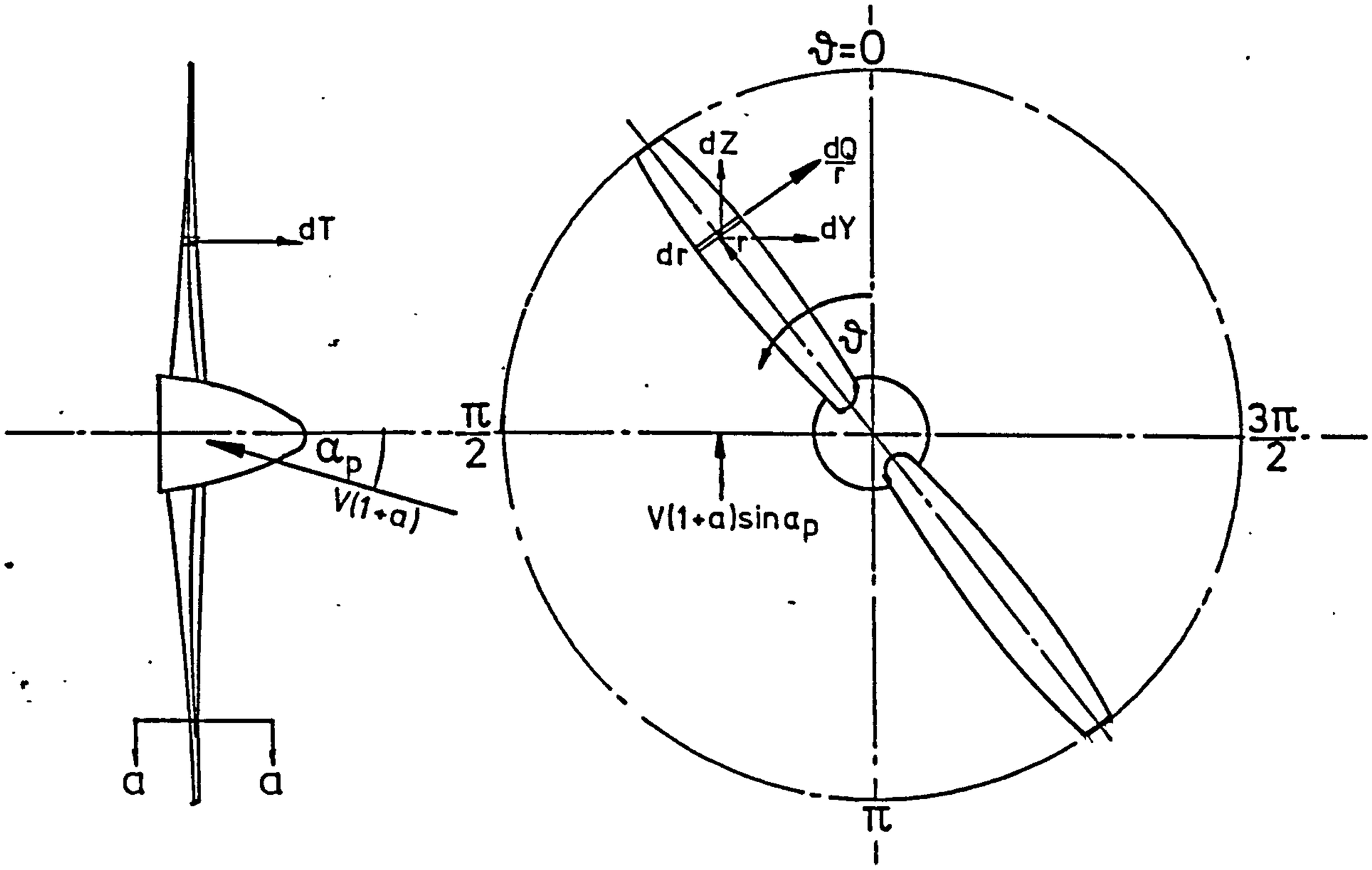

Propeller Section a—a.

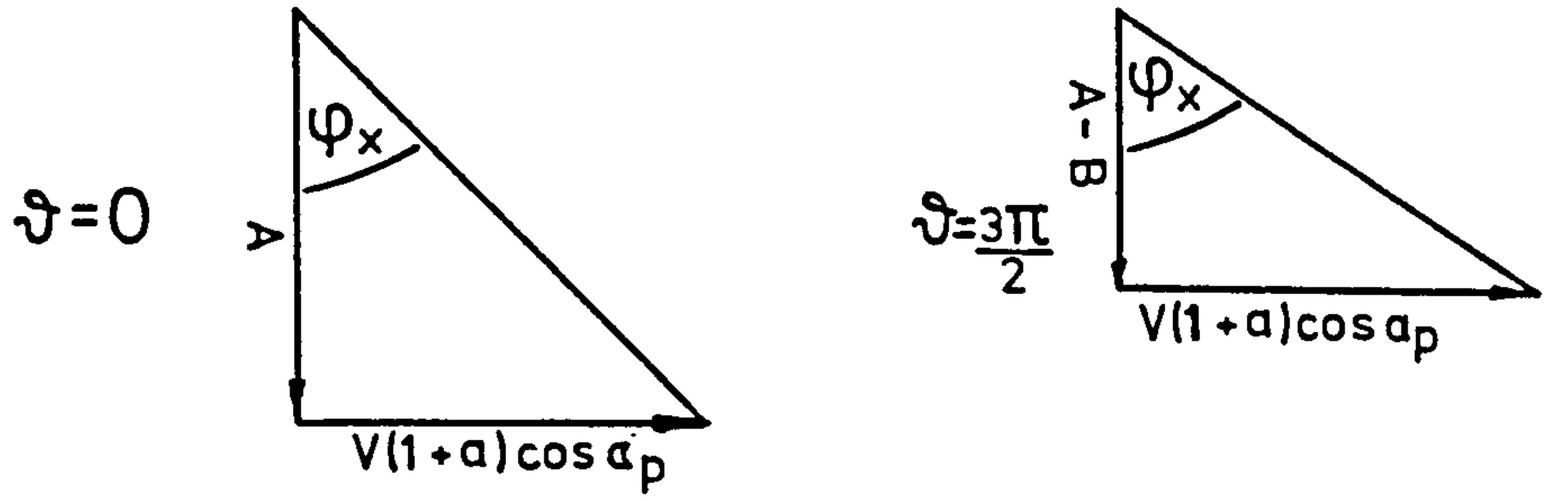

FIG.4. PROPELLER VELOCITY VECTORS AT INCIDENCE α_p

FIG. 5A PROPELLER TWIST

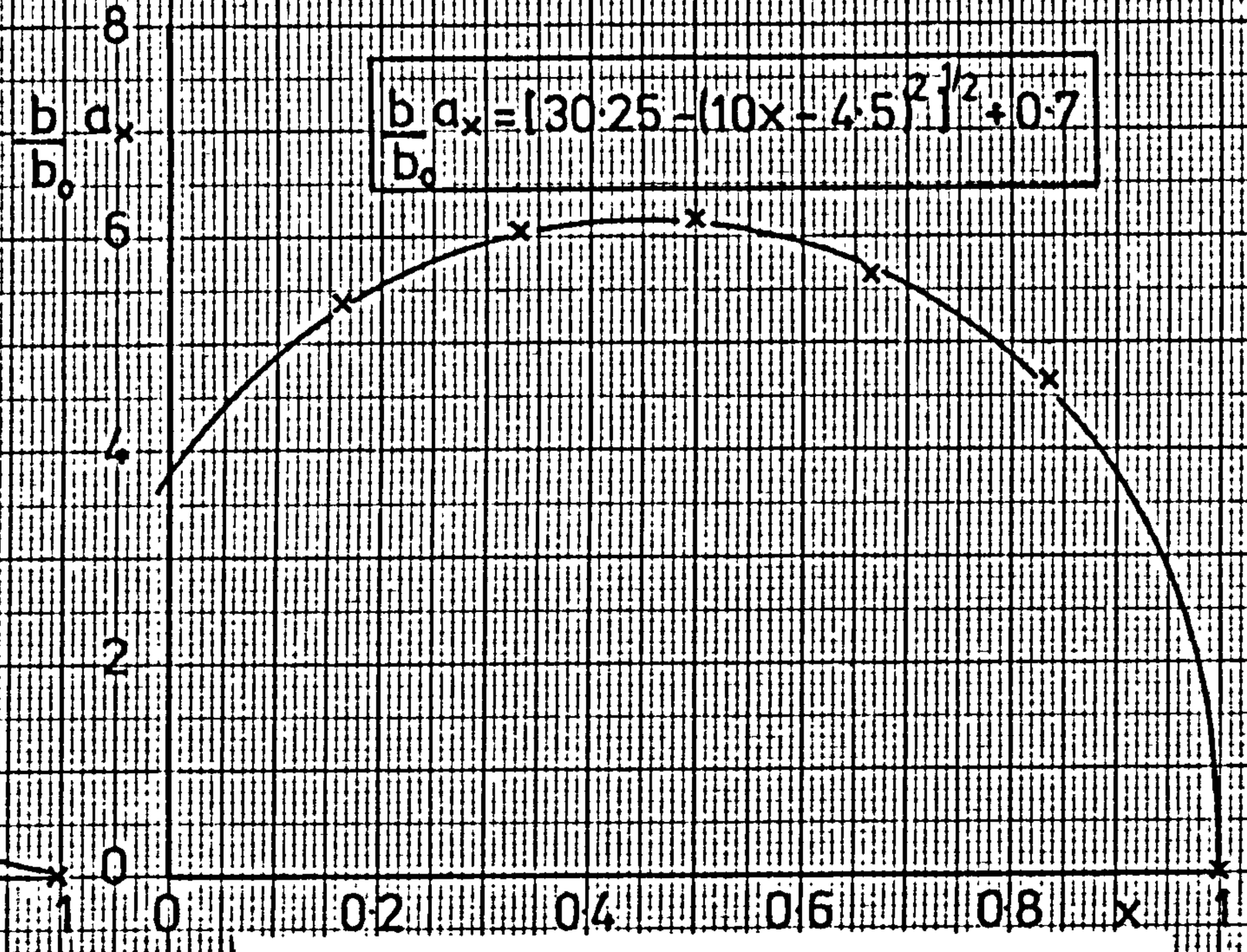

FIG. 5B BLADE ELEMENT LIFT PARAMETER

FIG. 5 PROPELLER BLADE CHARACTERISTICS, HARTZELL BLADE 7663

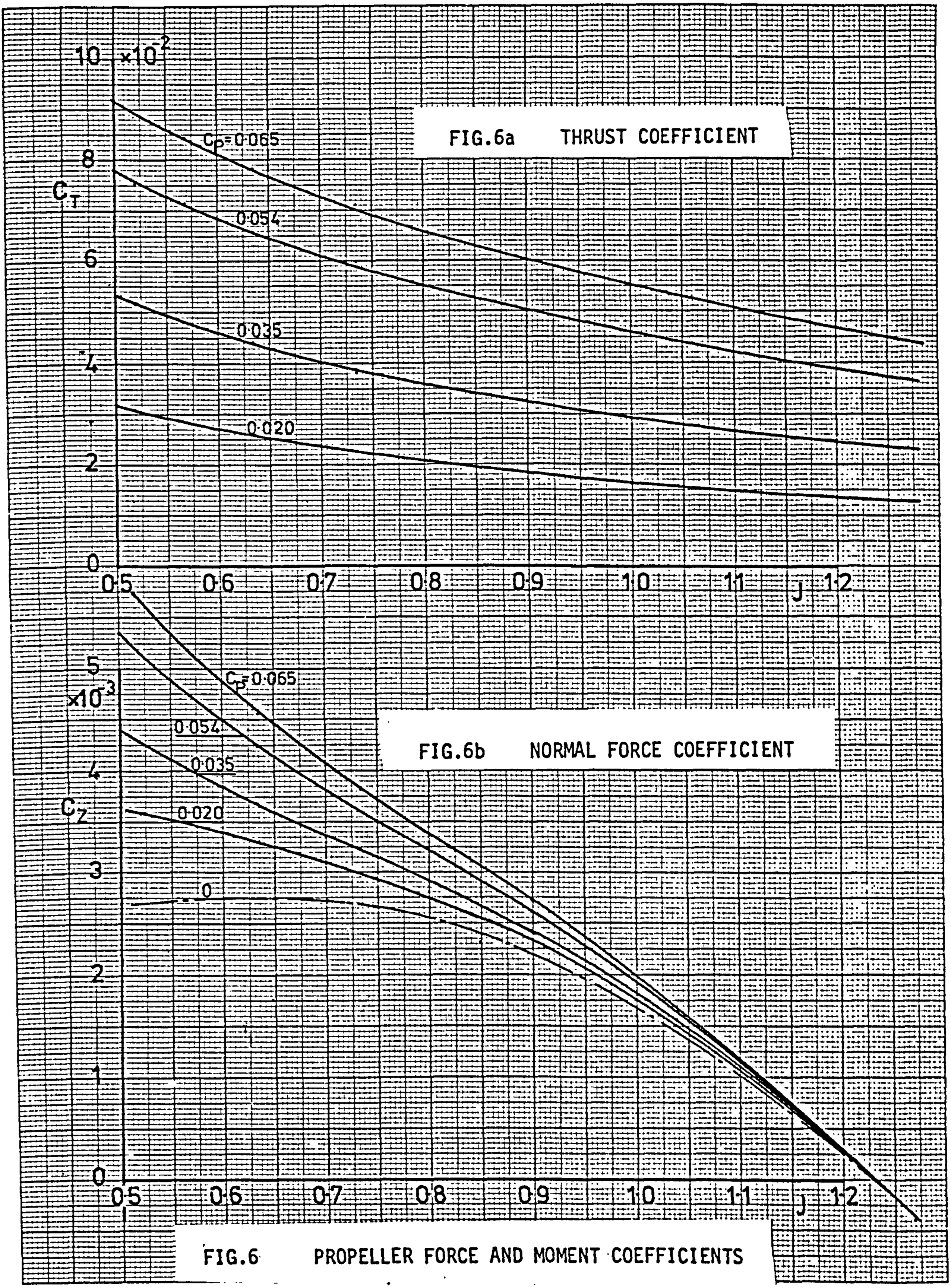

FIG.6a THRUST COEFFICIENT

FIG.6b NORMAL FORCE COEFFICIENT

FIG.6 PROPELLER FORCE AND MOMENT COEFFICIENTS

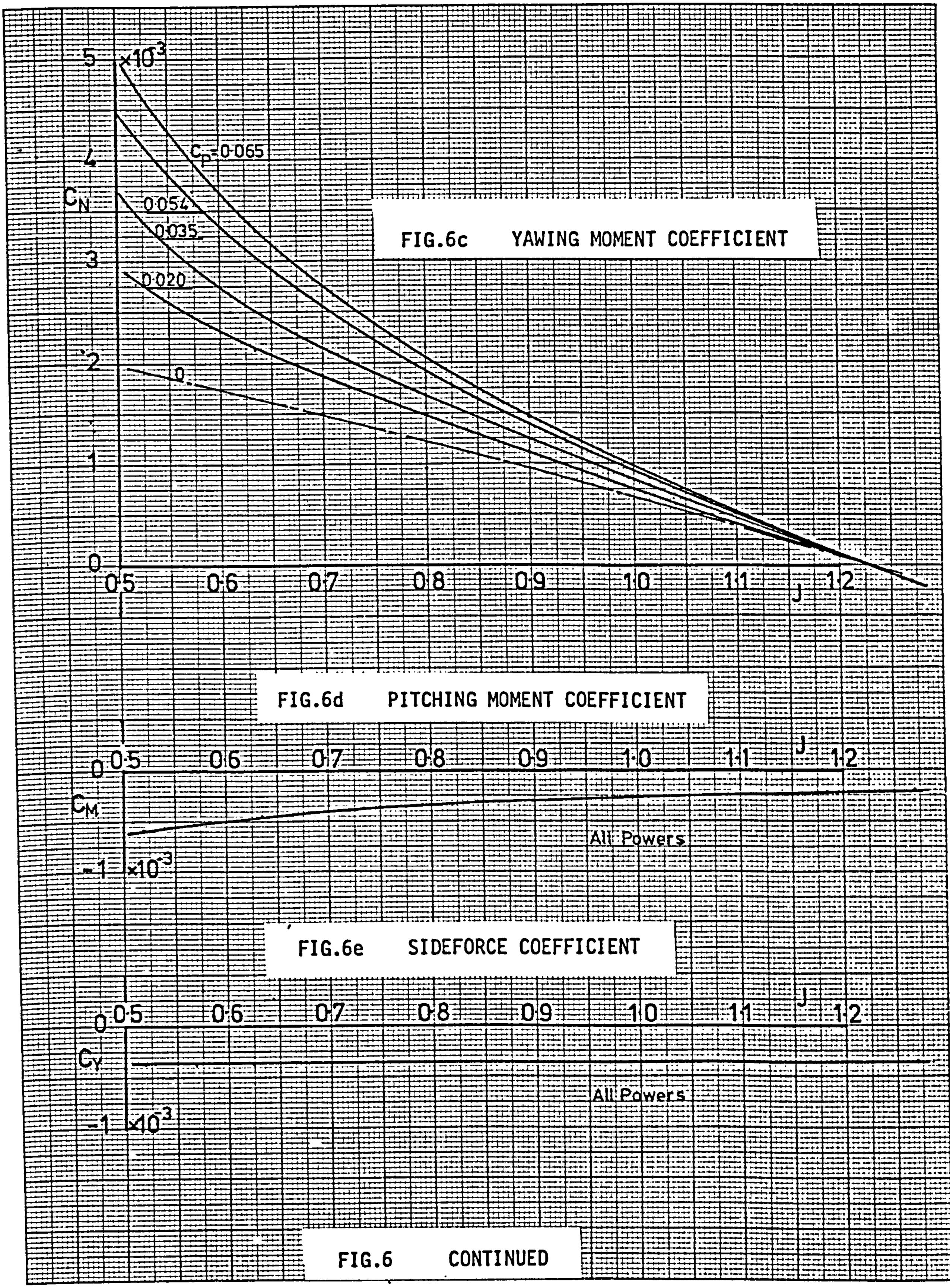

FIG.6c YAWING MOMENT COEFFICIENT

FIG.6d PITCHING MOMENT COEFFICIENT

FIG.6e SIDEFORCE COEFFICIENT

FIG.6 CONTINUED

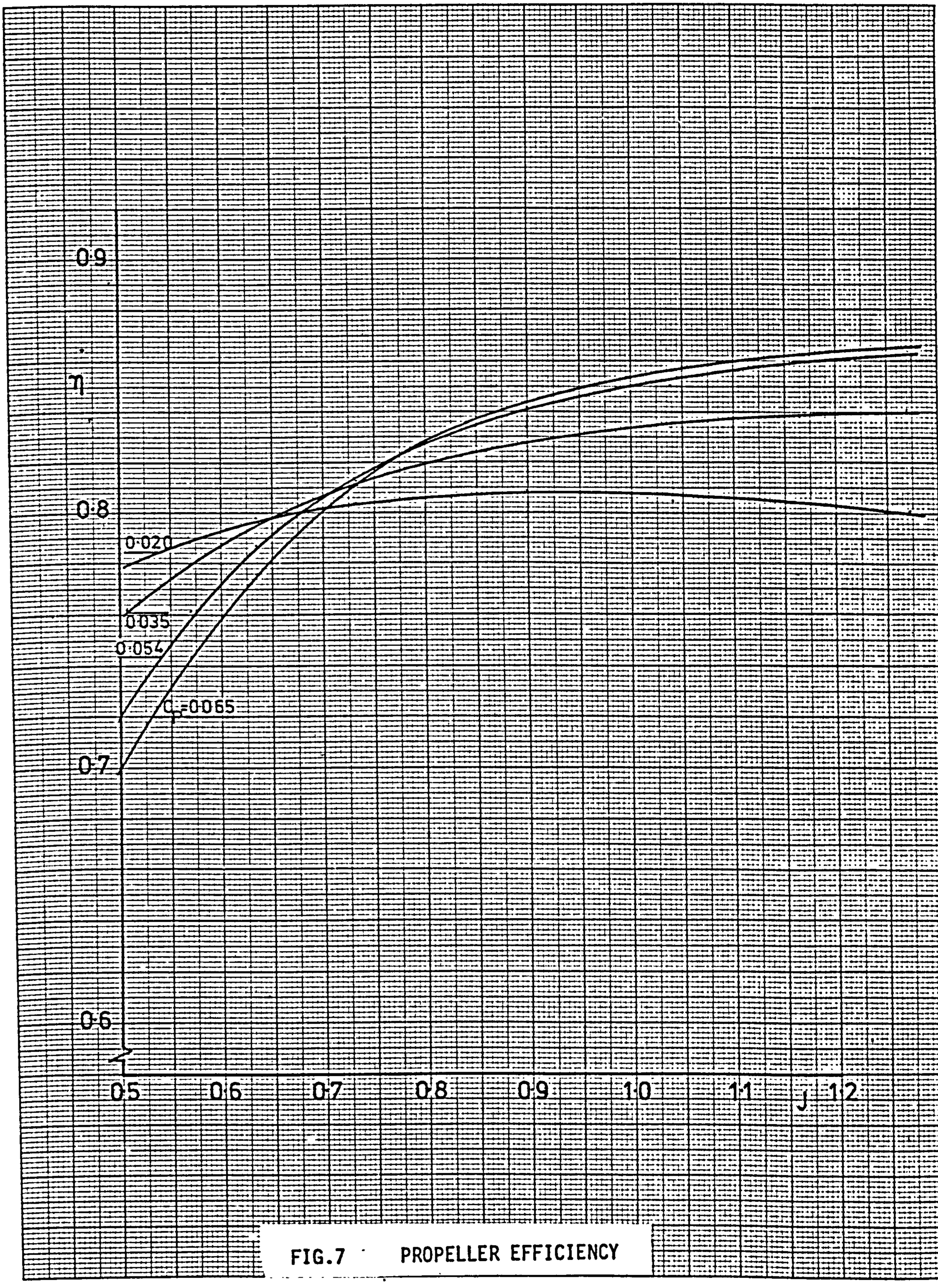

FIG.7 PROPELLER EFFICIENCY

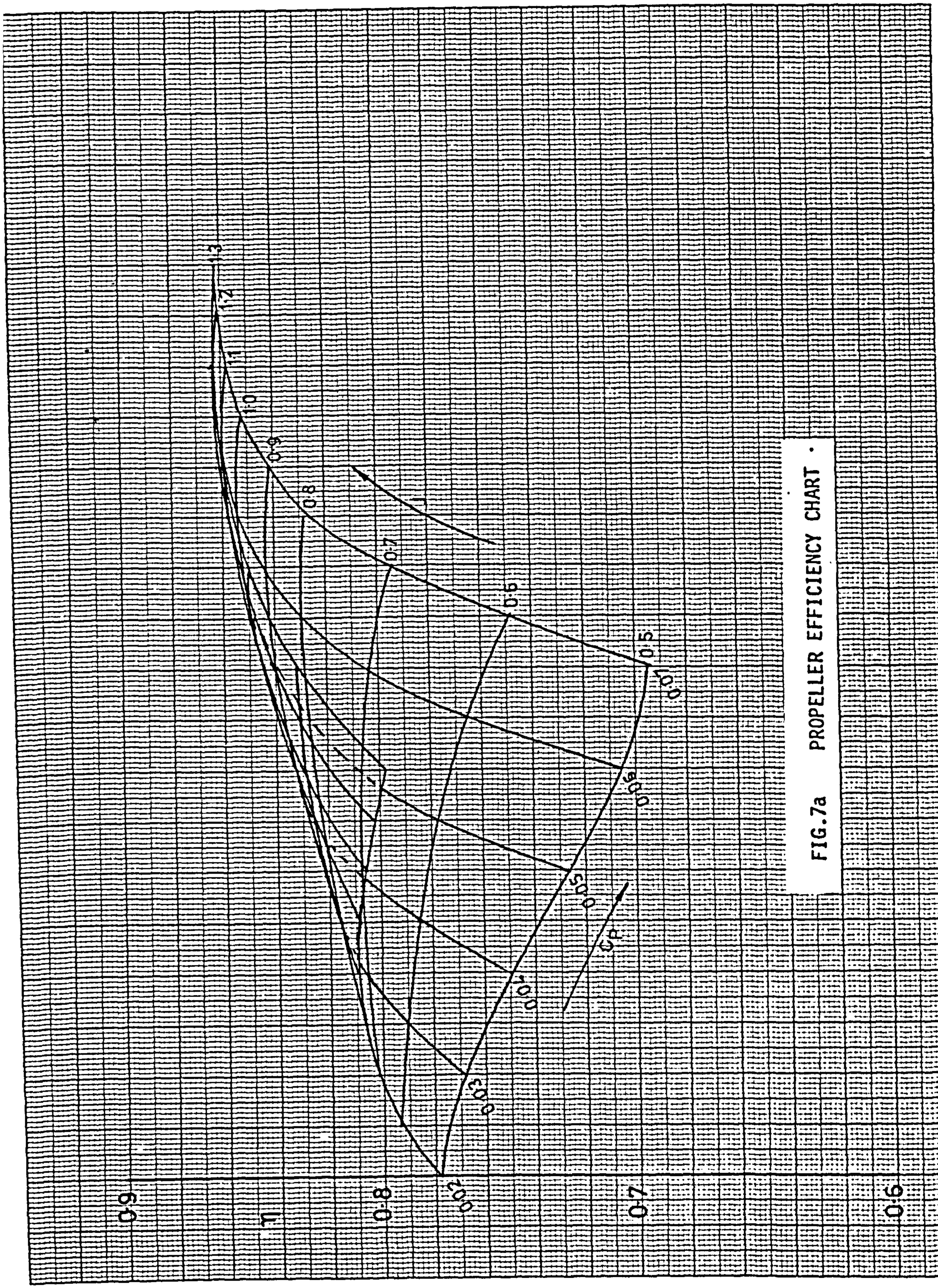

FIG.7a PROPELLER EFFICIENCY CHART

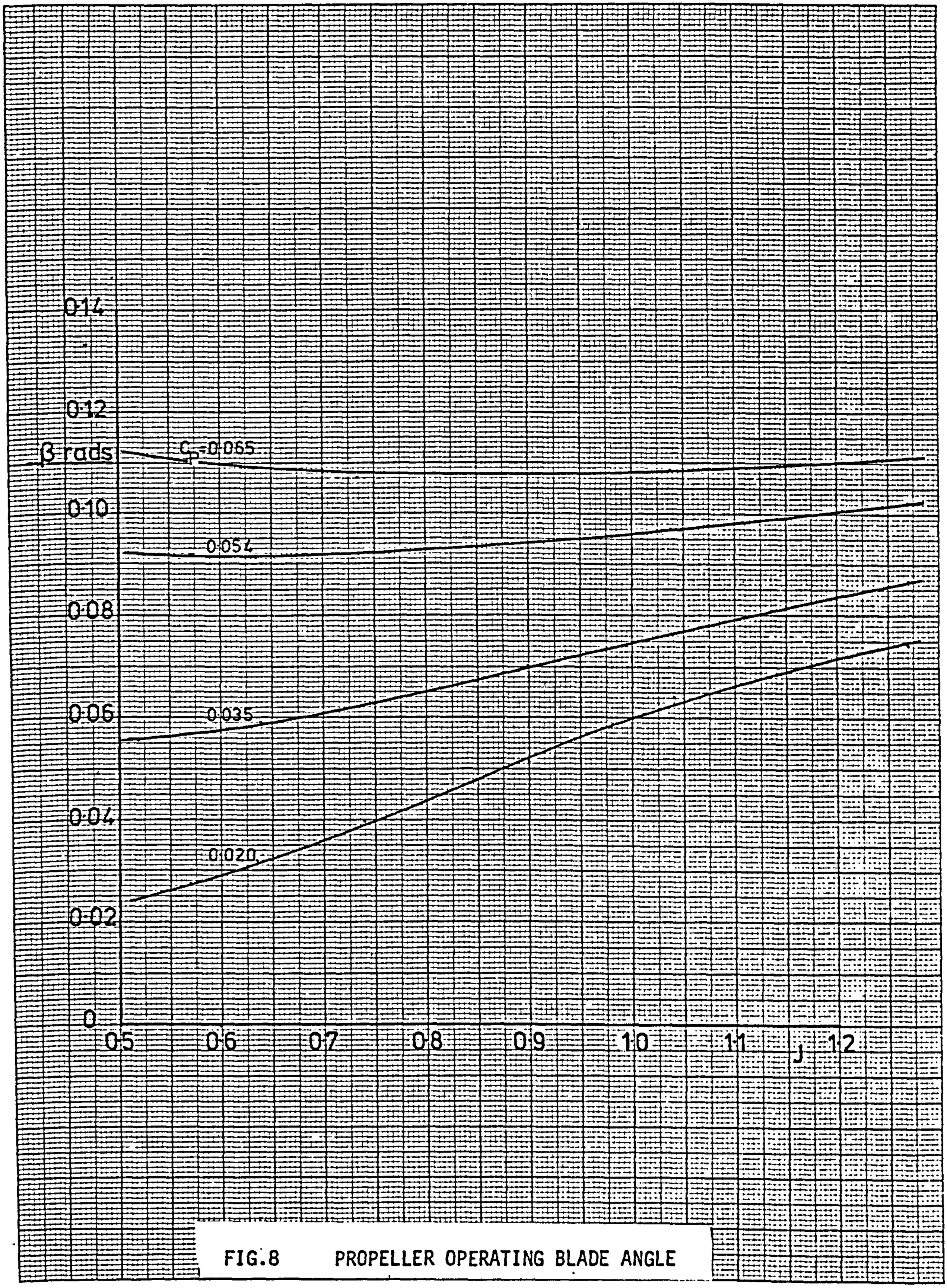

FIG.8 PROPELLER OPERATING BLADE ANGLE

REFERENCES

1. RIBNER, H.S. — Formulas for Propellers in Yaw and Charts for Side-force Derivatives. NACA T.R. 819 1945

2. RIBNER, H.S. — Propellers in Yaw. NACA T.R. 820 1945

3. PRIESTLEY, E. — Theory of the Propeller "Fin" Effect, including a Review of Existing Theories. R & M 2030 1943

4. LOCK, C.N.H., PANKHURST, R.C. & CONN, J.F.C. — Ship Theory Method of Calculations for Airscrews on High Speed Aeroplanes. R & M 2035 1945

5. BORST, H.V. — Summary of Propeller Design Procedures and Data. Vol I Aerodynamic Design and Installation. H.V. Borst & Ass. Rosemont Penn. 1973

6. GOLDSTEIN, S. — On the Vortex Theory of Screw Propellers. Proc. Roy. Roc. Av 123 1929

7. - — Handbook, Overhaul Instructions. Manual No.117-B Hartzell Propeller Inc.

8. HOERNER, S.F. — Aerodynamic Drag. Hoerner 1951

9. ABBOT, I.H. & VAN DOENHOFF, A.E. — Theory of Wing Sections. Dover Publications Inc. 1959

10. GLAUERT, H. — The Elements of Aerofoil and Airscrew Theory. C.U.P. 1959

REFERENCES (cont'd)

11. ESHELBY, M.E. — An Instrumentation System to Measure the Stability Characteristics of Light Aircraft. Cranfield Aero Memo No.101

12. ESHELBY, M.E. — The Influence of Running Propellers on Low Speed Longitudinal Static Stability Trim Curves. Cranfield Report, Aero No.34, 1976

13. WOLOWICZ, C.H. & YANCEY, R.B. — Longitudinal Aerodynamic Characteristics of Light Twin Engined, Propeller Driven Airplanes. NASA TN D-6800, 1972

APPENDIX A1

The Computer Programme for the Analysis of the Propeller Performance

The calculation of the propeller performance is carried out by the computer programme listed in table A1. The flow diagram, Fig.A1, describes the operation of the programme stage by stage, the language is Hewlett Packard BASIC.

The programme commences by printing its title and a format of headings for the identification of the output, it then requests an input of the weight, power and lift coefficient. On receipt of the input the aircraft weight (L) is inspected, if it is zero the programme is terminated, this is the only method of termination. If the weight is not zero then the flight conditions are calculated, these are the true airspeed (V0), propeller incidence (E1), advance ratio (J1) and power coefficient (P1). The programme then requests an input of the estimated propeller tip incidence β (B3) and propeller efficiency η_0 (E3). Both these parameters have to be estimated by the operator from experience of previous cases. Figs.7 and 8 show the form of the blade incidence and efficiency curves for the example computed.

The value of η_0 corresponds to the parameter K in equation (54) and the overall efficiency η_e (E0) is found by calculating the interference factors a and a' and iterating until $\eta_e = \eta$, when agreement to 1% is achieved the values of η_e, a and a' are accepted.

Using these values the calculation of the thrust and torque coefficients can commence. The thrust and torque forces on the blade elements are calculated at 17 equal intervals along the blade span from $r = 0.2$ to $r = 1$, these are then integrated by Simpsons Rule to give the nett thrust and torque of the blade at a rotational position $\theta = 0$. The blade is then rotated through a complete revolution in 50 equal intervals and the nett thrust and torque at each rotational position integrated by Simpsons Rule to give the total thrust C_T and torque C_Q of the propeller under the specified operating condition. The elemental thrust and torque force coefficient equations used to determine the propeller performance are given in equations (33)and (34).

The torque coefficient corresponding to the input power C_{Q_0} and the thrust coefficient C_{T_0} from the momentum theory are calculated using the calculated propeller efficiency η_e and compared with the values calculated by the integration. If $C_{T_0} = C_T$ and $C_Q = C_{Q_0}$, to within preset limits of ±1%, then it can be assumed that the integrated performance is equal to the gross performance both in respect to the power input (C_Q) and the output (C_T) and the model is therefore representing the operation of the propeller. The selected values of β and η_0 are acceptable and the programme can then proceed to the

final integration. If $C_T \neq C_{T_o}$ or $C_{Qo} \neq C_{Q_o}$ then a false assumption has been made in either β or n_o and a correction must be made. Initially corrections are made to β and the integration repeated until $C_T = C_{T_o}$ at which point, if $C_Q \neq C_{Q_o}$, the estimated efficiency n_o is corrected and the programme returns to the calculation of a new value of n_e. The iterative process continues until the conditions of convergence of C_T and C_Q are complete, printing intermediate data concerning β, n, C_T and C_Q after each iteration. When convergence is achieved the words "out of iteration" are printed indicating entry to the final integration routine. The corrections to β or n_o are proportional to the error between C_T and C_{T_o} or C_Q and C_{Q_o} respectively, it is sometimes necessary to change the constants of proportionality to avoid divergent iteration and therefore lines 890 and 910 may require minor changes to maintain stability under some operating conditions.

The final integration is similar to the integration for C_T and C_Q but calculates all six forces and moments using the previously established values of β and n_e and other operating variables.

The output consists of four lines of six parameters, these being:
Line 1, aircraft operating conditions
Line 2, propeller force and moment coefficients, non-dimensionalised by propeller characteristic groups ρnD
Line 3, as line 2, non-dimensionalised by aircraft groups ρVD
Line 4, propeller parameters used during the calculations.

On completing the output the next data case is requested and the programme returns to the input of the next data.

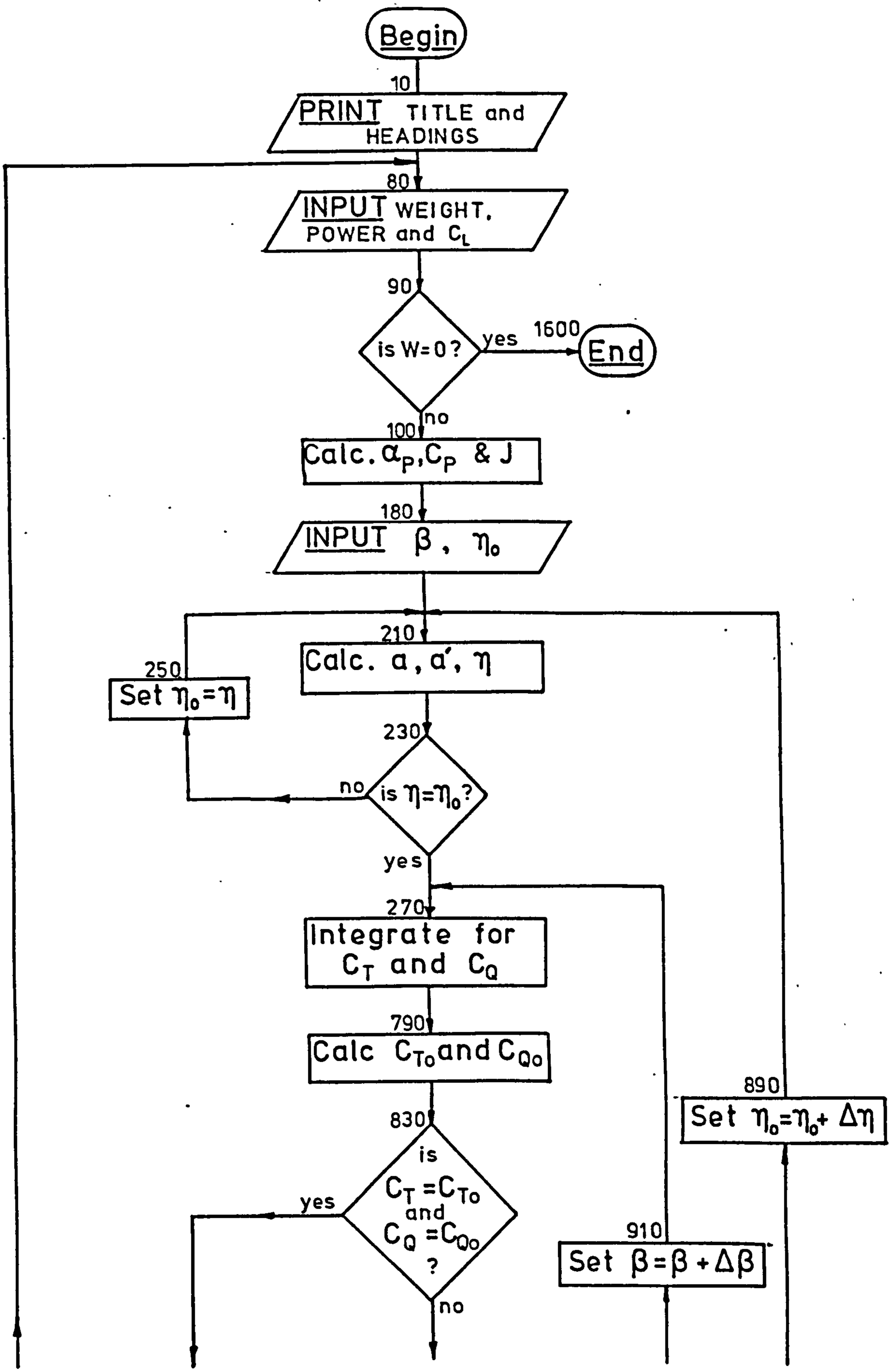

FIG A1 Programme Flow Diagram.

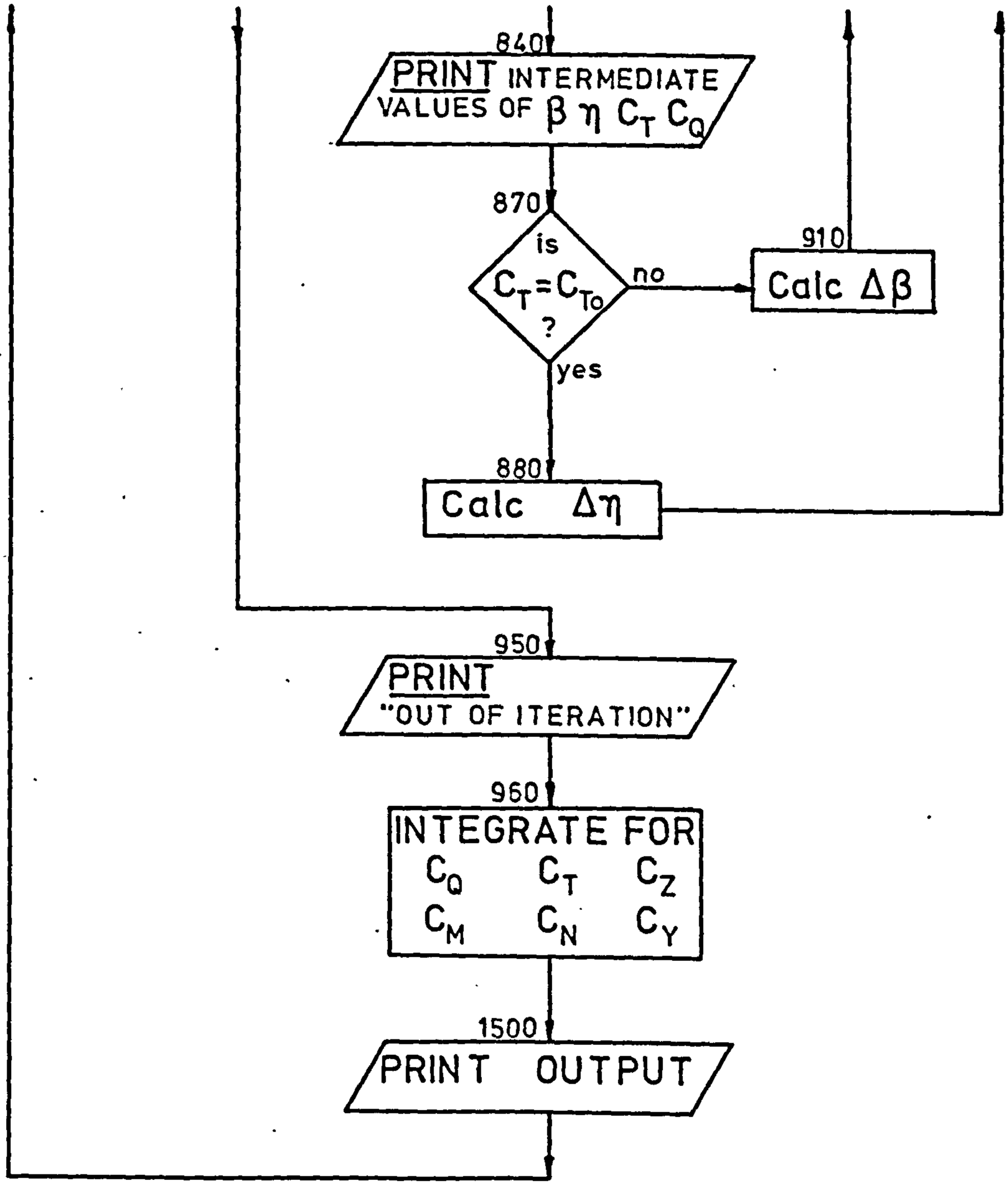
840
PRINT INTERMEDIATE VALUES OF β η C_T C_Q
870
is $C_T = C_{To}$?
no
910
Calc Δβ
yes
880
Calc Δη
950
PRINT "OUT OF ITERATION"
960
INTEGRATE FOR
C_Q C_T C_Z
C_M C_N C_Y
1500
PRINT OUTPUT

FIG A1 Cont.

```
10   PRINT "PROPELLER FORCE AND MOMENT PROGRAMME"
20   PRINT
30   PRINT "L        CL        P         VO        J         CP"
40   PRINT "CQ        CT        CZ        CM        CY        CN"
50   PRINT "QC        TC        ZC        MC        YC        NC"
60   PRINT "ETA       CT        a         a'        ALPHA     BETA 0"
70   PRINT "INPUT WEIGHT,POWER AND CL"
80   INPUT L,P,C
90   IF L=0 THEN 1600
100  V0=SQR(5.4835*L/C)
110  V1=.3216*L/V0
120  E=C/5
130  E2=ATN((V1*.96+V0*SIN(E))/(V1*.28+V0*COS(E)))
140  E1=E2-.0543
150  A2=V1/V0*SIN(E+.284)
160  J1=V0/240
170  P1=P*5.391E-04
180  INPUT B3,E3
190  D=.033
200  E9=E3
210  A=.637*E9*P1/J1↑3+A2
220  A1=.129*P1/(J1*(1+A))
230  E0=E3*(1-A1)/(1+A)
240  IF ABS((E9-E0)/E9)<.01 THEN 270
250  E9=E0
260  GOTO 210
270  REM ITERATION FOR CT AND BLADE SETTING ANGLE
280  B8=ATN(V0*(1+A)*COS(E1)/(754*(1-A1)))
290  FOR I=1 TO 51
300  T=.12566*(I-1)
310  FOR J=1 TO 17
320  X=.2+.05*(J-1)
330  X1=.56+X*COS(T)
340  X2=SQR(X1*X1+4)
350  E5=ATN(X1/2)
360  V1=2.01*L/(V0*X2*3)
370  E2=ATN((V1*COS(E5)+V0*SIN(E))/(V1*SIN(E5)+V0*COS(E)))
380  E1=E2-.0543
390  A2=V1/V0*SIN(E+E5)
400  A=.637*E9*P1/J1↑3+A2
410  B0=V0*(1+A)*COS(E1)
420  B1=754*(1-A1)*X+V0*(1+A)*SIN(E1)*SIN(T)
430  B2=ATN(B0/B1)
440  Z1=.01979*(J1*(1+A)*COS(E1)/SIN(B2))↑2
450  Z2=.19/X-.19+B3+B8-B2
460  Z3=SIN(B2)+D*COS(B2)
470  Z4=COS(B2)-D*SIN(B2)
480  Z5=.004*(2-X*1.35)
490  Z6=SQR(30.25-(10*X-4.5)↑2)+.7
500  DIM M[17,2]
510  M[J,1]=Z1*(Z6*Z2*Z4-Z5*SIN(B2))*2
520  M[J,2]=Z1*(Z6*Z2*Z3+Z5*COS(B2))*X
530  NEXT J
```

TABLE A1. Programme Listing

```
540   FOR K=1 TO 2
550   T7=T8=T9=0
560   T7=M[1,K]+M[17,K]
570   FOR J=1 TO 8
580   T8=T8+M[2*J,K]
590   NEXT J
600   FOR J=1 TO 7
610   T9=T9+M[2*J+1,K]
620   NEXT J
630   DIM N[51,2]
640   N[I,K]=(T7+4*T8+2*T9)/48
650   NEXT K
650   NEXT I
670   FOR K=1 TO 2
680   U1=U2=U3=0
690   U1=N[1,K]+N[51,K]
700   FOR J=1 TO 25
710   U2=U2+N[2*J,K]
720   NEXT J
730   FOR J=1 TO 24
740   U3=U3+N[2*J+1,K]
750   NEXT J
760   DIM S[2]
770   S[K]=(U1+4*U2+2*U3)/150
780   NEXT K
790   U9=E0*P1/J1
800   U0=P1/6.2832
810   Y1=(U9-S[1])/U9
820   Y2=(U0-S[2])/U0
830   IF ABS(Y1)<.01 AND ABS(Y2)<.01 THEN 950
840   PRINT B3,S[1],U9
850   PRINT D,S[2],U0
860   PRINT E3,E0,J1
870   IF ABS(Y1)>.01 THEN 910
880   E4=J1*S[1]/(6.2832*S[2])
890   E3=E3+(E4-E0)/2
900   GOTO 200
910   B3=B3+P1*Y1
920   PRINT
930   GOTO 290
940   REM INTEGRATION FOR FORCES AND MOMENTS
950   PRINT "OUT OF ITERATION"
960   FOR I=1 TO 51
970   T=.12566*(I-1)
980   FOR J=1 TO 17
990   X=.2+.05*(J-1)
1000   X1=.56+X*COS(T)
1010   X2=SQR(X1*X1+4)
1020   E5=ATN(X1/2)
1030   V1=2.01*L/(V0*X2*3)
1040   E2=ATN((V1*COS(E5)+V0*SIN(E))/(V1*SIN(E5)+V0*COS(E)))
1050   E1=E2-.0543
1060   A2=V1/V0*SIN(E+E5)
1070   A=.637*E9*P1/J1↑3+A2
```

TABLE A1. Continued

```
1080  B0=V0*(1+A)*COS(E1)
1090  B1=754*(1-A1)*X+V0*(1+A)*SIN(E1)*SIN(T)
1100  B2=ATN(B0/B1)
1110  Z1=.01979*(J1*(1+A)*COS(E1)/SIN(B2))↑2
1120  Z2=.19/X-.19+B3+B8-B2
1130  Z3=SIN(B2)+D*COS(B2)
1140  Z4=COS(B2)-D*SIN(B2)
1150  Z5=.004*(2-X*1.35)
1160  Z6=SQR(30.25-(10*X-4.5)↑2)+.7
1170  DIM F[17,6]
1180  F[J,1]=Z1*(Z6*Z2*Z3+Z5*COS(B2))*X
1190  F[J,2]=Z1*(Z6*Z2*Z4-Z5*SIN(B2))*2
1200  F[J,3]=Z1*(Z6*Z2*Z3+Z5*COS(B2))*2*SIN(T)
1210  F[J,4]=Z1*(Z6*Z2*Z4-Z5*SIN(B2))*X*COS(T)
1220  F[J,5]=Z1*(Z6*Z2*Z3+Z5*COS(B2))*2*COS(T)
1230  F[J,6]=Z1*(Z6*Z2*Z4-Z5*SIN(B2))*X*SIN(T)
1240  NEXT J
1250  FOR K=1 TO 6
1260  DIM G[51,6]
1270  T1=T2=T3=0
1280  T1=F[1,K]+F[17,K]
1290  FOR J=1 TO 8
1300  T2=T2+F[2*J,K]
1310  NEXT J
1320  FOR J=1 TO 7
1330  T3=T3+F[2*J+1,K]
1340  NEXT J
1350  G[I,K]=(T1+4*T2+2*T3)/48
1360  NEXT K
1370  NEXT I
1380  DIM H[6]
1390  FOR K=1 TO 6
1400  T4=T5=T6=0
1410  T4=G[1,K]+G[51,K]
1420  FOR J=1 TO 25
1430  T5=T5+G[2*J,K]
1440  NEXT J
1450  FOR J=1 TO 24
1460  T6=T6+G[2*J+1,K]
1470  NEXT J
1480  H[K]=(T4+4*T5+2*T6)/150
1490  NEXT K
1500  REM OUTPUT
1510  R=2/(J1*J1)
1520  PRINT L;C;P;V0;J1;P1
1530  PRINT H[1];H[2];H[3];H[4];H[5];H[6]
1540  PRINT H[1]*R;H[2]*R;H[3]*R;H[4]*R;H[5]*R;H[6]*R
1550  PRINT E0;U9;A;A1;E1*57296.;B3
1560  PRINT
1570  PRINT
1580  PRINT "NEXT CASE"
1590  GOTO 80
1600  END
```

TABLE A1. Concluded

PART II

Section 4

The Influence of Running Propellers on Low Speed Longitudinal Static Stability Trim Curves

Cranfield Report Aero No.34.

Cranfield Report Aero No.34

APRIL, 1977

CRANFIELD INSTITUTE OF TECHNOLOGY

The Influence of Running Propellers on Low Speed Longitudinal Static Stability Trim Curves

by

M.E. ESHELBY

Aerodynamics Division
College of Aeronautics

SUMMARY

The influence of running propellers on aircraft handling qualities has been known to be of considerable importance but until good estimates of the propeller performance operating under real flight conditions became available it was not possible to determine adequately the propeller contribution to the aircraft pitching moment and lift equations. In Ref.1 the thrust and normal force characteristics of a propeller were calculated for a particular aircraft as functions of engine power and flight conditions and in this report the findings are used to calculate the propeller contribution to the longitudinal static stability trim curves from which the handling qualities are assessed.

It is seen that the propeller can be considered to be similar to a canard wing producing a general destabilisation. The effect becomes more severe as speed is reduced and as power is increased leading to a deterioration of the handling qualities as the power on stall is approached. The analysis shows that the propeller characteristics calculated in Ref.1 are capable of accounting for these effects to a considerable degree and confirm that the propeller performance is being reasonably predicted.

The correction of the controls fixed neutral points to a propeller off condition shows that the propellers produce up to 3% chord forward shift of neutral point in the case considered. The controls free stability is not considered in detail as the control force data was not sufficiently reliable for the propeller effects to be separated.

CONTENTS

NOTATION

a	Lift curve slope of complete aircraft
a_1, a_2, a_3	Lift parameters of tailplane, elevator and elevator tab respectively.
C_L	Lift Coefficient
C_{LA}	Lift Coefficient, Aerodynamic (see eqn.4)
C_M	Pitching moment coefficient
$\bar{c}$	Mean aerodynamic chord (m.a.c.)
D	Propeller diameter
e	NASA span efficiency factor
h	C.G.position aft of L.E. of m.a.c.
h_0	Aerodynamic centre position aft of L.E. of m.a.c.
K_1	Normal force function (see eqn.6)
L	Lift
M	Pitching moment
N	Number of propellers
S	Wing Area
T	Thrust
T_c, C_T	Thrust coefficients (see P.2)
V	True airspeed
W	Weight
$\bar{x}$, $\bar{z}$	Propeller coordinates relative to L.E. of m.a.c.
x, z	Coordinates relative to C.G.
Z	Normal Force
Z_c, C_z	Normal Force coefficients (see p.2.)

NOTATION

α	Incidence
β	Elevator tab angle
γ	Flight path gradient
δ	Propeller thrust line inclination to m.a.c.
ρ	Air density
η	Elevator angle

Subscripts

C.G.	Relative to C.G.
o	Propellers off
p	Due to propeller, or propellers on
T	Tail

1. Introduction

The classical theory of static stability which is usually used as a measure of the handling qualities of the aircraft in a longitudinal sense does not contain any contribution due to the propellers. This omission is made on the assumption that the propeller effects are negligible and is reasonable providing that the propeller thrust line is not significantly displaced from the aircraft C.G. and that the propeller axis is closely aligned with the incident airflow. If however the propeller axis is at incidence with respect to the local flow direction the propeller will produce a force normal to its thrust axis in the pitching plane of the aircraft. As the aircraft changes speed, or C_l, its incidence will vary and so therefore will the incidence of the propeller to the local flow; this implies that a propeller normal force will exist and that it will be a function of C_l. The effect of the force will be to modify the pitching moment equation on which the assumed handling characteristics are based and therefore there will be a discrepancy between the predicted and observed handling qualities of the aircraft due to the power effects of the propellers.

The action of the propeller operating at incidence to the local airflow was considered in Ref.1 and characteristics of thrust and normal force were developed for a particular aircraft-propeller-engine combination. This showed that a very substantial normal force could be expected to occur and that it could be related to the engine shaft power and the flight lift coefficient. Having established the propeller characteristics as a function of the flight conditions it is now possible to include them in the static stability theory and to develop an expression for a correction to the simple classical theory to allow for the direct effects of the running propellers.

2. The Effect of the Propeller on the Longitudinal Trim of The Aircraft.

Since the propeller develops a normal force as well as a thrust force there will be two effects of the aircraft. Firstly there will be a normal contribution to the lift equation which will modify the apparent flight lift coefficient and, secondly the propeller will generate a pitching moment about the C.G. The influence of each of these on the longitudinal trim can be considered separately.

2.1 Propeller Contribution to Lift.

The flight lift coefficient C_L is considered to be given by the non-dimensionalised gross lift, L, of the aircraft normal to the flight path, thus

$$C_L = \frac{L}{\frac{1}{2}\rho V^2 S} \qquad (1)$$

where $L = W \cos \gamma$

and γ is the flight path gradient.

Now considering the forces acting normal to the flight path., fig 1

$$L = L_W + L_T + \{ Z \cos \alpha_p + T \sin \alpha_p \} N \qquad (2)$$

and parallel to the flight path

$$W \sin \gamma = D + \{ Z \sin \alpha_p - T \cos \alpha_p \} N \qquad (3)$$

where N is the number of propellers.

In steady flight equation 3 is balanced and the net force in the direction of flight is zero, thus speed is constant. Also for small values of γ (šay less than 10^0) the effect of γ is negligible and the lift can be assumed to equal the weight.

Non-dimensionalising eqn 2 gives

$$C_L = C_{L_W} + C_{L_T} \frac{ST}{S} + \{ Z_C \cos \alpha_p + T_C \sin \alpha_p \} \frac{ND^2}{S}$$

where $Z_C = Z/\frac{1}{2}\rho V^2 D^2$ and $T_C = T/\frac{1}{2}\rho V^2 D^2$

These coefficients should be compared with the non-dimensional coefficient based on the propeller characteristics used in ref 1.

$$C_Z = Z/\rho n^2 D^4 \quad \text{and} \quad C_T = T/\rho n^2 D^4$$

Thus $$Z_C = C_Z \cdot \frac{\rho n^2 D^4}{\frac{1}{2}\rho V^2 D^2} = \frac{2C_Z}{J^2}$$

and similarly $T_C = \frac{2\,C_T}{J^2}$

where J is the advance ratio V/nD

The wing and tail lift contributions can be combined into an aircraft lift coefficient, C_{LA}, corresponding to the aerodynamic lift generated by the aircraft. Thus the apparent flight lift coefficient C_L, is given by the sum of the propeller normal force and the aerodynamic lift,

$$C_L = C_{LA} + \{ Z_c \cos \alpha_p + T_c \sin \alpha_p \} \frac{D^2 N}{S} \qquad (4)$$

the value of C_{LA} being the effective lift contribution of the airframe to the lift equation.

Since only the overall lift can be measured in flight a correction to the flight lift coefficient to allow for the power contribution must be made. From equation (4) the effective lift contribution can be expressed as

$$C_{LA} = C_L - \{ Z_c \cos \alpha_p + T_c \sin \alpha_p \} \frac{D^2 N}{S} \qquad (5)$$

or, more conveniently, in the form

$$C_{L_A} = C_L - K_1 \tag{6}$$

where $$K_1 = \{Z_c \cos \alpha_p + T_c \sin \alpha_p\} \frac{D^2N}{S} \tag{7}$$

K_1 thus represents the modification of the lift equation due to the propeller and is a function of aircraft incidence and engine power.

2.2 Propeller Contribution to Pitching Moment

The propeller is generally situated at some distance from the aircraft C.G. and the forces generated by the propeller will produce a pitching moment about the C.G. From Fig.2 a general expression for the pitching moment due to the propeller, C_{M_P}, can be found.

The propeller is considered fixed relative to the mean aerodynamic chord (m.a.c.) at a distance $\bar{x}\,\bar{c}$ ahead of the leading edge and $\bar{z}\,\bar{c}$ above the m.a.c. with the thrust line inclined at some angle δ to the m.a.c. If the C.G. in $h\,\bar{c}$ behind the leading edge and $z\,\bar{c}$ above the m.a.c. then the propeller coordinates $(x_p\bar{c}, z_p\bar{c})$ relative to the C.G. will be given by

$$x_p = (\bar{x} + h) \cos \delta + (z - \bar{z}) \sin \delta \tag{8}$$

and $$z_p = (z - \bar{z}) \cos \delta - (\bar{x} + h) \sin \delta$$

Since the relative geometry of the propeller to the C.G. is fixed these coordinates will be independent of incidence.

The pitching moment due to the propeller M_{PCG} can therefore be expressed as

$$M_{PCG} = M_p + Tz_p\bar{c} + Zx_p\bar{c} \tag{9}$$

where M_p is the propeller direct pitching moment.

Non-dimensionalising equation (9) the pitching moment coefficient in terms of the aircraft wing area is given by

$$C_{mp} = M_c \frac{D^3N}{S\bar{c}} + \{T_c z_p + Z_c x_p\} \frac{D^2N}{S} \tag{10}$$

where M_c T_c and Z_c are the direct pitching moment, thrust and normal force coefficients of the propeller respectively and N the number of propellers.

The pitching moment coefficient due to the propeller about the C.G., C_{mp}, can now be included in the general pitching moment equation for the aircraft.

2.3 The Pitching Moment Equation including Propeller Effects

In its simplest form the pitching moment equation of an aircraft without propellers can be written,

$$C_{m_{CG}} = C_{m_o} + C_L (h - h_o) - \bar{V} \left\{ \frac{a_1}{a} C_L \left(1 - \frac{d\epsilon}{d\alpha}\right) + a_1 i_T + a_2 \eta + a_3 \beta \right\} \quad (11)$$

and the controls fixed static margin is given by differentiating with respect to C_L, assuming that η and β (and i_T) are constants, thus the propellers off static margin is given by

$$\left[\frac{dC_m}{dC_L}\right]_o = (h - h_o) - \bar{V} \frac{a_1}{a} \left(1 - \frac{d\epsilon}{d\alpha}\right) \quad (12)$$

With propellers on the additional terms from eqns (6) and (10) are included and the pitching moment equation becomes

$$C_{MC_G} = C_{M_0} + C_{M_P} + (C_L - K_1)(h - h_o) - \bar{V} \left\{ \frac{a_1}{a} (C_L - K_1)\left(1 - \frac{d\epsilon}{d\alpha}\right) + a_1 i_T + a_2 \eta + a_3 \beta \right\} \quad (13)$$

and the controls fixed static margin, propellers on, will be given by

$$\left[\frac{dC_m}{dC_L}\right]_p = \frac{dC_{mp}}{dC_L} + \left(1 - \frac{dK_1}{dC_L}\right) \left\{ (h - h_o) - \bar{V} \frac{a_1}{a} \left(1 - \frac{d\epsilon}{d\alpha}\right) \right\} \quad (14)$$

Comparing 12) and 14) gives the contribution to the static margin due to the propeller effects,

$$\Delta\left[\frac{dC_m}{dC_L}\right]_p = \left[\frac{dC_m}{dC_L}\right]_p - \left[\frac{dC_m}{dC_L}\right]_o = \left[\frac{dC_{mp}}{dC_L}\right] - \frac{dK_1}{dC_L} \left[\frac{dC_m}{dC_L}\right]_o \quad (15)$$

From equations 6) and 10) both C_{mp} and K_1 are functions of C_L and engine shaft power, therefore the conditions of flight under which the differentiation of 13) is performed must be established.

During the flight trials the engine was maintained at a constant shaft power by maintaining constant inlet manifold pressure and engine speed, thus the power coefficient, $C_p = P/\rho n^3 D^5$, was held constant. The lift coefficient was varied by changing the flight speed, V. Since the power was held constant and the speed varied the flight path angle γ would not be constant since a rate of climb or descent would be necessary in general to balance the drag, equation 3, and maintain constant speed. However the value of γ would normally be small, less than 10^0, and the effect on the lift equation can be considered negligible. In ref 1 the calculation of the propeller forces and moments was made on the assumption that the aircraft was flying at a constant power and a steady speed corresponding to a specified C_L and weight.

From eqn 15) the propeller produces two contributions to the static margin, a direct effect, $\frac{dC_{mP}}{dC_L}$, and an indirect effect due to the modification of the lift coefficient. The indirect effect is proportional to the static margin, propellers off, and thus the overall effect is a function of the static margin of the aircraft power off.

Since the static margin is measured in terms of the slope of the trim curves of elevator angle to trim, $\bar{n}$, (controls fixed) or elevator hinge moment to trim, C_H, (controls free) the propeller contribution can be expressed in terms of a correction to the trim curve slope,

Controls fixed

$$\Delta \left[\frac{d\bar{n}}{dC_L}\right]_P = \frac{1}{\bar{V}a_2}\left[\frac{dC_{m_P}}{dC_L}\right] - \frac{dK_1}{dC_L}\left[\frac{d\bar{n}}{dC_L}\right]_0 \qquad (16)$$

or, controls free

$$\Delta \left[\frac{dC_H}{dC_L}\right]_P = \frac{b_2}{\bar{V}a_2}\left[\frac{dC_{m_P}}{dC_L}\right] - \frac{dK_1}{dC_L}\left[\frac{dC_H}{dC_L}\right]_0 \qquad (16a)$$

Alternatively for the purpose of assessing the contribution of the propeller to measured values of the trim curves of an aircraft the measured value of the static margin with propellers on, $\left[\frac{dC_m}{dC_L}\right]_P$ can be corrected to give the propellers off value, $\left[\frac{dC_m}{dC_L}\right]_0$ from eqn 15).

$$\left[\frac{dCm}{dCL}\right]_0 = \left\{\left[\frac{dCm}{dC_L}\right]_P - \frac{dCmp}{dC_L}\right\}\left(1 - \frac{dK_1}{dC_L}\right)^{-1} \qquad (17)$$

This can also be expressed in terms of the controls fixed and controls free trim curve slopes,

Controls fixed,

$$\left[\frac{d\bar{n}}{dC_L}\right]_0 = \left\{\left[\frac{d\bar{n}}{dC_L}\right]_P - \frac{1}{\bar{V}a_2}\left[\frac{dCmp}{dC_L}\right]\right\}\left(1 - \frac{dK_1}{dC_L}\right)^{-1} \qquad (18)$$

and controls free,

$$\left[\frac{dC_H}{dC_L}\right]_0 = \left\{\left[\frac{dC_H}{dC_L}\right]_P - \frac{b_2}{\bar{V}a_2}\left[\frac{dCmp}{dC_L}\right]\right\}\left(1 - \frac{dK_1}{dC_L}\right)^{-1} \qquad (18a)$$

3. Contribution of the Propeller Effect to Longitudinal Handling Qualities

The analysis of the operation of a propeller under flight conditions, ref.1, has produced characteristics of thrust, normal force and pitching moment as functions of shaft power and aircraft lift coefficient, fig.3. These characteristics can be used to calculate the corrections to the static stability trim curve slopes to account for the effects of the propeller on the longitudinal trim of the aircraft.

The aircraft used for the flight trials was a Piper Twin Comanche 'A' series light aircraft described in APP A1. The aircraft is powered by two Lycoming IO-360-C engines each rated at 160 S.H.P. and driving Hartzell HCE-2YL-2B constant speed propellers, the engines were not counter-rotating.

The flight trials consisted of a series of steady speed trims through the speed range of the aircraft whilst maintaining a constant engine shaft power. The power was maintained constant by holding a constant value of manifold inlet pressure at a given engine speed governed by the propeller. At each trim condition the elevator angle to trim was measured and used to construct the trim curves, figs.7 to 10, of elevator angle to trim against flight lift coefficient. Each trim curve is based on a constant power condition. Since from ref.1 the propeller forces and moments are calculated at constant power as functions of advance ratio then the calculated propeller performance is compatible with the flight trials data since both advance ratio and lift coefficient are functions of incidence for a given aircraft weight. The trim curve slopes therefore correspond to the differentiation of the pitching moment equation at constant power.

The measured trim curves are shown in figs 7 to 10; two C.G. positions were used to enable an estimate of the neutral points to be made, and corrections for propeller effect are applied to each trim curve.

In eqn 15) it was shown that the propeller contribution consisted of a direct and an indirect effect on the static stability. The direct effect, due to the pitching moment, is shown in fig 4. Fundamentally the corrections to the forward and aft C.G. cases are of similar form but the shift caused to the longitudinal trim varies with power and is more marked at aft C.G. since the propeller moment arm about the C.G. is larger. The shift is due to the ratio between the thrust and normal force coefficients which varies with power. As power increases so the incidence at which zero propeller pitching moment occurs also increases causing the intercept of the curve with the C_L axis to vary as a function of power. The shape of the curves shows an inflection with a minimum slope at about $C_L = 0.6$, at higher speed the slope increases in approximate proportion to C_L and at lower speeds the slope varies as a function of power, fig.5. At low powers the slope continues to decrease (38 S.H.P.) as C_L increases but as power increases the slope, dC_{mp}/dC_L, becomes constant (65 S.H.P.) and then increases (100, 120 S.H.P.). This indicates that the propeller is generally destabilising at all speeds since dC_{mp}/dC_L is positive but the tendency is towards increased destabilisation at high

speed, (an incidence effect), and at low speeds (a combined incidence and power effect).

The indirect propeller effect is dependant on the static margin of the aircraft with propellers off and a component of the propeller force in lift, eqn.15). The lift contribution K_1, eqn.7, is a function of incidence and is shown in fig 6 for the aircraft considered. K_1 increases with C_L and power and the slope, dK_1/dC_L, is a linear function of C_L increasing with power. This produces an increasing contribution to the static stability as incidence increases and the contribution, which is destabilising, is proportional to the static margin propellers off. Thus its effect is more strongly felt at forward C.G.

Summing the two corrections they can be applied to the measured trim curve slopes to show the contribution to the static stability due to the propellers. Figs 7 to 10 show the measured trim curves at four constant power settings. The trim curves are constructed from the flight measured data and the trim curve slopes, propellers on, are measured from the trim curves. Using the measured trim curve slope, propellers on, together with propeller contributions the propellers off trim curve slopes can be estimated. These are shown at each constant power condition for comparison with the propellers on data.

The propellers are generally destabilising and the degree of destabilisation is a function of power, C.G. position and incidence. At low power (38 S.H.P. Fig.7) the propellers reduce the trim curve slope by approximately 0.3^o per C_L at high speed, $C_L = 0.2$ and by about 0.2^o per C_L at low speed, $C_L = 1.2$, with a slightly larger effect at forward C.G. compared to the aft C.G. As power increases the destabilising effect of the propeller increases and at high power (120 S.H.P., fig.10) the reduction of trim curve slope varies from about 0.3^o per C_L at high speed to 0.6^o per C_L at low speed, again the effect at forward C.G. is slightly larger.

By comparing the propeller off trim curve slopes at each power it can be seen that the curves now become very much closer to each other than the propellers on cases, fig.11. This indicates the degree to which the effects of power have been eliminated from the aircraft. At the higher powers, 65 S.H.P. and above, the correction is very nearly complete but at low power, 38 S.H.P., there is still a discrepancy between the curves although very much reduced. It is possible that at the low powers the engine power estimation may not be very accurate since the engine manufacturers power curves which were used to estimate the power had to be extrapolated to reach the low power conditions. Also the engine speed could not always be maintained at low forward speeds and the power may therefore have been over-estimated under these flight conditions.

One of the primary purposes of trim curve data is the prediction of neutral points by extrapolating the trim curve slope change with C.G. shift to determine the point at which the static stability becomes neutral. Fig.12 shows the predicted neutral points, controls fixed, for the aircraft propellers on and propellers off at each power condition. With propellers on there is a considerable variation of neutral point with power and a tendency for the neutral point to shift forward as C_L increases by up to 3% chord. Change in power also varies

the neutral point by about 2% at low speed. The propellers off neutral points are less scattered, generally within about 1% chord at low speed and the forward shift with C_L is reduced to about half the shift with propellers on. This gives a much more consistent prediction of neutral points although some power and incidence effects are still present.

Only controls fixed static stability has been considered since the controls free data relating to control forces was very scattered. This is thought to be due to friction in the control circuit which was holding considerable hinge moment at the elevator and making the control load measurement unreliable.

4. Conclusions

The application of the analysis of the propeller force system to the aircraft has shown that it is capable of accounting for a large proportion of the power effects on the static stability of the aircraft by correcting the measured trim curve data to a propellers off condition. The residue of the correction is probably due to slipstream interference with the wing and tail, this is considered in part in ref. 2.

The propeller has produced a general destabilisation throughout the operating speed range of the aircraft, this is analagous to a fixed canard surface at the propeller position and can be compared with the propeller "fin-effect" which is considered in asymmetic flight. The canard effect increases as speed decreases towards the stall and will cause a deterioration of the aircraft handling qualities which may lead to handling difficulties in an already difficult situation.

The parameters which most significantly affect the propeller contribution are the propeller incidence to the local flow direction and the propeller moment arm about the C.G. The moment arm will determine the magnitude of the "canard effect" whilst the incidence will determine the variation of its magnitude with C_L. These considerations are important in the case of modern light aircraft because of the tendency towards long engine nacelles. Aesthetic design in this respect could provide a source of reduced stability.

REFERENCES

1. ESHELBY M.E. — An Analysis of the Force System of a Propeller Cranfield Report Aero No.33 1977

2 ESHELBY M.E. — The Effect of Propeller Slipstream on Longitudinal Static Stability Trim Curves. Cranfield Report Aero No.32 1976

3 ESHELBY M.E. — An Instrumentation System to Measure the Stability Characteristics of Light Aircraft. Cranfield Aero Memo No.101

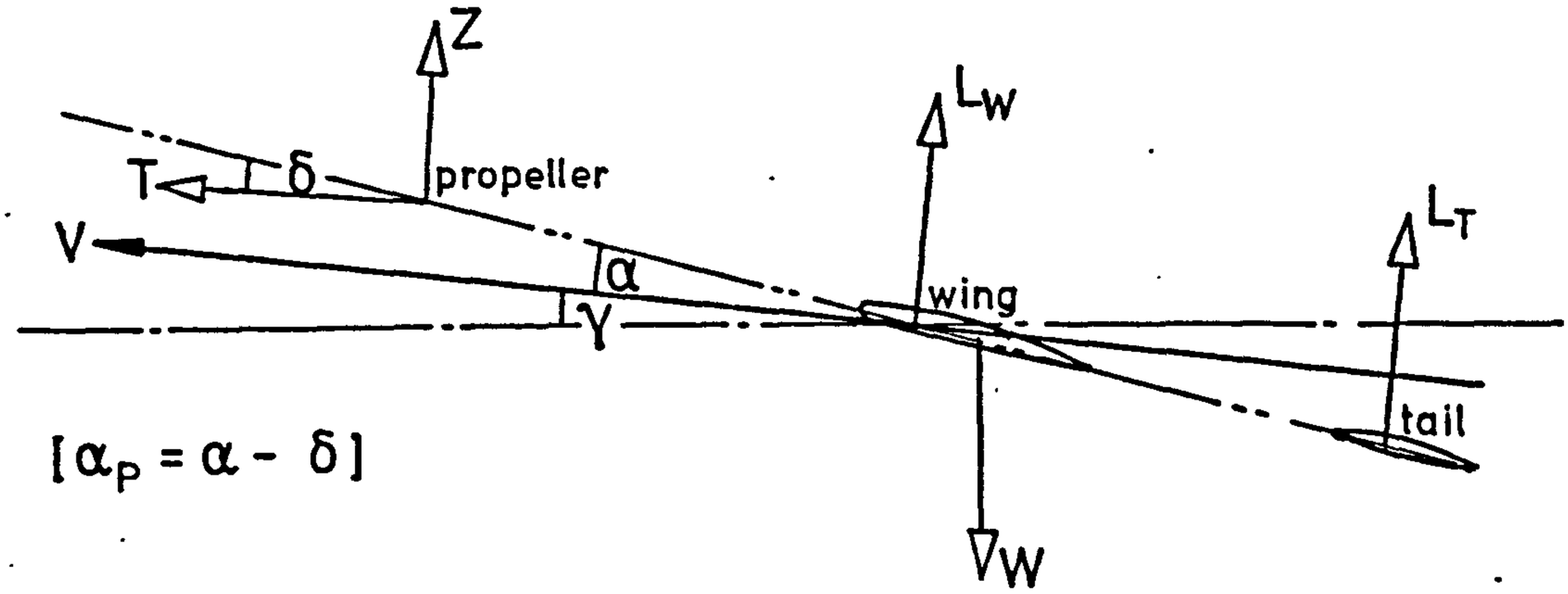

FIG.1. Aircraft Configuration.

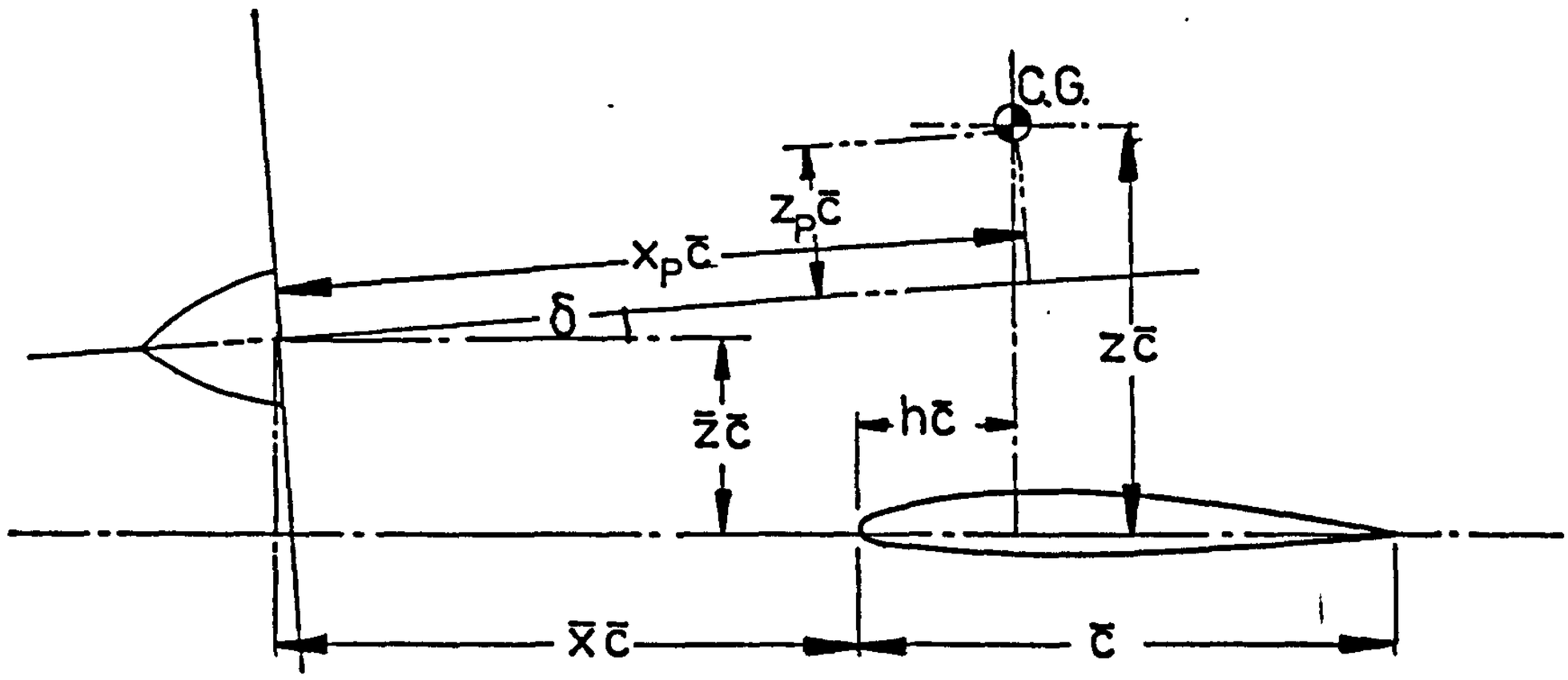

FIG 2 Propeller Moment Arm.

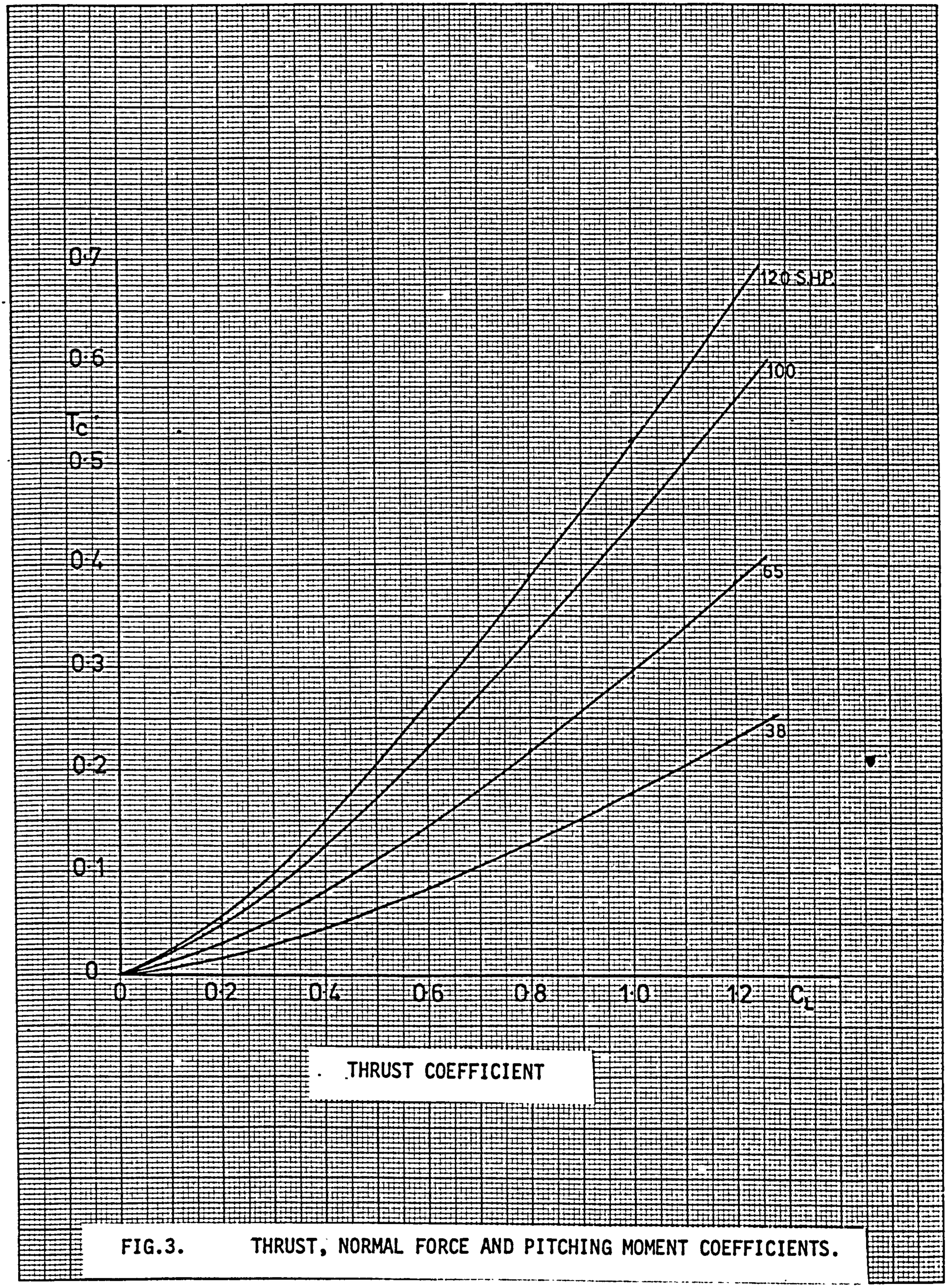

FIG.3. THRUST, NORMAL FORCE AND PITCHING MOMENT COEFFICIENTS.

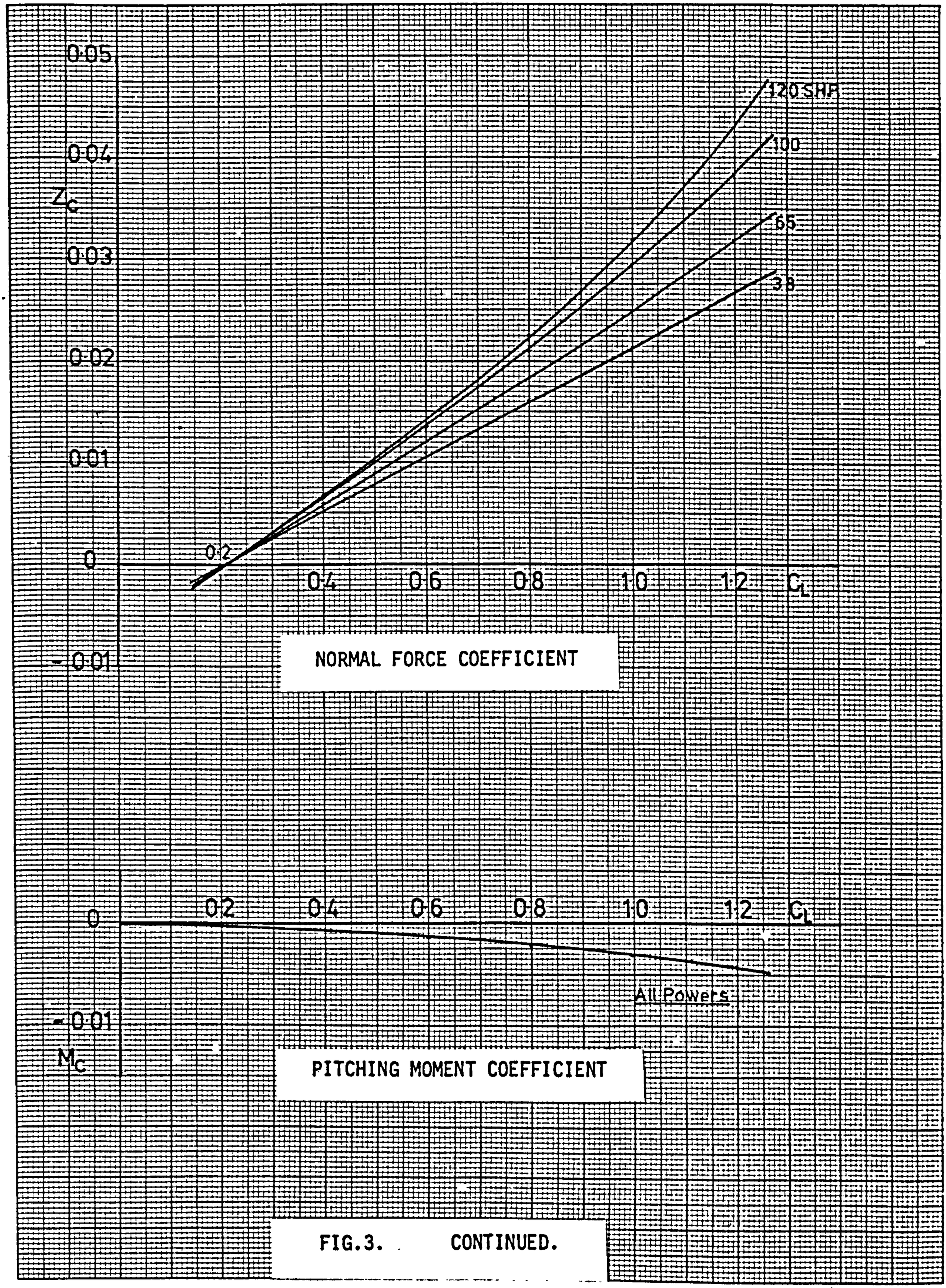

FIG.3. CONTINUED.

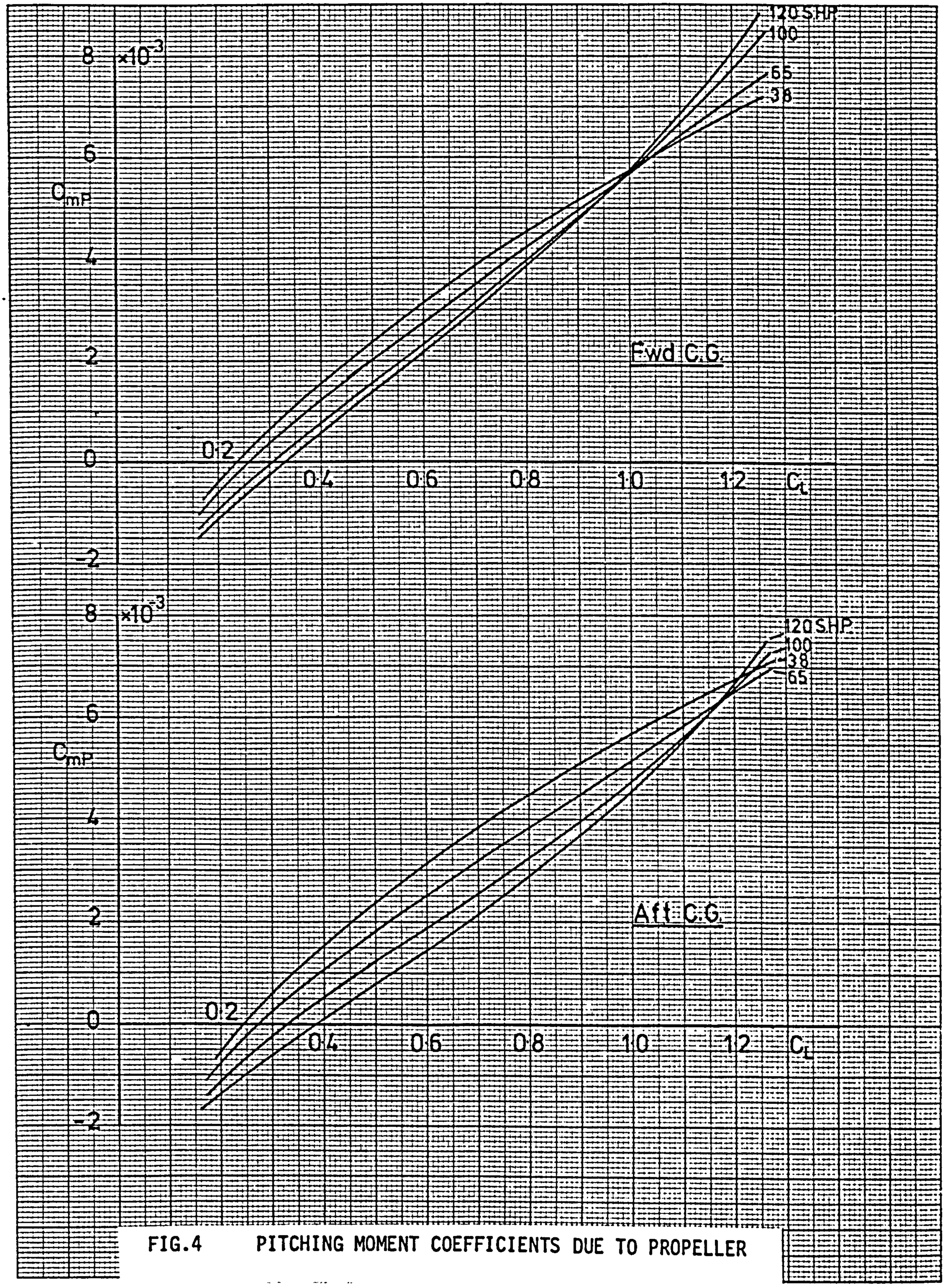

FIG.4 PITCHING MOMENT COEFFICIENTS DUE TO PROPELLER

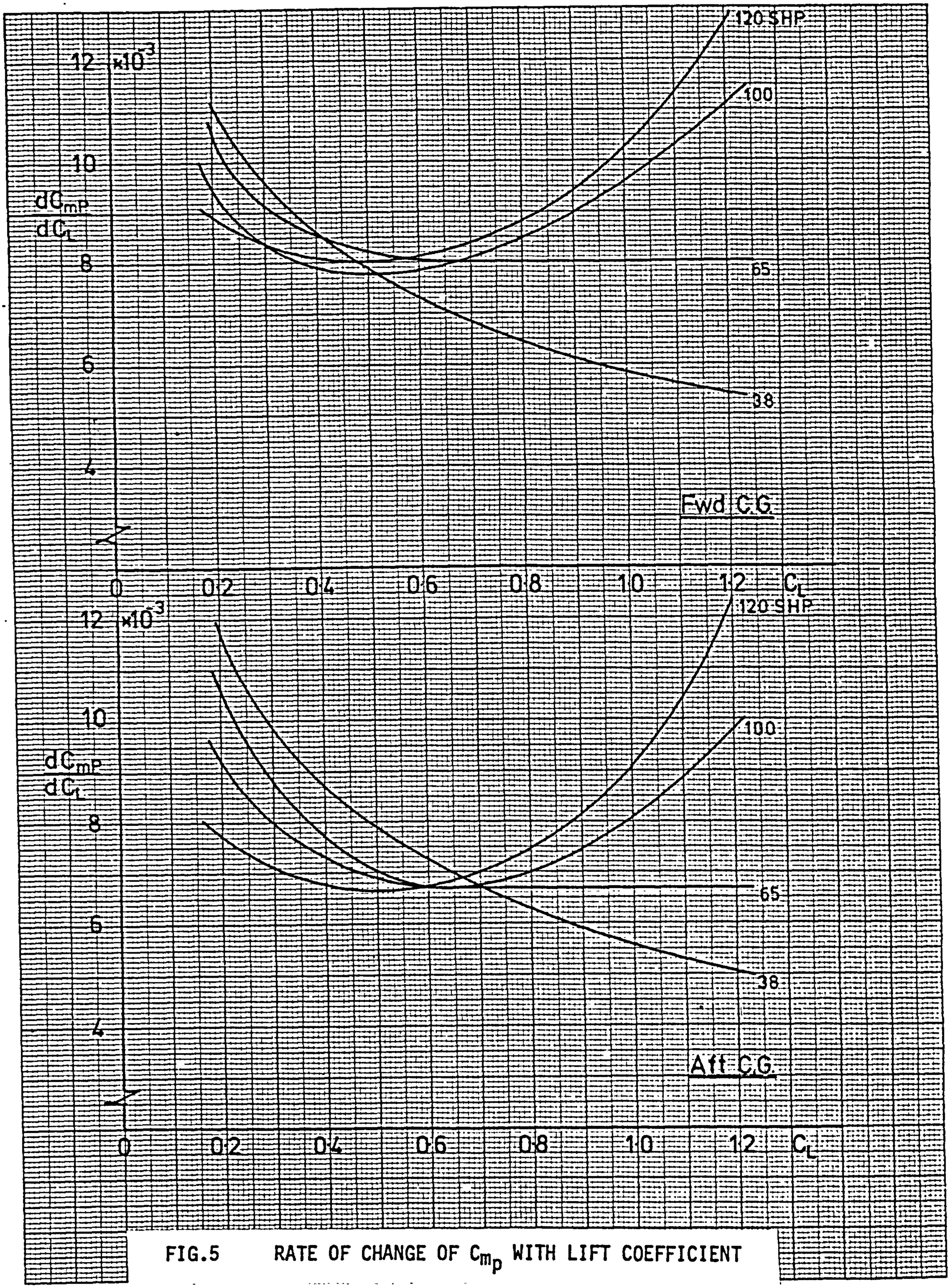

FIG.5 RATE OF CHANGE OF C_{m_p} WITH LIFT COEFFICIENT

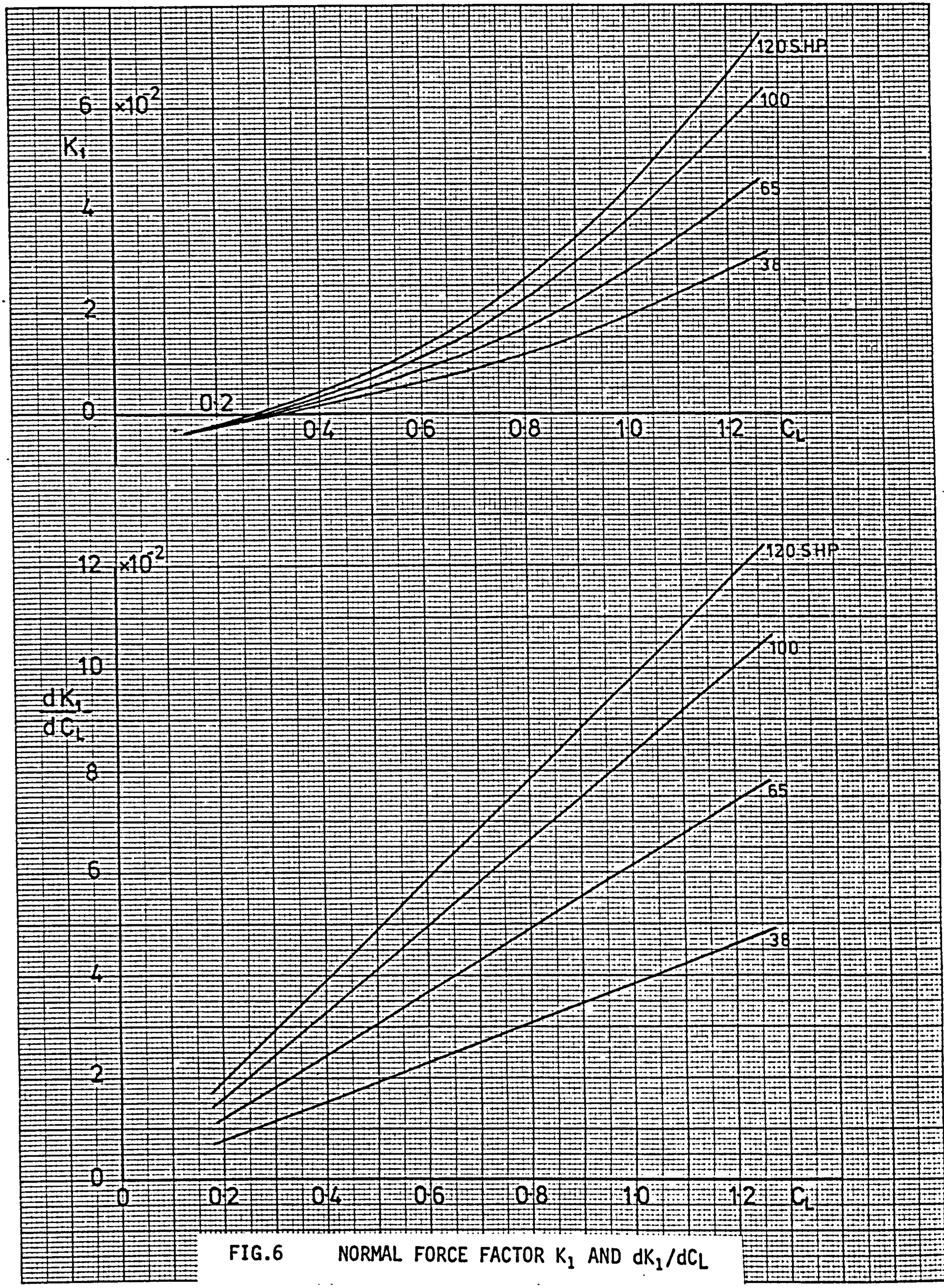

FIG.6 NORMAL FORCE FACTOR K_1 AND dK_1/dC_L

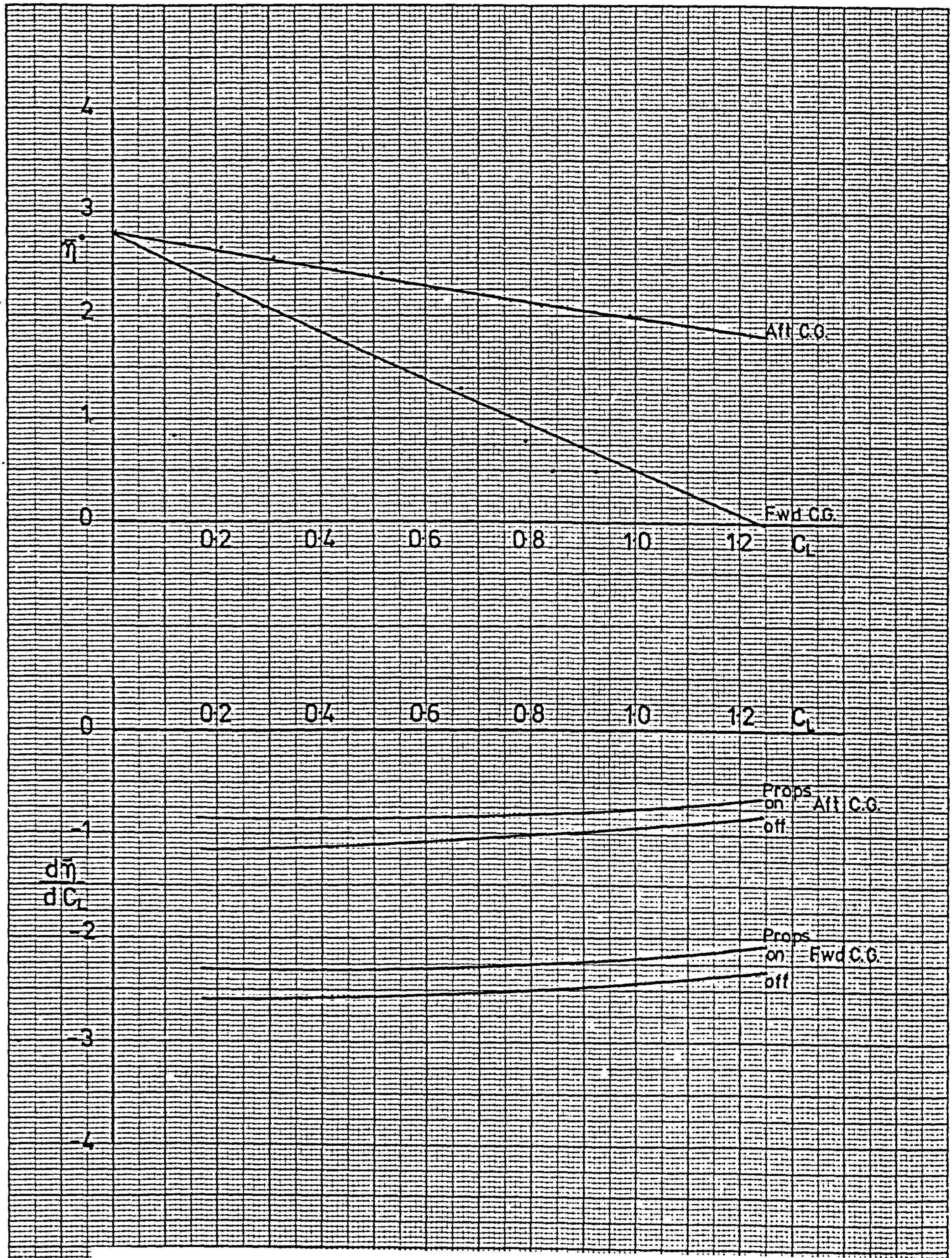

FIG.7. TRIM CURVES, CONTROLS FIXED, 38 S.H.P. (10"/2400 R.P.M.)

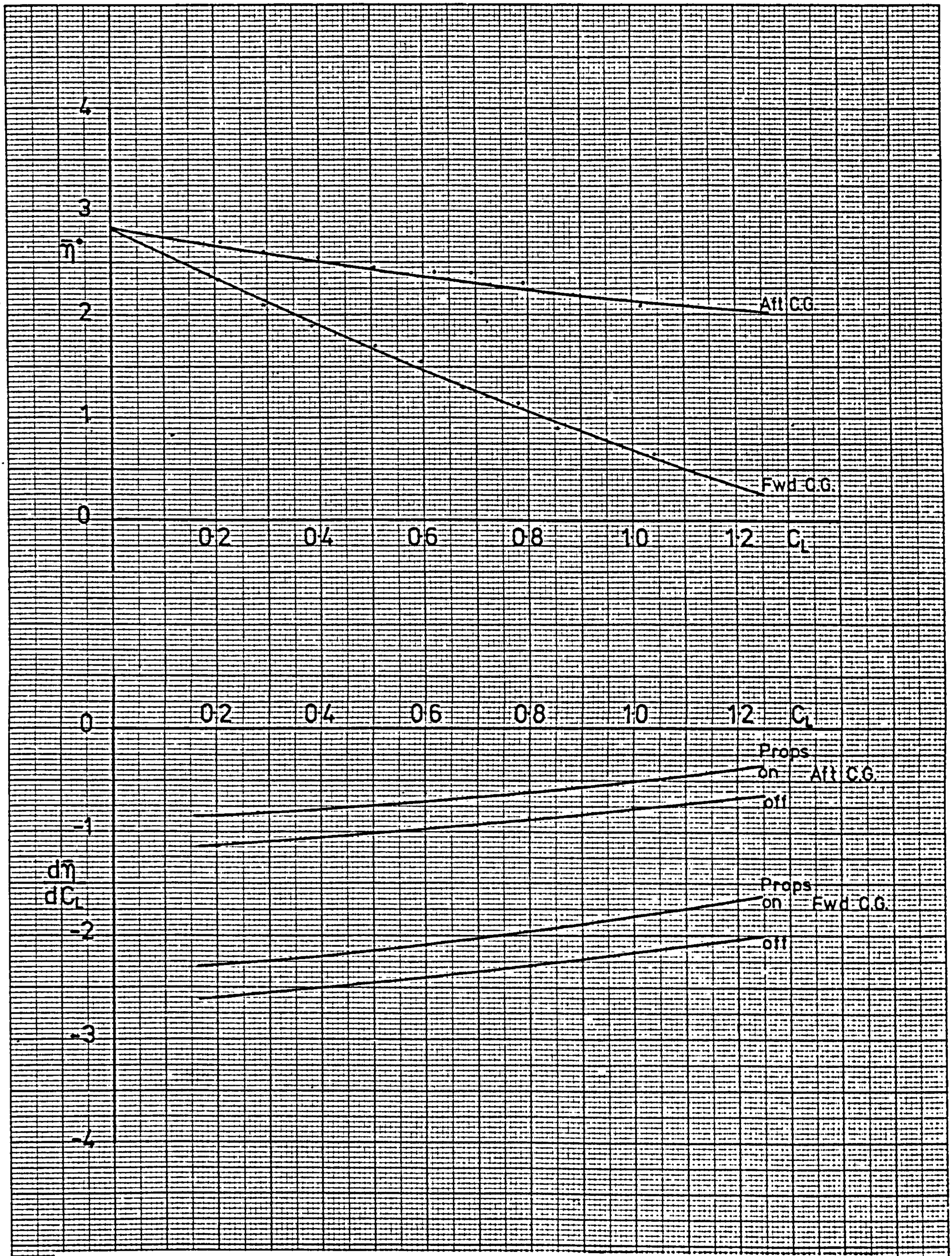

FIG.8. TRIM CURVES, CONTROLS FIXED, 65 S.H.P. (15"/2400 R.P.M.)

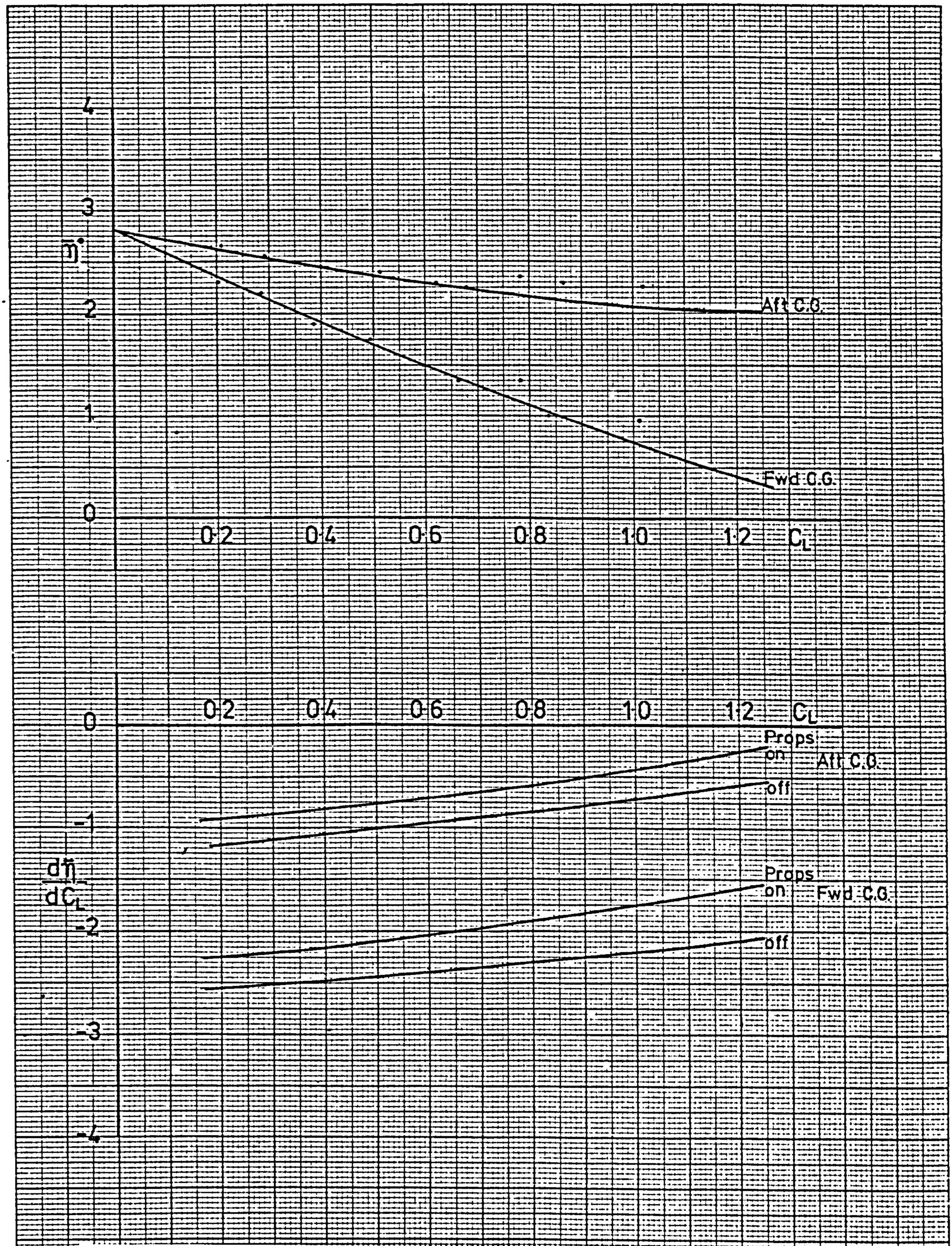

FIG.9. TRIM CURVES, CONTROLS FIXED, 100 S.H.P. (20"/2400 R.P.M.)

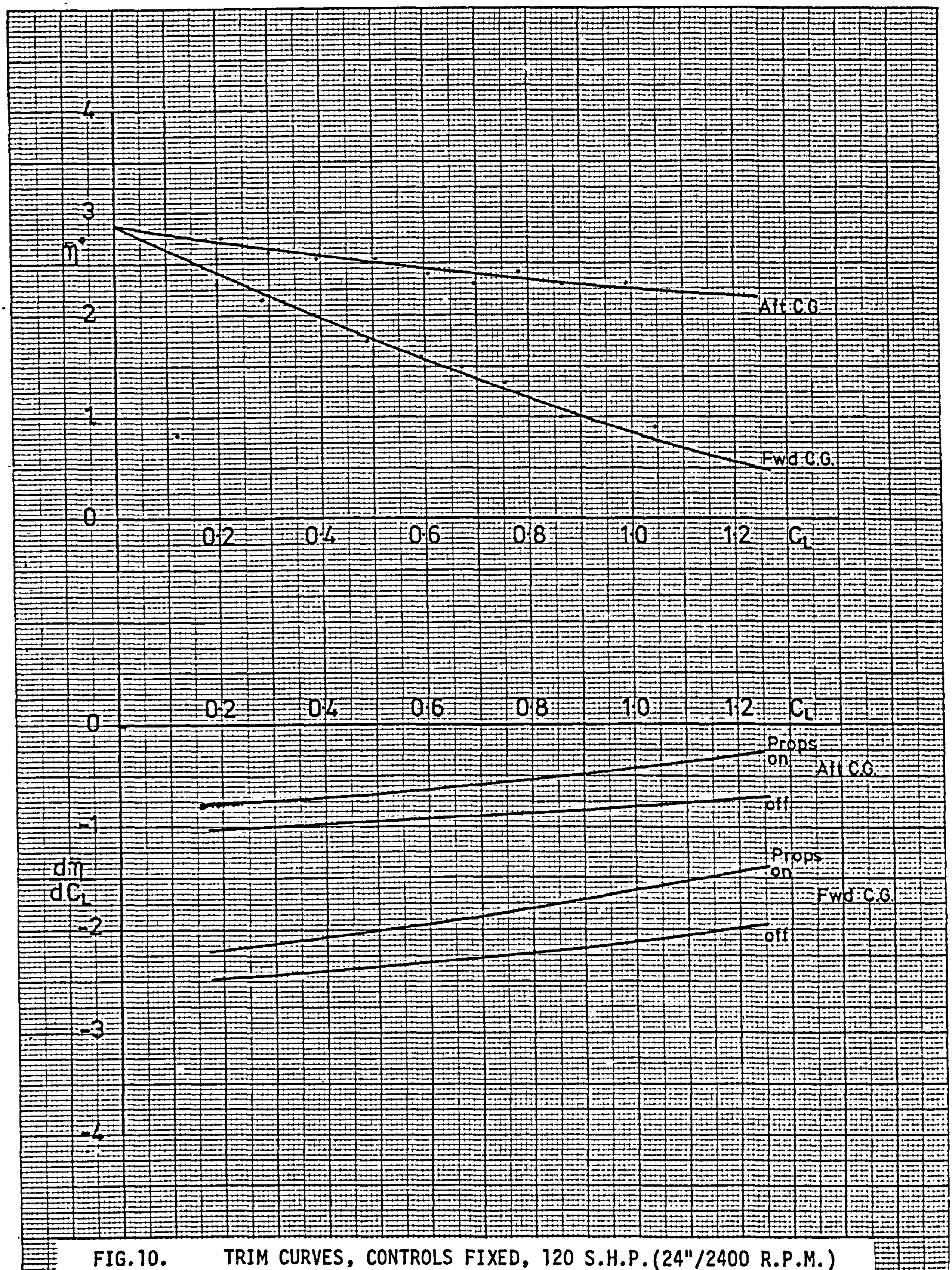

FIG.10. TRIM CURVES, CONTROLS FIXED, 120 S.H.P.(24"/2400 R.P.M.)

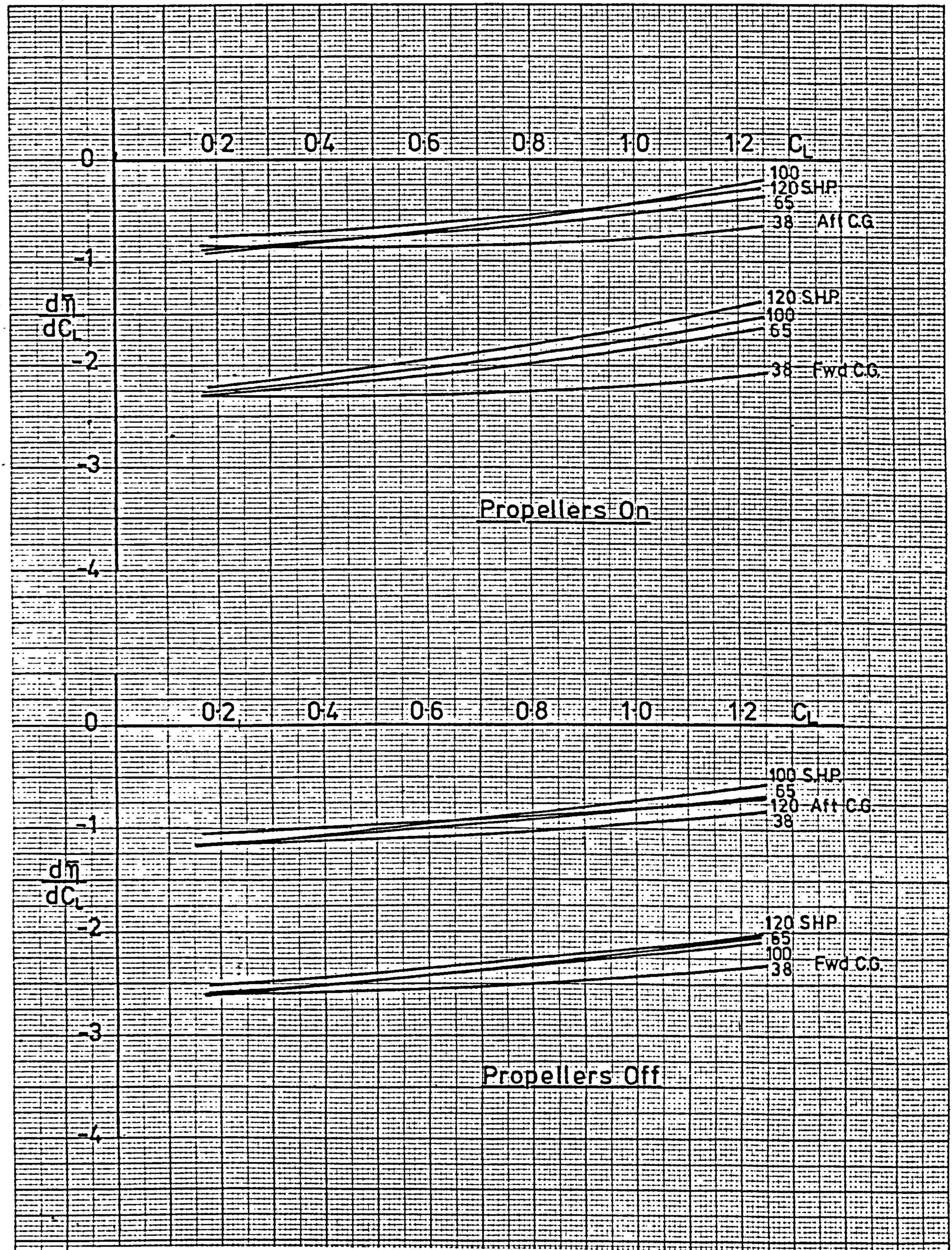

FIG.11. TRIM CURVE CLOPES, CONTROLS FIXED, PROPELLERS ON AND OFF

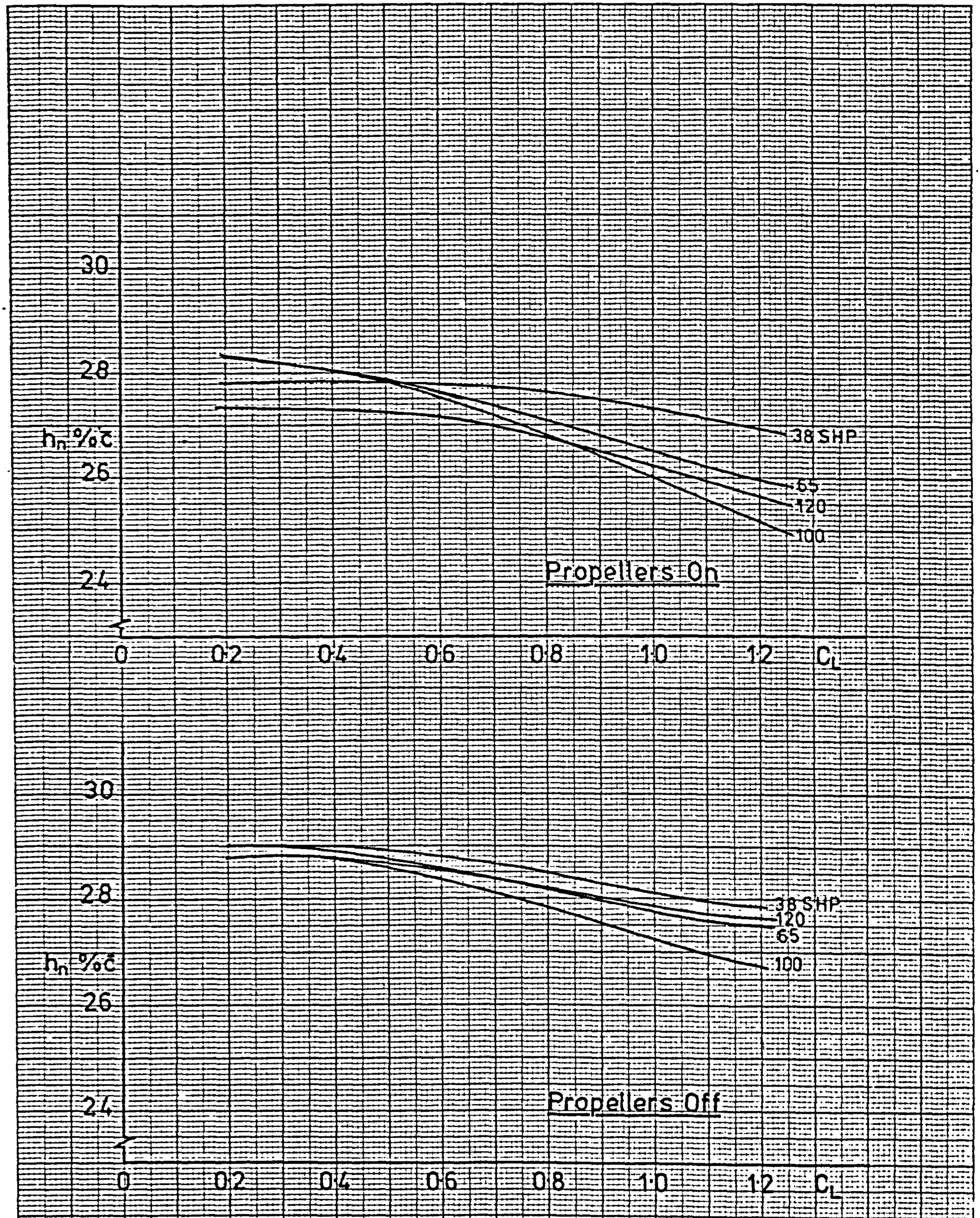

FIG.12. NEUTRAL POINTS, CONTROLS FIXED, PROPELLERS ON AND OFF.

APPENDIX A

AIRCRAFT DATA AND FLIGHT LOADINGS

1. Piper Twin Comanche 'A' Series

This is a light twin-engined aircraft extensively used in flying training establishments, by private owners and air taxi firms. It represents a very typical modern aircraft available for use by pilots of all levels of experience.

The aircraft used in the trials was a standard production model powered by 2-160 H.P. Lycoming 10-360-C engines. The instrumentation system installed for the test purposes was designed to have as little effect as possible on the exterior of the aircraft so that the handling characterisitcs would not be affected in any way. Ref.3. describes the instrumentation system in detail.

The loading conditions associated with the trial cases were:

	Weight	Horizontal C.G.	Vertical C.G.
Forward C.G.	3392 lb	17.36% $\bar{c}$	9.94% $\bar{c}$
Aft C.G.	3519 lb	23.95% $\bar{c}$	8.98% $\bar{c}$

The salient dimensions of the aircraft are shown in Table A1 and the outline G.A. in Fig.A1.

Wing

Section	NACA 64_2A215 (modified)
Area	178 ft^2
Span	35.98 ft
Mean aerodynamic chord	4.958 ft
Aspect ratio	7.28
Dehedral angle	5^o-00'
Incidence (root)	2^o-00'
Twist	0^o
Taper ratio	*0.513*

Tailplane

Section	NACA 0008
Area	32.50 ft^2
Span	12.50 ft
Mean aerodynamic chord	2.70 ft
Aspect ratio	4.8
Taper ratio	0.515

Tailplane Tab

Area	5.0 ft^2
Span	9.9 ft
Chord (% of local tail-plane chord)	18% $\bar{c}_T$

Tail Arm 14.40 ft

TABLE A1

Twin Comanche-Dimensions and Data

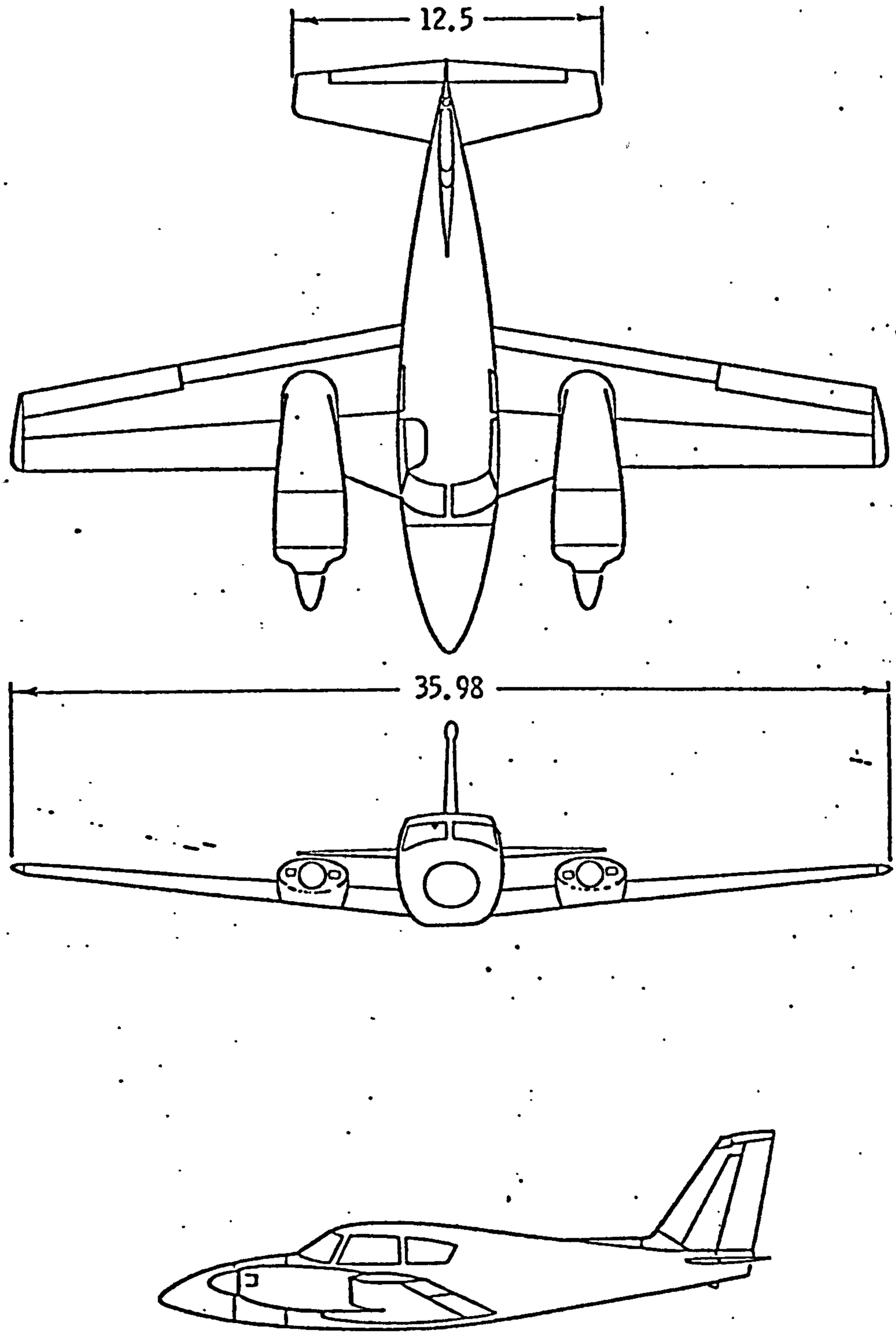

FIG. A1. PIPER TWIN COMANCHE.